THE ESTIMATION AND EVALUATION OF A SATELLITE-BASED DROUGHT INDEX USING RAINFALL AND EVAPOTRANSPIRATION

Maqsooda Mahomed

Submitted in fulfilment of the requirements for the degree of MSc Hydrology

Centre for Water Resources Research
School of Agriculture, Earth and Environmental Sciences
University of KwaZulu-Natal
Pietermaritzburg
08 December 2017

Supervisor: Ms KT Chetty
Co-Supervisor: Mr DJ Clark

In Memory of My beloved Grandmother,

Soogra Bee Bee Mahomed Ally

ABSTRACT

South Africa is naturally a water-scarce country and the climate is semi-arid hence, become particularly prone to droughts, which impact all facets of society and the environment. Climate change projections predict that droughts will worsen with the higher temperatures and fluctuating rainfall patterns. It is therefore vital that the country prepares for this natural phenomenon. In this study, drought estimation will be undertaken by using drought indices that have been utilised to analyse drought events in the past and by using the currently available sources of climatic data and satellite earth observation data. Since *Evapotranspiration* (*ET*) and rainfall drives the hydrological cycle, drought indices based on these variables will be investigated. The overall aim of this research study was to investigate, apply and evaluate a satellite-derived evaporative drought index in South Africa. The spatio-temporal evolution of droughts were analysed in the Upper Thukela and Umgeni Catchments, within the province of KwaZulu-Natal, South Africa for the study period 2011-2016. Drought analysis was carried out by using the Evapotranspiration Deficit Index (ETDI), the Standardized Precipitation Index (SPI) and the Standardized Precipitation Evapotranspiration Index (SPEI), at a monthly temporal scale. The LSA-SAF DMET product was used to obtain *actual ET* (ET_a) estimates for the study. A validation of the product against the surface renewal (SR) and eddy covariance (EC) systems within the Umgeni Catchment produced a correlation coefficient of 0.90 and a R^2 of 0.81. The satellite-derived Hargreaves-LST method was followed to obtain *reference ET* (ET_o) estimates; the approach was calibrated using the FAO Penman Monteith ET_o estimates and produced correlation coefficients of ≥0.86 for the selected quaternary catchment's (QC's). The SPI was calculated using *in-situ* data and the Famine Early Warning Systems Network African Rainfall Climatology (FEWS ARC 2.0) rainfall product for the Umgeni Catchment. This produced a R^2, ranging from 0.80-0.96, whilst between the FEWS ARC 2.0 and *in-situ* data for the Upper Thukela produced an R^2 that ranged from 0.55-0.72. The years, 2015 and 2016, was revealed as major drought years by the SPI, SPEI and ETDI, with prolonged dryness being detected for 2010 until 2016. The ETDI was compared using cross correlation analyses, which produced R^2 values that ranged from 0.31-0.73 for the Umgeni Catchment. Evaporative indices are suggested for use in semi-arid to arid regions as they contribute significantly to the water cycle. In addition, by utilizing satellite-derived drought indices, the analysis of the spatio-temporal patterns of droughts can contribute to an understanding of the mechanism of drought propagation and planning required for drought hazard mitigation.

DECLARATION PLAGIARISM

I, Maqsooda Mahomed declare that:

(a) the research reported in this dissertation, except where otherwise indicated, is my original work;
(b) this dissertation has not been submitted for any degree or examination at any other university;
(c) this dissertation does not contain other persons' data, pictures, graphs or other information, unless specifically acknowledged as being sourced from other persons;
(d) this dissertation does not contain other persons' writing, unless specifically acknowledged as being sourced from other researchers. Where other written sources have been quoted, then:
    (i) their words have been re-written, but the general information attributed to them has been referenced;
    (ii) where their exact words have been used, their writing has been placed inside quotation marks, and referenced.
(e) Where I have reproduced a publication of which I am an author, co-author or editor, I have indicated, in detail, which part of the publication was actually written by myself alone and have fully referenced such publications.
(f) This dissertation does not contain text, graphics or tables copied and pasted from the Internet, unless it is specifically acknowledged, and the source is detailed in the dissertation and in the References section.

Signed: …….
Maqsooda Mahomed

Supervisor: ……
Ms Kershani Tinisha Chetty

Co-Supervisor: …….
Mr David John Clark

PREFACE

The work produced and described in this dissertation was carried out at the Centre for Water Resources Research (CWRR), in the School of Agriculture, Earth and Environmental Sciences. The school is within the University of KwaZulu-Natal, in Pietermaritzburg. This dissertation was undertaken under the supervision of Ms KT Chetty and Mr DJ Clark.

The research presents the original and independent work by the author, Maqsooda Mahomed, and has not been published or submitted in any form, for any diploma or degree, to any tertiary institution. The work of other authors, where used, has been acknowledged appropriately.

ACKNOWLEDGEMENTS

First and foremost, I praise Almighty Allah for providing me with the knowledge, the physical and moral strength, and the capability to successfully complete my studies. His blessings are solely responsible for the successes and achievements in my life.

This Masters project, entitled “The Estimation and Evaluation of a Satellite Based Drought Index using Rainfall and Evapotranspiration”, has been funded by the NRF (National Research Foundation), in collaboration with ACCESS (Alliance for Collaboration on Climate and Earth Systems Science) and the DST (Department of Science and Technology). The financial assistance of the aforementioned institutions towards this research is hereby acknowledged. The opinions expressed and the conclusions arrived at, are those of the author and are not necessarily attributed to the NRF.

I also wish to acknowledge and express my sincere gratitude towards the following people and institutions:

I would like to thank my supervisor, Ms KT Chetty, for her sincerity, guidance and encouragement, which have led to the successful completion of this research. Her supervision and continual support have been a great help, from the commencement of this research study to its completion. Thank you for walking with me, and for being part of my development and providing a friendly and workable atmosphere.

I am also thankful to my co-supervisor, Mr DJ Clark for his invaluable advice and guidance. He had always been there to assist with the programming software that was used, without which the research would not have been possible. The amount of time and supervision you have given me has made a significant contribution to the successful completion of this research. The knowledge that you have imparted to me will form a strong foundation for my future ventures. A special thank-you for your patience during my first steps with the Python software.

Dr S Rees, thank you for your assistance with the editing of this dissertation. The time and effort extended towards this project is appreciated.

Mr Shaeden Gokool, I would like to express my deepest gratitude to you for your valuable comments and advice, which have improved my research. I have certainly learnt a lot from you. Thank you for being there for me every step of the way during my research. I deeply appreciate your support and the role that you have played for this study.

Dr Lauren Bulcock, I would like to express my appreciation for your support, invaluable advice and the words of motivation that you shared with me during this study.

Dr Joris Timmermans, thank you for your time, sound advice and for the provision of the scripts relating to the bulk processing of satellite data.

Dr Alistair Clulow, thank you for your advice and for the provision of the required validation data for this study.

I thank the Agricultural Research Council (ARC), the South African Weather Services (SAWS) and the South African Sugarcane Research Institute (SASRI) for their invaluable assistance and the provision of meteorological data used in this study. I would like to acknowledge the National Aeronautics and Space Administration (NASA), the EUMETSAT Satellite Application Faculty on Land Surface Analysis (LSA-SAF), the Satellite Applications and Hydrology Group (SAHG) and the Famine Early Warning Systems Network (FEWS) for providing freely-available datasets for my research study.

To all my CWRR colleagues and staff members at the Centre for Water Resources Research, thank you for enriching me with your valuable knowledge. I would like to express my deep gratitude for your support and friendship over the past 21 months.

My sincere thanks to my wonderful, loving parents, my sister, my dearest nephew, my family and friends, for their encouragement, endless love, moral support and advice, which have enabled me to complete my research study.

To my late grandmother, my heartfelt thanks for the love, support, encouragement and countless blessings that you have bestowed on me. Thank you for moulding me into the character I am. You will forever be cherished in my heart.

TABLE OF CONTENTS

LIST OF TABLES

Page

LIST OF FIGURES

Page

LIST OF SYMBOLS

$EDTI_{j-1}$	ETDI for initial month (dimensionless)
MSA_j	long-term median water stress of month j (dimensionless)
MaxWS	long-term maximum water stress of month j (dimensionless)
min WS_j	long-term minimum water stress of the month j (dimensionless)
$ET0_R$	ET values calculated using the reference FAO-PM method [mm]
$ET0_{lst}$	ET estimated using the Hargreaves empirical model and the MODIS LST [mm]
a and b	calibration parameters
$ET0_{ca}$	calibrated ET0 values [mm]
γ	psychometric constant [kPa/°C].
Δ	slope vapour pressure curve [kPa/°C]
e_s-e_a	saturation vapour pressure deficit [kPa]
ea	actual vapour pressure [kPa]
es	saturation vapour pressure [kPa]
u2	wind speed measured at 2 m height [m/s]
G	soil heat flux density [$MJ/m^2/day$]
ET_o	reference evapotranspiration [mm/day]
ET_a	actual evapotranspiration [mm/day]
T_{mean}	mean temperature [°C]
T_{min}	minimum temperature [°C]
T_{max}	maximum temperature [°C]
RA	extra-terrestrial radiation [$MJ.m^{-2}.d^{-1}$]
Ts	surface temperature [°C]
MET_j-1	previous ET values for the same pixel in considered day [mm]
MET_j	next existing ET values for the same pixel in considered day [mm]
h1	integration limit theoretically at 00:30 UTC
h2	integration limit theoretically at 24:00 UTC
L_v	latent heat of vaporization [$MJ.kg^{-1}$]
LAI	leaf area index
R_{ni}	partition of net radiation
H_i	sensible heat flux [$W.m^{-2}$]

LE_i	latent heat flux [W.m²]
G_i	heat conduction flux [W.m²]
Rn	net radiation [MJ/m2/day]
K	Kelvin
α	albedo
r_a	aerodynamic resistance
q_a	specific humidity
r_c	canopy resistance
q_{sat}	specific humidity at saturation
r_{aii}	aerodynamic resistance
L_i	Obukhov length [m]

LIST OF ABBREVIATIONS

ACCESS	Alliance for Collaboration on Climate and Earth Systems Science
ARC-ISCW	Agricultural Research Council-Institute for Soil, Climate and Water
ARC 2.0	African Rainfall Climatology 2.0
ASTER	Advanced Spaceborne Thermal Emission and Reflection Radiometer
ATBD	Algorithm Theoretical Basis Document
AVHRR	Advanced Very High Resolution Radiometer
AWS	Automatic Weather Station
BC	Blaney-Criddle
CRAN	Comprehensive R Archive Network
CRED	Centre for Research on the Epidemiology of Disasters
CRU TS	Climatic Research Unit Time-Series
CWRR	Centre for Water Resources Research
DMET	Daily evapotranspiration product
DOY	Day of Year
DWA	Department of Water Affairs
EC	Eddy Covariance system
ENSO	El Niño–Southern Oscillation
ET	*Evapotranspiration*
ET_o	*Reference Evapotranspiration* (mm)
ETDI	Evapotranspiration Deficit Index
ECMWF	European Centre for Medium Weather Forecast
ET_a	*Actual Evapotranspiration* (mm)
EUMETSAT	European Organization for the Exploitation of Meteorological Satellites
FAO	Food and Agriculture Organization
FAO-PM	Food and Agriculture Organization-Penman Monteith
FEWS ARC 2.0	Famine Early Warning Systems Network African Rainfall Climatology 2.0
FS	Free State Province
FTP	File Transfer Protocol
GDAL	Geospatial Data Abstraction Library
GIS	Geographic Information Systems
GOES	Geostationary Operational Environmental Satellite

GPCC	Global Precipitation Climatology Centre
GW	Ground Water
HDF	Hierarchical Data Format
LANDSAT	Land Remote-sensing Satellite
LAI	Leaf Area Index
LSA SAF	Land Surface Analysis Satellite Applications Facility
LST	Land Surface Temperature
MAD	Mean Absolute Deviation
MAP	Mean Annual Precipitation
MAPE	Mean Absolute Percentage Error
METREF	Reference evapotranspiration product
MODIS	Moderate Resolution Imaging Spectro-radiometer
MSG	Meteosat Second Generation
MSE	Mean Square Error
NAO	North Atlantic Oscillation
NASA	United States National Aeronautics and Space Administration
NDVI	Normalized Difference Vegetation Index
NetCDF	Network Common Data Form
NIMR	National Institute of Meteorological Research at Korea Meteorological Administration
NOAA	National Oceanic and Atmospheric Administration
NRF	National Research Foundation
NW	North-West Province
PET	Potential Evapotranspiration
PC-GLOBWB	PCRaster Global Water Balance
PN	Percent of Normal
PHDI	Palmer Hydrological Drought Index
Palmer Z	Short-term (monthly timescale) Palmer drought index
PDSI	Palmer Drought Severity Index
POF	Product Output Format
PUM	Product User Manual
QC's	Quaternary Catchments
R	Correlation Coefficient
R^2	Coefficient of Determination

RFE	African Rainfall Estimation
RMSE	Root Mean Square Error
RS	Remote Sensing
RDI	Reconnaissance Drought Index
RDDI	Rainfall Decile-based Drought Index
ReSET	Remote Sensing of ET Model
SEO	Satellite Earth Observation Data
SADC	Southern African Development Community
SAHG	Satellite Applications and Hydrology Group
SASEX	South African Sugar Association
SASRI	South African Sugarcane Research Institute
SAWS	South African Weather Service
SEBS	Surface Energy Balance System
SEBAL	Surface Energy Balance Algorithm for Land
SEVIRI	Spinning Enhanced Visible and Infrared Imager Radiometer
SPI	Standardised Precipitation Index
SPEI	Standardized Precipitation Evapotranspiration Index
SR	Surface Renewal system
SSI	Soil Saturation Index
SST	Sea Surface Temperature
SMDI	Soil Moisture Deficit Index
SPOT	Système Pour l'Observation de la Terre (French remote sensing satellite)
SVAT	Soil Vegetation Atmosphere Transfer
SWI	Standardised Water-level Index
SWSI	Surface Water Supply Index
TDTM	Time-Domain Triangle Method
TOPKAPI	Topographic Kinematic Approximation and Integration
TRMM	Tropical Rainfall Measurement Mission
USGS	United States Geological Survey
UKZN	University of KwaZulu-Natal
VegET	Vegetation Evapotranspiration Model
VCI	Vegetation Condition Index
VHI	Vegetation Health Index
VGT	Vegetation

VR	Validation Report
WPLM	Modified Palmer drought severity index
WACMOS	WAter Cycle Observation Multi-mission Strategy
WMO	World Meteorological Organization
WSA	Water Stress Anomaly
WS	Water Stress Ratio

1. INTRODUCTION

An essential element of life that is required by all inhabitants of our planet is water (Pedro-Monzonís *et al*., 2015). South Africa has been characterized as a semi-arid to arid country that has highly constrained fresh water resources, due to a highly variable climate (Dennis and Dennis, 2012; WRC, 2015). Climate change and variability impose weather extremes, which affect these finite water resources (UNFCCC, 2011; Dennis and Dennis, 2012; WRC, 2015). The unprecedented and rapidly-growing human population, as well as the need for water for socio-economic development in South Africa, have further impacted the availability of the already limited water resources (Shoko *et al*., 2013; WWAP, 2015). The country consists of a number of water resource consumers, who are all competing for a share of the limited resource (Jarmain *et al*., 2009). Coupled with the predominately arid environment of the country, the growing demand for water resources has led to a situation in which the demand surpasses the natural availability of water in many areas in South Africa (Molobela and Sinha, 2011).

Less than 500 mm of rainfall a year is received by three-quarters of the country (Dennis and Dennis, 2012; WRC, 2015), of which on average, South Africa receives about half the global mean annual precipitation (MAP) (860 mm) (Pitman, 2011; WRC, 2015). This natural water scarcity makes South Africa particularly prone to droughts (WRC, 2015). Hence, droughts are a regular feature of South Africa's climate due to the characteristic features of the country's greatly varied weather and climate extremes (Rouault and Richard, 2003**)**. Droughts are acknowledged as being disastrous natural phenomena that have an impact on the environment, on agriculture and on the socio-economic spheres (Bhuiyan, 2004; van Loon and Laaha, 2014; Winkler *et al*., 2017). Epidemics, famine, the relocation of populations and malnutrition are some of the severe consequences brought about by droughts (Rojas, 2011).

South Africa's climate is further characterized by dry spells, also known as El Niño (years experiencing below-normal rainfall), and by wet spells known as La Niña (years experiencing above-normal rainfall) (WRC, 2015). These alternating wet and dry periods often amplify drought situations and escalate the risks associated with widespread water shortages (WRC, 2015). In the late 2014 until the beginning of 2017, South Africa had been experiencing drought conditions, making the situation worse, the drought event had occurred within a prolonged dry period that had coincided with the El Niño phase. The country had therefore faced a severe

drought, with many of the country's dam levels being drastically reduced, water-restrictions being implemented and many areas in the country have had to deal with lower assurance of supply levels, as the drought conditions continued to intensify. This event had been recognized as a national drought, with the driest cropping season in more than 35 years (SADC, 2016). Seven of the country's nine provinces had to be declared as drought emergencies (SADC, 2016).

Furthermore, climate change may result in temperature increases and changes in rainfall patterns, leading to an increase in the frequency and intensity of droughts experienced worldwide (Burke *et al*., 2006; Lehner *et al*., 2006; Feyen and Dankers, 2009; Dai, 2011; Dai, 2013; Prudhomme *et al*., 2014; Trenberth *et al*., 2014; Wanders and Wada, 2014). As a result of climate change, a warmer climate and reduced summer rainfalls combined with increased evaporation is predicted to prevail, hence the danger of droughts increases and food- and water-security are placed at risk (UNFCCC, 2011).

The key to drought readiness and preparedness is about being knowledgeable regarding the how, when and what of the drought event (WRC, 2015). In order to achieve this goal, the capability of the observation networks, the scientific expertise to monitor and predict, as well as information systems to provide for early drought warnings need to be upgraded, focused and targeted (WRC, 2015). Drought indices are an efficient way of quantifying the impacts derived from droughts, for monitoring droughts in a real-time manner and for risk management (Vicente-Serrano *et al*., 2012a). There are several of drought indices that have evolved over the years and the different drought indices have been established on distinct hydrological variables, such as soil moisture, precipitation or *evapotranspiration* (*ET*).

Water is mainly consumed through evaporation (*E*), which accounts for water loss from the surface, and from transpiration, which accounts for water loss from vegetation (*T*), which are jointly termed *evapotranspiration* (*ET*) (Bastiaanssen *et al*., 2012; Sepulcre *et al*., 2014; Shoko *et al*., 2015). However, several authors state that the use of the term *ET* should be avoided, as it is a misleading term since it combines evaporation processes from different surfaces (Savenije, 2004; McMahon *et al*., 2012). Hence, in this document, evapotranspiration from a well-watered reference surface is termed *reference evapotranspiration* (ET_o) (Tian and Martinez, 2012), *actual evapotranspiration* (ET_a) refers to the quantity of actual water that is being removed from the earth's surface as a result of evaporation and transpiration processes

occurring while, *potential evapotranspiration* (*PET*) represents the amount of evaporation that will occur if an adequate water source is available.

It has been noted that 91% of the MAP that is received by the region of southern Africa, returns to the atmosphere by means of ET_a (Whitmore, 1971). ET_a is a key water cycle related variable, playing a crucial role in the carbon and energy cycles (Timmermans *et al*., 2010). Through these cycles, the estimation of ET_a is therefore vital for agricultural irrigation management, drought monitoring and weather forecast modelling (Timmermans *et al*., 2010). Drought conditions and the need for irrigation can be obtained from ET_a estimates, since they provide a direct forewarning of the growth rate and health status of crops. In addition, evaporation from open water bodies, soil water and plant transpiration merge as a lower forcing boundary parameter to the atmosphere which affects local and regional weather patterns (Timmermans *et al*., 2010).

In water-scarce regions of the world, the ET_a process dominates the hydrological cycle, hence, accurate ET_a estimation can prove to be very valuable for improving water resources management and irrigation, which, in turn, contributes to the improvement of agricultural production and water conservation (Elhaddad *et al*., 2011). The estimation of historical ET_a, as well as reliable short-term forecasts of ET_a, play a crucial role in understanding the water balance, which is a key element in water accounting for the management and monitoring of water resources as well as for evaluating water productivity (Mutiga *et al*., 2010; Shoko *et al*., 2013).

In the light of the impacts associated with droughts, there is a need to manage our water resources. Whatever the approach to the management of droughts may be (water management, water planning, and economy), it is necessary to understand the relationship between the physical variables, such as reservoir volumes, temperatures, precipitation, infrastructure management, water demands (ET_a), streamflows and piezometric levels, in order to enable the more efficient allocation of water resources. As a result, this study investigates the role of hydrological variables such as ET_a, precipitation and temperature for drought monitoring and risk management. The reason for this, by convention it is assumed that the water cycle begins with ET_a and it is through this process that increasing temperature in the coming decades as a result of climate change would most directly affect water resources. It is indicated that reduced summer rainfall with increased *PET* together with changes in seasonality and variability will

cause increased droughts (UNFCCC, 2011). As a result of the above-mentioned, the study places focus on ET_a, precipitation and temperature-based drought indices, based on satellite earth observation data (SEO), since the monitoring of drought and drought severity using *in-situ* data has often been difficult. This has been due to the lack of long-term data records, worsened by declining gauging networks and the incapability of *in-situ* data to capture the spatial and temporal coverage of such variables (Berhan *et al.*, 2011; Sheffield and Wood, 2011; Gokool, 2016).

In addition, there is a significant need to develop and expand our existing knowledge and to better understand and quantify ET_a at representative temporal and spatial scale to assist in assessing drought conditions. The conventional techniques used to estimate ET_a are unable to obtain large-scale spatial ET_a estimates, as they are only representative at point or localised field scales and cannot easily be extended over larger geographic scales (Gokool, 2016). Over the past four decades, the recent research and advances in satellite earth observation systems have provided new opportunities for obtaining hydro-meteorological data (Sorooshian and AghaKouchak, 2010). The utilisation of SEO has enabled us to capture hydro-meteorological data for large geographic scales, as well as for remote, ungauged areas, that are not easily accessible. Earth observational techniques provide near real-time, efficient and robust spatial and temporal data, which are applicable for extensive ET_a estimation for better water resources management.

As opposed to the conventional techniques, advances in modelling and the measurement of ET_a and other variables within the hydrological cycle, using satellite observations, are advocated more frequently (Sorooshian and AghaKouchak, 2010; Gokool, 2016). These estimates and hydro-meteorological data obtained through satellite earth observation techniques enable drought indices to be calculated and for the spatio-temporal analyses of droughts to be achieved (Berhan *et al.*, 2011).

1.1 Research Aims

The aim of this study was to investigate, apply and evaluate a satellite-derived evaporative drought index in South Africa, which can then be used to inform decision-making in water resources management, to assess drought conditions as well as to understand and to obtain

accurate estimates of ET_a on a greater temporal and spatial scale, by using satellite earth observational techniques.

1.1.1 Objectives

The specific objectives of this study include the following:

(i) The review of literature pertaining to current techniques, which utilize satellite derived earth observation data to estimate ET_a and ET_o.

(ii) The investigation and application of the Evapotranspiration Deficit Index (ETDI) in South Africa, using satellite derived earth observation data.

(iii) The estimation of ET_o from satellite earth observation data for use in the ETDI calculation.

(iv) The application and validation of a satellite-based ET_a product as an input for the ETDI calculation.

(v) The application of the Standardized Precipitation Index (SPI) and Standardized Precipitation Evapotranspiration Index (SPEI) to confirm the occurrence of drought events.

(vi) The assessment of the ETDI, using the SPI and SPEI as indicators of droughts in selected Quaternary level sub-Catchments (QC's) in South Africa.

(vii) The investigation of the use of satellite-based drought indices in an ungauged catchment.

1.1.2 Research questions

The following research questions will be investigated:

(i) Is the derivation of ET_a from satellite-based data a reliable way of obtaining an evaporative drought index to monitor droughts?

(ii) Is the calculation of an ETDI, using satellite earth observation data effective in the monitoring of droughts?

(iii) What is an appropriate method of estimating satellite-derived ET_o?

(iv) Can satellite data be used to calculate drought indices in an ungauged catchment? and

(v) How is the resulting information utilizing satellite earth observation data going to assist in monitoring droughts?

1.2 Organization of Dissertation

This dissertation is divided into five chapters, starting with introduction in Chapter One and ending with conclusion and recommendations in Chapter Five. An overview of the dissertation is presented as follows:

The literature review in the second chapter outlines the importance of droughts, drought monitoring and the different types of drought indices. An investigation of recent developments, specifically in the field of remote sensing (RS), which assist in drought monitoring using ET_a is also detailed. In addition, there is focus on the case studies and products that are based on SEO, which are used to obtain the parameters of the hydrological cycle to assess drought conditions. Chapter Two ends with an evaluation of the literature. It is a significant section, which summarizes the evaluated literature, reports on the gaps identified within the literature review and paves the way for the methodology, which is presented in Chapter Three. This chapter outlines the study areas and provides a detail description of the satellite data, meteorological data and validation data that were used in the study, along with details of the various procedures and techniques that were implemented. Chapter Four contains the results and discussion of the research study. The conclusion, limitations and recommendations are discussed in Chapter Five.

2. LITERATURE REVIEW

This chapter provides a review of literature pertaining to droughts, drought indices and the current techniques used to estimate ET_a and ET_o, using SEO. The use of SEO for providing the estimates of variables within the hydrological cycle is discussed, along with the use of the data used specifically for the monitoring of droughts. Information on satellite earth observation products is also contained in this review.

2.1 Droughts

Studies on droughts and drought management have gained increasing attention in recent years. Obtaining a unique definition for the term 'drought' is difficult, since there is no universally-accepted definition (Eden, 2012; Wilhite *et al*., 2014; van Loon, 2015). Drought is associated with dryness that is brought about by a shortage of water, or by levels of precipitation that are considered to be lower than normal (Petja *et al*., 2008; Zargar *et al*., 2011; Eden, 2012; Singleton, 2012; Wanga *et al*., 2015). It is commonly a result of climatic variations (Kershavarz, 2014; Wanga *et al*., 2015) and is also caused by an interaction between natural processes, such as the demand from humans and the environment caused by ET_a and precipitation factors (Eden, 2012). Relative humidity, wind and temperature are some of the important factors that should be included in the characterization of a drought (Mishra and Singh, 2010; WMO, 2012; Wanga *et al*., 2015).

A drought is usually described as a natural phenomenon or hazard that has an impact on many aspects of life, including society, the economy, the environment and agriculture (Bhuiyan, 2004; Petja *et al*., 2008; Singleton, 2012; Wilhite *et al*., 2014; Pedro-Monzonís *et al*., 2015; Russo *et al*., 2015). Droughts are perceived to be, costly and widespread, as well as one of the least understood natural disasters (Rivera and Penalba, 2014; Sheffield *et al*., 2014). The reason for this is the large spatial extent and lengthy duration that are attributed to droughts, and are driven by multiple regional or global features associated with this natural disaster such as the El Niño–Southern Oscillation (ENSO) (Rivera and Penalba, 2014; Sheffield *et al*., 2014). In addition, over a notable period of time, the repercussions of a drought are known to slowly accumulate and may last for many years after the event has occurred (Vicente-Serrano, 2006; Singleton, 2012; Wilhite *et al*., 2014). As a result of a lengthy period of dryness, precipitation

becomes inadequate to meet the needs of both humans and the environment. When compared to other natural disasters, droughts affect a larger proportion of a population (Sheffield *et al*., 2014). Furthermore, human activities such as land use changes, the poor management of water resources and deforestation, lead to drought conditions being further exacerbated. With most of the African continent being greatly dependent on rain-fed agriculture and with the impacts of drought on water resources and agriculture occurring over a large temporal and spatial scale, there are deleterious effects on food and water security (Sheffield *et al*., 2014; Masih *et al*., 2014). Droughts can occur anywhere in the world; however, the most severe drought consequences are felt in arid to semi-arid regions (van Loon, 2015).

The investigation of the temporal and spatial analyses of droughts is critical for sustained water resources management especially within semi-arid areas, as well as for their contribution to the climatic evaluation of an area (Rivera and Penalba, 2014). Furthermore, planning and preparing for droughts relies on how knowledgeable and informed one is about the severity, extent and duration of the event (Rivera and Penalba, 2014).

Droughts may be classified into different categories, based on their impact on the receiving environment. The different types of droughts are reviewed in the next section.

2.1.1 Types of drought

Droughts are known to be associated with timing (i.e. delays in the start of a rainy season, which is the main season of occurrence), as well as the effectiveness of rains (i.e. rainfall intensity, duration and spatial coverage) (Masih *et al*., 2014; Wilhite *et al*., 2014). According to Wilhite and Glantz (1985), climatology and hydrological parameters play an imperative role in assisting in the characterisation of droughts. Hence, a specific drought event is different in terms of its climatic and hydrologic characteristics, its impacts and spatial extent (Wilhite *et al*., 2014).

The four most common types of droughts are as follows (Wilhite and Glantz 1985; Petja *et al*., 2008; Wilhite *et al*., 2014):

a) **Agricultural drought:** The agricultural sector is affected by this type of drought. It frequently occurs when cultivated crops are harmed due to, a prolonged moisture

deficit (Eden, 2012). Since the water requirements of plants are not met, levels of ground water, soil conditions and plant characteristics are accounted for in this definition (Petja *et al*., 2008; Eden, 2012). A decline in crop yields result from this agricultural drought as well as crop development is affected (Pedro-Monzonís *et al*., 2015). Hence, the availability of soil water to aid crop and forage growth is commonly used to define an agricultural drought (Petja *et al*., 2008; Wilhite *et al*., 2014).

b) Meteorological drought: An extended period of dry weather is defined by this type of drought. Increases in temperature, the prolonged absence of rainfall and an accompanying decrease in humidity, which increases evapotranspiration results in the occurrence of a meteorological drought (Petja *et al*., 2008; Eden, 2012; Pedro-Monzonís *et al*., 2015).

c) Hydrological drought: As the name suggests, it relates specifically to hydro (water storage and flow) levels. It is a slow process drought that results when the supply of water from various water sources (lakes, streams and aquifers) drops below its normal level (Petja *et al*., 2008; Eden, 2012; Pedro-Monzonís *et al*., 2015). It may also be defined as the departure of surface and subsurface water supplies from an average condition occurring during various points in time. Hence, this type of drought occurs as a result of a deficiency in the water supply. (Petja *et al*., 2008; Wilhite *et al*., 2014; Pedro-Monzonís *et al*., 2015).

d) **Socio-economic drought:** Along with economic losses, this type of drought affects the social aspects. The demand for goods escalates, resulting in socio-economic impacts and famine or human starvation is usually inflicted. Supply-and-demand within a society is related to the socio-economic effect of the above-mentioned three droughts (Petja *et al*., 2008; Eden, 2012; Wilhite *et al*., 2014). This type of drought is therefore usually associated with the supply of a commodity, such as hydroelectric power, which is dependent on precipitation (Wilhite *et al*., 2014).

The aforementioned categories of droughts are all interrelated since they all emanate from a deficit of precipitation (Eden, 2012; Wilhite *et al*., 2014). Figure 2.1 portrays the interaction between the natural characteristics and human activities that rely on precipitation to supply sufficient water to meet the demands of the society and the environment (Wilhite *et al*., 2014).

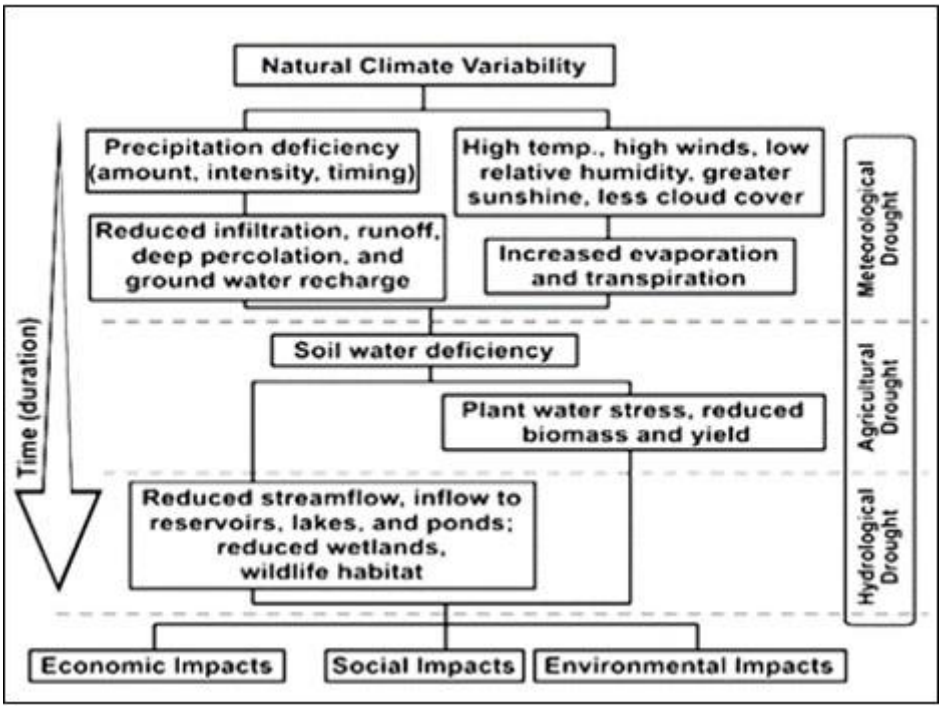

Figure 2.1 Drought types, the common sequence of occurrence and the causal factors of droughts (Source: National Drought Mitigation Center, University of Nebraska-Lincoln, US; cited by Wilhite *et al*., 2014)

From the above discussion, it is evident that drought conditions influence various spheres of life. The current pressures placed on our water resources and the country's climatic variability indicate that it is extremely crucial to administer water resources to satisfy the needs of a growing population and that there is a great need for sustainable water resource management practices. The monitoring of droughts and their impacts can be quantified through drought indices. This allows for a convenient way to express the level of risk associated with droughts. The beneficial use of drought indices for drought monitoring is elaborated on below.

2.1.2 Drought monitoring through drought indices

In an attempt to mitigate the negative impacts associated with droughts, proper methodologies and scientific approaches are needed to assist in developing policies and in decision-making, so as to reduce the hazardous consequences on both humans and the environment. Effective drought monitoring systems/techniques and improved forecasting and planning are some of the many ways that this can be done. For instance, through drought forecasting, farmers can make adaptive choices regarding crop varieties, technology investment and the source of labour.

They can also predict the duration of a drought event and improve their planning and resource allocation (Sheffield *et al*., 2014). Drought monitoring, forecasting and hydrological predictions have the capability to provide key information to an area for several reasons including urban and agricultural water supply, water resources management, as well as drought risk reduction.

Since droughts are often seen as creeping phenomena, with a slow onset and cessation, the provision of seasonal forecasts and the monitoring of drought development are crucial for drought risk reduction (Gillette, 1950, cited by Wilhite *et al*., 2014; Sheffield *et al*., 2014). Droughts are generally measured by an index or by the departure of a climatic variable such as precipitation or ET_a and the determination of impact is related to the duration of a drought event (Wilhite *et al*., 2014).

Drought indices are representative of an anomaly in respect of the past climate by means of models or observations (Heim, 2002). They have been established to assess, monitor and detect droughts (Pedro-Monzonís *et al*., 2015), easy to understand and are comparable in space and time (Heim, 2002). Over the years, a number of different types of drought indices have evolved specifically for the quantification and monitoring of droughts (Wanga *et al*., 2015). The following section details the various types of drought indices that exist.

2.1.3 Examples of different drought indices

According to Vicente-Serrano *et al.* (2012a), the quantification of impacts derived from droughts, together with the monitoring of droughts in a real-time manner so that it can be understood by users can be conducted through drought indices. Over the years, several different types of indices have evolved and are used widely for the monitoring, risk management and assessment of droughts. A drought index is frequently termed as a typical single value that is efficient for decision-making and for providing decision-makers with information regarding drought severities (Hayes *et al.*, 2007).

Drought indices are further defined as quantitative measures that identify droughts by assimilating climatic data (i.e. rainfall, temperature and streamflow) from one or several other variables into a single numerical value (Petja *et al*., 2008; Zagar *et al*., 2011). There is no quintessential index, as some indices may be more favourably suited to one region than to

another (van Loon, 2015). The selection of an index for drought monitoring is determined merely by the availability of climatic data and the ability of a specific index to detect temporal and spatial variations during a drought event (Morid *et al*., 2006). Therefore, the choice of an index plays a pivotal role in the execution of drought management plans.

It is important to identify the many types of drought indices that exist and which of them can be utilised for drought monitoring and management. Numerous drought indices have emerged to quantify droughts including the Standardised Precipitation Index (SPI), the Standardized Precipitation Evapotranspiration Index (SPEI), the Standardised Water-level Index (SWI), the Effective Drought Index (EDI), the Percent of Normal (PN), the Surface Water Supply Index (SWSI), the Evapotranspiration Deficit Index (ETDI), Four versions of the Palmer Indices (PHDI, WPLM, Palmer Z and PDSI), the Reconnaissance Drought Index (RDI), the Crop Moisture Index (CMI), the Deciles Index (DI), the Normalized Difference Vegetation Index (NDVI), the Vegetation Condition Index (VCI), the Temperature Condition Index (TCI), the Vegetation Health Index (VHI), the Rainfall Departure (RD), the Soil Moisture Deficit Index (SMDI) and the Rainfall Decile based Drought Index (RDDI). Information on these indices can be obtained from a variety of authors, including Heim (2002), Bhuiyan (2004), Morid *et al.* (2006), Hayes *et al.* (2007), Petja *et al*. (2008), Singleton, (2012), Vicente-Serrano *et al.* (2012), Jain *et al*. (2015), Vicente-Serrano *et al.* (2015b) and Wanga *et al*. (2015), amongst many other authors.

The above-mentioned indices are a few of the many indices that exist, with each index possessing its own strengths and weaknesses. The advantages and disadvantages of each of the aforementioned techniques are listed below in Table 2.1.

Table 2.1 A summary of the advantages and disadvantages of the different commonly used drought indices

Index	Advantages	Disadvantages	Source
SPI	Simple index to calculate and can be computed for multiple timescales. Requires one input parameter, precipitation, in order to function. Monitors wet and dry conditions.	No ratios can be calculated for ET_a since the index does not account for any soil water-balance component. Requires a minimum of at least 30 years of continuous precipitation data.	Morid *et al*., 2006; Petja *et al*., 2008; Singleton, 2012; Vicente-Serrano *et al*., 2012a; WMO, 2012; Jain *et al*., 2015
SWI	Measures hydrological drought intensity and allows for the scaling of groundwater recharge deficit.	Requires a long time series of observed data and the need to fit a probability density function.	Bhuiyan, 2004; Petja *et al*., 2008; Broek *et al*., 2014
EDI	Monitors duration and intensity of droughts over large areas, as well as wet and dry conditions. Calculates daily drought severity. Rapid detection and precise measurement of short-term drought.	Requires at least 30 years of precipitation data for calculation.	Morid *et al*., 2006; Petja *et al*., 2008; Jain *et al*., 2015
PN	Calculated for multiple time-scales, simplest measurement of rainfall for a location and very effective when used for a single region or a single season.	Mean precipitation not the same as the median precipitation. Not useful for analysing droughts based on a departure from normal.	Hayes *et al*., 2007; Petja *et al*., 2008; Morid *et al*., 2008
SWSI	Simple to calculate and represents water supply conditions unique to each basin. A good measure to monitor the impact of hydrologic drought on urban and industrial water supplies, irrigation and hydroelectric power generation.	Limits inter-basin comparisons and changes to data collection or water policies, or any extreme events that require new algorithms to be calculated. Not a suitable indicator for agricultural drought.	Narasimhan and Srinivasan, 2005; Hayes *et al*., 2007
ETDI	Accounts for the actual state of the land surface dryness, benefits of spatial coverage is attained (energy balance models) and provides a representation of the environmental demand of ET_a.	Long datasets required to calculate the water stress anomaly.	Narasimhan and Srinivasan, 2005; Eden, 2012; Trambauer *et al*., 2014
PDSI	Provides spatio-temporal representations of historical droughts and has been used to trigger actions associated with drought contingency plans. Measures wetness and dryness.	May not detect droughts as quick as the other indices, highly complex and less suited for high altitude areas or areas of frequent climatic extremes.	Narasimhan and Srinivasan, 2005; Hayes *et al*., 2007; Petja *et al*., 2008; Vicente-Serrano *et al*., 2012a; Vicente-Serrano *et al*., 2015b
CMI	More responsive to rapid changes in moisture conditions and responds to changes in weather conditions.	Not intended to assess long-term droughts.	Narasimhan and Srinivasan, 2005; Petja *et al*., 2008; Eden, 2012

Table 2.1 A summary of the advantages and disadvantages of the different commonly used drought indices (continued)

Index	Advantages	Disadvantages	Source
RDI	Can be computed at multiple time-scales.	Gives no valid values when ET_o is equal to 0, mainly when ET_o is calculated using empirical temperature-based methods.	Vicente-Serrano *et al*., 2015b
DI	Severity of droughts can be assessed.	Requires a long climatological record to calculate the deciles accurately.	Morid *et al*., 2006; Smakhtin and Hughes, 2007
NDVI/ VCI/TCI/VHI	Assessment of vegetative droughts. Vegetative and agricultural droughts reflect vegetation stress, provides a broad overview of the vegetation condition and spatial vegetation distribution in a region.	Strong ecological component subdues the weather component.	Bhuiyan, 2004; Rojas *et al*., 2011
SPEI	Sensitive to changes in evaporation demand, caused by temperature fluctuations and trends, through simple calculations and the multi-temporal nature of the SPI.	Does not represent soil water content and droughts are assumed to be influenced by the temporal variability of precipitation.	Vicente-Serrano *et al*., 2012a; Vicente-Serrano *et al*., 2015a
RD	A good indicator of dry and wet conditions for a given time over specified areas. It is easy to understand and simple to calculate.	Energy and water balances at the surface are not reflected, which indicates the effective amount of water left for agricultural purposes after runoff, evaporation and infiltration.	Parry *et al*., 2012; Jain *et al*., 2015
RDDI	The use of decile is advantageous due to the simplicity of its computation.	Conceptual difficulties and climates with highly seasonal precipitation may not be well suited to rainfall deciles.	Jain *et al*., 2015
SMDI	Useful for the monitoring soil moisture stress of crops and short-term droughts.	Data intensive.	Narasimhan and Srinivasan, 2005

Following the literature review on droughts and drought indices, the ETDI was the evaporative-based drought index selected for application in this study. The SPI and SPEI were also selected, to compare against the ETDI in determining the occurrence of a drought. As the ETDI, SPI and SPEI are prevalent in this study, a longer description is warranted. For the purpose of this study, the evaporative related drought index, ETDI, will be investigated for the monitoring of droughts. The ETDI was chosen because it is the only drought index that is based on an evaporation deficit (ET_o-ET_a) which has been found to be a good parameter for monitoring droughts. ET_a is an important component within the water cycle as the cycle begins with evaporation and ends, since it determines the amount of precipitation that is generation by the cycle as well as controls soil moisture.

Literature by Beguería *et al*. 2014, reports on the benefits of using ET_a as it accounts for water lost during real conditions hence, accounting for water available in soils, climate, physiological mechanisms, vegetation as well as crop type and state. ET_a is known to be dependent on the current water availability that prevails. Several research papers indicate that when a drought index is concerned, ET_a would be able to determine drought conditions as well as the surface water balance. ET_a allows for a better estimation of water that is transferred into the atmosphere, hence being more representative of the soil water balance than ET_o. Furthermore, climate change projections threaten increases in droughts due to increases in temperature and fluctuating rainfall patterns and it is through the process of evaporation that increases in global temperatures resulting from climate change is expected in the coming decades.

In addition, the ETDI requires a model output of ET_a, which can easily be obtained from remotely sensed models. Therefore, the advantage of ET_a estimation on a greater temporal and spatial scale as opposed to conventional techniques for obtaining ET_a estimates is made possible through RS techniques. Furthermore, with the ETDI accounting for ET_a, it is able to account for the actual state of the land surface dryness (Eden, 2012). This can be achieved by obtaining ET_a estimations from RS using energy balance models. Furthermore, the study will also seek to obtain ET_o estimates through RS methods, which will be used within the calculations of the ETDI.

Since droughts have spatial and temporal dimensions, achieving coverage of drought monitoring at large geographic scales through RS will provide a more comprehensive view of the development of a drought (Sheffield and Wood, 2011). With the application of the ETDI,

required inputs can be attained using RS techniques, which will allow this to be achieved. Hence, the monitoring of droughts over increasing spatial and temporal dimensions is permitted in this study.

In addition, the SPI and SPEI indices in this research study will be calculated to assess the potential/performance of the ETDI in detecting the occurrence of a drought. The SPI and SPEI have been used extensively in several hydrological and climatological studies. The SPI and SPEI are both based on the same concept: they are dimensionless and are classified into wet or dry categories (ten Broek *et al*., 2014). The SPI is a well-recognised and frequently-applied index, and it is valued for its robustness, versatility and theoretical development concerning drought analysis. The SPI has been utilised in operation, in more than 70 countries, as well as for research initiatives (WMO, 2012). This index is based on the input of precipitation data only and is widely accepted for the monitoring of droughts. Since droughts are associated with a deficit of precipitation and the SPI is based only on precipitation data, a comparative analysis between the SPI and ETDI will be performed in this study, to confirm the occurrence of a drought.

Despite rainfall being the main controlling factor for the occurrence of droughts, temperature has also been recognised in several studies as a key factor for explaining recent trends in water resources and for analysing droughts (Vicente-Serrano *et al*. 2011, 2012b, 2014; Schubert *et al*., 2014; Russo *et al*., 2015; Ceccherini *et al*., 2017). These studies have indicated an increase in temperature over the past 150 years along with climate models predicting a projected increase during the 21st century. Hence, the warming processes may have a negative impact on the availability of surface water, which are mainly driven by higher ET_a rates. The combined effect of higher temperatures and less rainfall is bound to lead to increases in the severity, magnitude and frequency of drought episodes. Hence, the use of indices accounting for temperature is preferable as the manifestation of droughts are often brought upon as a result of a lack of rainfall and soaring temperatures.

Hence, a drought index, SPEI was developed based on temperature and precipitation. These climate parameters are key drivers to the hydrological cycle. Similar to the PDSI, the SPEI is able to merge the sensitivity of changes in evaporation demand that result from temperature changes, with the multi-temporal nature and simplicity presented by the SPI.

The SPEI is similar to the SPI index, except that precipitation is not the only variable considered. This index takes into consideration the difference between the precipitation and evaporation variables (Trambauer *et al*., 2014). Hence, the SPEI uses a climatic water balance, thereby providing a more reliable measure of drought severity. Since the ETDI is calculated from evaporation variables and droughts are directly related to precipitation amounts, the SPEI will also be compared to the ETDI. The three indices used in this study all use some balance between the supply and demand of moisture, but each in their own unique way.

2.2 The Evapotranspiration Deficit Index (ETDI)

Narasimhan and Srinivasen (2005) developed the Evapotranspiration Deficit Index (ETDI). ETDI is a common agricultural drought indicator that was developed based on the weekly evapotranspiration deficit (Trambauer *et al*., 2014; Narasimhan and Srinivasen, 2005). It is calculated as a water stress ratio, which is the ratio between the ET_o and a model output of ET_a (Narasimhan and Srinivasen, 2005). The water stress values range from 0 to 1, where 0 is indicative of evapotranspiration occurring at the same rate as ET_o and 1 represents no evapotranspiration (Eden, 2012).

The water stress ratio (WS) for the month is calculated as follows (Narasimhan and Srinivasen, 2005):

$$WS = \frac{ET_0 - ET_a}{ET_0} \qquad (2.1)$$

where:

WS = monthly water stress ratio (dimensionless),
ET_o = monthly reference evapotranspiration (mm), and
ET_a = monthly actual evapotranspiration (mm).

Following the calculations of the WS, a water stress anomaly is calculated as expressed below (Narasimhan and Srinivasen, 2005):

$$WSA_{i,j} = \frac{MWS_j - WS_{i-j}}{MWS_j - minWS_j} * 100 \qquad \text{if} \qquad (WS_{i-j} = MWS_j) \qquad (2.2)$$

$$WSA_{i,j} = \frac{MWS_j - WS_{i-j}}{maxMWS_j - WS_j} * 100 \qquad \text{if} \qquad (WS_{i-j} > MWS_j) \qquad (2.3)$$

where:

WSA = monthly water stress anomaly,

MWS_j = long-term median water stress of month *j*,

$max\ WS_j$ = long-term maximum water stress of month *j*,

$min\ WS_j$ = long term minimum water stress of the month *j*, and

WS = monthly water stress ratio (for example: i = 2011-2016 and j = January-December).

During any month, the water stress anomaly (WSA) extends from -100 to +100, indicating very dry to very wet conditions with respect to evapotranspiration (Narasimhan and Srinivasen, 2005). Following the WSA calculations, a cumulating procedure is thereafter adopted for the ETDI to determine the severity of the drought due to the evapotranspiration deficit. This is given by Narasimhan and Srinivasan (2005) as follows:

$$ETDI_j = 0.5\ ETDI_{j-1} + \frac{WSA_j}{50} \qquad (2.4)$$

where:

$EDTI_{j-1}$ = the ETDI for the initial month, and

WSA_j = the monthly water stress anomaly.

2.2.1 Case studies: application of the ETDI

A concise description is presented below of a few studies that employ the ETDI, along with the key findings of these studies.

Narasimhan and Srinivasen (2005) used the distributed hydrological Soil and Water Assessment Tool (SWAT) model to simulate soil moisture and ET_a at a high spatial resolution (16 km^2) using GIS. By utilizing this data, the ETDI index was established. The index was based on a weekly evaporation deficit. The results showed that the developed index, the ETDI, could be used as a good indicator for monitoring soil moisture stress during critical growth periods of the wheat and sorghum crops. Furthermore, the ETDI is acceptable for agricultural

drought monitoring during short-term drought conditions. The key finding was that the ETDI was applicable for the monitoring of agricultural droughts.

Eden (2012) conducted a study to quantify the severity of drought by ET_a mapping in the Netherlands, for the period 2003-2010. The ETDI was used in the spatial and temporal distributional assessment of ET_a. The WACMOS (WAter Cycle Observation Multi-mission Strategy) methodology was pursued to obtain estimates of ET_a. The input data consisted of RS products from MODIS and meteorological data from the European Centre for Medium Weather Forecast (ECMWF). The results showed that the ET_a followed a seasonal trend in all years and that in which ET_a was greater for the growing seasons. The study also showed that the SEBS (Surface Energy Balance System) ET_a from MODIS 1km and the ECMWF could be used to estimate ET_a in the Twente region. The key finding was that ETDI and SPI are applicable for the assessment of droughts.

Trambauer *et al*. (2014) conducted a study in the Limpopo River Basin to analyse hydrological droughts using a fine resolution model, PCRaster Global Water Balance (PCR-GLOBWB). The ETDI was computed along with other indices. The overall results of the study indicated that the identification of hydrological droughts is possible with a carefully set-up process-based model, even if the model is largely uncalibrated. The results also described the significance of computing indicators that can be related to hydrological droughts as well as the value of identifying hydrological droughts. A key finding of the research was that the drought severity in the basin could be characterised. This was shown by its intensity, duration and time of occurrence.

2.2.2 The advantages and disadvantages of the ETDI

The main advantage of utilizing the ETDI is that the index considers ET_a and is able to account for the actual state of the land surface dryness (Eden, 2012). The index requires ET_a estimates that can be obtained either using *in-situ* data or satellite-derived estimates. By using an energy balance model to obtain these estimates, the benefits of RS may be attained, as ET_a estimation can be achieved over large geographic scales, accommodating for a more comprehensive view of the development of droughts. The ETDI also requires ET_o, which provides a representation of the environmental demand of ET_o. The main disadvantage of this index is the need for lengthy datasets to be able to calculate the WSA.

2.3 Standardized Precipitation Index (SPI)

SPI (McKee *et al*., 1993, 1995) is one of the most widely applied meteorological drought indices that is based only on precipitation data. According to the WMO (2012), the SPI index provides better representations than the PSDI and is recognisably a powerful, flexible index that is simple to calculate. This index has been primarily developed for characterizing and monitoring droughts (Jain *et al*., 2015; Botai *et al*., 2016). The SPI may also be beneficial and useful to determine periods of anomalously wet events/flood events.

The index is based on the probability of precipitation for multiple time scales which is thereafter transformed into an index (Narasimhan and Srinivasan, 2005; Zargar *et al*., 2011; WMO, 2012). In calculating the SPI, the precipitation record is first fitted to a Gamma distribution (Narasimhan and Srinivasan, 2005; Zargar *et al*., 2011; WMO, 2012; Trambauer *et al*., 2014; Jain *et al*., 2015; Kumar *et al*., 2016). The Gamma distribution is then transformed to a normal distribution, using an equal probability transformation (Narasimhan and Srinivasan, 2005; Zargar *et al*., 2011; Holloway *et al*., 2012; WMO, 2012; Trambauer *et al*., 2014; Jain *et al*., 2015; Kumar *et al*., 2016). The mean is set to a value of zero, which results in values above zero indicating a wet period and values below zero indicating a dry period (Zargar *et al*., 2011; WMO, 2012; Jain *et al*., 2015). During any given drought event, an SPI score is representative of how many standard deviations its cumulative precipitation deficit deviates from the normalized average (Zargar *et al*., 2011; Kumar *et al*., 2016). Hence, if a specific precipitation event produces a low probability on the cumulative probability function, then this is indicative of a possible drought event.

Several software tools have been developed to calculate the SPI and they can be could be operated both within a WINDOWS and a UNIX environment. Monthly precipitation values for at least 30 consecutive years, with 50-60 years (or greater) being optimal was preferred to run the programs (WMO, 2012; Jain *et al*., 2015). However, these programs have been replaced by an SPEI package within the R software, which also requires 30 years of continuous precipitation data. The SPEI R package is therefore recommended for use. Section 3.4.1 expands on the R software.

McKee *et al*. (1993) defined the drought intensities produced from the SPI, using the classification system shown in the SPI value table below (Table 2.2). When the SPI is negative and approaches an intensity of -1.0 or less, it is indicative of a drought event occurring during that period and ends when the SPI becomes positive. In addition, the positive sum of the SPI for all months present within a drought event may be defined as the drought's "magnitude" (WMO, 2012).

Table 2.2 Category of SPI values (McKee *et al*., 1993)

2.0 +	Extremely wet
1.5 to 1.99	Very wet
1.0 to 1.49	Moderately wet
-0.99 to 0.99	Near normal
-1.0 to -1.49	Moderately dry
-1.5 to -1.99	Severely dry
-2.0 and less	Extremely dry

The standardization technique of the SPI enables the index to determine the rarity of a current drought situation, as well as the probability of precipitation that is needed to end it (Table 2.3). Users are also given the opportunity to assess how frequent, or how rare a given drought event is (WMO, 2012).

Table 2.3 Probability of Recurrence (WMO, 2012)

SPI	**Category**	**Number of times in 100 years**	**Severity of event**
0 to -0.99	Mild dryness	33	1 in 3 years
-1.0 to -1.49	Moderate dryness	10	1 in 10 years
-1.5 to -1.99	Severe dryness	5	1 in 20 years
-2.0 and less	Extreme dryness	2.5	1 in 50 years

In addition, it is worth mentioning that a global SPI data set, with a spatial resolution of 2.5^{o} is presently available (Ziese *et al*., 2014). The data set is based on the NOAA NCEP CPC CAMS_OPI monthly precipitation data, which can be obtained using the following link, (http://iridl.ldeo.columbia.edu/maproom/Global/Precipitation/SPI.html?var=.SPI-CAMSOPI_12-Month#tabs-1). This dataset; however, has not been used in the study instead, *in-situ* data was used to provide more representative climatic conditions of the study areas.

2.3.1 The advantages and disadvantages of the SPI

The following advantages can be derived from the SPI:

- It is simple and relies only on precipitation data (WMO, 2012; Mu *et al*., 2013; Botai *et al*., 2016).
- The index provides a good indication of the history of droughts for a specific station by simply plotting a time series of the year against the SPI.
- By applying the SPI, the drought history of a site or region can be evaluated, including an analysis of the duration and frequency for a magnitude ranking of sorts.
- From a temporal point of view, the SPI index can be computed for different time scales (3-, 6-, 12-, 24- and 48-month timescales). This enables an analyst to study rainfall events at different time scales, as well as it provides early warning and assists in drought warning (Zargar *et al*., 2011; WMO, 2012; Mu *et al*., 2013).
- It is less complex in nature than the PDSI and several other indices (WMO, 2012).
- Since the SPI can be computed for longer time scales (greater than three months), agricultural and hydrological droughts/impacts can be reflected (Zargar *et al*., 2011).
- The SPI index is effective in analysing wet and dry climates and it can hence, be used to monitor dry periods (Zargar *et al*., 2011; WMO, 2012).
- It accounts for the stochastic nature of the drought event and therefore a useful measure of short- and long-term meteorological droughts (Narasimhan and Srinivasan, 2005).
- A comparison between different locations in different climates can be conducted as it is spatially consistent (WMO, 2012).

Some of disadvantages of the SPI include the following:

- Since it is based only on precipitation data, there is no direct connection to ground conditions (Trambauer *et al*., 2014; Zargar *et al*., 2011).
- The SPI does not consider the effect of crop growth, land use, temperature anomalies and land characteristics that play a key role for agricultural drought monitoring (Narasimhan and Srinivasan, 2005).

- The presence of limitations that may be attached to the precipitation data such as the number of gauging stations, the length of the record and the accuracy of measurements (Zargar *et al*., 2011; WMO, 2012; Mu *et al*., 2013).
- No ET_a ratios can be calculated, as the index does not account for any soil water-balance component (WMO, 2012).

2.4 Standardized Precipitation Evapotranspiration Index (SPEI)

Proposed by Vicente-Serrano *et al*. (2010b), the Standardized Precipitation Evapotranspiration Index (SPEI) is an extension of the SPI, which takes into account the effects of evapotranspiration. Hence, the SPEI is a modification of the SPI, which was developed to address water supply and water demand issues (Botai *et al*., 2016). The SPEI, like the SPI, can be computed at various time scales, enabling users to determine the time scale at which the response to a drought is the greatest. However, unlike the SPI, the SPEI is able to capture the major impact of temperature on the water demand (Vicente-Serrano, SM and National Center for Atmospheric Research Staff, 2015). The index is based on temperature and precipitation data and is capable of including the effects of temperature variability on drought assessments and exploring the climate change effects on drought conditions (Vicente-Serrano *et al*. 2010a; Beguería *et al*., 2010). The index is comparable to the self-calibrated Palmer drought severity index (sc-PDSI) as the index is based on a water balance. The SPEI combines the sensitivity of the PDSI to evaporative demand changes (due to temperature fluctuations and trends) with the capability and simplicity of the calculation of the SPI to represent drought events on a multi-temporal scale (Vicente-Serrano *et al*. 2010b; Trambauer *et al*., 2014; Botai *et al*., 2016). The SPEI is used by different science disciplines for the monitoring, detection and analysis of droughts.

According to Vicente-Serrano *et al*. (2010b), the SPEI can be computed at different temporal scales based on the non-exceedance probability of precipitation and *PET* differences. The SPEI is based on a monthly climatic water balance (PET-ET_o), which is adjusted by using a three-parameter log–logistic distribution. The values are accumulated at different time scales and converted to standard deviations, with respect to the average values (Vicente-Serrano, SM and National Center for Atmospheric Research Staff, 2015). In instances where limited climatic data is available, *PET* can be calculated using the simple Thornthwaite method (Vicente-

Serrano, SM and National Center for Atmospheric Research Staff, 2015). In cases where more data is available, a more complex method for estimating *PET* can be opted for, to produce an overall accounting of drought variability. However, additional variables can produce greater uncertainties (Vicente-Serrano, SM and National Center for Atmospheric Research Staff, 2015). Like the SPI, the SPEI R package requiring 30 consecutive years of precipitation and temperature data can be used to obtain SPEI values. The Section 3.4.1 elaborates further on the R software.

A complete description of the theory behind the SPEI, including the computational details, operational use and comparisons between other popular drought indices, such as the SPI and PDSI is provided by Vicente-Serrano *et al*. (2010a, 2010b, 2011, 2012a), Beguería *et al*. (2014), and Manatsa *et al*. (2017).

It is also beneficial to note that the Penman-Monteith method along with the CRU TS 3.2 input data have been utilised to produce a gridded SPEI data set for 1901-2011 (Vicente-Serrano, SM and National Center for Atmospheric Research Staff, 2015). The Thornthwaite method was used to generate a real-time SPEI for global drought monitoring. Finally, an R package is available for estimating SPEI from user-selected input data using the options of Penman-Monteith, Hargreaves or Thornthwaite methods (Vicente-Serrano, SM and National Center for Atmospheric Research Staff, 2015).

Furthermore, a "SPEI Global Drought Monitor" is presently available, which is based on precipitation data from the GPCC (Global Precipitation Climatology Centre), along with temperature data from the NOAA NCEP CPC GHCN_CAMS gridded data set (Ziese *et al*., 2014**)**. The *PET* is calculated based on the parameterization from the Thornthwaite (1948) method. The gridded data of the SPEI is produced at a 0.5^{o} spatial resolution, at a monthly time resolution and at a timescale of between 1 and 48 months (http://sac.csic.es/spei/). This SPEI dataset; however, has not been used in the study instead, *in-situ* data was used to provide more representative climatic conditions of the study areas.

2.4.1 Case studies: application of the SPI and SPEI

As a result of the SPI's reliability, and its ability to analyse droughts at multiple time steps for a variety of climatic regions, this index has been used extensively in several parts of the world.

A vast array of studies exist that have utilized the SPI; however, only a few selected case studies will be discussed in this section, along with their key findings. Studies by Rouault and Richard (2003), Sepulcre-Canto *et al*. (2014), Jain *et al*. (2015) and Kumar *et al*. (2016), amongst several others, can also be explored with regards to the application of the SPI. Various studies which utilise the SPI also include the SPEI, which is able to account for the role of ET_a and temperature within drought monitoring and hence, both indices are discussed in this section.

Palchaudhuri and Biswas (2013) applied the multi-temporal SPI to analyse the severity and spatial pattern of a meteorological drought in the Puruliya District, West Bengal, India. Some of the results and key findings of this study indicated that in the central portion of the study area, mild and moderate droughts occurred, whereas severe and extreme droughts occurred north-east, north-west and the south-west of the region. Overall, the study indicated that the SPI can be used for the assessment of droughts.

Trambauer *et al*. (2014) conducted a study to assess historical droughts in a highly water-stressed, semi-arid basin, by using different drought indicators. The Limpopo River Basin is recognised as one of the most water-stressed basins in Africa. A finer-resolution version of the global hydrological model (PCR-GLOBWB) was adapted to regional conditions in the basin. The model was then tested by comparing the simulated hydrological and agricultural drought indicators (ETDI, RSAI, SRI, GRI) in the period 1979–2010 with reported historic drought events in the same period. The SPI and SPEI drought indicators were also computed as a verification of the drought indicators and the type of drought. The key findings indicated that a combination of the drought indicators at different time scales (SPEI-3, SRI-6 and SPI-12 computed together) are worthy for distinguishing between agricultural to long-term hydrological droughts in the Basin. Furthermore, it was possible to identify drought severity in the basin, which was indicated by its time of occurrence, duration and intensity.

Botai *et al*. (2016) applied the SPI and the SPEI to investigate the historical evolution of drought within the Free State and North-West Provinces over the past 30 years. Monthly meteorological data, which were obtained from 14 weather/climate stations within the Free State (FS) and Northwest (NW) Provinces, were used to compute the drought indices. In addition to the computation of the drought indices, the meteorological data was also used to explore and identify variations in drought intensity, duration, frequency and severity in FS and NW Provinces during the period of 1985–2015. The key findings from this study indicated that

both the indices were able to display the drought development that was observed in the two provinces.

2.4.2 Advantages and disadvantages of the SPEI

The SPEI is simple to calculate and is based on the original SPI calculations. The index is particularly suited to monitoring, detecting and exploring the effects of global warming on drought conditions (Vicente-Serrano *et al*. 2010a, 2010b). Despite the index being relatively new, it has been used in several studies to analyse the variability of droughts (Potop, 2011; Paulo *et al*., 2012; Wei- Guang *et al*., 2012; Li *et al*., 2012; Spinoni *et al*., 2013; Sohn *et al*., 2013). This index is representative of a simple climatic water balance (Thornthwaite 1948), since the index is based on the difference between the precipitation and *PET*. The SPEI is also known to be applicable within any climatic region of the world. In comparison to the sc-PDSI, the SPEI has the advantage of being multi-scalar, which is critical for drought monitoring and analysis.

Some of the limitations of the SPEI may include more data is required than the SPI. Sensitivity is prevalent to the choice of method for calculating *PET*, due to the influence of global warming on the severity of droughts (Vicente-Serrano, SM and National Center for Atmospheric Research Staff, 2015). A long dataset that displays natural variability should be used (Vicente-Serrano, SM and National Center for Atmospheric Research Staff, 2015).

* * * * * *

Within the hydrological cycle, ET_a forms a vital component and greatly affects the availability of water resources present on earth. Globally, 64% of the precipitation is evapotranspired (Rivas and Caselles, 2004), of which the ET_a from land surfaces forms 97% and 3% forms open-water evaporation (Rivas and Caselles, 2004). Furthermore, in the region of Southern Africa, 91% of the MAP is returned to the atmosphere by means of ET_a (Whitmore, 1971). Hence, by monitoring ET_a, droughts can be effectively monitored and planned for future events. Since the ETDI, which is investigated in this study, is based on ET_a, the concept of ET_a and its role in the monitoring of droughts is therefore further elaborated on the next section.

2.5 The concept of Evapotranspiration

Evaporation is recognised as the process of water loss from the earth's surface and transpiration is the water loss from vegetation (Sepulcre *et al*., 2014). *Evaporation* (*E*) and *transpiration* (*T*) (jointly termed as *evapotranspiration* (*ET*)) constitute the processes of moisture evaporation from water bodies, soil and wet vegetated canopies and the transpiration from crops (NOAA, 2016). *ET* is recognisably one of the most effective variables in determining the water balance (Kiptala *et al*., 2013; Rahimi *et al*., 2015; Tian *et al*., 2015; Pandey *et al*., 2016). Several sources in literature report that the term *ET* should be avoided, as it accounts for evaporation from various surfaces (Savenije, 2004; McMahon *et al*., 2012). The term ET_a provides a clearer description of the movement of water from the earth surface to the atmosphere due to the processes of evaporation and transpiration (NOAA, 2016). The rate of ET_a is controlled by several environmental factors and, more so, by the availability of moisture to evaporate (NOAA, 2016). When holding all else equal, ET_a increases with increasing wind speed, temperature and sunshine (NOAA, 2016). While ET_a decreases with the increasing humidity, it is, however, always limited to the existence of moisture availability (NOAA, 2016).

ET_a plays a critical role in the understanding of land surface and atmospheric interactions as well as hydrological processes (Wang *et al*., 2007; Timmermans *et al*., 2010; Maeda *et al*., 2011; Bachour, 2013). Continuous and accurate estimation and forecasts of spatial and temporal ET_a variations are of paramount importance for enhancing climate change simulation and mitigation, water resources management, as well as drought detection (Jiang *et al*., 2009; Siska and Takac, 2009; Dorigo *et al*., 2010; Mutiga *et al*., 2010; Timmermans *et al*., 2010; Maeda *et al*., 2011; Huang *et al*., 2015; Rahimi *et al*., 2015; Minacapilli *et al*., 2016). As a result, ET_a estimations and forecasts provide an avenue for planning and scheduling purposes of reservoir operators, municipal water managers, as well as academic and operational hydrologists (NOAA, 2016).

Different types of *ET* exist in literature, such as *PET*, ET_o or ET_a. Abouali *et al*. (2013), Srivastava *et al*. (2013), Mutiga *et al*. (2010), Kovalskyy and Henebry, 2012, Cruz-Blanco *et al*. (2014), Salama *et al*. (2015) and Pandey *et al*. (2016) provide details on the aforementioned types of *ET*.

Various methods can be used for the estimation of ET_a, namely, field measurements, meteorological ground-based point data or remotely-sensed, spatially-explicit observations (Eden, 2012; Shoko, 2013). Conventional micro-meteorological-based techniques for estimating ET_a are established by using on-ground measurements, examples of which are the weighing lysimeter, the Bowen Ratio, surface renewal pan evaporation, sap flow, eddy covariance and the scintillometer (Bastiaanssen *et al*., 2012; Tian *et al*., 2015; Sur *et al*., 2015; Minacapilli *et al*., 2016). However, these field-based measurements are unable to represent the hydrological processes with sufficient reliability over large areas, while the cost of equipment and extensive labour restricts the use of these methods on a large scale (Wang *et al*., 2007; Bachour, 2013; Bastiaanssen *et al*., 2012; Tian *et al*., 2015; Hu *et al*., 2015).

In recent decades, the use of RS has enabled ET_a estimation to be conducted spatially over large areas (Bachour, 2013). The retrieval of the extensive distribution of land surface parameters such as albedo, vegetation and temperature indices through the estimation of ET_a by RS has been developed (Minacapilli *et al*., 2016). These provide a significant input into remotely sensed models that can be utilised for water resources, drought, flood and environmental planning and management (Minacapilli *et al*., 2016). The next section expands on the technique of obtaining ET_a estimates by using the SEO approach.

2.5.1 A brief review of current techniques to estimate evaporation based on satellite earth observation data

During the 1970's, the use of SEO was first proposed to estimate ET_a (Gokool, 2014). With the advent and advancement of SEO over the years, the spatial monitoring of ET_a over increasing spatial scales has improved (Shoko *et al*., 2013). Land surface parameters such as the Leaf Area Index (LAI), Albedo, NDVI, emissivity and temperature are retrieved through SEO and have been applied to drive ET_a based models. Over the years, the type of ET_a models that assimilate SEO to estimate ET_a have evolved moderately and are becoming more complex in nature (Jarmain *et al*., 2009).

According to Tian *et al*. (2015), four main categories of RS-based models have been established in recent decades to estimate ET_a. These include; (i) energy balance models, (ii) empirical statistical models, (iii) physical models, and (iv) water balance models. These models have been applied in many studies and in numerous areas; however, uncertainties are correlated

to the disadvantage of these models and their associated inputs, their scaling schemes and parameterization that still tend to exist (Tian *et al*., 2015). The increasing availability of measurements, the estimation of atmospheric and land surface parameters, as well as the enhancement of the model's performance through the integration of various techniques and data sources have led to RS techniques receiving world-wide interest (Tian *et al*., 2015).

Within the surface energy balance, ET_a is a crucial component, which is based on the partitioning of available energy into sensible and latent heat fluxes (Hu *et al*., 2015). Of particular interest is latent heat, as it is representative of the link between energy and the water budget equation (Sepulcre-Canto *et al*., 2014). It is directly related to the soil-vegetation system's moisture status and its integration over time, which generates the daily rate of ET_a (Sepulcre-Canto *et al*., 2014). Accurate estimates of terrestrial ET_a are vital for the study of regional and global climate change as well as net primary productivity, floods, droughts, irrigation and biogeochemical processes and cycles (Hu *et al*., 2015). Remotely sensed data have recently been utilised to characterize land surface biophysical processes and properties and to serve as the major forcing to several different ET_a models (Hu *et al*., 2015).

In the recent years, several global and continental ET_a products have been produced on satellite retrievals (Hu *et al*., 2015). These monitoring systems exploit either polar or geostationary satellite data. The different data sets vary in terms of the governing equations used, the forcing data employed and their spatial and temporal scales. Table 2.5 displays the available remotely sensed global ET_a products.

ET_a alone cannot indicate water stress; the variable is also influenced by water availability and factors like solar radiation and windspeed (Sepulcre-Canto *et al*., 2014). For this reason, ET_a is commonly normalized by the *PET* or ET_o to characterize water stress (Sepulcre-Canto *et al*., 2014). The term "Evapotranspiration deficit" which is defined as the difference between ET_o and ET_a, is said be a good parameter for evaluating the drought conditions of a landscape on an agricultural level (Siska and Takac, 2009). For the purpose of this study, the ETDI will be applied, which is based on the estimation of ET_a and ET_o. The variable ET_o plays a significant role in hydro-meteorological applications, effects catchment water balance, and hence water yield and groundwater recharge (Srivastava *et al*., 2013). Obtaining accurate estimates of ET_o from cropped surfaces is required for efficient irrigation scheduling and management (Srivastava *et al*., 2013).

2.5.2 Reference evapotranspiration (ET_o)

Rainfall and ET_o are the most significant and fundamental water-cycle related variables in hydrological modelling. ET_o is usually termed as the *ET* from a well-watered reference surface (Tian and Martinez, 2012). Crop water requirements can be estimated from ET_o values (de Bruin *et al*., 2010). Over the past decades, several methods have been developed and recommended for the estimation of ET_o under different climatic conditions. Measurements of weather variables, such as solar radiation, air temperature, dew point and wind speed, are usually required for the estimation of ET_o. Accurate estimates of ET_o have become available through the Penman-Monteith equation with the aid of ground-based observations. Several other techniques exist for estimating ET_o. The A-pan or British Standard tank (S-tank) is an example of a micro-meteorological based method that can be used. Literature by Chen *et al.* (2005), provides further details on this method. Some of the most widely-used, meteorologically-based conventional techniques for estimating ET_o are shown in Table 2.4.

Table 2.4 Estimating reference evapotranspiration (ET_o), using meteorological-based conventional techniques

Technique	Meterological Variables required	Additonal parameters required
Penman-Monteith (1948)	Atmospheric pressure, relative humidity, wind speed radiation, daily temperature,	Vegetation characteristics
Thornthwaite (1948)	Mean daily temperature	Latitude, daytime length
Makkink (1957)	Mean daily temperature, radiation	___
Turc (1961)	Mean daily temperature, relative humidity, radiation	___
Blaney- Criddle (1962)	Sunshine hours, wind speed, relative humidity, daily temperature	___
Priestley-Taylor (1972)	Mean daily temperature, radiation	Calibration constant
Kimberly-Penman (1982)	Atmospheric pressure, radiation, wind speed, daily temperature	___
Hargreaves-Samani (1985)	Daily temperature, radiation	Day of year (DOY), latitude

The FAO Penman-Monteith (FAO-PM) technique given by Allen *et al*. (1998), has beeen recognised as the most reliable method for precise ET_o estimation (Tian and Martinez, 2012; Bachour, 2013; Cruz-Blanco *et al*., 2014; Pandey *et al*., 2016). This technique is applicable globally under a wide range of climatic conditions and regimes. As a result, it has been regarded as the standard method for the verification of other meterological based methods and the

validation of RS methods (Maede *et al*., 2011). Despite this, the relatively large number of atmospheric variables required by the Penman Monteith method limits the widespread use of this equation.

The techniques mentioned in Table 2.4 are based on meterological data, which are usually obtained from meterological stations that are often unevenly distributed spatially (Srivastava *et al*., 2015). In addition, these variables are generally unavailable over ungauged catchments in many regions (Tian and Martinez, 2012; Srivastava *et al*., 2013). Coverage of small areas is only conducted with ground-based observations (Srivastava *et al*., 2013). Furthermore, the above-mentioned approaches tend to be very expensive and labour-intensive (Srivastava *et al*., 2013). However, the use of RS as an approach allows for efficient, robust and instantenous ET_o estimation for the better management of our water resources (Winkler *et al*., 2017). This strategy has become promising, offering greater spatial and temporal coverage with variablity, as highilighted in Section 2.5.1. In addition, to overcome data inadequacy issue, various methods like the Hargreaves-Samani, Makkink, Turc and Priestly-Taylor are explored for the estimation of ET_o with limited weather data. Table 2.7 displays some of the aformentioned techniques that have incorporated remotely-sensed data.

A review was undertaken of the case studies pertaining to the various methods that can be utilised to obtain ET_a (see Table 2.6) and ET_o (see Table 2.7), by using SEO to enable the calculation of the ETDI. Table 2.5 displays the global ET_a products that have been derived for use at different spatio-temporal scales.

Table 2.5 Remote sensing-based global ET_a products

ET-Product	Algorithm	Input Dataset	Grid Size	Temporal Resolution	Time Span	Reference	Data Source
MOD 16-ET	Penman-Monteith	Actual vapour pressure, solar radiation, daily temperature, NDVI, LST and LAI	1 km	Daily	2000-2013	Mu *et al*. (2007)	GMAO, MODIS
Zhang-ET	PM of Vegetation + PM Soil evaporation	Net radiation, daily temperature, NDVI	8 km	Monthly	1983-2006	Zhang *et al*. (2010)	NCEP/NCAR, GEWEX SRB, GIMMS
GLEAM ET	Priestley & Taylor	Air temperature, Precipitation, Net Radiation, Vegetation optical depth, Snow water equivalents, Skin Temperature Soil Moisture,	0.25 deg.	Daily	1984-2007	Miralles *et al*. (2011)	GEWEX SRB, CMORPH NSIDC, ISCCP, TMMI+AMSR-E
CHEN-ET	Surface Energy Balance	canopy height, soil Moisture (*ET* partition), Air temperature, pressure, wind speed, humidity, Downward/upward shortwave/longwave radiation, albedo, LST, NDVI, FPAR, LAI	5 km	Monthly	2000-2014	Chen *et al*. (2014)	ERA-I, MODIS, GlobAlbedo, ESA CCI
EARS	Surface Energy Balance	Temperature, Albedo	5 km	Daily, Monthly, Yearly	2000-2011	Rosema, 2006; Rosema *et al*. (2008)	FengYun-2c Meteosat
LSA-SAF: DMET	Surface Energy Balance	Air temperature, specific humidity, air pressure, wind speed, surface, soil temperature, soil moisture, land cover, solar radiation, long-wave radiation, albedo	3- 5 km (dependent on latitude and distance to nadir view)	Daily	2009-Present	LSA-SAF 2010:Algorithm Theoretical Basis Document (ATBD) available at: http://landsaf.meteo.pt/	ECMWF, ECOCLIMAP, MSG-SEVIRI

Table 2.6 Summary of studies utilizing different remote sensing techniques/methods for the estimation of ET_a

Reference	Temporal/Spatial scale/sensor	Method	Data Requirements	Key Findings
Jiang *et al*., 2009	1998 and 1999,regional, Advanced Very High Resolution Radiometer (AVHRR) aboard NOAA-14 satellite.	*ET* estimation algorithm developed by merging satellite and *in-situ* data.	Remotely sensed surface temperature, vegetation index (NDVI) and net radiation data obtained from *in-situ* data.	• The proposed algorithm seems to be powerful and has the ability to provide near real-time land surface evapotranspiration at a very fine spatial and temporal resolution over wide heterogeneous areas.
Elhaddad *et al*., 2011	2006,Catchment, Landsat (Land Remote-sensing Satellite)	Remote Sensing of *ET* (ReSET) Model	Landsat imagery	• The ReSET model is encouraged to be utilised as a tool for water management. • Slight differences were obtained between ReSET *ET* estimates and conventional *ET* methods.
Bastiaanssen *et al*., 2012	2007,regional, Advanced Microwave Scanning Radiometer (AMSR-E) aboard Aqua satellite	ETLook remote sensing model	Surface soil moisture, spectral vegetation index, surface albedo, atmospheric optical depth, land use and land cover (LULC), soil physical properties, and meteorological data(e.g., air temperature, relative humidity and wind speed) at 1 km resolution .	• Satellite data must be available at all times, for an operational *ET* monitoring system. • The total *ET* value derived from the water balance for irrigated areas as one total system for the study areas were in agreement with the *ET* value from the ETLook surface energy balance computations. • ETLook is established as a novel model that can be operationalized further.

Table 2.6 (continued) Summary of studies utilizing different remote sensing techniques/methods for the estimation of ET_a

Reference	Temporal/Spatial scale/sensor	Method	Data Requirements	Key Findings
Kovalskyy and Henebry, 2012	2002-2008,Field,MODIS and AVHRR	VegET model	Daily time series of 2 m air temperature [K]; 2 m specific humidity [kg kg^{-1}]; surface pressure [Pa]; U wind component [m s^{-1}];V wind component [m s^{-1}; downward shortwave radiation [Wm^{-2}]; downward longwave radiation [Wm^{-2}]; total precipitation[kg/m^2]; soil permanent wilting point and water holding capacity at each study site; descriptions of crops and grasses; MODIS and AVHRR NDVI's.	• Taking into account phenology enhances the accuracy of ET_a estimation by the VegET model. • Utilising climatologies result in VegET overestimating daily ET_a during the actual growing season and durations of seasons.
Park *et al*., 2012	1 day (2009), Regional, Aqua·Terra/MODIS, SPOT/VGT satellite	NIMR (National Institute of Meteorological Research at Korea Meteorological Administration) daily ET_a algorithm	Satellite data and ground based meteorological data (wind speed (10 m), air temperature (2 m), relative humidity, precipitation).	• NIMR daily evapotranspiration displays fairly well in agreement with validation data as R^2 is 0.671, RMSE is 0.067 $mm \cdot d^{-1}$ and Bias is 0.09 $mm \cdot d\text{-}^{1}$.
Kiptala *et al*., 2013	2008–2010, Catchment, MODIS	SEBAL (Surface Energy Balance Algorithm for Land) Model	MODIS datasets; Daily rainfall data; Land Use and Land Cover Types; ground meteorological Data.	• SEBAL overestimates ET_a during dry periods. SEBAL ET_a estimates were compared with global ET_a from MODIS 16 algorithm (R50.74; R250.32; RMSE of 34% and MAE of 28%) and a 95% confidence level.

Table 2.6 (continued) Summary of studies utilizing different remote sensing techniques/methods for the estimation of ET_a

Reference	Temporal/Spatial scale/sensor	Method	Data Requirements	Key Findings
Rahimi *et al*., 2015	February to July 2011, catchment, MODIS images located on Terra satellite	SEBAL (comparing with calculated values by the FAO-PM)	Temperature, wind velocity, relative humidity with a 6-hour period and MODIS imagery.	• No significant difference between SEBAL algorithm and FAO-PM method in both hourly and daily states of ET_a estimation. • The SEBAL algorithm produces ET_a values of acceptable accuracy. • Considering the spatial resolution and freely available MODIS imagery, utilisation of such imagery is acceptable and practical for the estimation of daily water requirements, irrigation scheduling and management.
Minacapilli *et al*., 2016	Observation period: 2010–2012,regional, MODIS and MSG-SEVIRI sensors	Time-Domain Triangle Method (TDTM)	Remotely sensed vegetation indices, day–night time land surface temperature differences	• Estimation of daily ET_a with reasonable accuracy for practical purposes. • TDTM regarded as a straightforward and effective tool to predict ET_a at regional scale, temporal and spatial scale changes

Table 2.7 A limited list of different methods which can be used to calculate ET_o based on satellite earth observation data

Reference	Method	Description	Requirements	Advantages	Disadvantages
Rivas and Caselles, 2004	Simpler form of the Penman–Monteith equation	A simplified Penman–Monteith equation is used to produce spatial reference evaporation estimates from remotely sensed surface temperature and local meteorological data.	NOAA-AVHRR imagery and ground weather data.	Study demonstrates the potential of calculating ET_o by integrating the surface temperature from satellite imagery with conventional weather information.	Meteorological data is necessary to estimate reference ET_o.
Hart *et al*., 2009	ASCE-ET Formulation	Meteorological data is merged with hourly NOAA Geostationary Operational Environmental Satellite (GOES) visible satellite data to produce spatial daily ET_o.	Hourly GOES satellite imagery and ground-based meteorological data.	Demonstrates an approach of creating daily ET_o maps by fusing satellite and ground station data.	-Data intensive. Requires ground-based meteorological data. -Difficult to get accurate ET_o estimation where ground-based meteorological data is missing.
Maeda *et al*., 2011	Use of Empirical models (Hargreaves, Thornwaite and Blaney-Criddle)	ET_o is estimated using remote sensing and empirical models in a region with limited ground data.	Land surface temperature (LST) data (MODIS).	Only air temperature data is required. The Hargreaves model produced results that were consistent with data collected in ground station and works well in semi-arid environments.	Ground based LST data are required to calibrate the Hargreaves model. The Blaney Criddle and Thornwaite models are sensitive to temperature differences.

Table 2.7 (continued) A limited list of different methods which can be used to calculate ET_o based on satellite earth observation data

Reference	Method	Description	Requirements	Advantages	Disadvantages
Cruz-Blanco *et al*., 2014	MA + LSE approach	Established on the Makkink-Advection (MAK-Adv) equation together with remotely sensed solar radiation and a numerical weather forecast of near surface air temperature.	Rs and Ta (EUMETSAT LSASAF, a RS tool, and ECMWF products).	Does not require local meteorological data. Produces good ET_o estimates under semi-arid environments.	Comparison of ET_o values from MA + LSE approach with the PM-FAO56 method values display a small underestimation in the ET_o assessment using the MA + LSE approach.
Rahimikhoob and Hosseinzadeh, 2014	Blaney-Criddle (BC) model	Daytime surface temperature is obtained from the AVHRR/NOAA sensor instead of air temperature in the BC equation for the estimation of ET_o.	NOAA/AVHRR imagery and ground weather data.	Allows for the estimation of daily ET_o in the areas where meteorological data is unavailable.	-Limitation of NOAA/AVHRR imagery due to cloudy conditions. -FAO-56 PM model used to calibrate BC model.
Castro and Parra, 2015	Multiple regression model	ET_o is estimated, at a regional scale, using data provided by the MODIS sensor on board the TERRA satellite platform. The input data assumed by the model include the Normalized Difference Infrared Index (NDII) and the earth's surface temperature.	Meteorological data and data provided by the TERRA/MODIS sensor.	Monthly ET_o can be estimated based on the NDII vegetation index and surface temperature.	Meteorological data is required to train and validate the model by utilising the FAO-PM model.

Many methods have been developed to assess ET_a and ET_o from meteorological data. However, existing weather station networks around the world is not sufficient to capture the spatial heterogeneity of these variables (Winkler *et al*., 2017). This poses as a greater challenge for developing countries. To improve water management, the contribution of SEO at various spatial scales has increased significantly over the years. Table 2.6 and Table 2.7 indicate recent studies, which display the combination of ET_o models with satellite data as a feasible alternative for obtaining spatial and temporal data on the biophysical variables (Wagner *et al*., 2008). As a result, one of the components of this study seeks to apply a method that utilises SEO to attain reliable estimations of ET_o. The Hargreaves method is a potential solution to the above problem, as the method requires only temperature data and radiation data to estimate ET_o.

The above-mentioned case studies in Table 2.7 expand on a few of the many approaches that one can adopt to obtain ET_o values that are based on SEO. These, and several other case studies, indicate the methods used to attain satellite ET_o values. Literature by Gavilan *et al*. (2006), Patel *et al*. (2006), Su *et al*. (2010), De Bruin *et al*. (2010), Aguilar and Polo (2011), Hart *et al*. (2012), Cammalleri and Ciraolo (2013), Miralles *et al*. (2015), Zheng and Zhu *et al*. (2015), Sur *et al*. (2015) and Pandey *et al*. (2016) provide details on such methods.

The Hargreaves model was specifically chosen from the above-mentioned case studies, to be applied in this study (Table 2.7). The reasons for this choice are that it is simple to use, it is less demanding, as it only requires LST data, and it is a frequently-applied method. In addition, when compared to the Blaney-Criddle and Thornthwaite models, the Hargreaves model estimates closely follow the reference (FAO-PM) results, it achieves the best results in linear regression and the analysis of errors, which prove to be consistent with those results obtained in previous studies (Maeda *et al*., 2011). The Hargreaves model has been found to be most feasible method for application under semi-arid conditions. A few of the studies that have utilised the Hargreaves approach are Gavilan *et al*. (2006), Aguilar and Polo (2011), Maeda *et al*. (2011), and Zheng and Zhu (2015), amongst several others.

It is also noteworthy to mention that the EUMETSAT LSA-SAF has produced an ET_o product known as METREF. The LSA-SAF METREF provides daily ET_o estimates from the daily global radiation derived from SEVIRI/MSG, as this is recognised as the main driver of ET_o over a reference surface. However, the LSA-SAF METREF product does not utilise atmospheric humidity and only presents a slight dependency on near surface temperature. The

product is also not affected by local effects such as local advection or surface aridity. The LSA-SAF documents provide further details on the product, describes the algorithm and can be accessed from the website http://landsaf.ipma.pt. De Bruin *et al*. (2015) also provide further details on the product. The product is disseminated in HDF (Hierarchical Data Format) and has been available since 07th August 2016. Due to the short data period, the product could not be used in this study; hence, the Hargreaves-LST approach was adopted to produce satellite based ET_o estimates.

In addition, several initiatives have been conducted to integrate different types of SEO and *in-situ* observations to produce integrated data for key variables of the water cycle such as rainfall and temperature. This integrated initiative is certainly paving the way for a new era in water management. Through such integration, data and products are being produced that are more robust and useful in data-sparse areas.

Knowledge obtained from the above literature reviews and case studies indicate that satellite earth observation techniques can prove to be very useful for obtaining estimates of parameters within the hydrological cycle, which can be used within drought indices to enable the monitoring of droughts. Hence, the following section discusses the monitoring of droughts by utilising the satellite earth observational approach.

2.6 Drought Monitoring using Satellite Earth Observation/Remote Sensing

Globally, the gathering of reliable information on land surface conditions using, RS or satellite earth observational techniques has been studied by many researchers. Su *et al*. (2001), Petja *et al*. (2008), Gibson *et al*. (2009), Anderson *et al*. (2012), Gokmen *et al*. (2012), Gibson *et al*. (2013), Mu *et al*. (2013), Shoko *et al*. (2013) and Byun *et al*. (2014), amongst several other studies give more detailed information on such studies.

The term “RS” or “satellite earth observation" is associated with aerial photography and satellite imagery, which are utilised to obtain information about the features present on the earth’s surface (Gibson *et al.,* 2009). It is a technique that allows for spatial and temporal coverage and it enables information to be retrieved from places that are inaccessible to man (Eden, 2012). Information from accessible areas can also be obtained. Further insights into RS are provided by Vinukollu *et al.* (2011) and Romaguera *et al*. (2014).

RS sensors are devices that allow data, relating to an object, to be captured remotely. Landsat, MODIS, IKONOS, SPOT, NOAA-AVHRR and MSG-SEVIRI are amongst the most commonly-used sensors in hydrology. These sensors produce imagery that provides an understanding of the relationship between various parameters of the hydrological cycle. RS techniques make it possible to measure various components of the hydrological cycle on the land surface, as well as the state of natural vegetation and agriculture, often at very high spatial resolution (<1 km) depending on the purpose of the data and in near–real time, which is fundamental for early drought warning (Sheffield *et al*., 2014; Sepulcre-Canto *et al*., 2014).

Concerning droughts, the approximation of the LST by thermal-infrared imagery that is captured by RS sensors such as, Landsat enables the mapping of ET_a at the spatial scale at which water is being used. The monitoring and assessment of droughts can be performed, using this procedure. Drought events tend to occur with uneven spatial and temporal features (Petja *et al*., 2008). The wealth of available information and tools that are based on RS offer great opportunities for identifying the geospatial differences attributed to drought events and drought hot spots (Masih *et al*., 2014). The input of surface variables carried out by using RS techniques, into surface energy balance models enables the detailed mapping and monitoring of drought conditions/water stresses to be conducted (Sepulcre-Canto *et al*., 2014). A substantial and increasingly large body of literature currently exists on the potential for drought monitoring, (for example, in Anderson *et al*. (2011), Houborg *et al*. (2012), Sheffield *et al*. (2012) and Mu *et al*. (2013)).

Specifically in the case of water management, RS techniques are currently in a growing market because of the complex environmental issues, climate change concerns as well as continuous increases in the demand for water, under the umbrella of global change (Bastiaanssen and Harshadeep, 2003). The scope of providing a holistic and consistent view of droughts has recently been broadened, by merging RS data with land surface hydrological modelling, either directly via assimilation (for example satellite retrievals of soil moisture), or indirectly via input drivers (for example precipitation) (Sheffield *et al*., 2014). Van Dijk and Renzullo, (2011), Anderson *et al*. (2012) and Winkler *et al*. (2017) are amongst several studies that have displayed this potential. Recently, an increasing number of satellite-based ET_a products, at various temporal and spatial scales, has recently been generated (Hu *et al*., 2015).

The benefits of employing satellite-based techniques can be extremely useful for water resources management; however, it is crucial to take note that this technique also possesses limitations and disadvantages. Some of these limitations are attributed to all satellite-based techniques while, certain limitations are specific to the technique applied (Mertz, 2010). The next section will discuss details of these advantages and disadvantages/limitations.

The listed advantages and disadvantages discussed below are not the only ones that exist with the utilisation of satellite techniques, but merely provide a brief overview of just a few.

2.6.1 Advantages of remote sensing for drought monitoring

Some of the several advantages relating to the use of RS for drought monitoring include the following:

(i) In recent years, advancements in remote-sensing ET_a models have paved the way for more accurate estimates of ET_a to be obtained. This forms an essential component for understanding the consumptive use and availability of water resources (Schneider *et al*., 2008).

(ii) Specifically in the fields of hydrology and agriculture, the availability of land surface information at a wide range of temporal and spatial scales through space-borne RS measurements is attainable, compared to *in-situ* measurements (Bastiaanssen *et al*., 2000). It is useful for producing more accurate estimates of ET_a and providing a more comprehensive view of drought development.

(iii) The necessary water resource-related information can be made available to the public, consultancies, policy-makers and researchers to assist them in formulating legislation, for planning purposes as well as for impact assessments (Bastiaanssen *et al.*, 2000).

(iv) Spatial estimates of various water-cycle related variables provide water managers with the opportunity to use them for estimating water usage by alien invasive species, monitoring water rights, determining the allocation of water amongst the many sectors, monitoring drought and food insecurity and evaluating climatic models (Anderson *et al*., 2012).

(v) The assessment of water use, crops biomass and yield production can be performed as a result of the recent developments in the use of RS information (Jarmaine *et al.*, 2014).

Hence, the amount of ET_o and ET_a loss from crops and surfaces including water bodies can be accounted for and the assessments of the severity of droughts can be conducted.

(vi) The high temporal resolution of geostationary satellites allows for the continuous monitoring of different applications and the availability of long-term data series to allow for studies to be directed towards possible change detection (Hu *et al*., 2015**)**.

(vii) Some sensors are well-suited for carrying out certain tasks, as opposed to others. For example, Landsat is useful for monitoring of the earth's surface, for environmental monitoring and for vegetation and land cover classification. SPOT is used mainly for farming, fisheries, mapping and forestry, geology, land management and planning, security and defence as well as for risk mitigation, while NOAA satellites or ASTER are useful for providing information on the topography of an area.

(viii) RS data obtained from polar-orbiting satellites are able to produce spatial and temporal information continuously over vegetated surfaces which is beneficial for monitoring surface variables that affect *ET* (Mu *et al.*, 2013). This assists in producing more accurate ET_a estimates to develop drought indices for the monitoring of droughts.

(ix) The archives of RS imagery provide excellent sources of historical data for research, and other purposes (Gibson *et al.*, 2009). This enables the comparison and analysis of drought events and it helps water resource managers to plan for the future.

2.6.2 Disadvantages/limitations of remote sensing for drought monitoring

The disadvantages and limitations associated with the use of RS include the following:

(i) The high costs of training and providing the necessary skills for technicians depending on the models, products and images used (Bastiaanssen *et al*., 2000).

(ii) There are differences between the spatial and temporal scales of satellites.

(iii) The under-utilisation of RS data by water resource managers (Bastiaanssen *et al.*, 2000). This is because remotely-sensed products are often expensive and difficult to obtain, which prohibits or limits their use (Boyle *et al.*, 2014).

(iv) Difficulties prevail in relating observed radiances to landscape features in the absence of ground truth data (Kustas and Norman, 1996).

(v) Satellite revisit and repeat cycles play a key role in the availability of images and thereby determine the amount of ET_a estimates that can be produced (Schneider *et al*., 2008).

(vi) Cloud coverage has a great influence on the reflected radiation for both optical and thermal wavelengths; hence, the number of images that can be processed is dependent on the availability of cloud-free imagery. This limits the number of ET_a estimates that can be produced for the calculation of drought indices and hence, for the monitoring of droughts.

(vii) The indirect nature of the retrieval of physical variables and changes in satellite sensors that can lead to temporal inhomogeneity's (Sheffield *et al*. 2014). More specifically, the non-closure of the water budget, errors in individual products and inconsistencies between products imply that the use of RS to be accrued out with caution (Sheffield *et al*. 2014).

Given the potential advantages and associated benefits of utilising satellite imagery as a data input, the use and development of models and ET_a algorithms incorporating this data present themselves as an attractive collaborator or alternative to conventional ET_a measuring methods for use in areas with limited ground station networks (data-sparse areas). Consequently, this research study explores the EUMETSAT LSA-SAF ET_a product as a satellite-derived ET_a product for incorporation into the ETDI index in this study. The list of globally available ET_a products are displayed (in Table 2.5). However, the EUMETSAT LSA-SAF ET_a product was chosen as it is a global product that is obtained by using a surface energy balance, which enables the spatial coverage of droughts to be captured. The product is freely available, has a high temporal resolution (daily) and, most importantly, the dataset is available for current years, in comparison to the other global datasets. Therefore, the EUMETSAT LSA-SAF ET_a was chosen for use in this study. A detailed description of this product is provided in the next section.

2.7 EUMETSAT Satellite Application Facility on Land Surface Analysis (LSA-SAF) ET_a Product

The LSA-SAF ET_a product based on the SEVIRI sensor onboard the Meteosat Second Generation geo-stationary satellites (MSG-SEVIRI) is one of the few available operational products (Ghilain *et al*., 2011; Sepulcre-Canto *et al*., 2014; Hu *et al*., 2015). According to Hu *et al*. (2015), LSA-SAF MSG ET_a and the MOD 16 (Mu *et al*., 2007) are two of the operational moderate spatial resolution ET_a products that are based on satellite data at a global and continental scale. The LSA-SAF MSG ET_a product is distributed by the EUMETSAT (European Organization for the Exploitation of Meteorological Satellites) Satellite Application

Facility on Land Surface Analysis (LSA-SAF) and the University of Montana, respectively (Hu *et al*., 2015). The major benefit of using this product is its spatial coverage, as it is generated over four geographical areas (Europe, North Africa, South Africa and the eastern part of South America) within the MSG disk and it is produced operationally in near-real time (every 30 mins in the case of ET_a) (Figure 2.2) (Ghilain *et al*., 2011; Sepulcre-Canto *et al*., 2014; Hu *et al*., 2015). The model does not take into account the Land Surface Temperature (LST) for an all-weather evaluation of ET_a as a mandatory input of the model, since this would restrict the model's evaluation to cloud-free sky conditions (Ghilain *et al*., 2011). Hence, ET_a maps are produced for all weather conditions, allowing the model to provide continuous ET_a series that are useful in various applications (Ghilain *et al*., 2011; Hu *et al*., 2015).

The LSA-SAF includes the following two ET_a products:

(a) **MET:** These are instantaneous ET_a estimates, with a time interval of 30-minute (MET). A quality flag image is produced together with the ET_a map, providing information on a pixel-by-pixel basis. The quality of input variables and if pre/post-processing (gap filling) was performed on input or output data are contained within the quality flag image.

(b) **DMET:** This is the daily ET_a product that is produced by integrating the instantaneous values of each day (DMET) (Hu *et al*., 2015). Accompanying the DMET product are two images which are indicative of the number of values (slots) missing for each pixel and the percentage that it represents respectively.

Table 2.8 includes the characteristics of the SEVIRI based ET_a products. The method follows a physical approach and the model is forced with radiative data derived from MSG satellites, together with information on land-cover characteristics as displayed in Figure 2.3 and ancillary meteorological data from the NWP (Numerical Weather Prediction Model) (Ghilain *et al*., 2011; Sepulcre-Canto *et al*., 2014).

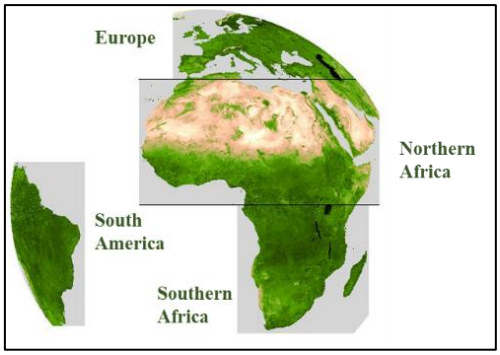

Figure 2.2 The four geographical areas covered by the LSA-SAF ET_a products: Europe, Northern Africa, Southern Africa, and South America (http://landsaf.meteo.pt/)

Table 2.8 ET_a product requirements, in terms of area coverage, resolution and accuracy (LSA-SAF, 2015)

ET Product	Product		Resolution		Threshold	Accuracy Target	Optimal
	Identifier	Coverage	Temporal	Spatial			
MET: ET	LSA_16	MSG Disk	30 min	MSG pixel resolution	30 %	MET> 0.4mm /h: 25%;	10%
DMET:ET	LSA_17	MSG Disk	1 Day	MSG pixel resolution	30 %	MET<0.4 mm/h: 0.1 mm/h : 0.2 20%	10%

2.7.1 Data requirements of model

The ET_a is obtained by modelling the energy exchange between the atmosphere and the earth's surface (soil and vegetation). The model is driven by input data ('forcings') produced by the LSA-SAF MSG.

The main input data necessary to retrieve MET and DMET include the following:

A. **Radiative data:** The required LSA-SAF MSG data inputs to the ET_a algorithm are fractional vegetation cover, LAI, albedo, snow cover, down-welling shortwave and

longwave fluxes and land cover (Hu *et al*., 2015). These atmospheric model inputs are obtained from corresponding LSA-SAF products produced from the MSG-SEVIRI.

B. **Meteorological data:** The meteorological data is provided by the ECMWF numerical weather prediction analyses and forecasts (Gellens-Meulenberghs *et al*., 2007; Ghilain *et al*., 2011). The input non-satellite data are ECMWF four-dimensional variational (4DVAR) reanalysis data (Hu *et al*., 2015). This data is originally obtained at ECMWF spatial resolution, which is thereafter transposed into the MSG grid and spatially interpolated. Currently, the meteorological variables used by the MET algorithm include the following: 2m temperature (K), soil temperature for 4 soil layers (K), 2m dew point temperature (K), atmospheric pressure at sea level (Pa), 10m wind speed (m/s) and soil moisture for 4 soil layers (m^3/m^3).

C. **Land cover:** ECOCLIMAP land cover classification (Masson *et al*., 2003) is used in the current versions for identifying and characterizing the land cover at 1 km resolution and the vegetation parameters required in SVAT (Soil Vegetation Atmosphere Transfer) models.

Figure 2.3 Schematic representation of a MSG pixel composition (bare soil, forest, crops and grassland (LSA-SAF, 2015)

For detailed information about the capabilities and validation of the LSA-SAF MET and DMET product Version 4.0, one should consult the Product User Manual (PUM) and Validation Report (VR) (Gellens-Meulenberghs *et al*., 2007, 2008, 2009; Arboleda *et al*., 2011; Ghilain *et al*., 2011, 2013). The VR gathers all the results of performed validation tests as well as details of the possible causes of uncertainty and it leads the way towards further improvements. In the PUM, it is stated that the product in its current state is useful for many applications, such as environmental monitoring, for assimilation in models, for long-term studies on ET_a (that are) linked to climate and for regional ET_a estimates, where no measurements exist.

2.7.2 Calculation of the ET_a and model description at tile level

To produce ET_a products, the model is based on the specific parameterization of the TESSEL SVAT scheme (Viterbo and Beljaars, 1995; van den Hulk *et al*., 2000; Balsamo *et al*., 2009; Ghilain *et al*., 2011). The area for which ET_a has to be assessed is divided into independent pixels, in a one-to-one correspondence with the pixels of a satellite image. Within the model, each pixel is interpreted as a mix of homogenous tiles, representing particular land cover types. The land cover types include deciduous, coniferous and evergreen broadleaf trees, bare soil and rocks, rainfed and irrigated crops and natural herbaceous plants (Sepulcre-Canto *et al*., 2014). For each respective pixel, a maximum of four tiles (three vegetation tiles and bare soil) are allowed (see Figure 2.3).

Hence, the energy balance equations are solved at a tile level and the global pixel value is obtained through the weighted contribution of each pixel (Sepulcre-Canto *et al*., 2014). The surface dimension represented by the pixel varies in the function of its location (longitude and latitude) and is 3x3 km at the MSG sub-satellite point. This is one of the first methods to derive ET_a operationally over large areas (Arboleda *et al*., 2011).

The MET algorithm is an energy balance model that aims to compute, for each tile *i* in the considered pixel, the partition of net radiation (R_{ni}), the sensible heat flux (H_i), the latent heat flux (LE_i) and the heat conduction flux into the ground (G_i), according to (Equation 2.5 below):

$$Rn_i - H_i - LE_i - G_i = 0 \qquad (2.5)$$

2.7.3 Daily evapotranspiration product (DMET)

The temporal integration of instantaneous values produced by the MET algorithm yields daily evapotranspiration according to Equation 2.6:

$$DMET = \int_{h_1}^{h_2} MET_i(t)dt \qquad (2.6)$$

where:

MET_i = the instantaneous evapotranspiration estimated by the MET algorithm every 30 minutes for a day.

The integration limits (h_1, h_2) relate to the first (theoretically at 00:30 UTC) and last (theoretically at 24:00 UTC) existing slots for a day. In an ideal situation, 48 images in total are generated, which is interpreted as being that, for each MSG pixel, 48 ET_a values have to be integrated. To generate a daily consistent value for each pixel, a linear interpolation between the closest slots is applied according to Equation 2.7:

$$MET_j = MET_{j-1} + 0.5\left(MET_j + MET_{j-1}\right)N \quad (2.7)$$

where:

MET_{j-1} and MET_j = previous and next existing ET_a values for the same pixel in considered day, and

N = the number of time steps between previous and next existing ET_a values.

For a more detailed description of the LSA-SAF MSG ET_a products regarding; the model, the methodology, theoretical framework and mathematical description of the algorithms, documents by the LSA-SAF are available and include: the PUM, the Algorithm Theoretical Basis Document (ATBD), the VR and the Product Output Format (POF), which are available at: http://landsaf.meteo.pt/. Literature by Ghilian *et al*. (2011) and Hu *et al*. (2015), amongst many others also provide details on the LSA-SAF MSG ET_a products.

2.7.4 Processing scheme

As detailed within the PUM, the execution of the algorithm is performed in three steps. The first step corresponds to the pre-processing, where all the input data is verified by the algorithm, the gap-filling procedure over the missing DSLF pixels values over land is conducted, internal structures are initialised and input data is loaded into internal arrays. The second step corresponds to the equation-solving process, where the first pixel on the image is the starting point for the algorithm. If all necessary input data is available, the algorithm solves the set equations for each tile and, if convergence is reached, the ET_a for the whole pixel is computed. Depending on the performances of the algorithm and the quality of input data, a quality flag value is generated for the pixel. Finally, the third step is the output formatting. In this step, the scaling factor for the whole image is set by the algorithm, data type casting is carried out, the

data and attributes are set and the output is written in HDF5 format. Thereafter, used memory is freed by the algorithm, it returns the control to the wrapper and stands idle until the next call. Figure 2.4 below provides a generalised view of the procedures that were followed.

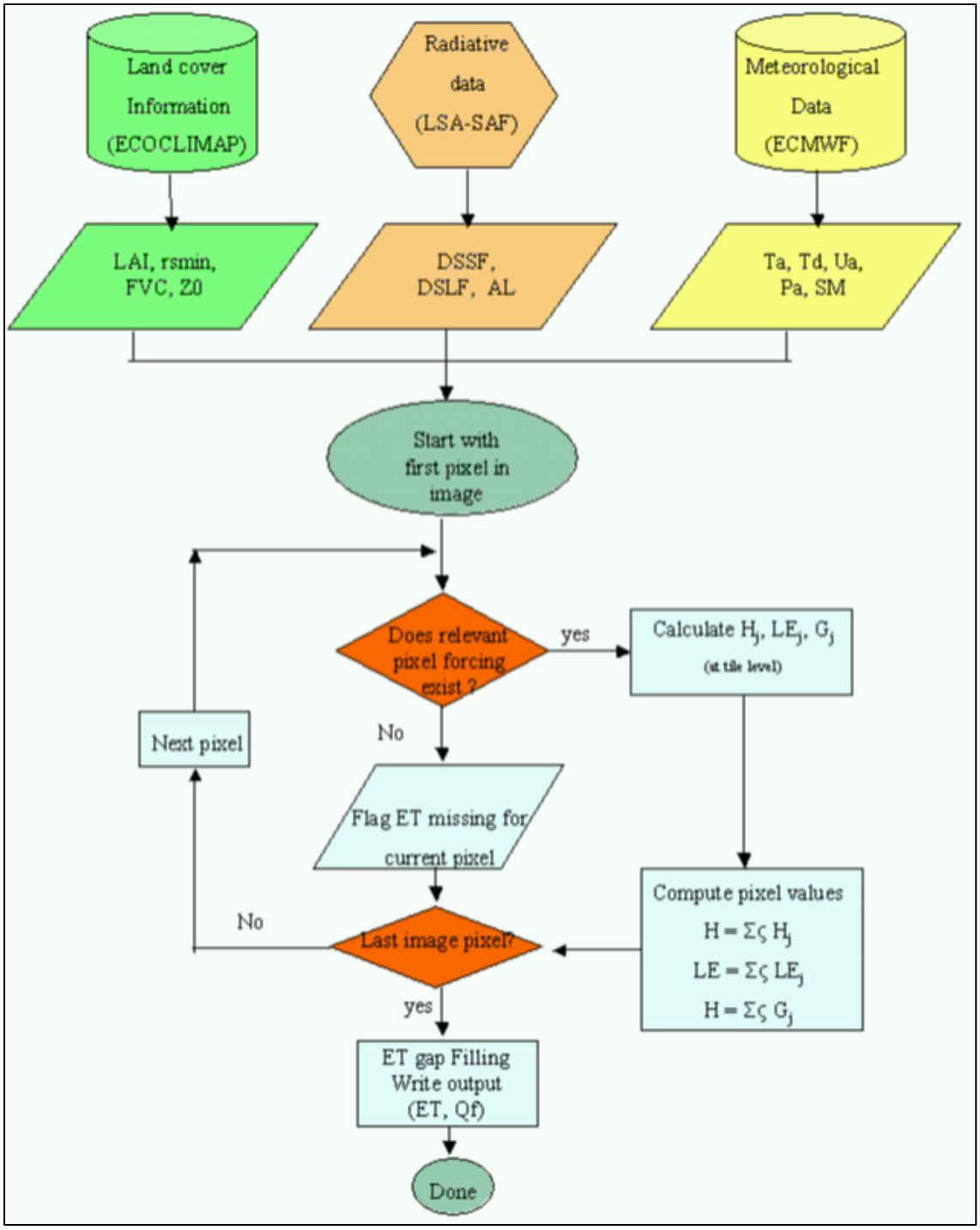

Figure 2.4 The diagram of ET_a processing chain (LSA-SAF, 2015)

2.8 Synthesis of Literature

Given projections of an increase in the occurrence and severity of extreme climate events for many regions around the world, it is imperative that nations now move towards more risk-based strategies to drought management. It is quite clear from the literature review that scientific research and expertise is needed to monitor and predict natural hazards such as droughts. Drought indices are one of the approaches that can be used to assess and monitor droughts.

Monitoring drought and drought severity using *in-situ* data has often been difficult due to the lack of long-term data records, worsened by declining gauging networks. Traditionally, local risk management approaches placed emphasis only on short-term climatic events without accounting for long-term climate changes. To fill this gap, drought indices that consider different variables and time scales in their formulation (SPI, SPEI) may be utilised, more so for investigating future climate change scenarios. Nowadays, drought monitoring using SEO has been receiving a significant amount of attention. As opposed to obtaining point measurements from *in-situ* methods, which do not represent spatial characteristics of different meteorological and climatic variables, satellite earth observation approaches are able to capture the spatial and temporal coverage of such variables. Since droughts are known to have spatial and temporal dimensions, achieving coverage of drought monitoring over large geographic scales through satellite earth observation will assist in providing a more comprehensive view of the development of a drought. This will enable better management of water resources and improved disaster risk management.

Quantification of the hydrological cycle components is fundamental to managing water resources. ET_a is one of the critical variables in semi-arid and arid countries like South Africa. In water scarce regions around the world, ET_a or crop water use is the greatest water user, hence a vital parameter in assisting water resource management. Thus, ET_a estimation is a vital element in water accounting for water resources monitoring and management. Through the investigation of how the content of ET_a varies in time and space, a crucial component of the water cycle may be understood and quantified. Conventional techniques of ET_a estimation possess capacity constraints such as time and expenses as well as they contain poor spatial resolution as they only representative at point or localized field scales. However, recent advances in modeling and estimating ET_a using satellite observations, which generate hyper-

or multi-spectral digital images, have become more sought after by many water resources managers and planners due to cost-effective and time-less means of acquiring spatial representative ET_a. These techniques were not available in the past, however due to technological advances, spatial and temporal coverage and resolution have improved. Nowadays, there is a growing number of earth observational products derived from satellite images available at a global and continental scale for the estimation of hydrological cycle-related variables such as precipitation, ET_a and soil moisture to name a few.

The focus on this research is on a satellite based, spatially derived evaporative drought index, the ETDI. The evaporative drought index accounts for ET_a thereby accounting for the actual state of the land surface dryness. Within the ETDI calculation, ET_o is also required which will be calculated from satellite data. With the incorporation of satellite data, drought monitoring over large-scales can be achieved, providing a more comprehensive view of drought development over differing spatial scales.

From the literature reviews conducted, it was further found that all droughts emanate from a deficit of rainfall; hence, the SPI, which is the most widely used drought index based on rainfall was used to assess the ETDI in detecting the occurrences of droughts. The SPEI accounts for the deficit between ET_a and precipitation, which are vital drivers to droughts. Furthermore, the SPEI accounts for temperature and in drought analysis it is found to be beneficial, more so for climate change analysis as scientists have predicted a marked increase in temperature over the years. Therefore, the SPEI, which is based on the SPI algorithm incorporating ET_a was utilised in addition to the SPI as a comparison to the ETDI. The use of satellite data and the associated products to obtain estimates for the various components within the hydrological cycle was reviewed and used to display the relationship between droughts and the various hydrological parameters.

The literature reviews undertaken in this section brought to light many research gaps, which informed this research study. Some of the many research gaps found within the literature included:

a) There is a significantly increasing number of scientific studies and information on various aspects of drought. However, these studies often do not incorporate satellite data as well as the spatial scale perspective.

b) Relatively few studies that focus on evaporative drought indices exist despite, evapotranspiration being one of the most critical water-cycle related variables in semi-arid and arid areas.

c) The ETDI determines drought severity based on an *ET* deficit, which is a good parameter for evaluating drought conditions of a landscape on an agricultural level. Despite this, the ETDI has not been applied in many regions of the world and especially not in those countries where agricultural productivity is a dominate sector.

d) Alternate methods of obtaining estimates of ET_o based on satellite earth observational data presents themselves as feasible approaches of obtaining spatial and temporal data on this biophysical variable, hence should be explored and investigated.

e) There is demand for more accurate and reliable drought monitoring studies along with forecasting systems/approaches for South Africa.

The knowledge gained from the above literature along with the findings has assisted in, informing the methodology that will be used for this study. The following chapter details the methodology to be carried out for this research study.

3. METHODOLOGY

The methodology component of this research stems from the evaluation of literature gaps identified in the previous chapter. The overall aim is to estimate a satellite-based spatially-derived drought index from the hydrological system drivers. This study investigated a methodology for estimating drought indices by combining satellite earth observation data (SEO) with conventional *in-situ* data. This chapter details the general methodology, a description of the research areas, the ETDI, SPI and SPEI indices along with the inputs, necessary calculations and procedures that were required to obtain the spatial and temporal drought monitoring results.

3.1 General Methodology

The general methodology adopted in this study aimed to achieve the research objectives that were posed in Chapter One, which included:

i. an investigation into, and the application of, the ETDI in South Africa, using satellite-derived earth observation data,
ii. an estimation of ET_o from satellite earth observation data (SEO) for use in the ETDI calculation,
iii. the application and validation of a satellite-based ET_a product as an input for the ETDI calculation,
iv. the application of the SPI and SPEI to confirm the occurrence of drought events,
v. the assessment of the ETDI, using the SPI and SPEI as indicators of droughts in selected Quaternary level sub-Catchments (QC's) in South Africa, and
vi. an investigation into the use of satellite-based drought indices in ungauged catchments.

The first section of this study was aimed at monitoring historical droughts using SEO through the calculation of the ETDI from two key water-cycle related variables, namely, ET_a and ET_o. The research work carried out in this section of the study was divided into three main phases. Phase One involved the use of a global daily evapotranspiration product, to generate the ET_a estimates. The LSA-SAF product was downloaded for the period 01st January 2011 to 31st

December 2016 and furthered processed using Python scripts. With respect to Phase Two, as a result of a declining availability of meteorological data from ground stations in poor and developing regions, and due to maintenance and cost-related issues, data from such stations are insufficient to represent the spatial-temporal variation of ET_o. An alternative method that can be used in poor and developing countries, such as South Africa, is a combination of the Hargreaves Model (Hargreaves and Samani, 1985) and RS (remote sensing) data, which enables a spatial-temporal variation of ET_o to be calculated, thereby assisting for the proper management of water resources. The final and third phase of this section was the calculation of the ETDI from the WSA.

The methodology for the second section of the research work focused on calculating the SPI and the SPEI from the R software package. The research work carried out in this section of the study was divided into five main steps. The first step involved obtaining the SPEI-R package, while Steps 2 and 3 consisted of creating 30-year historical records of continuous rainfall data and temperature from different sources to form the data inputs into the SPEI package within the R software and to enable the calculation of the SPI and SPEI. Step 4 consisted of structuring the data and creating the text input files for the SPEI-R package. Finally, running the R software to obtain results formed the fifth step.

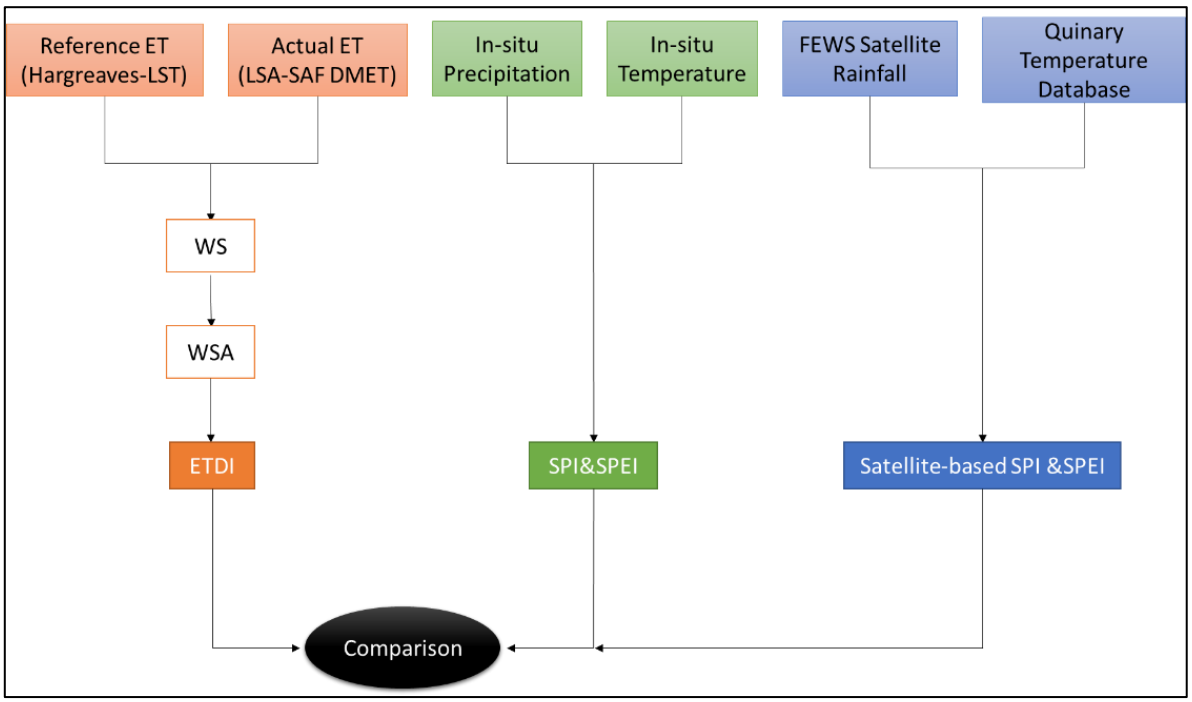

Figure 3.1 General methodology for drought assessment

3.2 Description of the Study Area

Upper Thukela and Umgeni Catchments, located in the KwaZulu-Natal province in South Africa, were selected for this research study (Figure 3.2). In 2015, 2016 and at the beginning of 2017, these catchments were severely affected by an ongoing drought event, which coincided with an El Nino event. This research study was thus undertaken in the above catchments in an attempt to depict the drought event that had occurred and to assist in improving the water resources management by advocating the use of SEO. This will attempt to contribute to a better understanding of the spatio-temporal patterns of droughts, which is needed for implementing strategies of drought risk planning and management.

Additionally, drought analysis in these catchments is important as the 2015/2016 drought caused significant economic losses, whilst the urban and agricultural water demands have increased considerably. This has further highlighted the need to understand the temporal behaviour of droughts and their spatial patterns in order to assist in the development plans for future risk mitigation. This study reports and detects the important drought events that have occurred within these catchments.

In South Africa, a classification system is used to categorize hydrological unit boundaries, which are endorsed by the Department of Water Affairs (DWA) (Maherry *et al*., 2013). These range from primary, secondary and tertiary, with the smallest operational unit being the quaternary catchment (Maherry *et al*., 2013). To enable the validation of the LSA-SAF ET_a product, a quaternary level sub-catchment (QC) was selected, which is located immediately next to the QC's within the Umgeni Catchment of the study area. QC U40C was chosen to be the validation site. The Two Streams Research Catchment is located within the QC from which data was received (Figure 3.2).

3.2.1 Upper Thukela Catchment

The Upper Thukela Catchment extends from the river's headwaters in the Ukhahlamba-Drakensberg Mountains (3000 m above sea level) and flows to the Indian Ocean (de Winnaar *et al*., 2010; Andersson *et al*., 2011; Graham *et al*., 2011). The catchment covers an area of approximately 29 297.54 km^2, within which the Department of Water Affairs (DWA) has delineated 86 QC's (Kongo *et al*., 2011). More recently, other researchers have delineated the

QC's further into 235 sub-catchments (Kongo *et al*., 2011). The focus of this study are 55 of the headwater QC's that make up the Thukela Catchment, which are located in the upper Thukela within the secondary catchments V1, V2, V6 and V7, and cover an area of 16265.41 km^2.

The catchment is diverse in terms of its culture, landscape and climate (Andersson *et al*., 2011). Various land uses occur within the study area of the Upper Thukela Catchment, as shown in Figure 3.3. In respect to the climate characteristics of the Upper Thukela Catchment, it is highly seasonal, with warm summers and dry cool winters, and a large variation of precipitation is exhibited (Andersson *et al*., 2011). The mean annual potential evapotranspiration of the catchment ranges between 1600 to 2000 mm (Andersson *et al*., 2011). The MAP ranges from approximately 2000 mm in sections of the Drakensberg mountains to as low as 550 mm in the drier lower valley regions (Lynch, 2004; Kongo *et al*., 2011). Several large reservoirs that are used for hydropower and other downstream services are fed by the abundant runoff received from the Drakensberg Mountains (Wilk *et al*., 2013). The conditions are known to be generally good for farming, which stretches over much of the catchment (Graham *et al*., 2011).

3.2.2 Umgeni Catchment

The Umgeni Catchment (4 481.25 km^2) is located in the Province of KwaZulu-Natal, South Africa (see Figure 3.2). The catchment extends between the longitudes of 29°47'6.90"E and 31°3'28.73"E and the latitudes of 29°13'6.35"S, 29°50'12.37"S. The Umgeni Catchment is strategically and economically important for South Africa. Water resources from the Umgeni Catchment supplies nearly 15% of the country's 41 million inhabitants as well as a region that is known to produce approximately 20% of the country's Gross Domestic Product (GDP) (Schulze *et al*., 2004; Warburton *et al*., 2010).

Sub-tropical climatic conditions prevail within the catchment with an average annual temperature ranging from 12°C in the escarpment areas to 20°C towards the coastal areas of the catchment (Warburton *et al*., 2010; Dube and Mutanga, 2015, 2016). The altitude in the catchment extends from 1913 m a.s.l in the western escarpment of the catchment to sea level at the catchment's outlets to the Indian Ocean (Warburton *et al*., 2010). The MAP varies between 730 mm in the drier middle sections of the catchment and 1500 mm in the dominant water source areas found in the west of the catchment (Dube and Mutanga, 2015, 2016). The

rainy season occurs in the summer months from October and February, with the high summer rainfall providing favourable conditions for the production of timber in commercial plantations (Dube and Mutanga, 2015). The mean annual potential evaporation ranges between 1 567 mm and 1 737 mm (Warburton *et al*., 2010). The area is characterised by moderately steep and undulating slopes stretching between 644 m and 1266 m above sea level (Dube and Mutanga, 2015, 2016).

There are intensive cultivation of commercial timber and sugar plantations as well as subsistence crop husbandry (Schulze *et al*., 2004). There are also irrigated crops/pastures and over-grazed areas present within the catchment (Schulze *et al*., 2004). The aforementioned contrasting agricultural systems affect hydrological responses in vastly different ways (Schulze *et al*., 2004). The land cover types present within the catchment are shown in Figure 3.3.

Four major dams (Midmar dam, Albert Falls, Inanda dam and Nagle dam), are located within the Umgeni Catchment that form the water engineering system of the Umgeni (Warburton *et al*., 2010). For this study, 12 QC's that make up the Umgeni catchment were the main focus for the study. These QC's form part of the U20 tertiary catchment. Figure 3.2 displays the location of the catchment.

3.2.3 Validation site: Two Streams Research Catchment

The Two Streams Catchment was chosen as the validation site for the LSA SAF DMET product based on the availability of *in-situ* measurements (Figure 3.2). The catchment is located 70 km northeast of Pietermaritzburg, in the seven Oaks District (Lorentz *et al*., 2004; Bulcock and Jewitt, 2012; Everson *et al*., 2014) and is at an altitude of approximately 1050 m (Lorentz *et al*., 2004). Mucina and Rutherford (2006) classified the area as the "Midlands Misbelt Grassland" (Bulcock and Jewitt, 2012; Everson *et al*., 2014), with a rolling landscape and the majority of the land is arable (Everson *et al*., 2014). Commercial forestry dominates the areas, with Eucalyptus, pine (*Pinus*) and wattle (*Acacia*) being the genera of choice (Lorentz *et al*., 2004; Bulcock and Jewitt, 2012). Sugarcane plantations are also grown where the drainage of cold air is good to ensure that light or no frost occurs (Bulcock and Jewitt, 2012). The climate is humid, with an annual summer rainfall of 659 mm to 1139 mm (Bulcock and Jewitt, 2012; Everson *et al*., 2014) and most rainfall occurs during the summer months from October to March (Bulcock and Jewitt, 2012). During the winter months, dry and windy conditions prevail

with occasional low frontal systems. Heavy mists, frost, hail, Berg winds and droughts are common to the area (Mucina and Rutherford, 2006; Everson *et al*., 2014).

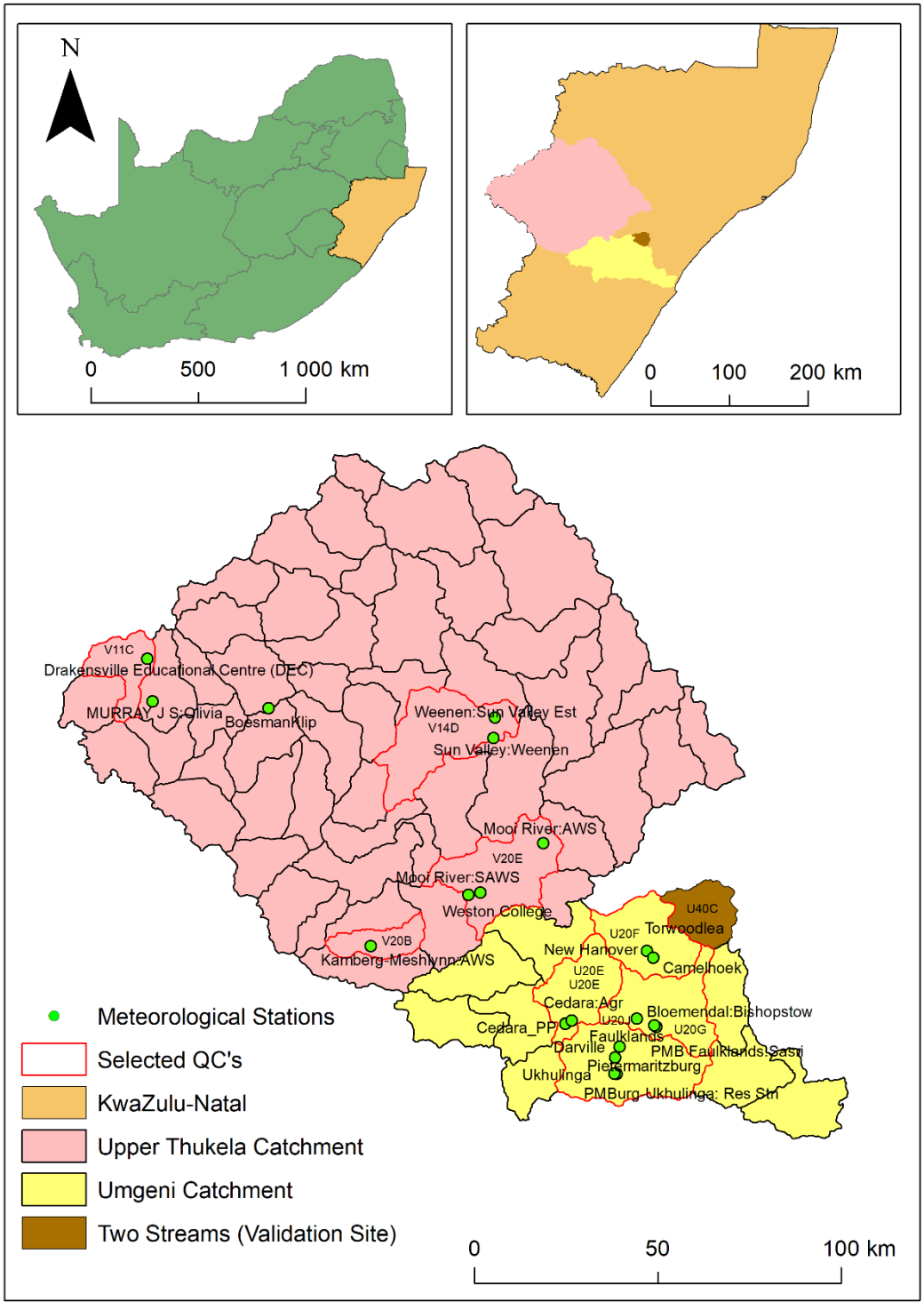

Figure 3.2 Location of the Umgeni and Upper Thukela Catchment within the province of KwaZulu-Natal, South Africa, along with the location of the 22 meteorological stations used to obtain precipitation and temperature data

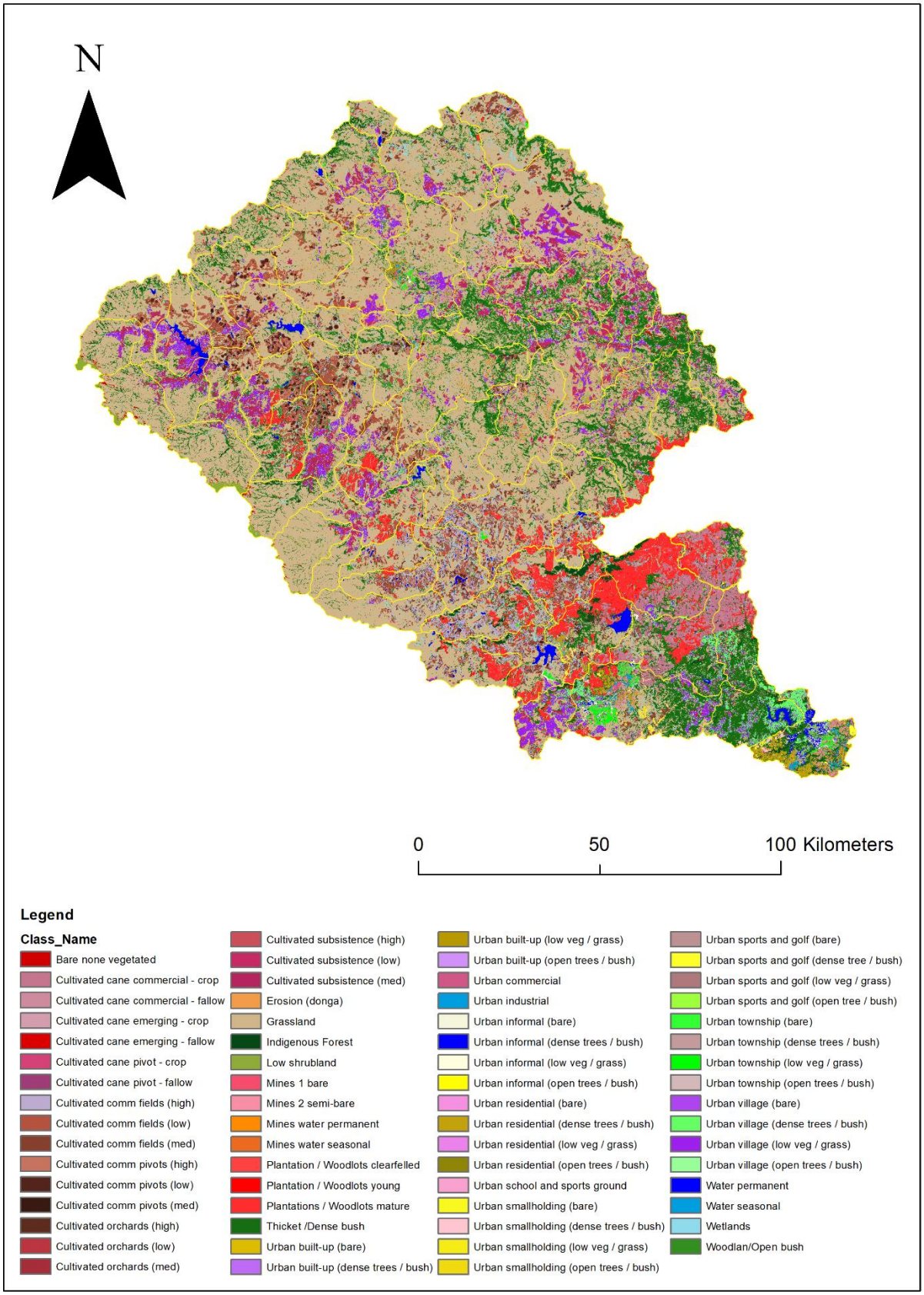

Figure 3.3 Land cover map for the research study sites (GEOTERRAIMAGE, 2015)

3.3 Monitoring Droughts with the Evapotranspiration Deficit Index (ETDI)

The research work involved in this component of the study focused on calculating the ETDI to enable the monitoring of droughts. The methodology was divided into three steps. The first step required obtaining ET_a estimates, while the second step looked at calculating ET_o using a satellite-based technique. In the third step, ET_a and ET_o were used to calculate the ETDI.

3.3.1 Actual evapotranspiration estimates (ET_a)

This study uses the daily ET_a product known as DMET (Hu *et al*., 2015), which is produced by integrating instantaneous 30 min ET_a values (MET product) over an entire day (mm/d^{-1}). Section 2.7 describes the method briefly and presents the main equations; however, the complete procedure is described in the User Manual and various supporting documents for the product (LSASAF, 2011).

3.3.2 Imagery retrieval and processing

The LSA-SAF DMET product was downloaded from the EUMETSAT's LSA-SAF website (http://landsaf.meteo.pt/), which is an FTP site. Registered users have free access to LSA-SAF ET_a results through the LSA-SAF website (see http://landsaf.meteo.pt/) or via EUMETCast (http://www.eumetsat.int/ Home/Main/DataAccess/EUMETCast/index.htm) dissemination in near-real time. Off-line distribution to users is also possible via ftp (http://landsaf.meteo.pt) or on request from helpdesk.landsaf@meteo.pt. Prior to the date 11/11/2015, four areas (Europe, North Africa, South Africa and South America) were available; the area of South Africa was downloaded for this study. However, after the above specified date, only the full MSG-Disk was available and had to be downloaded. The area of South Africa was therefore chosen (prior to 11/11/2015), and the MSG Disk was chosen afterwards due to a change in the product format. The files were downloaded in HDF format for a six-year period (2011-2016). A total of 2170 DMET files were utilised in this study.

Provided that optimal conditions prevail, one image is available per day. Each image is stored in an HDF5 file, which also contains information about the quality of the generated output. Every output file is composed of three images containing: (i) the DMET estimates, (ii) the number of values (slots) missing for each pixel, and (iii) the percentage it represents

respectively. The product has a one-day distribution delay and a spatial resolution of 3-5 km, which is dependent on the latitude and the distance to the nadir view (Sepulcre-Canto *et al*., 2014). The product has been operationally available since the 13th of December 2010.

Once the DMET HDF5 files are downloaded, HDFView software (http://www.hdfgroup.org/hdf-java-html/hdfview/index.html#download_hdfview) can be utilised to view the data, for basic statistics, line-plotting and histogram generation. The three files contained within the ET_a product in the HDFView software can be displayed using colour palettes, the files can be inspected and the dataset attributes can be viewed.

GIS tools are required for the visualization and analysis. The HDFView is a tool that provides for a quick inspection, while GIS tools are more useful for map-making, visualization and analysis. However, most GIS tools cannot recognize LSA-SAF coordinate information; therefore, the files need to be projected, hence an MSG toolbox has been provided by the LSA-SAF for geo-referencing LSA-SAF products.

Within the MSG toolbox, HDF5 files can be converted to a geotiff format, which is based on an interchange format for georeferenced raster imagery that is suitable for further processing in GIS software. The toolbox offers other file format conversions such as for ILWIS (.mpr) and IDL-ENVI/SPIRITS (.img). Temporal compositing, quality filtering and composite files based on daily composites, periodic composites and a number of observations using minimum, maximum, sum or average of the values, are some of the various options provided by the toolbox. However, this toolbox has not yet been adapted to work with the full MSG disk. The LSA-SAF has been contacted and it was envisaged that the modified version of the toolbox would work with the full MSG disk and be released by July 2017. However, due to delays the modified version was not yet ready when this study required it.

Open source tools such as GDAL, Proj and Qt4 have the ability to work as a geo-reference tool for the LSA-SAF products. Python scripts using GDAL were written to further process the DMET product for this study. A scaling factor of a 1000 was applied as indicated by the metadata supplied by the files and the images were clipped according to the study area. The ET_a data was obtained in HDF5 format; therefore, Python was employed to convert the DMET files into a geotiff format (World Geodetic System 1984 datum) for further processing within the GIS (Geographical Information System) software as well as for extracting a time series of

the ET_a estimates for the chosen study sites. Since LSA-SAF data are kept in native geostationary projection, centred at 0º longitude and latitude, specific longitude and latitude files had to be downloaded from the website. A quality control procedure was also introduced and carried out within the scripts, whereby those images that possessed >30% "bad pixels" within a shape file were excluded. These "bad pixels" included missing pixel values and scan lines. This step was undertaken to ensure that accurate estimates of the ET_a could be obtained. A few images from the year 2011 had to be discarded due to significant scan line issues. Significant scan lines were detected only for the year 2011 and ended in May of the same year. The dates of the eight discarded images as a result of the scan lines were: 2011/01/09, 2011/02/02, 2011/02/03, 2011/02/20, 2011/03/19, 2011/03/22, 2011/05/10 and 2011/05/11. Overall, 2162 good images were processed and utilised to obtain ET_a estimates.

3.3.3 Validating the LSA SAF DMET product

In-situ ET_a estimates obtained from the surface renewal (SR) and eddy covariance (EC) systems were sourced from Dr Alistair Clulow in the Hydrology Department of the University of KwaZulu-Natal, for the Two Streams Catchment. These ET_a estimates were obtained as part of a WRC project by Everson *et al*. (2014). These estimates were used together with LSA-SAF ET_a estimates to enable the validation of the DMET product for use within the study site.

3.3.4 Reference evapotranspiration estimates

For the purpose of this section of the study, literature by Maeda *et al*. (2011) was utilised as the key reference paper. ET_o estimates were attained by applying the Hargreaves equation (Hargreaves and Samani, 1985) on the basis of surface temperature being sourced from remotely sensed products.

Hargreaves and Samani (1985) developed the Hargreaves equation by using eight years of daily lysimeter data that had been obtained from Davis and California (Maeda *et al*., 2011; Zheng and Zhu, 2015). The method was applied and tested in different locations, including Haiti, Australia and Bandgladesh (Maeda *et al*., 2011; Zheng and Zhu, 2015). Since the development of the method, the Hargreaves Model has been successfully applied throughout the world (Gavilán *et al*., 2006; Maeda *et al*., 2011; Aguilar and Polo, 2011; Zheng and Zhu, 2015).

The Hargreaves method requires only maximum and minimum air temperatures and extra-terrestrial radiation data. The equation can be expressed as follows:

$$ET_o = 0.0023\ x\ RA\ x\ ((Tmax - Tmin))^{0.5}\ x\ (Tmean + 17.8) \quad (3.1)$$

where:

ET_o = the reference evapotranspiration [mm.day^{-1}],
RA = the extra-terrestrial radiation [mm.day^{-1}],
Tmax = the maximum temperature [^{o}C],
Tmin = the minimum temperature [^{o}C], and
Tmean = mean temperature [^{o}C].

The extra-terrestrial radiation (*RA*) was calculated from the solar constant, the catchment's latitude, the solar declination and the time of year using the following equation (Zotarelli *et al*., 2013):

$$RA = (\frac{24\ (60)}{\pi}\ G_{sc} d_r \left[\left(\omega_s sin_\varphi sin_\delta\right) + \left(cos_\varphi cos_\delta sin_{\omega_s}\right)\right]/2.45) \quad (3.2)$$

where:

RA = the extra-terrestrial radiation [mm.day^{-1}],
G_{sc} = solar constant (0.0820 MJ m^{-2}),
d_r = inverse relative distance Earth-Sun,
φ = latitude (radians),
δ = solar declination, and
ω_s = sunset hour angle (radians).

3.3.5 Data input and collection

The use of meteorological data from ground-based weather stations as input to models is known as the traditional approach for estimating ET_o. However, as previously mentioned, in poor, developing countries, the availability of data from weather stations is insufficient for it to be representative of the spatial distribution of ET_o at a detailed spatial scale. Obtaining long records of near surface air temperature is often complex especially in developing countries due

to the limited availability of ground-based weather stations. Satellite earth observation techniques are used to obtain estimates for various meteorological variables such as temperature. However, deriving near surface air temperature from LST, which is derived from satellites, is not simple. This is because the near surface and LST vary strongly, depending on cloud cover, seasonality and ecosystems.

In order to obtain the minimum and maximum temperatures for input into the Hargreaves equation, remotely-sensed data was sourced from the Moderate Resolution Imaging Spectroradiometer (MODIS).

LST products, that have been produced, include the LST from NOAA-AVHRR, which has an 8 km spatial resolution, a daily temporal resolution and it is available for 1995-2000. While the LST from MODIS (Aqua and Terra) possesses a 1 km and 5km spatial resolution, daily, eight-day composites, monthly temporal resolution and is available from 2000-present (Aqua) over Africa. Examples of the various MODIS LST products include the MOD11_L2, MOD11A1, MOD11B1, MOD11A2, MOD11C1, MOD11C2 and MOD11C3 (http://www.icess.ucsb.edu/modis/LstUsrGuide/usrguide_intro.html). This study utilised a quality-flagged MODIS Aqua/Terra land data product known as the eight-day LST (MOD11A2-Version 6) (http://modis-land.gsfc.nasa.gov/temp.htm). Various MODIS LST products exist; however, the choice of the averaged eight-day product was more suitable due to its high spatial resolution of 1 km and the computational ease, since the ETDI is calculated on a monthly basis.

On board the Terra and Aqua polar-orbiting satellites is the MODIS sensor, which possesses 36 spectral bands over a wide range at moderate resolutions (250, 500, and 1000 m) with a nearly daily coverage of the earth (http://modis.gsfc.nasa.gov). The MOD11A2 Version 6 product contains both day- and night-time surface temperature bands together with their quality indicator layers, MODIS Bands 31 and 32 as well as 8 observation layers. The LST day and night data is stored as an average eight-day, per-pixel LST within a 1200 x 1200 kilometre grid and a pixel size of 1 km. The compositing period of eight days was chosen primarily since twice that period is the exact ground tracking repeat period of the Terra and Aqua platforms.

The temporal extent of the MOD11A2- Version 6 product is from March 2000 until the present. The product also possesses a global spatial extent. Each file size is ~3.86 MB along with an

HDF file format and a sinusoidal coordinate system. The LST obtained from MODIS is representative of the radiometric temperature corresponding to the thermal infrared radiation (TIR) that is emitted from the land surface and observed by an instantaneous MODIS observation (Maeda *et al*., 2011). MOD11A2 products are validated over a wide range of conditions, with product uncertainties being well-defined. Furthermore, the products have been applied within a variety of scientific studies producing; satisfactorily results (Maeda *et al*., 2011). The daytime LST correlates to measurements obtained around 10:30 am, while the night-time LST is obtained at around 22:30 pm (Maeda *et al*., 2011). These times are regarded as local solar time.

In total, 274 LST images corresponding to the complete MOD11A2 dataset for the years 2011-2016 were obtained from the USGS Earth Explorer website (https://earthexplorer.usgs.gov/), through a free download procedure. MOD11A2 datasets can also be retrieved from the Land Processes Distributed Active Archive Center (LP DAAC). Within the NASA LP DAAC collections, the MODIS MOD11A2 Version 6 product was downloaded to obtain the day and night LST values. The data was received in HDF format and the HDFView tool was used to provide a quick inspection of the datasets contained within the product.

The images were thereafter processed using Python scripts. Within the Python scripts, imagery file names were converted from a Day of Year (DOY) format to a date format (year, month, day) as understood by the Python scripts. Following this step, LST day and night sub datasets were then extracted from the main dataset along with the application of the scaling factor (x 0.02). All images were then converted to a geotiff file format and clipped according to the study sites. A quality control step was also introduced and carried out within the scripts, whereby images containing >30% “bad pixels” within a shape file were excluded. This was done to ensure that accurate estimates of the LST could be retrieved. LST values were then converted to degrees Celsius from the original Kelvin units within the software. Finally, time series of daily LST values were extracted using the Python scripts. These values where then used within Excel to be complied into monthly averaged LST values.

3.3.6 Calibrating the Hargreaves-LST equation

The empirical nature of the Hargreaves-LST approach means that local calibration should be conducted. Hence, the calibration of the empirical equation is usually performed using the

FAO-PM approach (Allen *et al*., 1998). The FAO-PM approach is recognised as being the standard ET_o method and it is able to produce the most precise and reliable results compared to other equations tested in various regions across the world.

Although, inherent errors and uncertainties are contained within the FAO-PM approach, this method has been shown to perform considerably well under different climatic conditions (Maeda *et al*., 2011). The validation and calibration of empirical equations such as the Hargreaves-LST are therefore performed using this approach.

The FAO-PM method (Allen *et al*., 1998) is given as:

$$ETo = \frac{0.408\Delta(R_n - G) + \gamma \frac{900}{Tmean+273} u_2 (e_s - e_a)}{\Delta + \gamma(1 + 0.34u_2)} \quad (3.3)$$

where:

ETo = reference evapotranspiration [mm.day^{-1}],
Rn = net radiation at the crop surface [MJ.m^2.day^{-1}],
G = soil heat flux density [MJ.m^2.day^{-1}] which can be neglected (G=0),
Tmean = mean air temperature [°C],
u_2 = wind speed measured at 2 m height [m.s^{-1}],
es = saturation vapour pressure [kPa],
ea = actual vapour pressure [kPa],
e_s-e_a = saturation vapour pressure deficit [kPa],
Δ = slope vapour pressure curve [kPa/°C], and
γ = psychometric constant [kPa/°C].

For this study, FAO-PM ET_o estimates for selected QC's were obtained from the Institute for Soil, Climate and Water of the Agricultural Research Council (ISCW-ARC), whereby the calibration of the Hargreaves equation was performed. ET_o values were also calculated for these QC's using the MODIS LST data together with the empirical model. The details of the stations from which the FAO-PM ET_o estimates were obtained can be seen in Figure 3.2.

Allen *et al*., 1998; defined the calibration parameters using Equation 3.4 below:

$$ETo_{cal} = a + b\,.ETo_{lst} \quad (3.4)$$

where:

ETo_{cal} = the calibrated ET_o values [mm],

a and *b* = the calibration parameters obtained from a regression analysis that uses as reference the FAO-PM method, and

ETo_{lst} = the ET_o values that are estimated using the Hargreaves empirical model, and MODIS LST as data input [mm].

3.3.7 Calculation of the ETDI

Once the two parameters that are significant inputs for the ETDI calculation, namely ET_o and ET_a have been calculated, the ETDI estimates can then be obtained. The ETDI values were calculated following the WS and WSA calculations. The WS, WSA and ETDI equations are described in section 2.2. Following these equations, ETDI estimates were produced to enable the monitoring of drought conditions within the Upper Thukela and Umgeni Catchments.

3.3.8 Comparison of the ETDI with variables from the hydrological cycle

Once the results for the ETDI were obtained, a spatial comparison between the ETDI and various hydrological variables such as ET_a, ET_o, precipitation, elevation, soil moisture and temperature was performed to determine the relationship between them. In addition, the spatial and temporal analysis of a drought contributes significantly to the evaluation of the dynamic climate in an area.

MAP (Lynch, 2004) and elevation (Weepener *et al*., 2011) raster images were obtained from the University of KwaZulu-Natal's Centre for Water Resources Research (CWRR). ET_o and ET_a were retrieved as detailed in the above sections, while temperature was retrieved using the MOD11A2 product. Soil moisture values were retrieved from the Satellite Applications and Hydrology Group (SAHG) website http://sahg.ukzn.ac.za/soil_moisture/sm/.

An outcome of one of the South African Water Research Commission funded projects (Sinclair and Pegram, 2010) on soil moisture estimation is the Soil Saturation Index (SSI), which was produced by automated real-time computations of the TOPKAPI hydrological model in the LSM mode using three-hourly rainfall and ET_a forcing. Using the above-mentioned forcing datasets, the percentage of soil saturation was automatically computed once daily, for each of the 6984 TOPKAPI cells at three-hourly time-steps. The SSI product is an estimate of the soil moisture state over South Africa at a three-hour time steps on a 0.125^o spatial grid. Literature by Sinclair and Pegram, (2010) gives the details of the SSI, the results of which are easily obtained from the SAHG website (http://sahg.ukzn.ac.za/). The website provides FTP access to results in geo-referenced ASCII and geotiff formats.

For the comparison between soil moisture and ETDI, 247 geotiffs at 3-hourly intervals for the month of May 2015 were downloaded for the SAHG website. The 247 geotiff's were then combined to create daily images and then into a monthly image for May 2015 within the ArcGIS software. A clip tool within the ArcGIS software was used to produce spatial monthly SSI maps for the study areas.

3.4 The Standardized Precipitation Index (SPI) and the Standardized Precipitation Evapotranspiration Index (SPEI)

The research work involved in this section was aimed at calculating the SPI and SPEI using the inputs of rainfall and temperature data in the SPEI-R software. The calculation of these indices were divided into five steps, which are detailed below.

3.4.1 SPEI-R package

The first step involved downloading and obtaining the R software, as well as gaining insight on the necessary documents and requirements needed to run the software. The SPEI R package (Vicente-Serrano *et al*., 2010) consists of a set of functions to compute SPI and SPEI (Penman-Monteith, Thornthwaite and Hargreaves methods) as well as many widely used drought indices, which currently include the SPI and the SPEI. The SPEI-R package requires monthly input data for 30 years.

The SPEI R library can be obtained from the Comprehensive R Archive Network, CRAN (https://CRAN.R-project.org/package=SPEI). Several versions of the package exist with different corrections and modifications made to each. The current version, Version 1.7 was used in this study. The SPEI R package has been used to calculate SPI and SPEI in several studies. Literature by Vicente-Serrano *et al*. (2010a), (2010b), (2011), (2012a), (2012b), (2015) and (2016), as well as by Begueria *et al*. (2010) and (2014), provide further details on the SPEI library. The following website also details the SPEI R package, http://spei.csic.es.

3.4.2 *In-situ* precipitation data

The second step entailed obtaining 30 years of historical precipitation data (1986-2016) for the Upper Thukela and Umgeni study areas. As a result of insufficient meteorological data for each of the QC's within the study areas, four QC's within each study area were chosen based on those QC's which had the longest record of meteorological data. Figure 3.2 displays the location of the 22 ground stations that were used to obtain rainfall and temperature data for the selected QC's to enable the calculation of the SPI and SPEI. Hence, SPI and SPEI results are only produced for the four selected QC's within the two study sites.

Precipitation data was obtained from the South African Weather Service (SAWS), from the ISCW-ARC as well as from the South African Sugarcane Research Institute (SASRI). Despite all efforts in trying to source precipitation data from the various Institutes, the Upper Thukela Catchment had very few gauges. To address the challenge of obtaining a reliable 30-year record of precipitation data for the Upper Thukela Catchment to enable SPI and SPEI calculations, satellite based rainfall estimates were used. The estimates were obtained from the satellite rainfall product, Famine Early Warning System Network African Rainfall Climatology, version 2.0 (FEWS ARC 2.0) (Novella and Thiaw, 2012), which is elaborated in the following section.

3.4.3 Satellite-based rainfall data

The FEWS ARC 2.0 product was chosen for use in this study as it had a suitable spatial and temporal coverage as well as its applicability to climate and hydrological studies has been proven (Novella and Thiaw, 2012; Bangira 2013; Bayissa *et al*., 2017). The product was further decided for use over others as it has the longest stable data record period of more than 30 years.

Although it is considerably costly to produce these datasets, they are provided at no cost to users and can be downloaded from the Internet. Novella and Thiaw (2012), describe the details and algorithm of the new daily remotely sensed precipitation product, ARC 2.0. ARC 2.0 was developed by utilising datasets of historical rain gauge data as well as IR (Infrared) data. The ARC 2.0 product can also be used to identify wet and dry periods, extreme rainfall events along with the peaks, onset and departure of seasonal trends (Novella and Thiaw, 2012). The new dataset provides more than 30 years of reliable precipitation estimates using reliable inputs, which allows for climate variability and change to be understood.

The study by Novella and Thiaw (2012) indicates that the ARC 2.0 rainfall estimates are consistent with other long-term datasets. In addition, the study proves that the ARC 2.0 estimates compared more favourably to the other products with long-term rainfall datasets, when validated against rain gauge measurements. All FEWS products and data are available via http:// and CPC's ftp server: ftp://ftp.cpc.ncep.noaa.gov/fews/.

Various analyses and comparisons with representative rain gauge rainfall data were carried out in the Umgeni Catchment, prior to the use of the satellite rainfall product in the Upper Thukela Catchment. The FEWS ARC 2.0 rainfall product was obtained by first creating and setting up a personal FTP site, after which, the images were downloaded from the following website: http://www.cpc.ncep.noaa.gov/fews/fewsdata/africa/arc2. The images were downloaded as zipped geotiff files and a total of 11 110 daily files were downloaded. The Python scripts were then used to unzip the compressed files, to extract the satellite rainfall data for the relevant study sites and to perform the necessary steps to produce a daily time series of rainfall estimates for the Upper Thukela Catchment. The following QC's and years indicate the period for which satellite rainfall was used, while for the remaining years, *in-situ* rainfall data from weather stations were used to complete the 30 year data record (1986-2016): V11C = 1986-2009, V14D = 1986-2002, V20B = 1986-2002 and V20E = 1986-2000.

3.4.4 Temperature data

The third step was to obtain air temperature (minimum and maximum) data records for 30 years (1986-2016) for the four selected QC's within each of the two study areas. As previously mentioned, sufficient temperature data was obtained from SAWS, ISCW-ARC and SASRI, to form 30-year records (1986-2016) for the Umgeni Catchment; however, the presence of very

few gauges within the Upper Thukela Catchment was a limitation to form historical 30-year records.

Hence, to enable the SPEI to be calculated within the Upper Thukela Catchments, the Database of Gridded Daily Temperatures for Southern Africa by Schulze and Maharaj, (2003); was used together with available data from weather stations within the catchment to extend and form historical 30-year temperature records. The monthly temperature records for the eight selected QC's within the two study sites were accessed from the University of KwaZulu-Natal's CWRR. Schulze and Maharaj (2003) detail the development of the gridded daily temperature database for Southern Africa.

3.4.5 Calculation of the SPI and SPEI indices

The fourth step involved setting up text files containing the rainfall and temperature data of the selected QC's, which were structured into a specific format as required by the SPEI R package. The final and fifth step was running the SPEI-R package to obtain SPI and SPEI statistics and graphs for the Umgeni and Upper Thukela Catchments.

4. RESULTS AND DISCUSSION

This chapter intends to present the results and discussion of the various aspects of the research study. The section will detail the following aspects:

(i) The validation of the LSA-SAF DMET product with a representative *in-situ* ET_a dataset for the Two-Streams Research Catchment.

(ii) Producing a spatial averaged illustration of the satellite-derived ET_o estimates for the research study area, which have been derived by using the Hargreaves-LST approach.

(iii) The calibration of the Hargreaves-LST data with available meteorological data.

(iv) A detailed investigation into the spatial and temporal distribution of ET_a obtained from LSA-SAF and ET_o using satellite-derived estimates to calculate water stress ratio's and water stress anomaly's to enable the calculation of the ETDI index for drought assessment.

(v) A spatial and temporal investigation into land surface variables such as ET_a, ET_o, precipitation, soil moisture and temperature as notable driving forces to droughts.

(vi) An assessment of the use of satellite rainfall estimates for the calculation of the SPI and SPEI.

(vii) An investigation into the SPI and SPEI to assess the link between meteorological droughts and the estimated ETDI.

(viii) A cross-comparison of the drought indicators in order to investigate the potential of synergy.

The types of analyses that have been implemented in this research study include:

(i) A time series analysis;

(ii) The correlation coefficient (r) and coefficient of determination (R^2):

(iii) The Nash- Sutcliffe efficiency index;

(iv) Paired t-test; and

(v) Standard statistics namely: the Mean Absolute Deviation (MAD), Mean Square Error (MSE), Root Mean Square Error (RMSE) and Mean Absolute Percentage Error (MAPE) were computed using the following equations (Douglas *et al.*, 2009; Maeda *et al.*, 2011) :

$$MAD = \frac{\sum_{t=1}^{n} |ETO_{cal} - ETO_R|}{n} \quad (4.1)$$

$$MSE = \frac{\sum_{t=1}^{n} (ETO_{cal} - ETO_R)^2}{n} \quad (4.2)$$

$$RMSE = \sqrt{\frac{\sum_{t=1}^{n} (ETO_{cal} - ETO_R)^2}{n}} \quad (4.3)$$

$$MAPE = \frac{\sum_{t=1}^{n} \left|\frac{ETO_{cal} - ETO_R}{ETO_{cal}}\right|}{n} \text{ x } 100 \quad (4.4)$$

The above-mentioned statistical analyses are amongst the most commonly-used analyses in current satellite-based studies. These selected analyses have also been considered appropriate for the various aspects of the research project to generate reliable conclusions. The selected statistical analyses are not used in every result section, but they are rather selected for use in appropriate sections.

4.1 Validation of the LSA-SAF DMET Product

In recent years, several global products and datasets derived from earth observation have been made available to the public. One of the key objectives of this research project is the use of earth observation data to enable the calculation of an evaporative drought index. As detailed in Section 2.2, one of the required inputs into the drought index calculation is the ET_a variable. In order to achieve this, this study opted to use a freely available global ET_a (LSA-SAF DMET) product to provide the spatial estimates of ET_a.

To validate the DMET product, correlations and linear regression models between *in-situ* measurements and satellite estimates at a daily temporal resolution were evaluated. Due to the absence of *in-situ* measurements within the research area, the Two Streams Research Catchment found in QC U40C, which is within the same climatic region as the Umgeni Catchment was used. Figure 3.2 illustrates the QC used for the validation of the DMET product.

The *in-situ* measurements were conducted at the Two-Streams Research Catchment site, which is found at the coordinates of 29°11’47.99” S and 30°39’58.73” E. Satellite-derived ET_a

estimates were processed using Python scripts as detailed in the methodology in Chapter 3 and averaged over the QC.

The comparison between the *in-situ* measurements and the satellite-derived ET_a product were evaluated by means of classical statistical indicators (a time series analysis, 1:1 line, paired t-test, Nash index, R^2 and Pearsons correlations). For *in-situ* measurements, the surface renewal (SR) and eddy covariance (EC) systems were used to obtain ET_a estimates for the period between 27 October 2011 and 25 October 2013 as data was only available for this period (Figure 4.1). The time period was considered adequate for the validation procedure since wet (summer) and dry (winter) periods were included within the data record. The SR and EC systems were used alternatively to ensure that a complete dataset of ground-based ET_a estimates were obtained, because in some instances where one system may have experienced technical failure, the alternative system was utilised. As illustrated in Figure 4.1, to patch a period of missing data, a relationship between ET_a and net radiation (Rn) was observed and this relationship was used to patch the missing data period.

A time series analysis was plotted to visually interpret and compare the performance of the satellite LandSAF DMET product in estimating ET_a and the *in-situ* data set. The satellite-derived LandSAF daily ET_a temporal behaviour correlated to the *in-situ* measured ET_a at the Two Streams site for the period of 27 October 2011-25 October 2013 (Figures 4.1 and 4.2). As shown in Figure 4.1, the LandSAF DMET estimates follow the same trend as the *in-situ* data set. The LandSAF DMET estimates correlate to *in-situ* ET_a data better during the summer months (wetter period) compared to the winter months (drier period). Although the DMET estimates are seen to underestimate ET_a throughout the data period when compared to *in-situ* data, the underestimation is more visible during the drier periods.

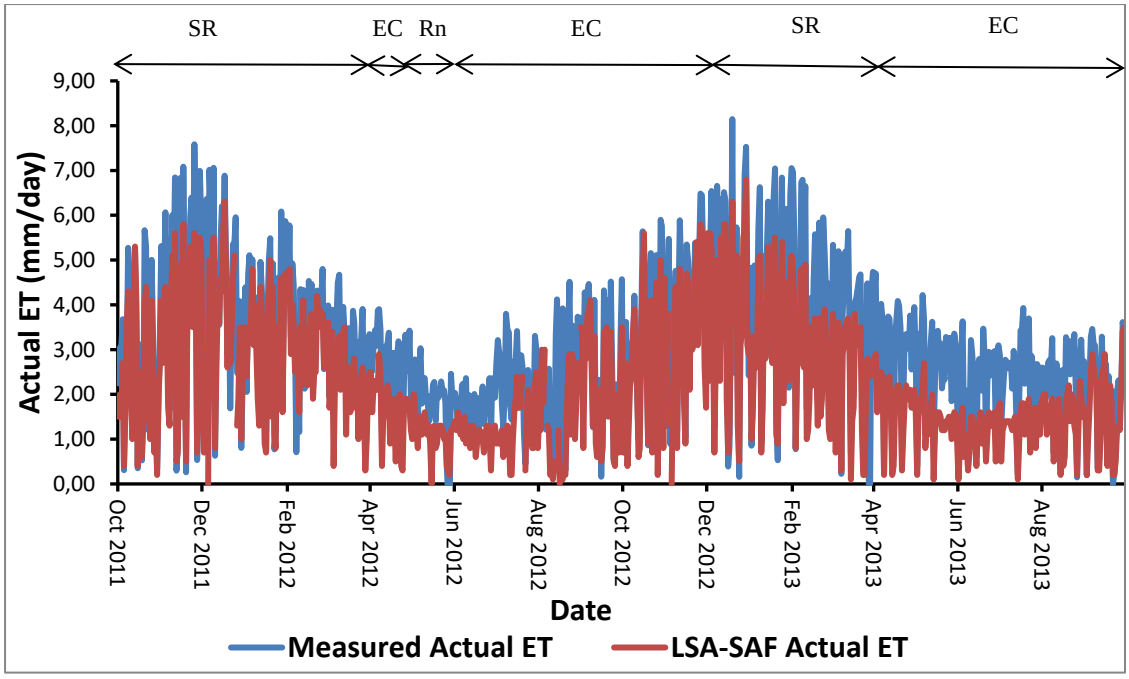

Figure 4.1 Daily *in-situ* and LSA-SAF DMET ET_a estimates for the validation site: Quaternary Catchment U40C

The DMET's product validation report also illustrated an underestimation of ET_a for the Sahelian savannah in Africa, which has a semi-arid climate. The potential sources attributed to this error are discussed in the validation report, with the main reasoning being the input variables of soil moisture and the vegetation characteristics. The ECMWF soil moisture provides lower values than *in-situ* measurements and this is attributed to the difference in spatial scale between the ECWMF grid and the *in-situ* measurements. The ECOCLIMAP/MSG tile may not fully correspond to the vegetation type of the QC, namely, the fraction of vegetation cover (FVC) and leaf area index (LAI), which may influence the estimates of ET_a from crop types, conditions and phenology characteristics. For example, the research area used in this study does consists of crops such as maize, sugarcane and commercial forestry. In the case of commercial afforestation, trees are able to access soil water or ground water deeper down that is why they are stable, able to have higher water use and transpire for a longer period.

Other sources of error result from input variables, including the differences in solar radiation, which is the main driver of the algorithm, vegetation characteristics and available soil moisture that are caused either by the model errors or spatial scale differences which could explain the difference between the product and *in-situ* measurements. Overall, it can be seen that the DMET product followed the general trend of the *in-situ* ET_a variations. There were differences

between the datasets, as the DMET product was generally slightly lower than the *in-situ* dataset. This difference was more noticeable during the winter months.

A scatter graph was plotted with the measured ET_a estimates on the x-axis and the satellite-derived daily LandSAF ET_a estimates on the y-axis (Figure 4.2). From Figure 4.2, it can be seen that the majority of the points are below the 1:1 line (red), however they are in close proximity to the 1:1 line. The negative y-intercept of 0.1629 is indicative of an underestimation of the DMET product when compared to measured ET_a estimates. The slope is 0.7943 and this value is representative of the relationship between the variables plotted, with respect to their increases and decreases. Since the value is close to 1, this indicates that there is a good correlation between both data sets. Judging by the 1:1 line, the LandSAF ET_a tends to underestimate compared to observed ET_a values.

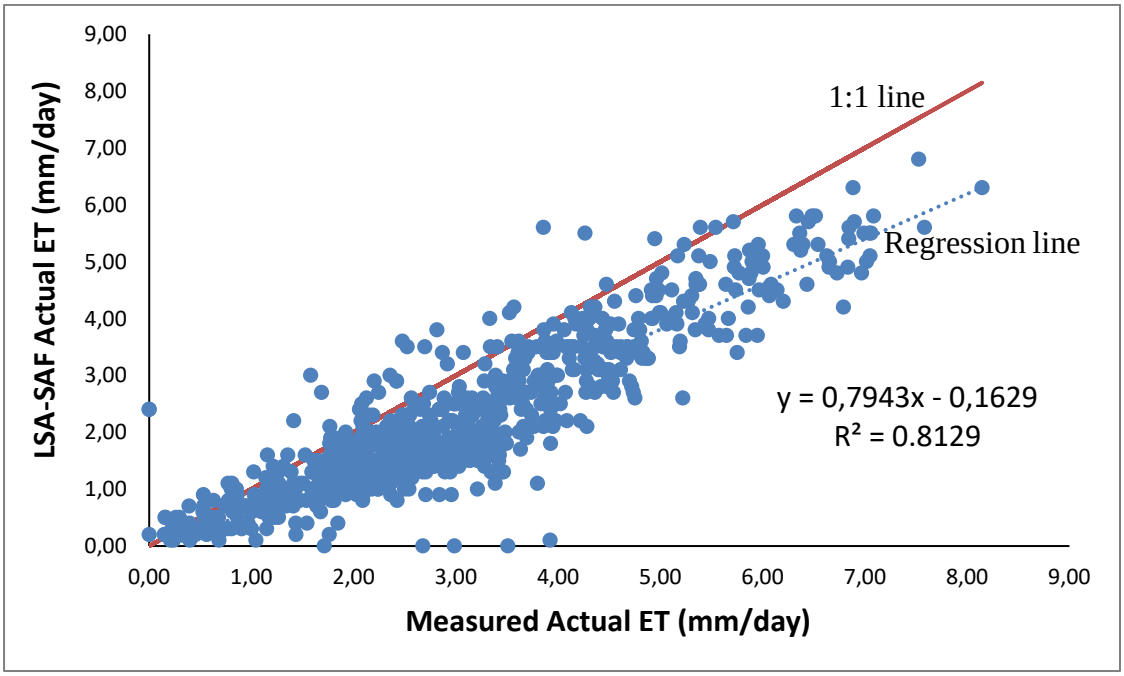

Figure 4.2 Relationship between *in-situ* ET_a and satellite-derived daily LandSAF ET_a estimates.

The R^2 is 0.81. The correlation between the data was determined by a Pearson correlation coefficient for the daily integration of the measured and estimated data, which was 0.90, and the relationship was statistically significant. A Pearson correlation coefficient is a measure of the strength of the association between the two data variables. Since the value 0.90 is close to 1, there is a good relationship between the two variables. The Nash-Sutcliffe efficiency index

yielded a value of 0.57. This statistic is used to assess the predictive power of model when compared to observed data. A MSE of 1.09 and a RMSE of 1.04 was also obtained between the datasets.

A paired t-test was also conducted on the two data sets (Table 4.1). From Table 4.1, it can be seen that the mean of the LSA SAF DMET product is lower than that of the *in-situ* dataset, which results in the t-stat value being positive. These statistics further support the above results and prove that the LSA SAF product underestimates ET_a.

Table 4.1 T-test of *in-situ* against LSA SAF estimates

	In-situ	**LSA SAF**
Mean	3,01	2,23
Variance	2,53	1,96
Observations	719	719
Pearson Correlation	0,90	
Hypothesized Mean Difference	0	
df	718	
t Stat	30,49	
P(T<=t) two-tail	1,17E-131	
t Critical two-tail	1,96	

The inconsistences seen in the data comparison can be attributed to the previously mentioned reasons as well as the following reasons. The *in-situ* dataset that was used to validate the DMET product was not the actual average of the QC, but it was rather obtained from a point within the QC. If the sensors were placed at different locations in the QC, the *in-situ* dataset could be different. Overall, despite the underestimation that was observed, it can be seen that the DMET product followed the trend and correlated well with the *in-situ* data ($R^2 = 0.81$, $r = 0.90$), hence was suitable to provide spatial estimates of ET_a for the ETDI calculation.

Ghilian *et al*. (2011) compared LSA-SAF satellite ET_a estimates with *in-situ* measurements, which produced an overall good confidence in the ET_a results. Ground measurements were retrieved from FLUXNET eddy correlation towers, which displayed positive overall performances, as a correlation between 80%-90% was noted. The product's user manual further stated that the DMET product produces globally lower estimates when compared to the ECMWF, especially in Africa and South America. The validation report also indicates that the model tends to underestimate ET_a in dry climatic conditions, such as the African dry savannah.

The possible reasons for the discrepancies between the model and ground observations are explained in the validation report in detail, with more research and improvements suggested for African countries

In addition, Jovanovic *et al*., (2014) conducted a study in the Western Cape in South Africa that evaluated the reliability of the LSA-SAF MET (30-min estimates) and DMET (30-min estimates) products by comparing it with *in-situ* measurements obtained through a scintillometer system. The study was undertaken at the Riverlands Nature Reserve located in the Western Cape, South Africa. The results produced by the study included Pearsons correlation coefficients of 0.85 and 0.91, and linear regressions produced R^2 values of 0.72 and 0.75 for the MET and DMET products, respectively.

Overall, these results, along with those of a study undertaken in South Africa by Jovanovic *et al*. (2014), show that the results obtained in this study are within the range of correlations and that the satellite derived ET_a estimates correspond relatively well to the ground-based measured ET_a at a daily temporal scale. Hence, the product is able to reproduce a temporal development of ET_a with values comparable to observations. However, it is significantly important that the model quality should be further investigated due to the limited validation in the driest regions of the world (mainly in African countries). It is also important for the model to be validated over other land covers to further improve the results globally.

4.2 Spatial and Temporal Distribution of Actual Evapotranspiration Estimates obtained from the LSA-SAF DMET Product

This section will display the spatial annual mean ET_a maps that were calculated from daily ET_a over the six-year period (2011-2016) and derived from the LSA-SAF DMET product (Figure 4.3). ET_a values were extracted for the Umgeni Catchment at a tertiary and QC level, while the Upper Thukela Catchment values were extracted for the entire Upper Thukela (V) and at a secondary level (V1, V2, V6, V7) as well as at a QC level.

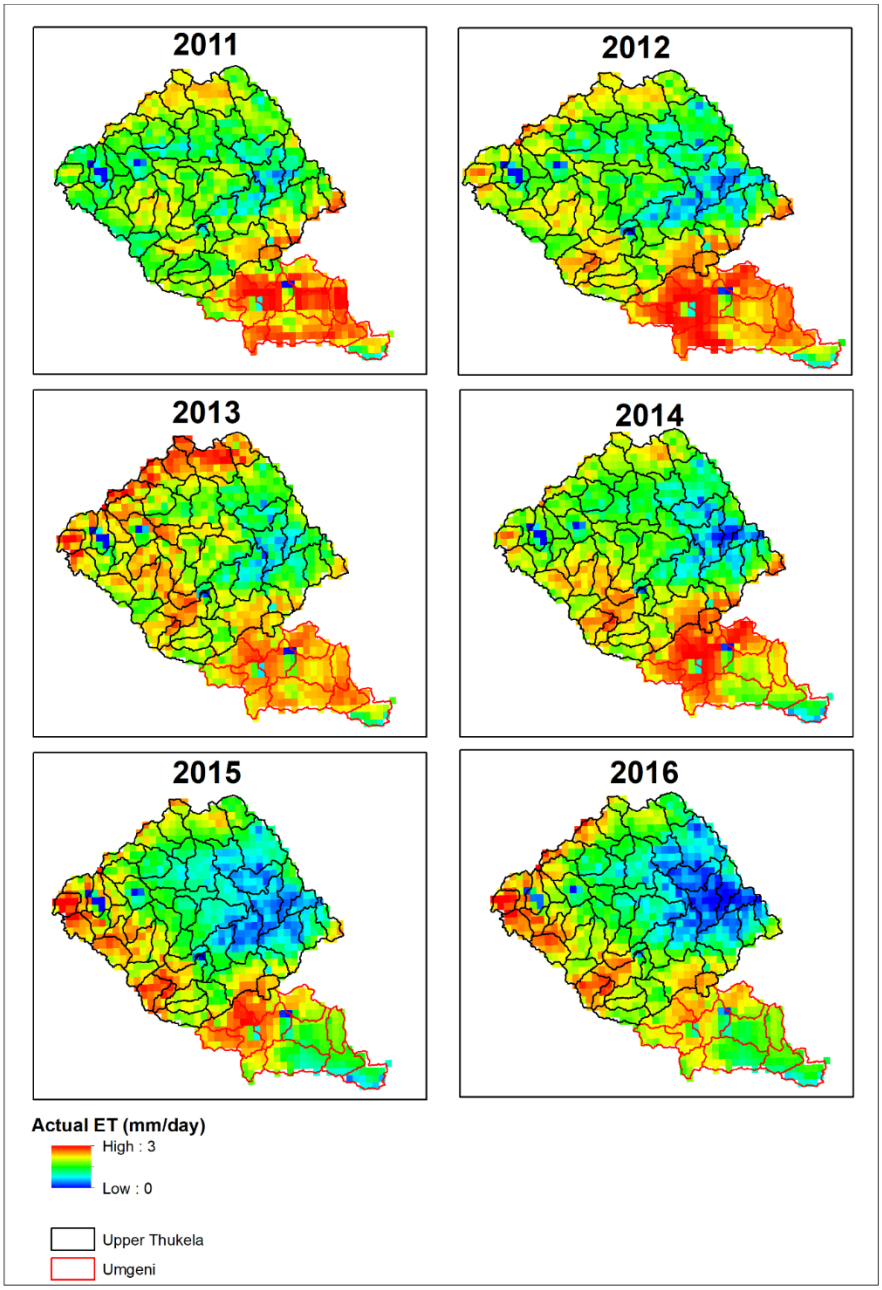

Figure 4.3 Annual averaged ET_a estimates for 2011-2016

From Figure 4.3, it can be seen that ET_a values are higher in the Umgeni Catchment in comparison to the Upper Thukela Catchment. Furthermore, higher ET_a values are shown for the years 2011, 2012, 2013 and 2014 in comparison to the years 2015 and 2016 for the Umgeni Catchment. This could be due to the catchment experiencing higher rainfall for the years 2011 to 2014 than for the years 2015 and 2016, which have been labelled as the "drought years" that have negatively impacted the Umgeni Catchment. Therefore, years 2011 to 2014 had adequate rainfall, hence a higher availability of water for evaporation to occur which resulted in higher ET_a values. This is illustrated further in

Figure 4.4. Annual rainfall totals for QC U20J indicate a decreasing trend in rainfall over the years (2011-2016) as seen in Figure 4.4. As depicted by Figure 4.4, 2011-2013 displays higher rainfall totals explaining the higher ET_a while, 2014-2016 display lower rainfall totals. Figure 4.3 displays high ET_a values for 2014, which may be due to the ET_a that was being detected following the higher rainfall experienced in the previous year.

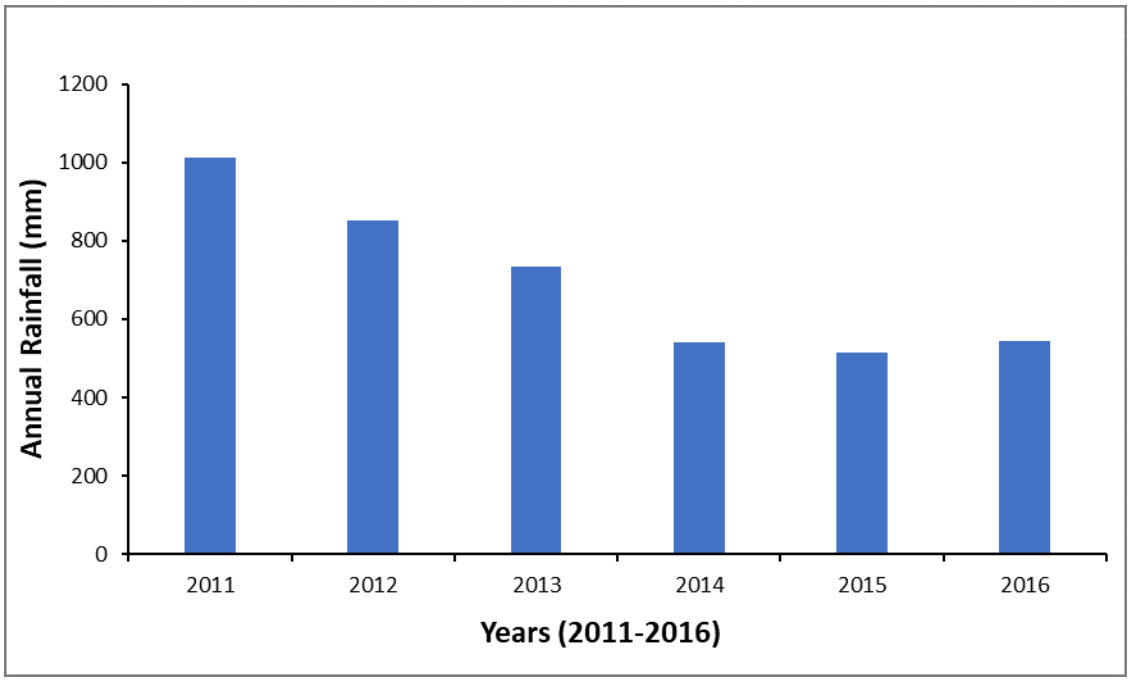

Figure 4.4 Annual rainfall totals for U20J, in the Umgeni Catchment (2011-2016)

The Upper Thukela Catchment located directly north of the Umgeni Catchment, displayed higher ET_a values along the Upper Thukela Catchment boundary, where high elevation occurs as compared to the rest of the catchment. The high ET_a values seen at a higher elevation for the Upper Thukela can be a result of more rainfall occurring in these areas due to the rising and cooling of air, which results in rainfall, and hence there is adequate moisture to allow for ET_a processes to occur. Overall, low ET_a values for the Upper Thukela are seen for years 2015 and 2016 indicating dry conditions within the catchment.

4.2.1 Trends of LSA-SAF derived actual ET

The trend of derived ET_a from 2011-2016 was analysed at a tertiary level (U20) for the Umgeni Catchment and for the Upper Thukela Catchment as shown in Tables 4.2 and 4.3. The ET_a values over the six year period at a monthly timescale have been used for the temporal

distribution analysis in drought assessment in order to display trends in the seasons (Figures 4.5 and 4.6).

Table 4.2 Daily averaged ET_a (Umgeni)

Daily actual ET tertiary averaged for Umgeni Catchment (U20)						
	2011	**2012**	**2013**	**2014**	**2015**	**2016**
Jan	1,94	3,28	3,03	3,05	2,75	2,38
Feb	2,18	2,89	3,18	2,85	2,71	2,64
Mar	1,77	2,69	2,34	2,45	2,26	2,30
Apr	1,26	2,13	2,29	1,95	1,74	1,63
May	1,24	1,53	1,63	1,37	1,19	1,28
Jun	1,22	1,11	1,24	0,99	0,60	0,78
Jul	0,95	1,10	1,17	0,94	0,72	0,71
Aug	1,63	1,58	1,40	1,04	0,93	1,35
Sep	1,80	1,56	1,38	1,13	1,14	1,31
Oct	2,05	1,86	1,72	1,59	1,37	1,63
Nov	2,37	2,46	2,70	2,01	1,75	1,92
Dec	2,83	3,08	2,44	2,48	2,45	2,38

Table 4.3 Daily averaged ET_a (Upper Thukela)

Daily actual ET primary averaged for the Upper Thukela Catchment (V)						
	2011	**2012**	**2013**	**2014**	**2015**	**2016**
Jan	2,73	2,94	3,34	2,97	3,04	2,46
Feb	2,62	2,94	3,09	2,78	2,81	2,77
Mar	1,87	2,33	2,25	2,48	2,35	2,24
Apr	1,44	1,45	1,99	1,73	1,45	1,10
May	1,02	0,83	1,41	0,89	0,76	0,64
Jun	0,82	0,46	0,87	0,49	0,32	0,37
Jul	0,55	0,50	0,69	0,46	0,48	0,39
Aug	1,16	0,92	0,75	0,57	0,54	0,79
Sep	0,95	1,37	0,60	0,53	0,61	0,78
Oct	1,35	1,80	1,06	1,39	0,91	1,17
Nov	1,74	2,87	2,26	2,23	1,04	1,85
Dec	2,57	3,22	2,72	2,75	2,22	2,11

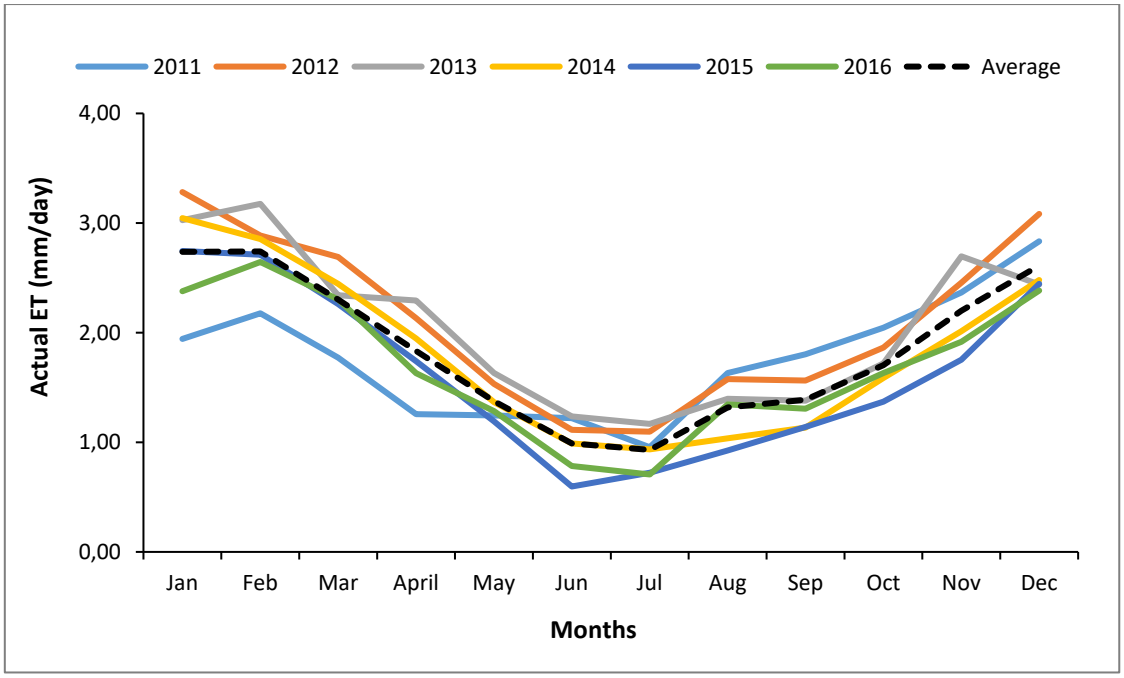

Figure 4.5 ET_a trend for 2011-2016 for catchment average (Umgeni)

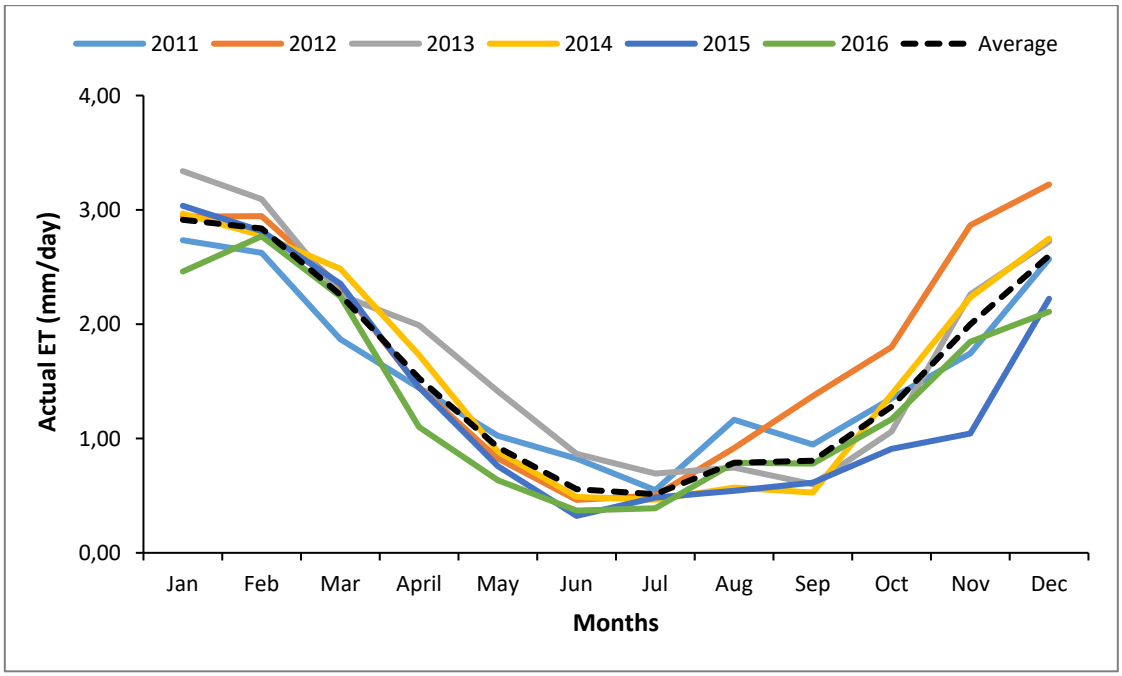

Figure 4.6 ET_a trend for 2011-2016 for catchment average (Upper Thukela)

Tables 4.2 and 4.3 display the ET_a trend for different years from the averaged monthly values for the Upper Thukela and Umgeni Catchments. Tables 4.2 and 4.3 display higher ET_a values during the summer months in comparison to the winter months (seasonal fluctuations). This is attributed to wetter periods that occur during the summer as a result of, rainfall generating sufficient moisture for ET_a processes to occur. Other factors that influence ET_a estimates may

include higher temperatures and solar radiation as well as increases in the vapour pressure deficit (VPD) during the summer seasons. For both catchments, the lowest ET_a values during the summer and winter months were recorded for years 2015 and 2016. From Figures 4.5 and 4.6, the highest average ET_a is observed for the year 2013 during the summer period. The black dotted line in both graphs shows the mean ET_a over the six-year period, while the rest display the monthly averaged ET_a. The monthly values of averaged daily ET_a values fall within the range of 0-3.5 mm.day^{-1}, with the highest average ET_a values being recorded during the summer months. Hence, the temporal trend of ET_a for all years are following a seasonal trend with maximum ET_a values occurring during the growing season (summer months).

4.3 Estimating Reference Evaporation using Remote Sensing and the Hargreaves Empirical Model

During the duration of this study, the search for ET_o estimates from ground stations turned into a complex task. ET_o estimates especially in the high mountainous areas within the Upper Thukela Catchment were not available. In addition, ground stations are found to be insufficient to represent the spatial and temporal variation of ET_o. The lack of meteorological data from ground stations is a barrier to the management of water resources within a country, especially in developing countries. The study undertaken by Maeda *et al*. (2011) was used as a reference paper in this section of this study.

This study employed and evaluated the temperature-based Hargreaves empirical equation and to overcome the poor availability of meteorological data, LST data acquired by the MODIS sensor were tested as an alternative input into the model. Chapter 3 discusses the methodology that has been adopted by this study. Since LST data was used to replace the air temperature from ground stations, the Hargreaves model will be hereafter be referred to as the Hargreaves-LST. LST maps obtained from the MOD11A2 product for the study period (2011-2016) are shown in Figure 4.7.

Spatially, the distribution of the MOD11A2 LST product over the period from 2011 to 2016 for the study areas is represented in Figure 4.7. Temperature fluctuations are seen to occur during the different months in response to the seasonal differences. The maps depicted a clear spatial pattern with higher LST values during the spring-summer months and lower LST values during the autumn-winter months and in high altitude areas.

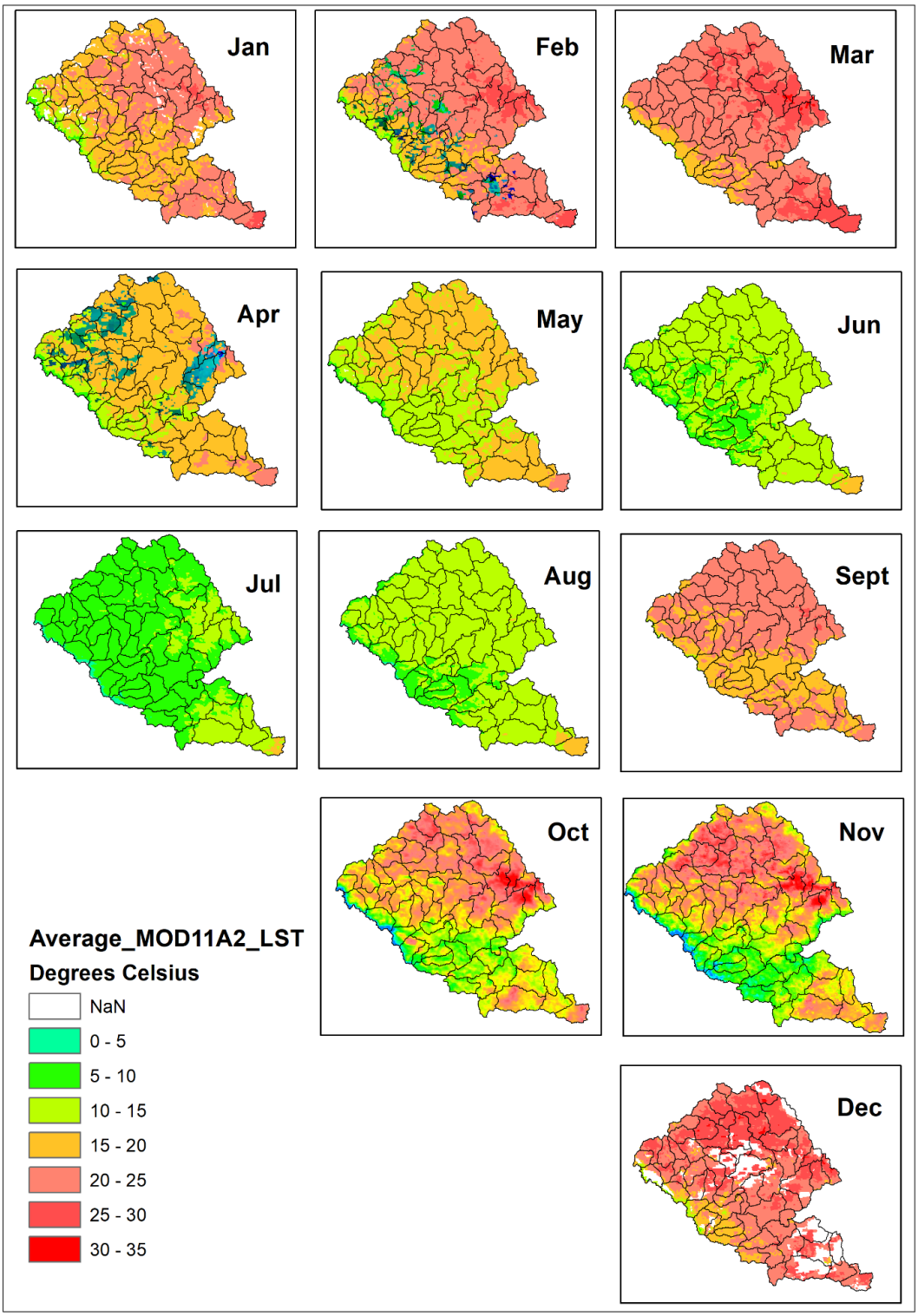

Figure 4.7 Monthly average MOD11A2 Land Surface Temperature (LST) maps for the Upper Thukela and Umgeni Catchments for 2011-2016

The estimates from the MOD11A2 product were used as an input into the Hargreaves model to enable the calculation of satellite-derived ET_o estimates. Spatial distribution of the Hargreaves-LST estimates for the period 2011 to 2016 is shown below in Figure 4.8.

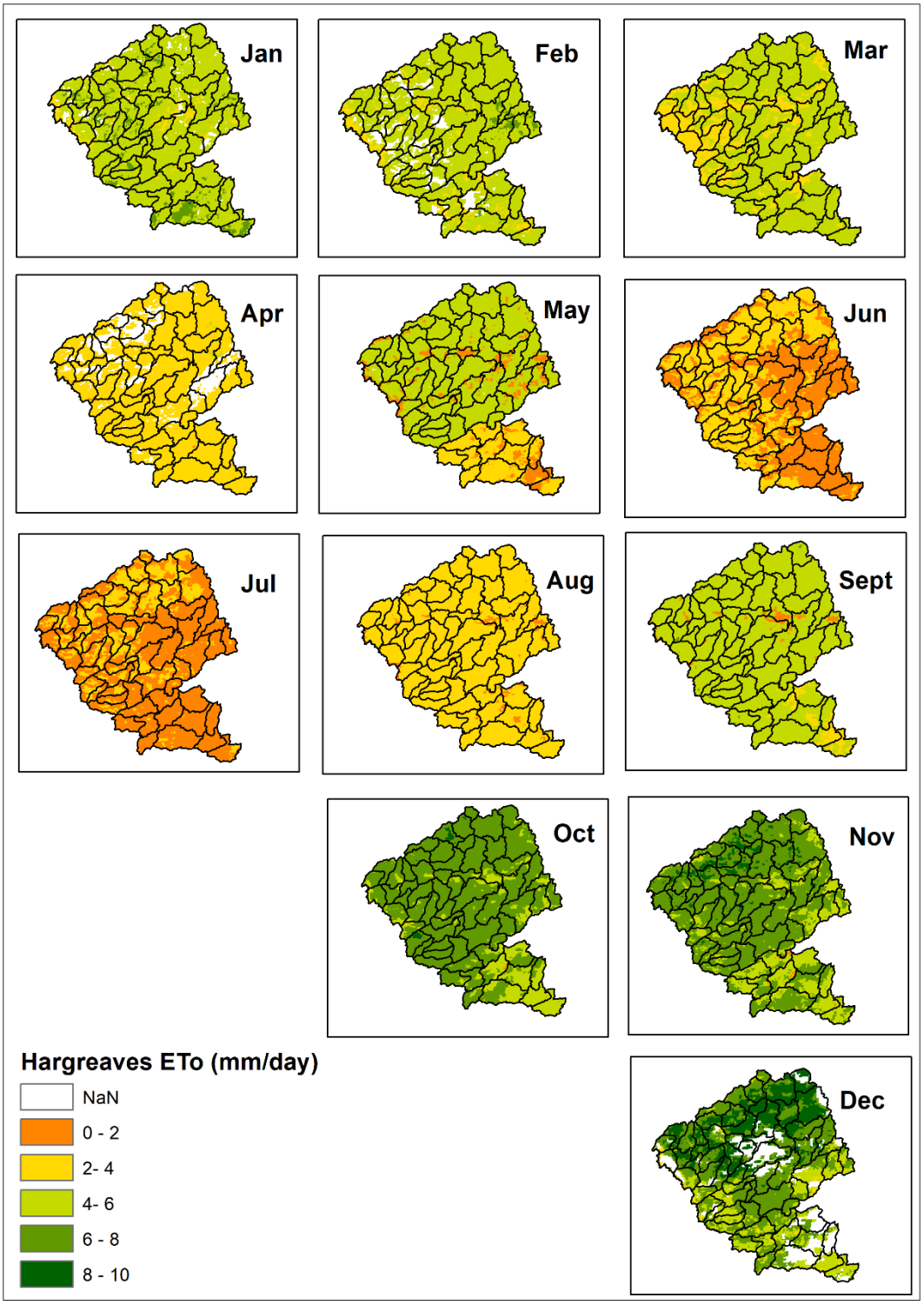

Figure 4.8 Monthly average Reference Evapotranspiration (ET_o) maps obtained using the Hargreaves model and averaged 8-day LST records from 2011-2016

Changes in the ET_o over the months can be attributed to differences in land surface and atmospheric temperature. In general, the spatial distribution in all the maps depicted a clear seasonal spatio-temporal pattern of ET_o, which was higher between September to March, and

which reached the lowest values between April to August. During the winter season, clear changes in the spatial patterns are displayed with low ET_o values being detected due to drier conditions prevailing and a lower availability of water/moisture for evaporation to occur. Overall, these maps displayed the potential of the Hargreaves-LST methodology in providing information over large spatial areas as well as in mountainous areas, which are not often provided by weather stations.

4.3.1 Calibrating the Hargreaves empirical model

Studies that have applied the Hargreaves model report on the effectiveness of the model in estimating ET_o; however, the empirical nature of the model makes local calibration necessary (Maeda *et al*., 2011). This study utilised available FAO-PM estimates from the ISCW-ARC ground stations within the study area. The calibration procedure of the empirical model was conducted only on selected QC's within the research study area due to the limited availability of meteorological data. In total, eight calibrations were completed. Four calibrations were completed within the Umgeni Catchment and four calibrations were completed within the Upper Thukela Catchment. The selected QC's on which the calibration was performed can be seen in Table 4.4 along with the respective station's necessary information.

A comparison between the air temperature data measured at the respective weather stations and the LST data obtained by the MODIS sensor is presented for each QC within the Umgeni Catchment in Figure 4.9, while comparisons for the Upper Thukela Catchment are presented in Figure 4.10. The Figures display the monthly averages from 2011 to 2016.

Table 4.4 List of selected Quaternary Catchment's used in the calibration of the Hargreaves empirical model. A summary of the coordinates of the selected meteorological weather stations, including their respective altitudes

UMGENI CATCHMENT				
Quaternary Name	**Station Name**	**Altitude (m)**	**Longitude**	**Latitude**
U20E	Cedara_PP	1068	30.26498	-29.54190
U20F	New Hanover	822	30.50000	-29.36666
U20G	Faulklands	660	30.52147	-29.55431
U20J	PMB; Ukhulinga	809	30.40615	-29.66787
UPPER THUKELA CATCHMENT				
Quaternary Name	**Station Name**	**Altitude (m)**	**Longitude**	**Latitude**
V11C	Drakensville Educational Centre (DEC)	1226	29.12320	-28.61337
V14D	Weenen; Sun Valley	699	30.08891	-28.78301
V20B	Kamberg-Meshlynn: AWS	1552	29.72355	-29.33741
V20E	Weston College	1469	30.03594	-29.21299

As depicted in Figure 4.9, a close fit between the mean air temperature (T_{mean}) and the mean MODIS LST is observed as well as, between the minimum air temperature (T_{min}) and the night MODIS LST. However, variations in the comparison between the maximum air temperature (T_{max}) and day MODIS LST are displayed. In QC U20J, seasonal variations are visible between the maximum air temperature and the day LST, while QC's U20E, U20F and U20G have similar variations from September to December. The reason for the discrepancies between the maximum air temperature and day LST are discussed further below.

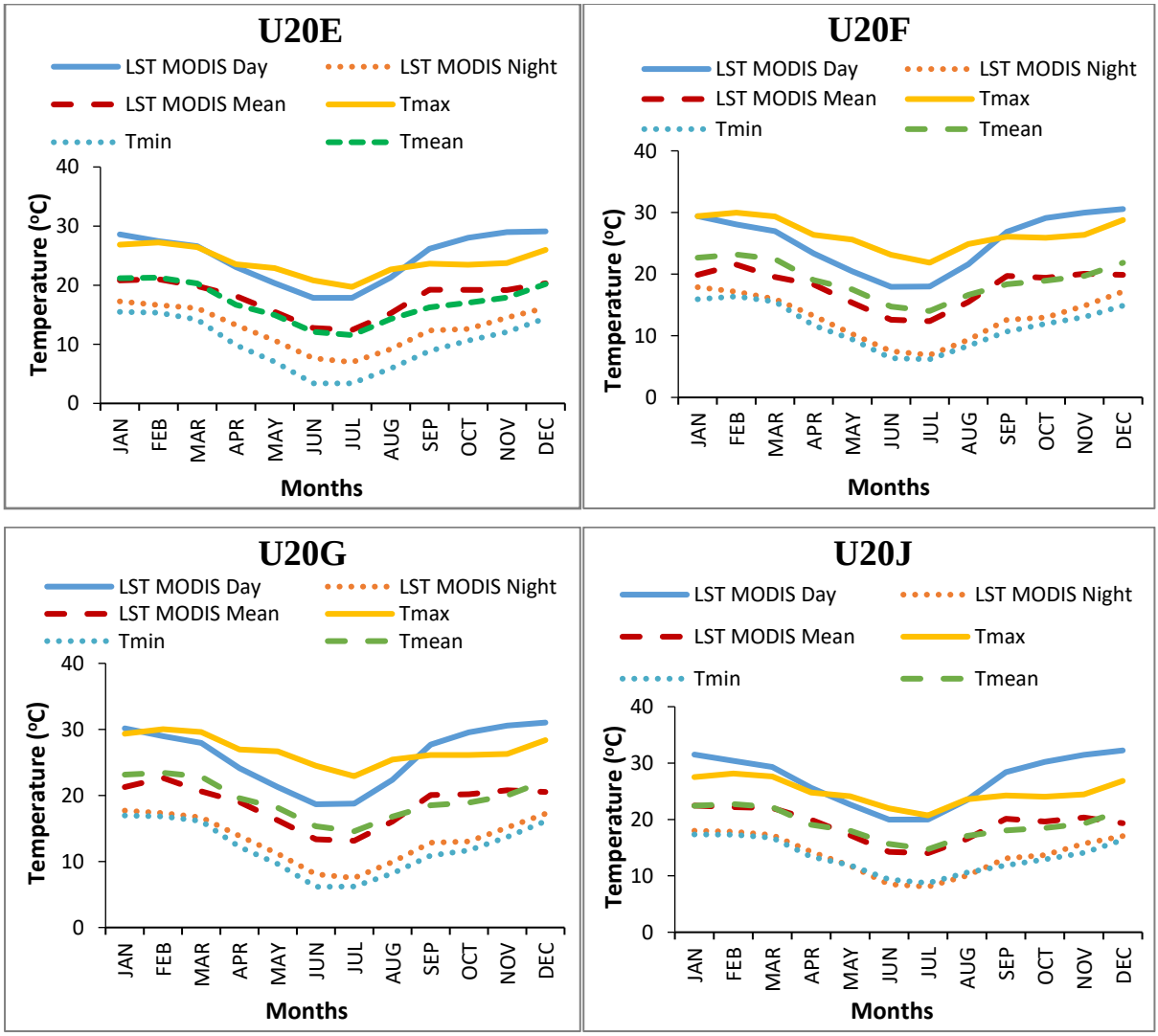

Figure 4.9 Monthly averages of maximum, minimum and mean air temperature for selected Umgeni QC's, along with monthly averages of day, night and mean Land Surface Temperature (LST)

From Figure 4.10, as also seen in Figure 4.9 there is a close fit between the mean air temperature (T_{mean}) and the mean MODIS LST as well as between the minimum air temperature (T_{min}) and the night MODIS LST for the Upper Thukela quaternaries. Variations in the comparison between the maximum air temperature and day LST were once again observed.

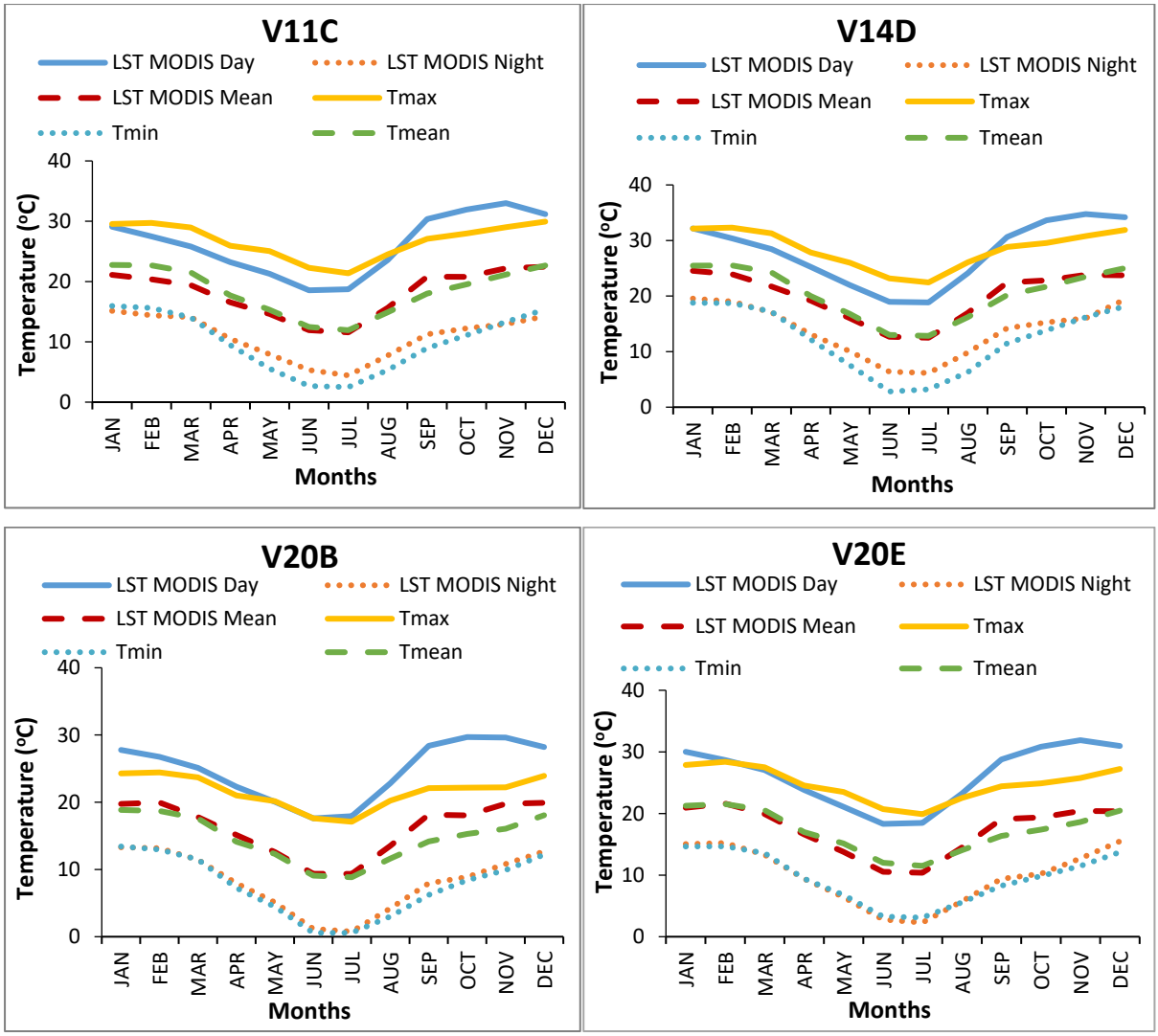

Figure 4.10 Monthly averages of maximum, minimum and mean air temperature for selected Upper Thukela QC's, along with monthly averages of day, night and mean Land Surface Temperature (LST)

The differences observed between the MODIS-LST maximum temperature data and day air temperature have already been reported in literature especially season differences. Authors suggest that changes in the vegetation phenology during the summer play a key role in reducing the correlation between LST and max/min air temperatures (Ceccato and Dinku, 2010; Vancutsem *et al.*, 2010). Vancutsem *et al.* (2010) compared the MODIS day LST with the maximum air temperature in Africa over different ecosystems. These authors reported that in addition to seasonality factors, the discrepancies between day LST and T_{max} may vary, in accordance with the solar radiation, cloud cover and ecosystems. The IRI Technical Report (Ceccato and Dinku, 2010), reported on comparisons between the air temperature and MODIS temperature, MODIS night-time products displayed a good estimation of minimum air

temperature over all ecosystems in Africa. However, comparisons between maximum air temperature and MODIS daytime data showed differences that varied with the ecosystems, cloud cover, seasonality and solar radiation. This indicates that further research needs to be undertaken on robust methods to retrieve maximum air temperature data.

With respect to the reliability of the MOD11A2 product, it has been noted to have been extensively tested using radiation-based validation and that it has *in-situ* values (Wan *et al*., 2002, 2004; Wan, 2008; Coll *et al*., 2009). The results produced by these tests indicated that in the majority of cases the MODIS LST error is found to be lower than 1 Kelvin. Therefore, intrinsic errors of air temperature data should also be accounted for as a possible cause of the discrepancies observed. Despite the fact that the surface air temperature data used in this current study was screened to eliminate missing records, it is noted that various other sources of error can be identified from the ground station records. The sources of such error may include, but may not be limited to, failure in equipment, uncalibrated and old equipment that usually cause low quality measurements or unskilled operators. Overall, it can be seen that the MOD11A2 is suitable for providing spatial estimates of LST for use within the Hargreaves-LST approach to enable the calculation of the ETDI.

The performance of the model was determined by using standard statistics and linear regression analysis, with the reference dataset being the surface air temperature data obtained from meteorological weather stations. The performance of the Hargreaves-LST estimates was also evaluated using the following: the Mean Absolute Deviation (MAD), the Mean Square Error (MSE), the Root Mean Square Error (RMSE), the Mean Absolute Percentage Error (MAPE) and the Pearson correlation coefficient. The coefficient of determination was considered to be a measure of precision. The results obtained in the evaluation of the model are summarized below in Table 4.5, while graphs of the regression analysis are shown in Figure 4.13 and Figure 4.14. These figures provides a visual illustration for ET_o estimates using different inputs to allow for visual interpretation and comparison of the models performance in estimating ET_o.

Table 4.5 Summary of the results obtained from the model's error analysis between the calibrated Hargreaves-LST and the FAO-Penman Monteith estimates obtained from the ARC.

UMGENI CATCHMENT					
Quaternary Name	**MAD**	**MSE**	**RMSE**	**MAPE**	**Correlation Coefficient (r)**
U20E	0,21	0,06	0,25	7,23	0,90
U20F	0,23	0,08	0,28	7,24	0,92
U20G	0,25	0,09	0,31	8,84	0,88
U20J	0,20	0,05	0,23	6,48	0,93
UPPER THUKELA CATCHMENT					
Quaternary Name	**MAD**	**MSE**	**RMSE**	**MAPE**	**Correlation Coefficient (r)**
V11C	0,15	0,03	0,17	4,28	0,98
V14D	0,37	0,20	0,44	9,35	0,93
V20B	0,19	0,05	0,22	6,35	0,91
V20E	0,28	0,11	0,33	8,38	0,86

As described in Equations 4.1, 4.2, 4.3 and 4.4, these standard statistics were used to quantify the differences between the ET_o that was estimated by using the reference method (FAO-PM), which was obtained from the ISCW-ARC and the estimates obtained by using the Hargreaves equation parameterized using MODIS LST data. The statistics are similar for each of the QC's. The MAD, which describes the sum of the absolute differences, ranged between 0.20 $mm.m^{-1}$ to 0.25 $mm.m^{-1}$ for the Umgeni Catchment, while it ranged between 0.15 $mm.m^{-1}$ to 0.37 $mm.m^{-1}$ for the Upper Thukela Catchment.

MSE ranged between 0.05 $mm.m^{-1}$ to 0.09 $mm.m^{-1}$ for the Umgeni Catchment and between 0.03 $mm.m^{-1}$ to 0.20 $mm.m^{-1}$ for the Upper Thukela Catchment. RMSE ranged between 0.23 $mm.m^{-1}$ to 0.31 $mm.m^{-1}$ for the Umgeni Catchment, and between 0.18 $mm.m^{-1}$ to 0.44 $mm.m^{-1}$ for the Upper Thukela Catchment. The smaller the RMSE value, the closer the predicted and observed values are. The MAPE known as the error percentage was found to be between the range of 6.48 % to 8.83% for the Umgeni Catchment and between 4.28% to 9.35% for the Upper Thukela Catchment. The MAPE showed no statistically significant errors as; all errors were below 10 %. The correlation coefficient *r*, which is a measurement of the strength of the linearity relationship that occurs between two variables on a scatterplot, ranges between +1 to -1, with a value closer to 1 indicating that the datasets correlate better. For the Umgeni

Catchment, *r* ranged between 0.88 to 0.93, while with respect to the Upper Thukela Catchment *r* values ranged between 0.86 to 0.98.

The monthly MSE and RMSE obtained by the Hargreaves-LST model were found to be consistent with the results observed in other studies. For instance, a study undertaken by Ahmadi and Fooladmand (2008) in the South of Iran achieved monthly errors, which ranged from 0.37 to 0.62 mm day^{-1} and the average RMSE obtained was 0.47 mm day^{-1}. A study by Gavilán *et al*. (2006), which focused on the evaluation of the Hargreaves equation under a semi-arid environment, was carried out in Southern Spain. The results of this study produced an RMSE ranging from 0.46 to 1.65 mm day^{-1}, which were found to be compatible with the results produced by the above study by Gavilán *et al*. (2006). Narongrit and Yasuoka (2003) compared the Hargreaves-LST model with the FAO-PM method, which achieved an R^2 of 0.57 and 0.60.

Maeda *et al*. (2011) performed a study evaluating the Hargreaves-LST model in Kenya and produced results that consisted of a RMSE of 0.47 mm $day^{-1}$and a correlation coefficient (r-value) of 0.67 when compared to the FAO-PM method. The above studies are among many other studies that have showed the same ranges. Another study by Zheng and Zhu *et al*. (2014), which was undertaken in North China incorporated MODIS LST data into the Hargreaves model, while a study by Castro and Parra (2015) proposed a multiple regression model to estimate ET_o using MODIS/TERRA data. Results from that study indicated the feasibility of utilising data from satellite sensors, particularly from the MODIS/TERRA sensor for estimating ET_o as the images consists of known spatial ranges. From the results of the mentioned studies and the results produced from these studies, it is clearly understood that the results achieved in this study are consistent with those results observed in previous published research. Overall, by taking into account the above statistics, the model performed well.

The monthly average values of ET_o estimates for the period 2011 to 2016 with respect to the Umgeni Catchment are shown in Figure 4.11. It illustrates the profiles obtained by the reference method (denoted as "ARC-ET0" in the graphs) that were obtained from the ISCW-ARC along with three more profiles, which utilised different LST inputs. "Hargreaves-LST" refers to the non-calibrated ET_o estimates, "Hargreaves-Calibrated" refers to the calibrated ET_o estimates and "Hargreaves-ARC" refers to the Hargreaves approach, which used ground station temperature values as an input into the model.

The profile of the curve formed by the calibrated Hargreaves-LST model estimates closely follows the profile obtained by using the reference method (ARC-ET0) during the entire study period. The worst fit profiles are the non-calibrated Hargreaves-LST and the Hargreaves methods using ARC temperature as an input. It is therefore recommended that the calibrated Hargreaves-LST estimates be used if sufficient data is available to allow the calibration procedure to be performed.

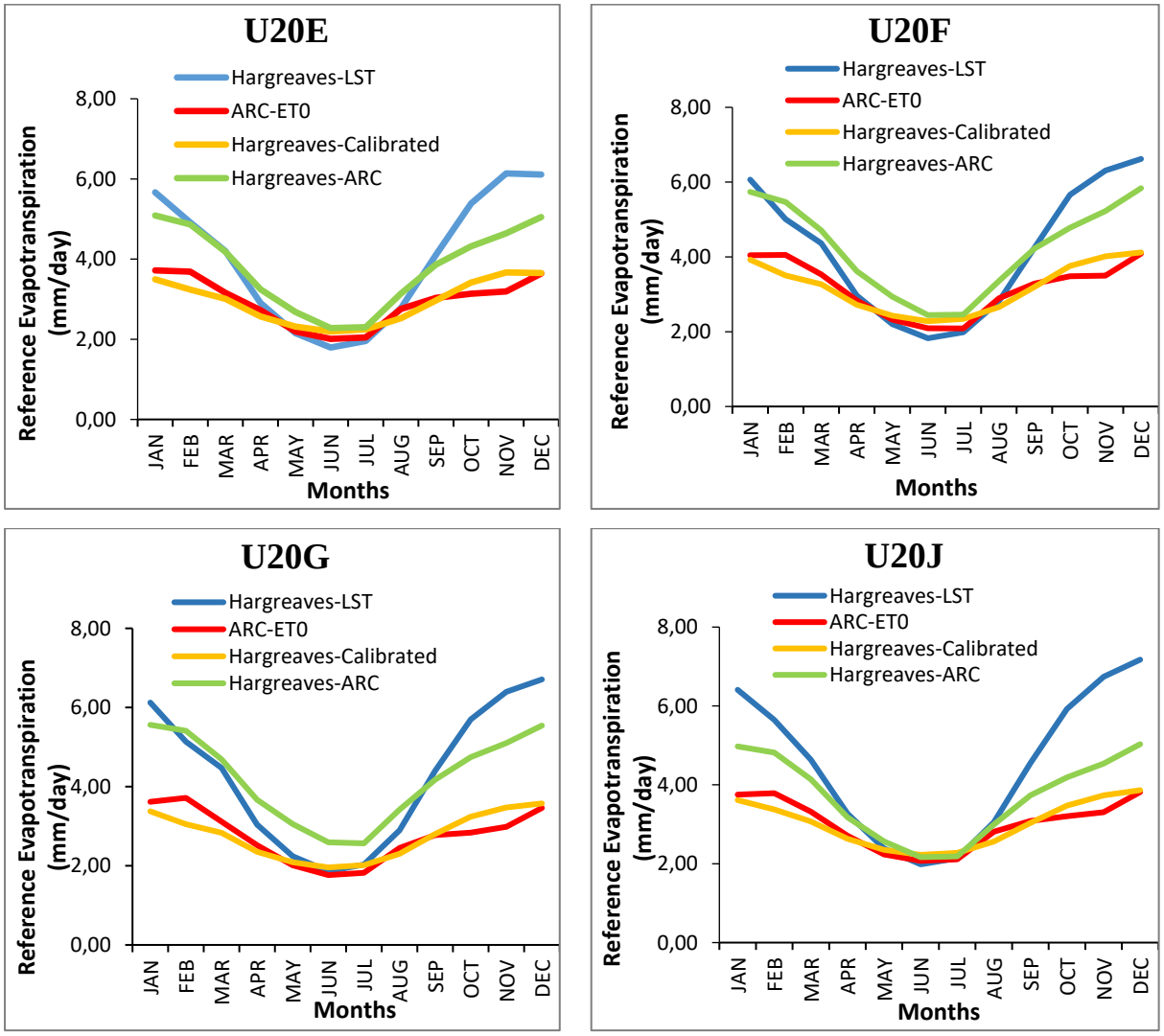

Figure 4.11 Monthly average distribution of ET_o estimated by the ARC and compared with the values calculated by the Hargreaves method using different LST input data for selected QC's within the Umgeni Catchment (2011-2016)

Figure 4.12 shows the monthly averaged values of the ET_o estimates for the Upper Thukela Catchment for the period 2011 to 2016. Once again, the profile curve formed by the calibrated Hargreaves-LST model estimates correlate well with the profile obtained using the reference

method (ARC-ET0) for the entire study duration. The worst fit profiles are the non-calibrated Hargreaves-LST and the Hargreaves methods using ARC temperature as an input for V20B and V20E, while these profiles for QC's V11C and V14D display seasonal QC's fluctuations with a close fit visible during winter months while significant comparisons are seen during the summer months. It should be noted that QC's V11C and V14D have higher altitudes compared to V20B and V20E, which may have influenced the results achieved.

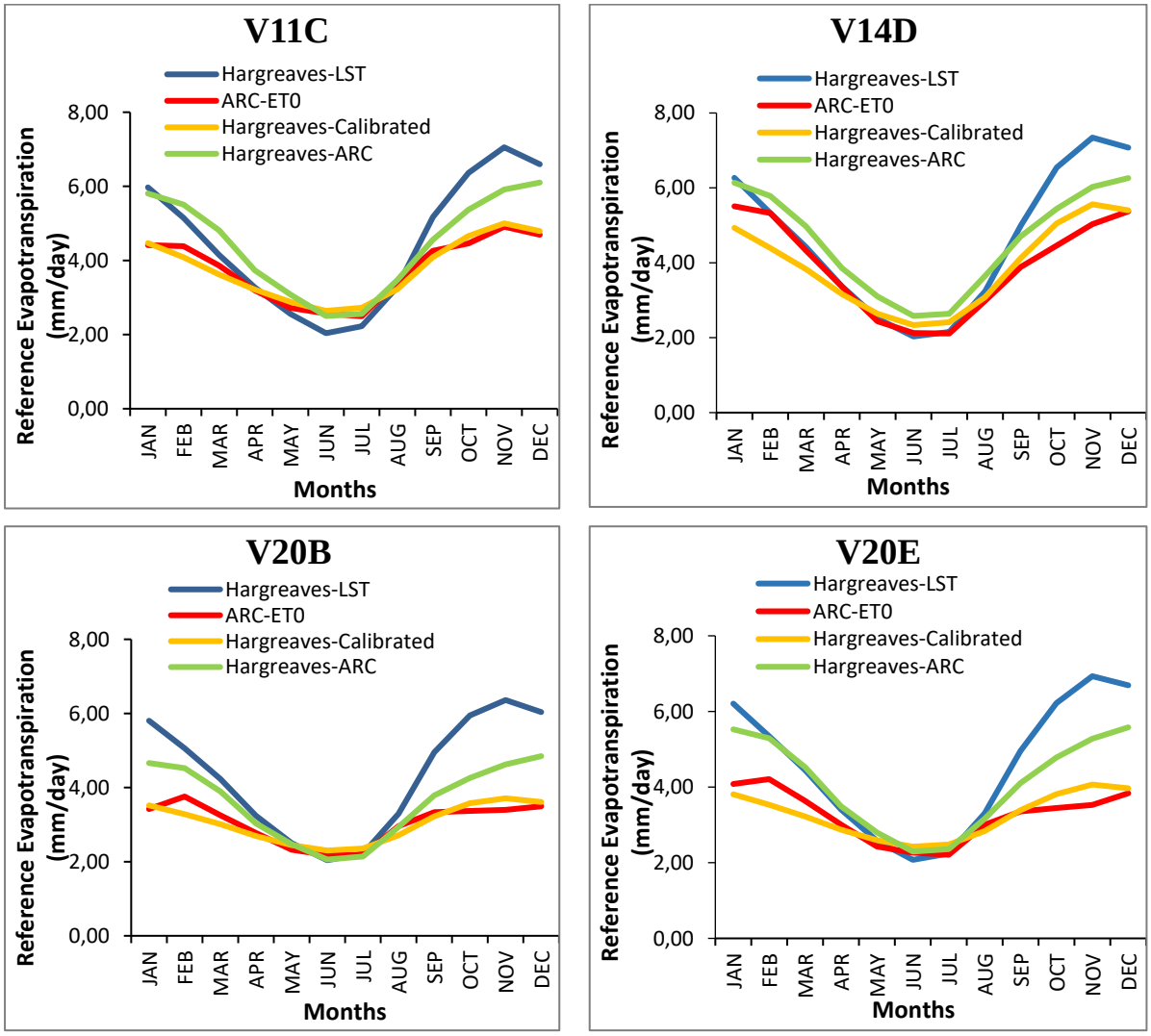

Figure 4.12 Monthly average distribution of ET_o estimated by the ARC and compared with the values calculated by the Hargreaves method using different LST input data for selected QC's within the Upper Thukela Catchment (2011-2016)

Overall, if sufficient data is available to allow the calibration procedure to be performed, it is recommended that the calibrated Hargreaves-LST estimates be used as the model is empirically based therefore local rigorous calibration is needed.

The fitted regression lines obtained in the regression analysis was performed using the reference and calibrated model are displayed in Figure 4.13 for the Umgeni Catchment and in Figure 4.14 for the Upper Thukela Catchment.

The Hargreaves-LST model performed well for the Umgeni and Upper Thukela Catchments. R^2 values ranging between 0.74 to 0.96 are produced for the Umgeni and Upper Thukela Catchments indicating a good fit between the data and the regression lines. The negative y-intercepts of 0.0187 and 0.0844 for QC's V11C and V14D, which are located at higher altitudes compared to the other QC's are indicative of an underestimation of ET_o estimates produced by the Hargreaves-LST approach when compared to the reference estimates. The remaining QC's with a positive y-intercept represent a slight over-estimation of ET_o estimates produced by the Hargreaves-LST approach in comparison to the reference estimates.

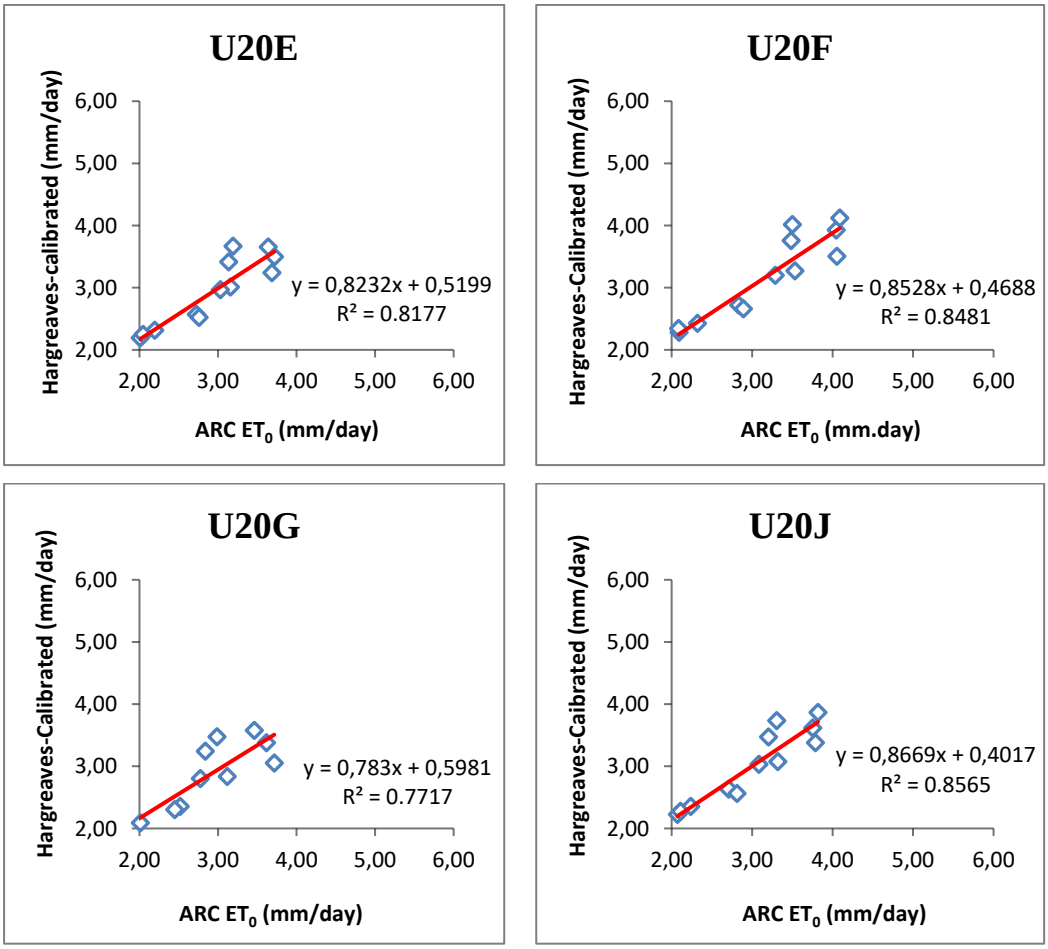

Figure 4.13 Fitted regression lines obtained from the regression analyses performed using the reference method (ARC-ET0) and the calibrated Hargreaves-LST method for the Umgeni Catchment

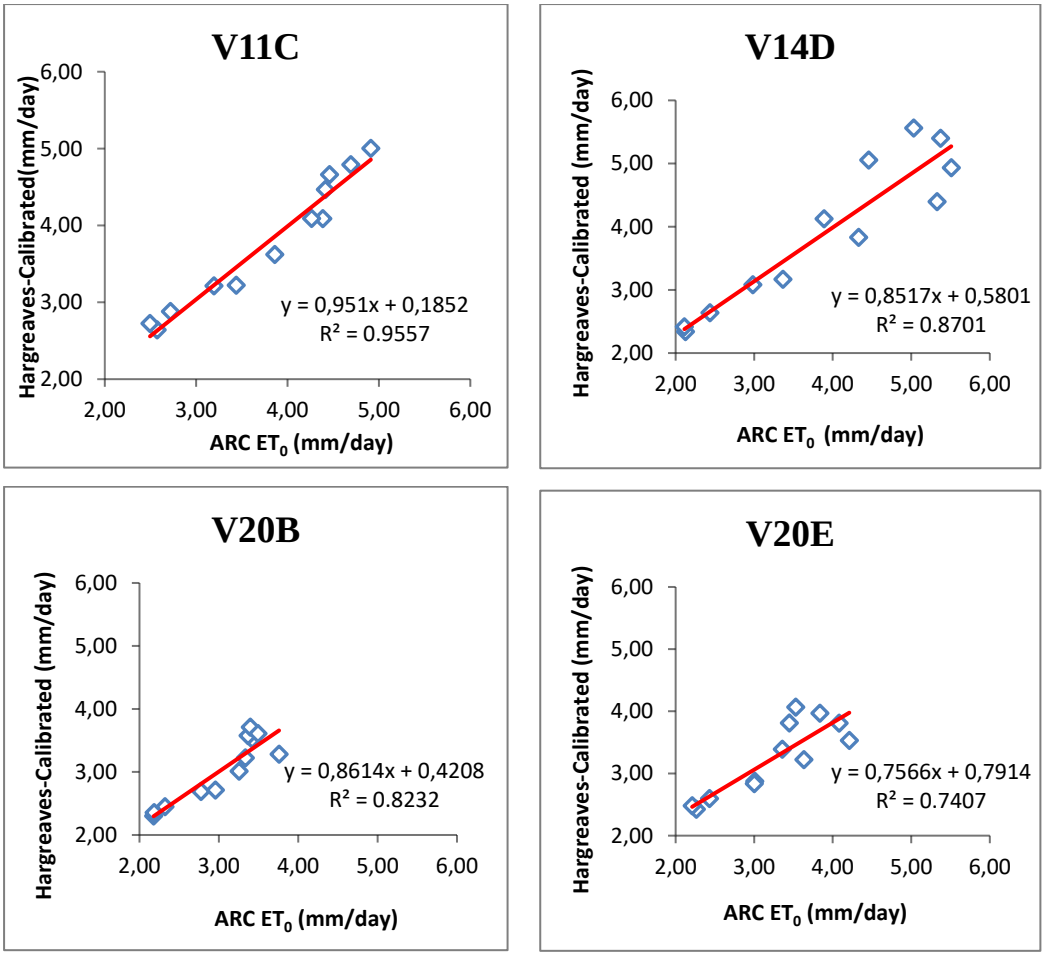

Figure 4.14 Fitted regression lines obtained from the regression analyses performed using the reference method (ARC-ET0) and the calibrated Hargreaves-LST method for the Upper Thukela Catchment

Considering the results achieved in this study and the comparisons with previous studies, it is concluded that the calibrated Hargreaves-LST model achieved good results in the linear regression and in the analysis of errors, and that they are consistent with results obtained in previous studies. In addition, studies by Ahmadi and Fooladmand (2008) and Gavilán *et al.* (2006) utilised ground data from weather stations as input for the evaluation of the Hargreaves model. However, the results produced from the above studies and the results produced by this study were seen to be consistent, yet this study evaluated the Hargreaves model, using MODIS-LST as an input. Despite this empirical model being initially developed using air temperature, this particular study demonstrated that similar results can be attained by using SEO of land surface temperatures (MODIS-LST) as an alternative input in areas within South Africa and areas where the availability of ground data is poor. Nevertheless, Figures 4.9, 4.10, 4.11 and 4.12 indicate that the errors and accuracy of this method may vary with the season and different

ecosystems. However, it is feasible to assert that this methodology is appropriate for this study, which incorporates RS data.

It is also worth mentioning that the use of LST data from orbital sensors presents the benefit of enabling the spatial analysis of ET_o at a greater spatial resolution. The benefit of using a spatially-explicit technique is portrayed in the maps in Figure 4.8 which allow for the identification of the spatio-temporal variation of ET_o at different spatial scales. This advantage would be technically impossible using conventional methods, which utilise data from ground stations. A spatially-explicit characteristic of the ET_o model can benefit the monitoring of droughts, provide relevant information on crop water requirements, risk assessments, improve water resources management, play a role in policy decision-making for land use allocation and the forecasting of agricultural yields.

This section of the research study presented an alternative for estimating ET_o using LST data from the MODIS sensor and an empirical model, for use in South Africa. Based on the statistics and regression analysis, the Hargreaves-LST approach is appropriate for use within South Africa. Despite some drawbacks when utilising the maximum LST data as input into the model, the MOD11A2 LST product was satisfactorily incorporated into the model. The results and outcomes of this approach are consistent with previous research, including research that utilised air temperature obtained from ground stations. Furthermore, the uncertainties and errors associated with the LST data can be tolerated when accounting for the limited availability of ground data. The methodology presented in this study can be noted to be a feasible alternative for estimating ET_o in South Africa without additional cost since the MODIS LST product is freely available and it can be improved with the use of low cost direct methods such as the use of lysimeters to calibrate the empirical model. It must be noted that calibration is necessary to signify the changes in climatic variables.

The Hargreaves model with its respective calibration parameters and the input data acquired by the MODIS sensor was applied in this study to represent the averaged spatio-temporal distribution of the ET_o in the study area. In addition, the ET_o estimates were further used as an input into the ETDI calculation for the assessment of droughts.

4.4 Drought Assessment Results

For this study, the ETDI was used to analyse drought conditions for the period 2011 to 2016. The assessment was based on the spatial and temporal distribution of ET_a and ET_o which were used to calculate ETDI. The use of SEO as a potential data source for monitoring droughts to assist in water resources and disaster management in South Africa was investigated. Since, the ETDI requires ET_o as an input, which used LST data from the MOD11A2 product and the other input being ET_a, was obtained from the LSA-SAF DMET product, the study was able to utilize the spatial benefits provided by SEO.

Given the difficulties in defining the beginning and end of drought events, their slow development and multiple climatic features, the temporal and spatial characteristics of the ETDI were produced. The investigation of the spatial and temporal characteristics of a drought provide a framework for sustainable water resources management, especially in semi-arid regions. Maps expressing the quantitative monitoring of drought occurrences in terms of the drought severity characteristics obtained from the ETDI drought indicator, such as duration, magnitude, and spatial extent, are produced for the study areas, which constitute part of a hazard assessment. A four-month consecutive period was found to be suitable for displaying the spatial development of droughts for this study (April to June).

The drought indices were calculated at different catchment levels in an attempt to display the development of a drought at different spatial scales. For the Umgeni Catchment results were produced at a tertiary and QC level, while for the Upper Thukela results were obtained for the entire Upper Thukela Catchment as well as at a secondary and QC level. Greater details are discussed at a QC level, as this level was considered most appropriate for decision-making in water resources management.

4.4.1 Evapotranspiration Deficit Index (ETDI)

The ETDI is calculated as described in Section 2.2 using a monthly water stress ratio (WS) and a monthly water stress anomaly (WSA). An average monthly WSA value ranges from -100 to +100, representing very dry to very wet conditions, respectively. The monthly WS ranges from 0 to 1, whereby 0 is indicative of evapotranspiration occurring at the same rate as reference evapotranspiration and 1 represents no evapotranspiration (Eden, 2012). The investigation of

the temporal trend of a drought is conducted through WS, WSA and ETDI analyses for the two study sites at different spatial scales. Spatially, the WS and ETDI maps were produced for the years, which were the driest during the 2011-2016 research period, namely 2015 and 2016. Spatially averaged maps were not produced for every level at which calculations were done but rather at appropriate levels to display drought patterns, considering that the calculations were obtained as a spatial average and not at a pixel by pixel basis.

Umgeni Catchment: Tertiary Level

With respect to the Umgeni Catchment, results are displayed at a tertiary and QC level. To investigate the temporal trend of drought within the Umgeni Catchment, the WS, WSA and ETDI were analysed using the Hargreaves-LST derived ET_o and the LSA-SAF ET_a as inputs. Figures 4.15, 4.16, 4.17, 4.18, 4.19, 4.20 and 4.21 display the results, respectively. Spatial maps are illustrated where necessary.

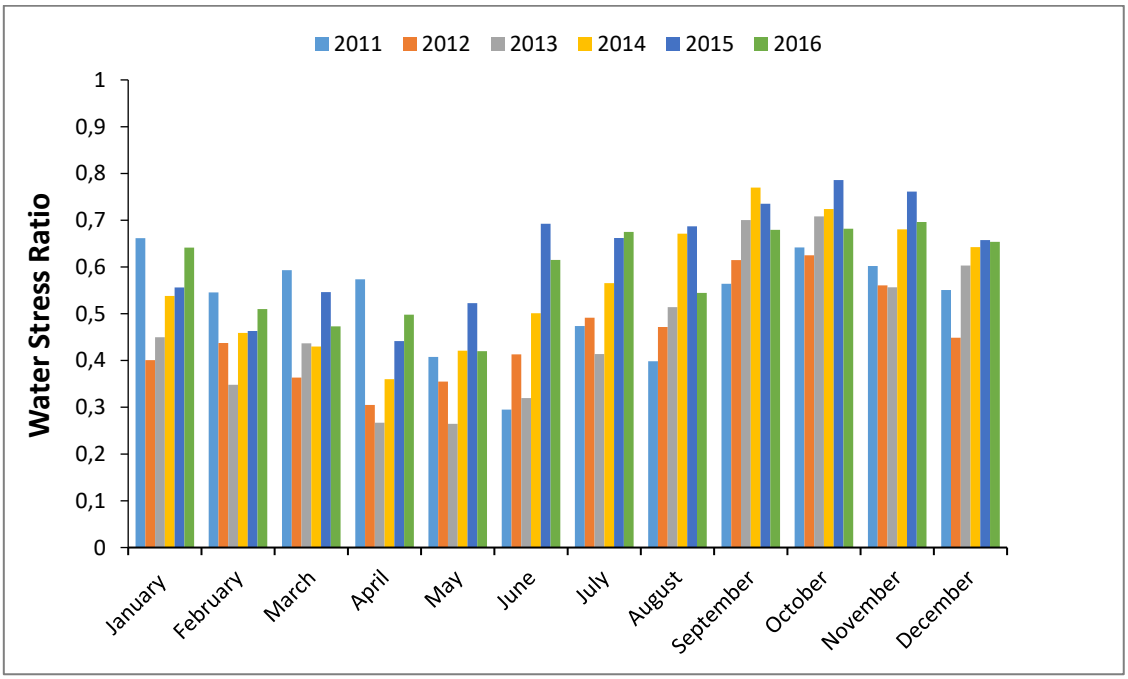

Figure 4.15 Water stress ratio for the Umgeni Catchment at a tertiary level (2011-2016)

The WS at a tertiary level for the Umgeni Catchment is shown in Figure 4.15. The WS ranges from 0 to 1 and is useful for providing information on the presence of moisture within the area. A WS of 0 indicates there is sufficient water/moisture available for ET_a to take place at the same rate as ET_o, while a value closer to 1 is indicative of insufficient moisture/rainfall being

present; hence, no evapotranspiration can occur as the catchment is stressed. In the year 2012 the lowest WS of 0.46 was shown, while the year 2015 indicated the highest WS of 0.62, followed by the year 2016 with a ratio of 0.59. In the year 2011 a WS of 0.52 was displayed, 2013 a ratio of 0.46 and the year 2014 yielded a ratio of 0.56.

The above results indicate that the years 2015 and 2016 displayed severe stress within the catchment, due to insufficient moisture/rainfall being available. Furthermore, in the year 2015, the month of October displayed the highest WS within the entire study period (2011-2016). A ratio of 0.79 was obtained.

A spatial investigation of the WS is shown in Figure 4.16. The maps show the WS's for the driest years (2015 and 2016) within the duration of the study. The maps display three summer months and three winter months for the dry years, ensuring that the seasonal trends can be seen. Spatially, the distribution of the significant water stress that occurred within the catchment during 2015 and 2016 was displayed in the map (Figure 4.16). Winter months display more water stress compared to the summer months. This is due to the changes in weather conditions brought by seasonal differences.

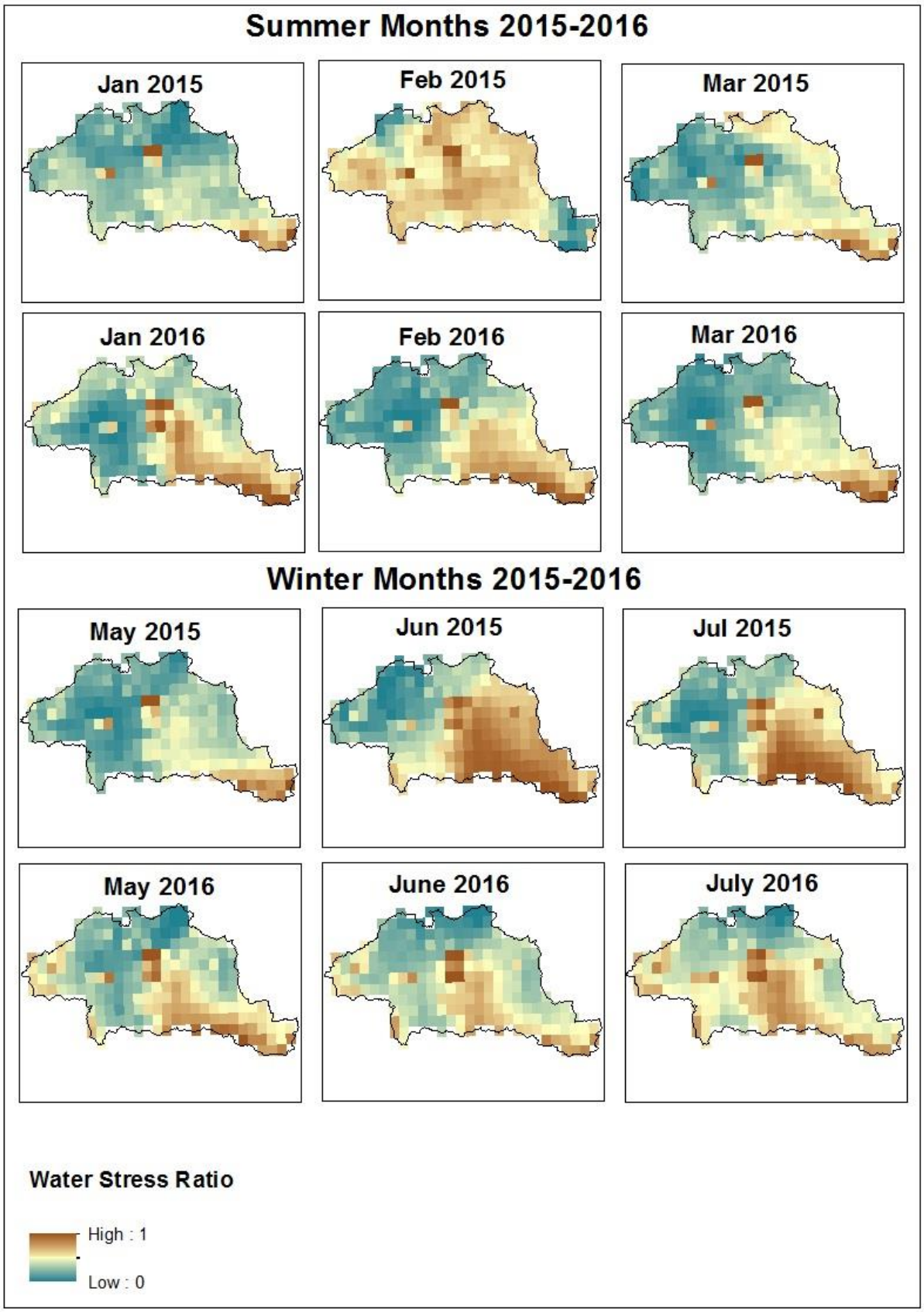

Figure 4.16 Water stress ratio maps for 2015 and 2016 for the Umgeni Catchment at a tertiary level

To further investigate the temporal trend of drought, WSA and ETDI were analysed at tertiary level and QC level for Umgeni, as shown in Figures 4.17, 4.18, 4.19 and 4.20, respectively.

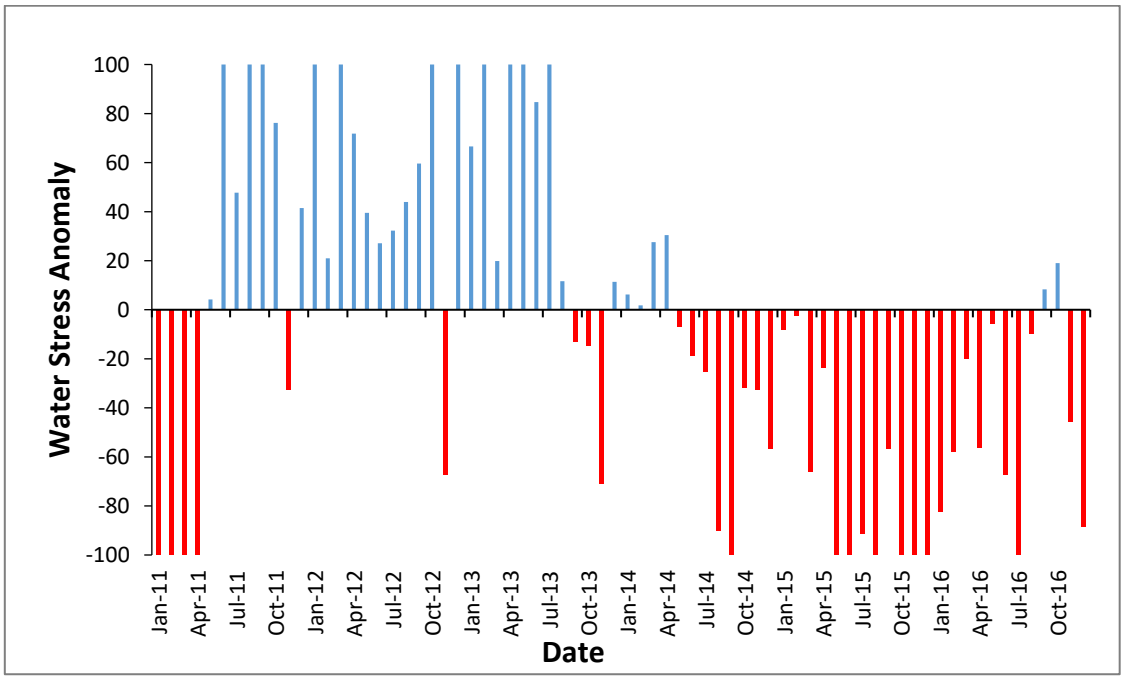

Figure 4.17 Water stress anomaly for the Umgeni Catchment at a Tertiary level (2011-2016)

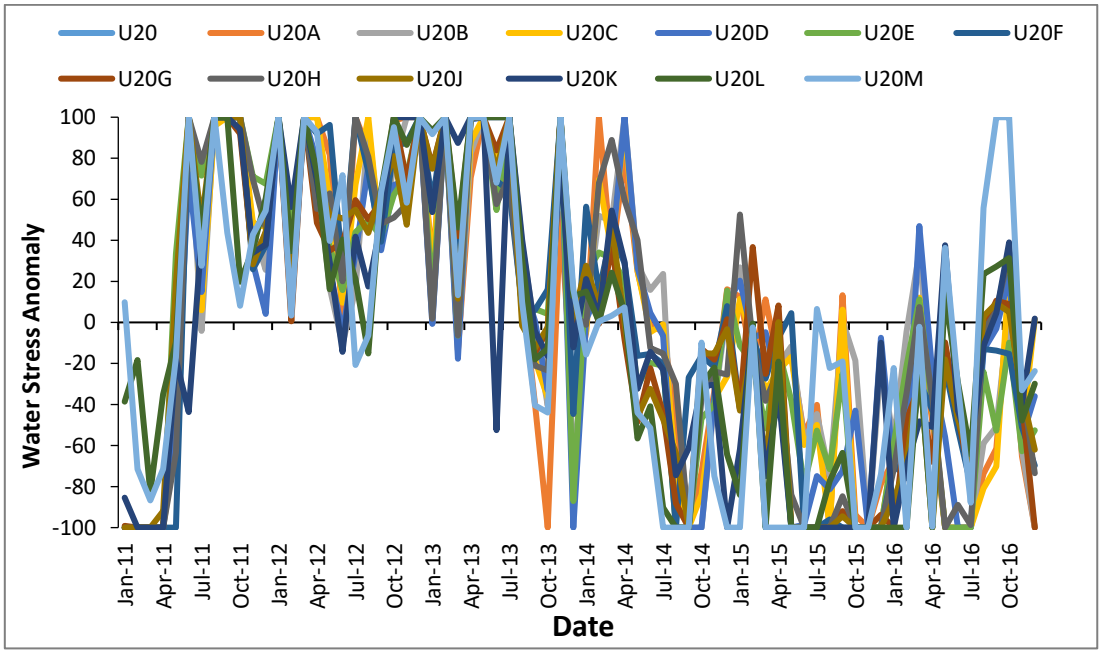

Figure 4.18 Water stress anomaly for the Umgeni Catchment at a QC level (2011-2016)

Average monthly WSA values ranged from -100 to +100, displaying very dry to very wet conditions, respectively.

Tertiary level: In Figure 4.17, the red bars represent the dry months and blue bars represent the wet months. The beginning of 2011 as well as October displayed dryness, while the remaining months, wet conditions prevailed. 2012 and 2013 are the years with the most wet months namely October 2012, August 2013, September 2013 and October 2013. 2012 is the year with the majority of significantly wet months and this correlates with the lowest WS of 0.46, indicating that sufficient moisture was present for the year within the catchment to allow for processes of ET_a to occur, hence a higher ET_a was experienced. A continuous trend of dryness is shown from May 2014 until December 2016. This indicates a period of extreme dryness lasting for almost two consecutive years. The WSA is in agreement with the results achieved from the WS. The WS for the years 2014-2016 ranged from 0.56-0.62, which were the highest of the WS's for the study period displaying the presence of a great deal of water stress in the catchment.

QC level: In Figure 4.18, the WSA for the tertiary level represented by U20 as well as for the 12 QC's (U20A-U20M) are illustrated. The WSA at tertiary level as well as for the 12 separate QC's within the catchment follow the same trend. The beginning of 2011, displays dry conditions, while the rest of the months going into the year 2013 display wet conditions. April 2014 until December 2016 displays dry conditions, while U20M, the month of September and October had a WSA of +100 indicating extreme wetness.

Overall, both levels follow a similar trend. The drought severity due to the deficit of ET_o-ET_a was calculated based on a cumulating procedure, which gave the ETDI results as shown below (Figures 4.19 and 4.20):

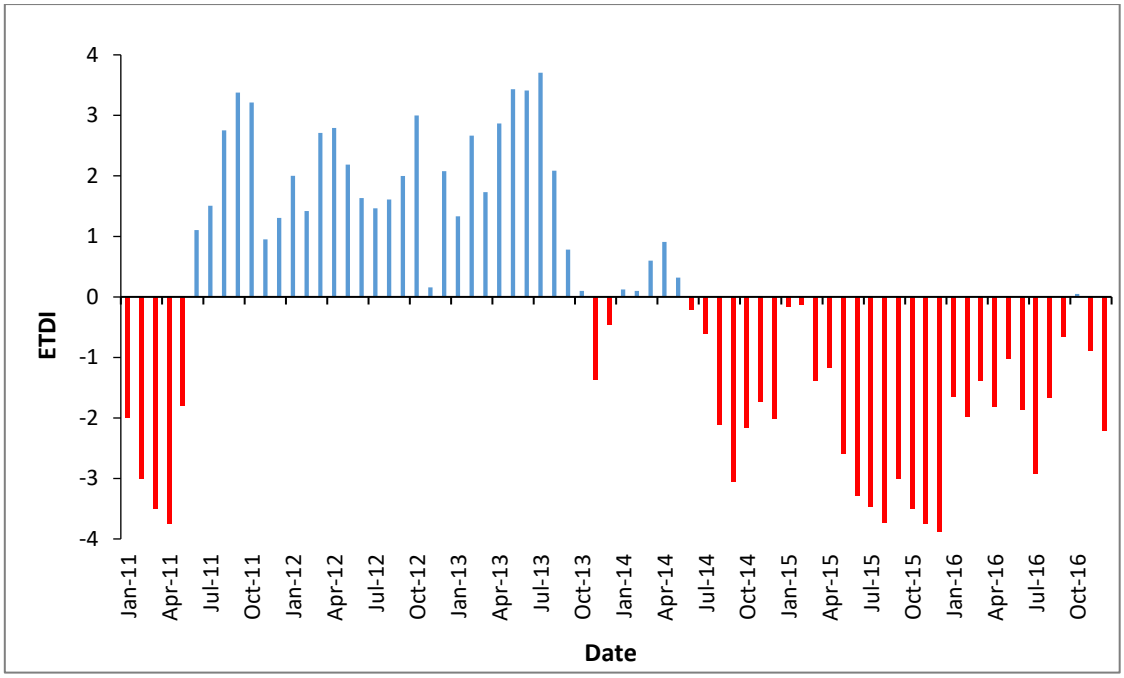

Figure 4.19 ETDI plot for the Umgeni Catchment at a tertiary level (2011-2016)

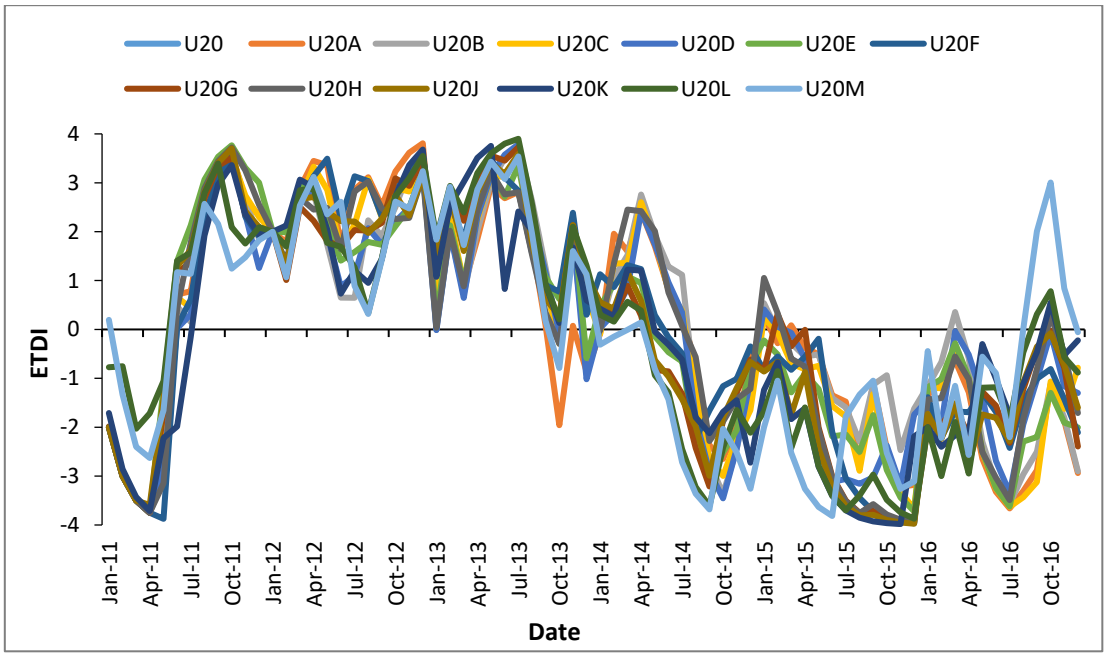

Figure 4.20 ETDI plot for the Umgeni Catchment at a QC level (2011-2016)

Tertiary level: Figure 4.19 similar to the WSA, displays red bars which represent dry months and blue bars, which represent wet months. The ETDI ranges from -4 to +4 indicating wet and dry conditions, respectively. In 2011, from January to April, all the remaining months showed positive ETDI indicating wet conditions with ETDI reaching almost +4 in September. The entire year of 2012 was wet and displayed a positive ETDI. In 2013, except for November and

December, all months showed a positive ETDI. In 2014, January to May were wet but with an ETDI not greater than +1. From May 2014 until December 2016, all months were dry, with most months having an ETDI greater than -2. Slight wetness was displayed in October 2016 with an ETDI of 0.05 that is almost near normal. Extreme dryness with an ETDI approaching -4 was displayed for October to December of 2015. In November 2015, the second highest negative ETDI of -3.50 was displayed, with the highest for the study period being December 2015 of -3.87. This correlates to ARC-ISCW (Agricultural Research Council-Institute for Soil, Climate and Water) issue for the month of November 2015 (ARC-ISCW, 2015). The report stated that hot and dry conditions prevailed in November 2015, with the month being extremely dry for the northern areas of KwaZulu-Natal. The SPI map produced within the report showed that severe to extreme drought conditions were confined to the parts of KwaZulu-Natal and the *PET* remained low. The Standardized Difference Vegetation Index (SDVI) indicated drought stress over the northern parts of KwaZulu-Natal.

According to the Centre for Research on the Epidemiology of Disasters (CRED), South Africa experienced a heat wave during week three in 2016 (January 11-January 17) (CRED, 2015). The ETDI result for this period at tertiary level was -1.65 indicating dryness, while the ETDI for the QC also displayed low negative ETDI values representing the dry conditions that were experienced as a result of the heat wave. CRED also reported on a drought event experienced in South Africa during week 46 in 2015 (November 9-November 15). The ETDI value produced for this drought period for the tertiary level was -3.75, which was the second highest negative ETDI value for the entire study period and which is indicative of the severe dryness. The QC also illustrated extremely low negative ETDI's well above -2 which is representative of dryness.

The results produced by ETDI are in agreement with results produced by the WS and WSA. Year 2012 was highlighted as a wet year and year 2015 was highlighted as the driest year. Continuous dryness was displayed from 2014 until the end of 2016.

QC Level: The ETDI ranged between -4 to +4 representing wet and dry conditions. The results produced by the ETDI (Figure 4.20) are in agreement with the results produced by the WSA. The ETDI of the separate QC's and the ETDI at tertiary level follow the same trend with same months indicating wetness and same months displaying dryness. The spike caused by U20M for October 2016 explains the extreme wetness that was depicted by the WSA in Figure 4.18.

A spatial distribution of the ETDI at a QC level is illustrated in Figure 4.21. The spatial maps are produced for four consecutive months within the most driest year (2015). These maps were produced to investigate and display the development of a drought over a large spatial scale. Droughts are known for their spatial and temporal dimensions, hence achieving coverage of drought monitoring over a vast area, allows for a more comprehensive view of the development of droughts to be seen. Figure 4.21 below displays that an area affected by a drought is rarely static; as a drought event emerges and intensifies, the core area affected by the drought and its spatial extent, spreads throughout the duration.

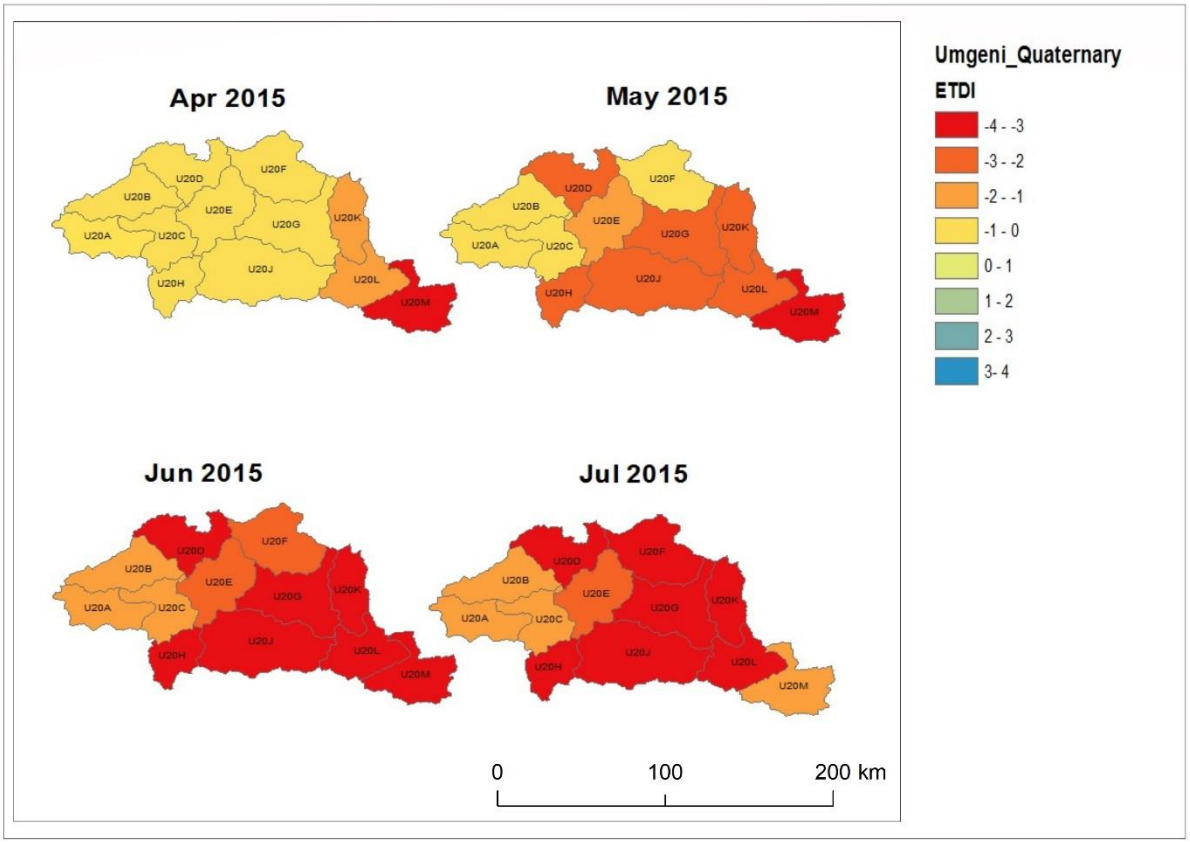

Figure 4.21 ETDI maps for 2015 for the Umgeni Catchment at a QC level

From these maps, the progression and onset of an intensifying drought over the Umgeni Catchment is shown, which had been previously detected by the spatial and temporal trends of the WS, WSA and the temporal trend of the ETDI. The effect of the drought accumulates gradually over the four-month period, displaying the slow-onset, creeping effect of the natural hazard (van Loon, 2015). The ETDI displays the drought as slowly gripping one quaternary at a time, eventually tightening its grip over the months as illustrated in Figure 4.21. The characteristics (duration, intensity and spatial coverage) of a drought are shown to be

interrelated by Figure 4.21, whereby with an increase in duration, the intensity of the drought intensifies and spreads slowly over a spatial area. A study by Demuth and Stahl emphasizes the need to study the characteristics of droughts at different temporal and spatial scales. Since there is the possibility for the characteristics and propagation of droughts to differ under different spatial scales.

Upper Thukela Catchment

With respect to the Upper Thukela Catchment, results are displayed for the entire catchment and at a secondary as well as QC level. To investigate the temporal trend of drought within the Upper Thukela Catchment, the WS, WSA and ETDI were analysed using the Hargreaves-LST derived ET_o and the LSA-SAF ET_a as inputs. Figures 4.22 to 4.29 display the results. Spatial maps were further generated to investigate the spatial distribution of droughts over a geographic area.

WS was calculated for the Upper Thukela Catchment and the results are displayed in Figure 4.22. WS were calculated from ET_o and ET_a estimates and therefore provide beneficial data on the presence of moisture within an area. In the year 2013, the lowest WS of 0.60 was displayed followed by the year 2012, which had a WS of 0.62. A WS of 0.62 was displayed for the year 2014. The highest WS were obtained for the years 2015 and 2016 with values of 0.72 and 0.71, respectively.

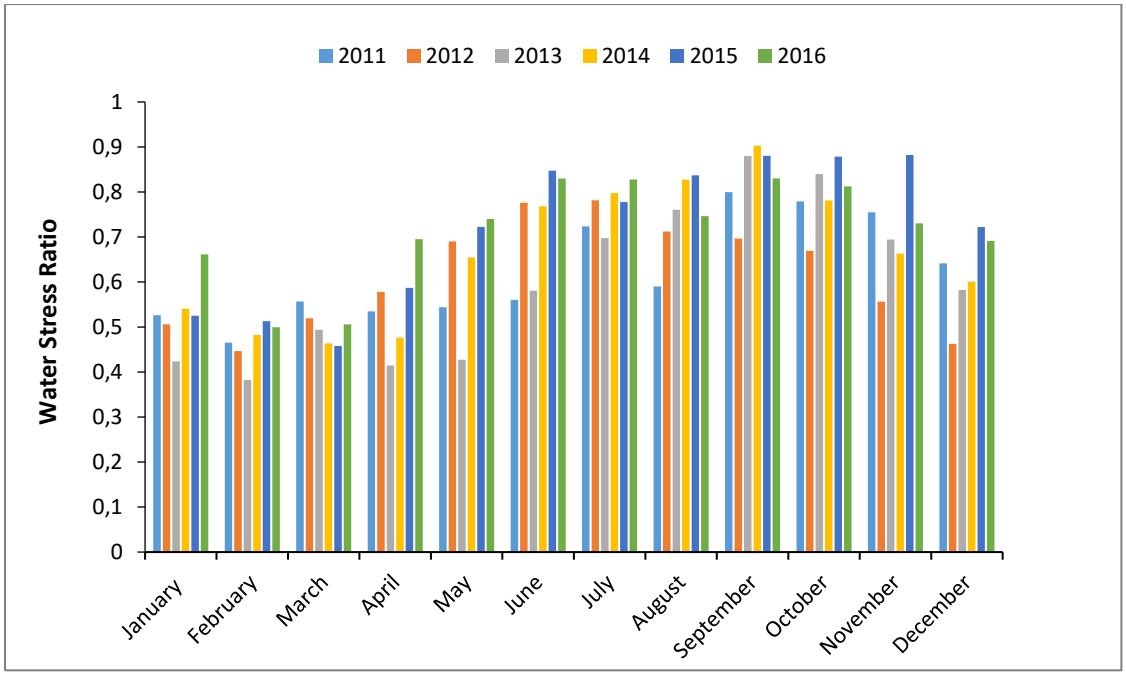

Figure 4.22 Water stress ratio for the Upper Thukela Catchment (2011-2016)

The above WS values are mostly found to be closer to 1 suggesting that the catchment was stressed as insufficient moisture was available for evapotranspiration to occur. The year 2015 and 2016, displayed the highest WS indicating extreme dryness and lack of moisture. The months from September to November in 2015 and the months between June and October of 2016 showed the highest WS over 0.80.

An investigation of the spatial trend of the WS for the catchment was shown in Figure 4.23. Spatial maps of WS were produced for the driest years, namely; 2015 and 2016. Maps are displayed for three summer months and the three winter months as result of seasonal differences. Moisture stress within the catchment is clearly depicted in Figure 4.23. Severe stress is further highlighted for the winter months as a result of the weather conditions brought about by the season. During winter, less rainfall and moisture are present compared to the summer months, which further worsen the stress within the catchment.

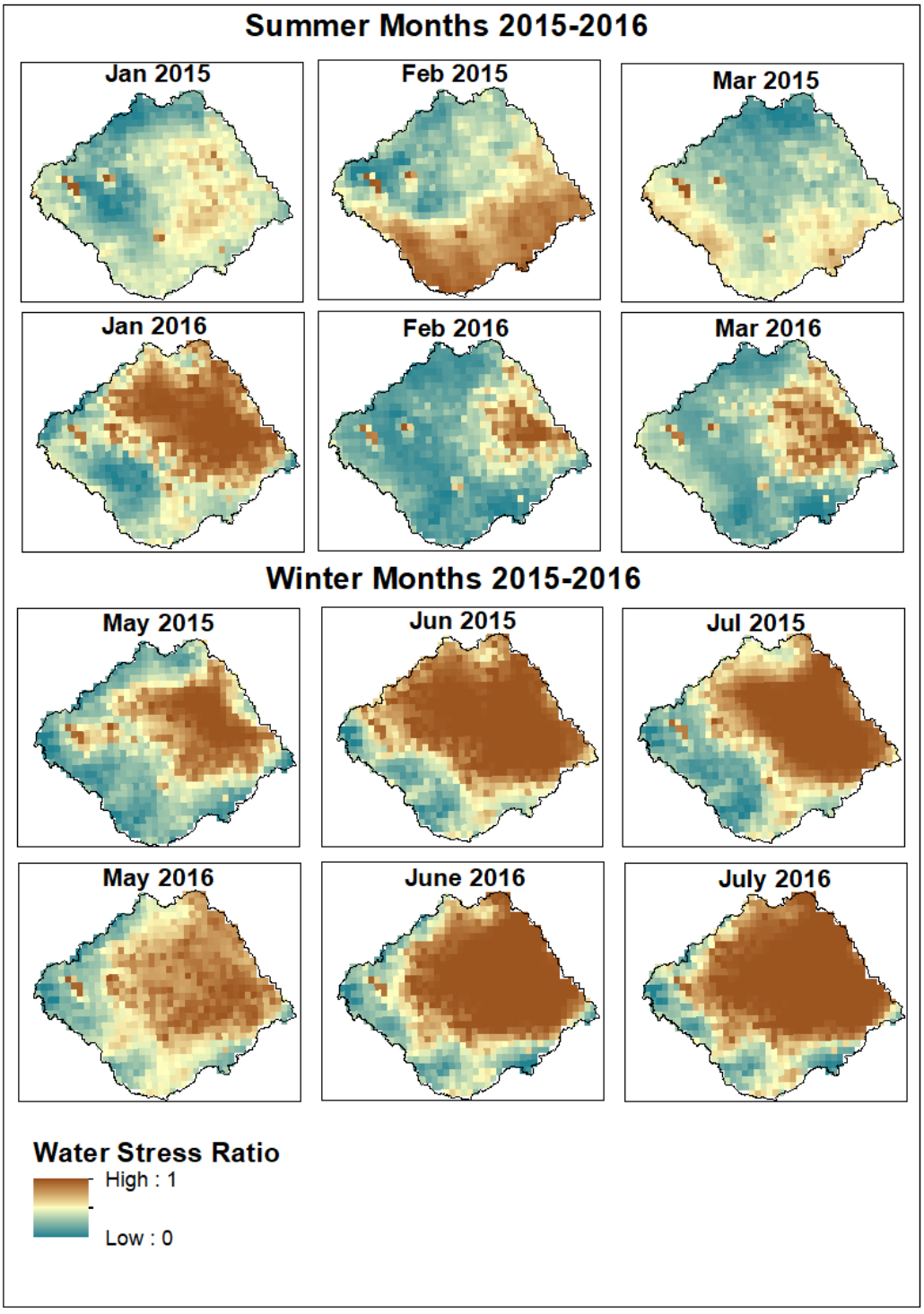

Figure 4.23 Water stress ratio maps for 2015 and 2016 for the Upper Thukela Catchment

To investigate the temporal trend of droughts, WSA and ETDI were analysed for the Upper Thukela Catchment and at a secondary level, as shown in Figures 4.24, 4.25, 4.26 and 4.27, respectively. However, for the investigation of the spatial development of drought, ETDI maps were produced at a secondary and QC level. These spatially averaged maps are shown in Figures 4.28 and 4.29.

Catchment level: In Figure 4.24, the red bars are representative of dry months and the blue bars are presentative of wet months. At a catchment level, January, March and November of 2011 displayed dryness and rest of the months were displayed as wet. March to July 2012 experienced dry conditions, while the remaining months of 2012 were wet. The majority of the months for 2013 displayed wetness, which is in agreement with the lowest WS of 0.60 that was produced, indicating a wet year with high ET_a experienced. August, September and October of 2013 were the exception as they displayed dry conditions. For 2014, apart from the dry months January, February, July and September, the remaining months were wet. The two-year period (2015-2016) indicated extreme dryness, while January 2015, March 2015, August 2016 and September 2016 displayed wetness. The extended period of dryness within these two years (2015-2016) correlated with the highest WS that were produced for the years 2015 and 2016 with values of 0.72 and 0.71, respectively. These results indicate that the year 2015 and 2016 were extremely dry years with a low ET_a experienced.

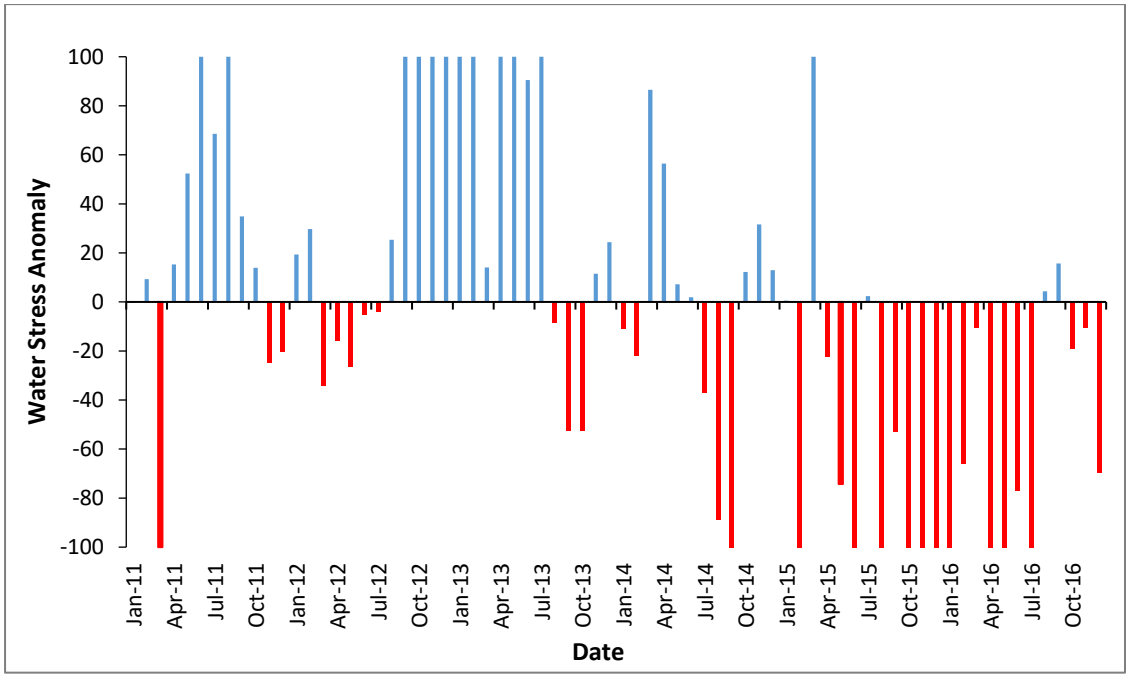

Figure 4.24 Water stress anomaly for the Upper Thukela Catchment (2011-2016)

Secondary level: Figure 4.25 illustrates the WSA for the secondary level catchments (V1, V2, V6, V7) as well as for the whole catchment (V). The WSA at a secondary level follow the same trend as the WSA on a catchment level. The majority of wet months during 2013 indicate a wet year and the extreme dryness for the years 2015 and 2016 was clearly depicted.

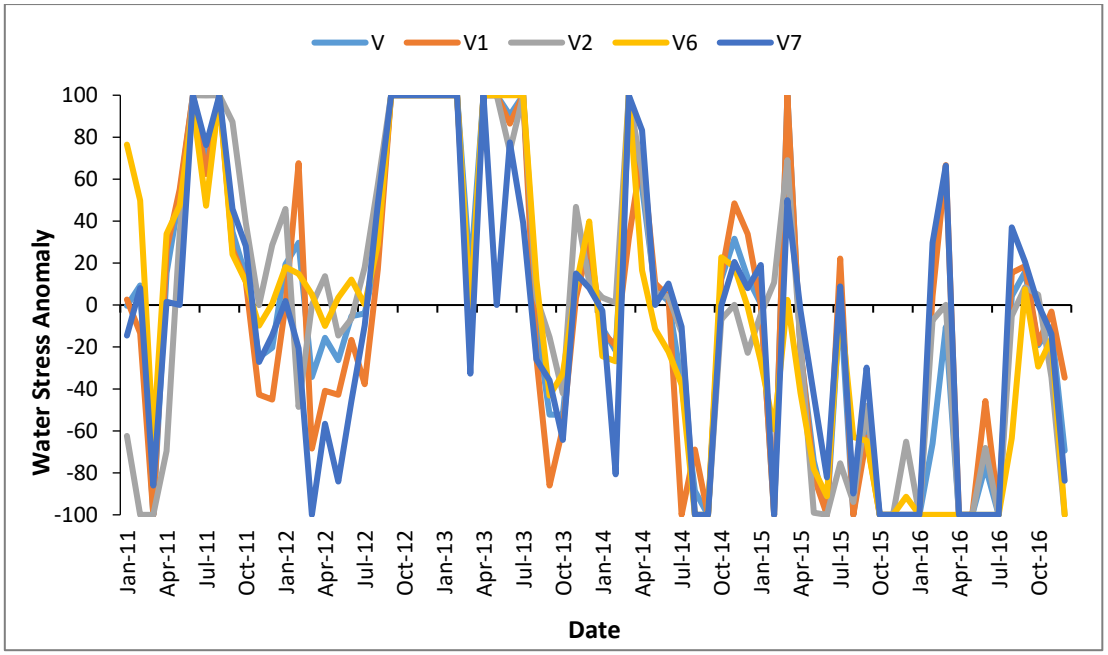

Figure 4.25 Water stress anomaly for the Upper Thukela Catchment at a secondary level (2011-2016)

Overall, both levels follow a similar trend with no significant changes noted in the difference between the levels. The drought severity due to the deficit of ET_a was thereafter calculated based on a cumulating procedure, which gave the ETDI results as shown below (Figures 4.26 and 4.27). The range of ETDI is between -4 to +4, which is representative of wet and dry conditions, respectively.

Catchment Level: Figure 4.26 displays red bars that represent dry months and blue bars that represent wet months, similar to the WSA. In 2011, the majority of the months displayed a positive ETDI indicating wetness with the exception to the months January, March, April and December, which displayed dry conditions and produced a negative ETDI. For 2012, the months from March to July showed a negative ETDI indicating dryness while the remaining months were wet. In 2013, a positive ETDI was displayed for the majority of the months indicating a wet year, while the months September to November displayed a slight dryness, with low negative ETDI values (-0.32- -1.14). January, February, July, August, September and October indicated dryness with a negative ETDI, while the remaining months displayed wet conditions. Years 2015 to 2016 all displayed negative ETDI values, with January and April 2015 displaying near normal values (0.01, 0.05).

November 2015 produced a negative ETDI of -3.59, which was amongst the extremely high negative ETDI values for the study period. This correlated to UMLINDI: The Watchman issue for the month of November 2015 (ARC-ISCW, 2015), which reported November 2015 was characterized by extremely hot conditions, with the month being extremely dry for the northern areas of KwaZulu-Natal. These results were in agreement with results achieved by the WS and WSA, which pointed out a two-year consecutive period of dryness.

As previously stated, CRED reported on the heat wave in South Africa during January 2016 as well as the drought experienced in South Africa in November 2015. The ETDI for the catchment for November 2015 was -3.60 which was amongst the highest ETDI's experienced during the study period, while for January 2016 an ETDI of -2 was achieved. These ETDI results indicate the severely dry conditions that were experienced as reported by media reports. While for the secondary level catchments, during November 2015, ETDI's produced were all reaching close to -4 and for the month January 2016, low negative ETDI were achieved, representative of the dry conditions and the dryness that was experienced.

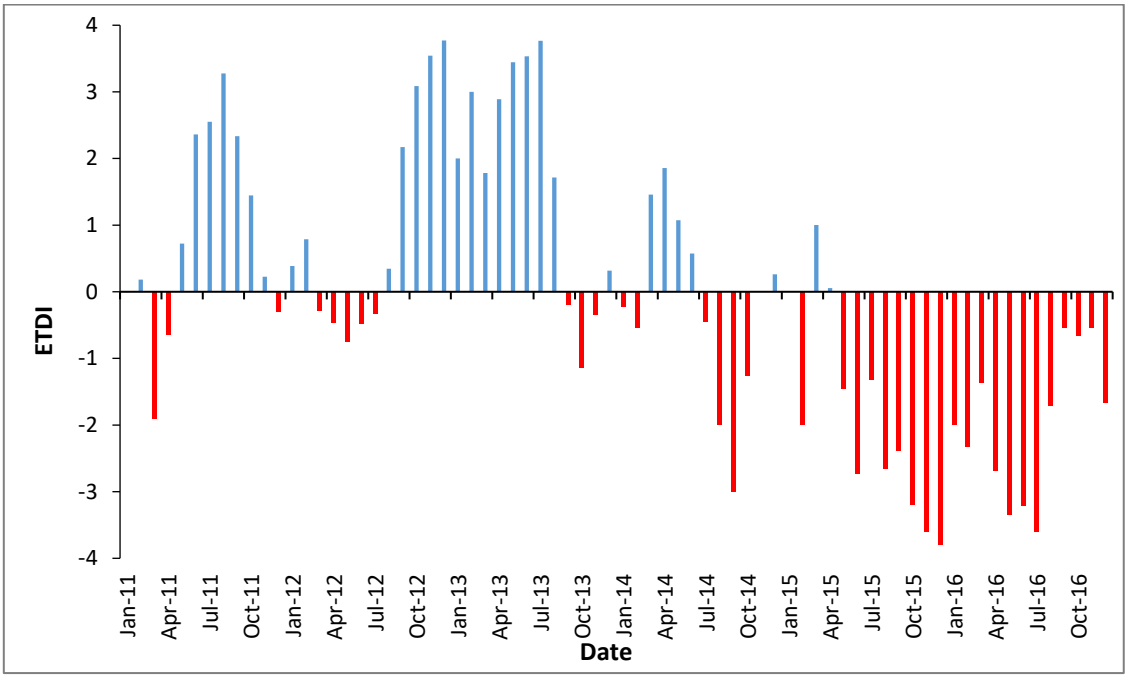

Figure 4.26 ETDI plot for the Upper Thukela Catchment (2011-2016)

Secondary Level: Figure 4.27 shows that the ETDI results at a secondary level follow the same trend of the ETDI produced at a primary level for the Upper Thukela, with same months

indicating wetness and same months displaying dryness. Hence, no significant difference are noted for the WSA and ETDI calculated at different levels.

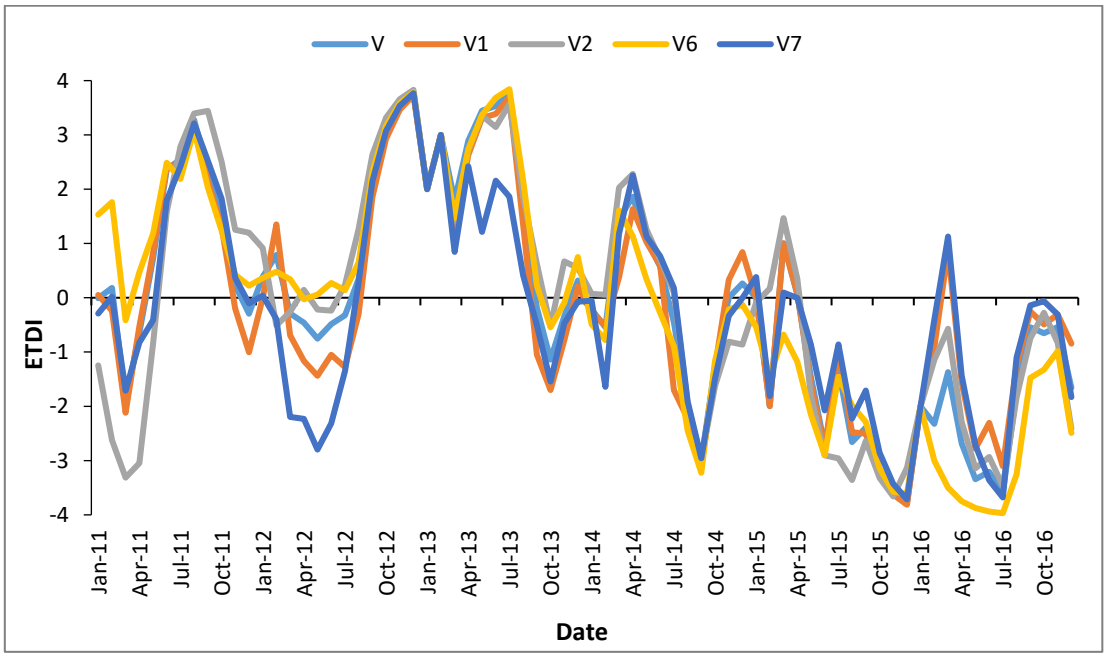

Figure 4.27 ETDI plot for the Upper Thukela Catchment at a secondary level (2011-2016)

To investigate the spatial distribution of a drought, spatial maps were produced at a secondary (Figure 4.28) and at a QC level (Figure 4.29). The spatial maps are produced for four consecutive months within the driest year (2015). These maps were generated to investigate and display the development of a drought over different spatial scales.

A study by Leelaruban and Padmanabhan, (2017) indicated that drought conditions at a state level differs from those of a country, whereby the drought information of a smaller area could be masked when the drought is reported at a state level. This is because the more homogenous hydrological conditions enable sudden variations of the area coverage of certain drought intensity. The recognition of this feature is important from a drought management perspective across scales because the small scales are subject to sudden drought and can be unnoticed at a larger spatial scale, which is evident from this figures displayed below. Spatial maps are produced at a secondary (Figure 4.28) and at a QC level (Figure 4.29) for the Upper Thukela study site.

Spatially, at a secondary level, ETDI maps are displayed in Figure 4.28, while Figure 4.29 displays the ETDI maps at a QC level. There is considerable variability with regards to the different classes of droughts. The smaller scales are a subset of the larger spatial scales. The number of drought events appear to be increasing from a larger spatial scale to a smaller spatial scale. In Figure 4.28 the secondary catchments are classified broadly, hence the ETDI values are generalized and do not detect the severe dryness occurring within particular QC's within the secondary catchments as displayed in Figure 4.29. It is therefore advised that spatial investigations of droughts be conducted at a QC level, as this level provides greater and finer details that can assist in water resources management and drought assessment.

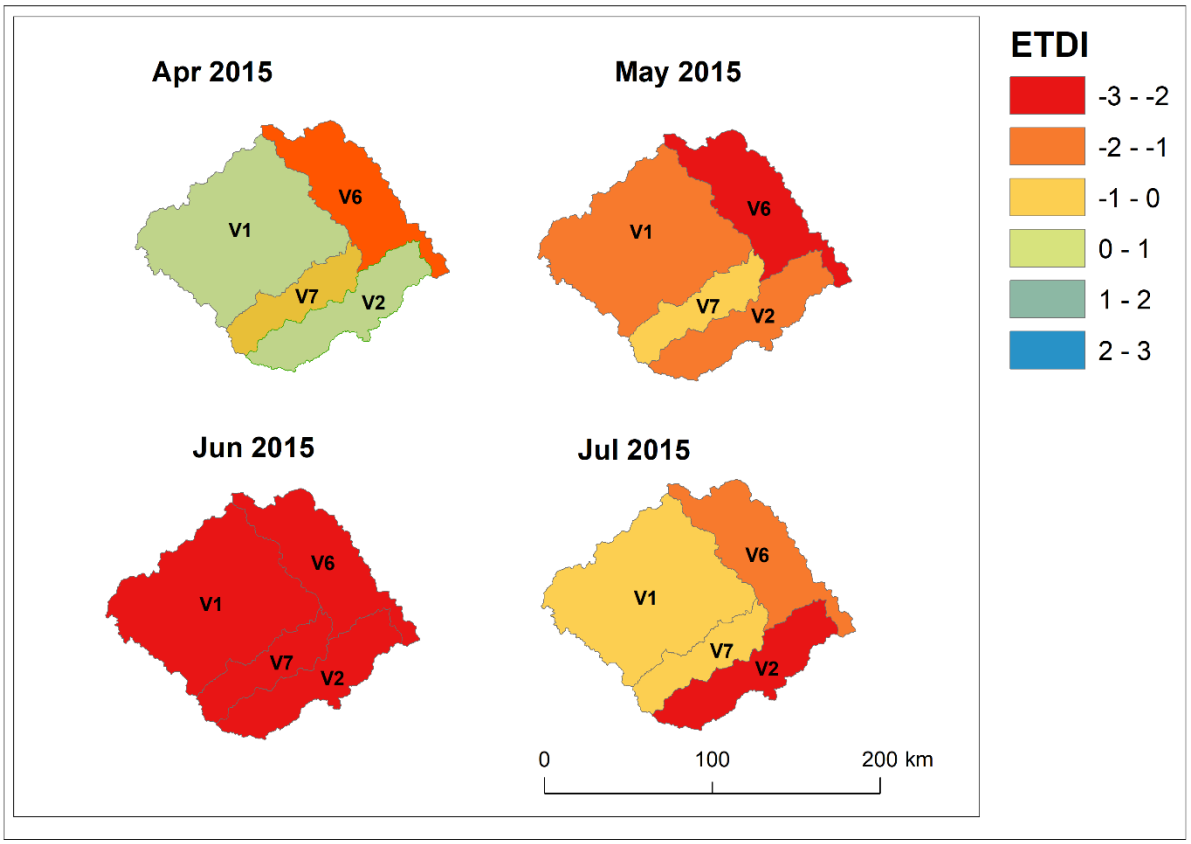

Figure 4.28 ETDI maps for 2015 for the Upper Thukela Catchment at a secondary level

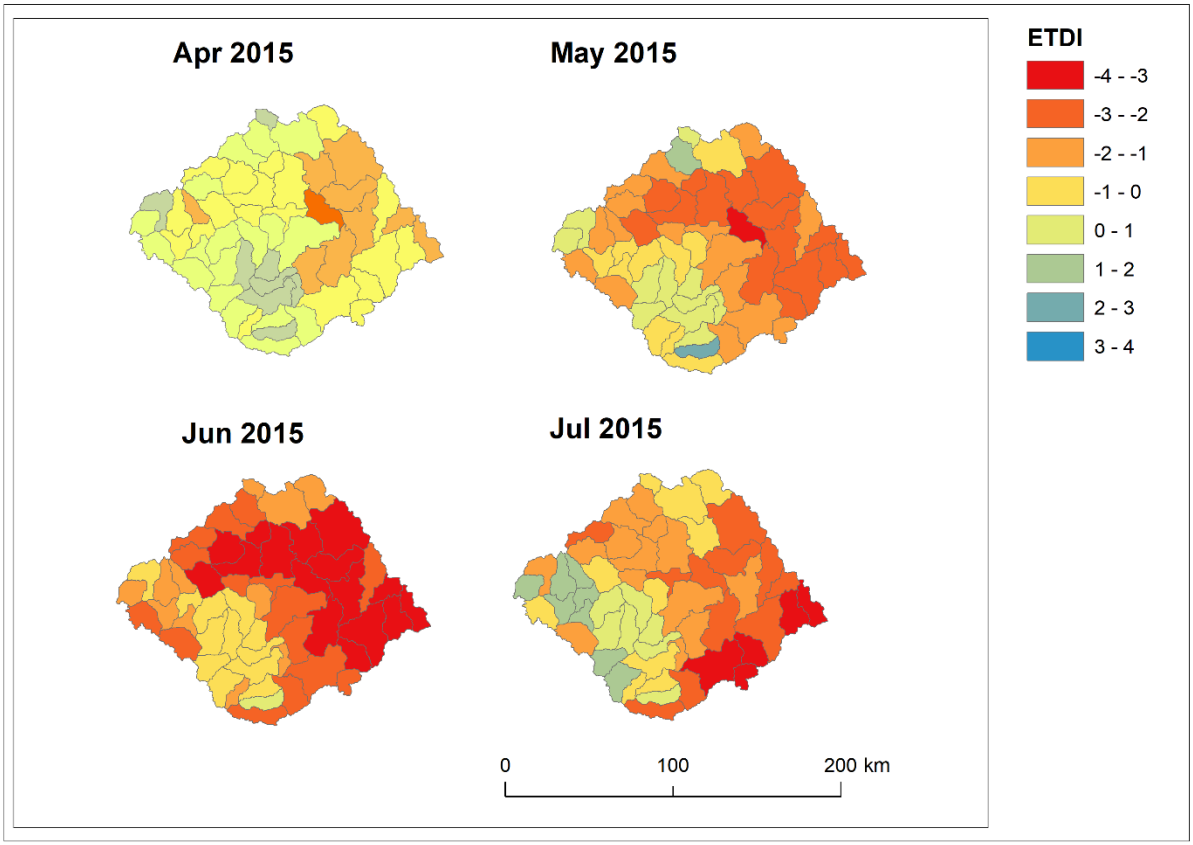

Figure 4.29 ETDI maps for 2015 for the Upper Thukela Catchment at a QC level

Episodes of droughts affect wide areas over long periods of time. The spatial patterns of droughts are seemingly complex as it is common for an area to suffer dry conditions, whilst the neighbouring areas experience humid or normal conditions (Figure 4.29). Vicente-Serrano (2010b) accounts for such variation by mentioning atmospheric circulation patterns, as droughts cannot be associated with one single atmospheric conditions, more specifically; spatial variability in precipitation and its variability are the attributable causes. Thus, the determination of areas over which drought development is homogenous becomes difficult.

The spatial maps show that more intense droughts occur spatially at a QC level and are less intense when the QC is spatially connected to form the secondary catchments. The study by Leelaruban and Padmanabhan (2017) indicates that the spatio-temporal features of the propagation of a drought event can significantly change with spatial scale. The same drought may appear to have different characteristics when viewed at different spatial scales, and this needs to be considered in drought management. This study is in line with the results shown in previous research.

Overall, the results produced by the ETDI for the Umgeni Catchment and for the Upper Thukela Catchment were consistent with several research and media articles and reports produced for the region of South Africa. According to a report produced by the SADC (Southern African Development Community), South Africa was amongst the SADC's regions that experienced a rather devastating drought that was said to be associated with the 2015/2016 El Niño event. The 2015/2016 rainfall season in South Africa was delayed, which was evident as both catchments during the period 2015-2016 displayed prolonged dryness. The Umgeni Catchment between January 2015 to December 2016 negative ETDI were achieved indicating dry conditions with an exception to October 2016 (EDTI = 0.05) with near normal condition. While with respect to the Upper Thukela, January 2015 and April 2015 displayed near normal conditions, while the remaining months between January 2015-December 2016 showed dryness.

A rainfall analysis performed by the SADC indicated that the period between October to December 2015 was the driest in more than 35 years along with higher than averaged temperatures occurring consistently within the same period (SADC, 2016). In addition, the October 2015 report on drought conditions across the country indicated that drought conditions were being experienced in KZN. These drought conditions and the intense dryness that was displayed between these months were depicted by the ETDI for both study areas. In the Umgeni Catchment, the ETDI for months October 2015 - December 2015 were amongst the highest negative values for the entire study period (2011-2016). October 2015 had an ETDI of -3.50, November 2015 was -3.75 and December 2015 was -3.87. For the same months, the Upper Thukela Catchment also produced an extremely high negative ETDI of -3.19 for October 2015, -3.59 for November 2015 and -3.79 for December 2015. The extremely high negative ETDI therefore indicated the intense dryness that was experienced in the respective catchments.

Following the dry conditions heavy rains occurred for approximately 30 days between 21 February 2016 to March 2016. However, these rains followed several months of poor rainfall; hence, they were insufficient for the rainfall deficits since October to be eliminated. The rainfall was reported to have amounted to twice the normal amount for South Africa. The ETDI for the Umgeni for February was -1.98 and for March it was -1.39 whereas, for the Upper Thukela, February was -2.32 and March was -1.37. These Figures remained negative despite heavy rains because the rains were insufficient. However, an extremely high negative ETDI of above -3 was noticed for October –December 2015, and the ETDI for February and March was lower

due to the effect of the heavy rains. The results produced by the ETDI for both study sites correlated with the report since, January-December 2014 for both catchments majority negative ETDI's for majority of the months within the period were achieved. For the Umgeni Catchment, January 2014-May 2014 were nearly normal, while the rest of the months were negative ETDI, indicative of dryness. For the Upper Thukela Catchment, positive ETDI's were not greater than +2 in 2014, while negative ETDI's were as high as -3 with the highest for August 2014 (-2) and September 2014 (-3).

As a result of the investigation into the ETDI in the assessment of droughts, it can be concluded that it is a useful indicator for monitoring drought conditions. The ETDI was able to simulate the wet and dry conditions within the study areas reasonably well. The spatial variability analysis showed that the spatial variability in ET_a is critical in ETDI for identifying drought conditions. The ET_a deficit calculated by the ETDI can be a good parameter for the evaluation of drought conditions within a landscape, at an agricultural level.

High totals of ET_a can evoke the occurrence of droughts more frequently as indicated by the WS and the WSA. With that being said, crop sections and water saving rotation can play a role in assisting and minimizing the impacts of droughts within an area. In Morocco, drought tolerant crops such as winter chickpea are grown as a drought mitigation strategy. These crops make beneficial use of the autumn and winter rains. Such techniques can substantially improve and stabilize crop yields, protect the environment and reduce the impact of droughts on society.

A combination of the spatial analysis and temporal analysis of droughts can help to develop an improved understanding of agricultural droughts and droughts in general. Additionally, it can be beneficial in the monitoring and planning of droughts to mitigate their impacts. The spatio-temporal analysis can enable the monitoring of moisture within any space and time scale. The ETDI is a spatial indicator that can be estimated at any location within an area. From the spatial analysis, it could be seen that droughts are characterised by their duration, intensity and spatial coverage. Spatially-averaged maps displayed how affected/ severely affected areas gradually evolve and how the QC's of maximum intensity expand.

Depending on the size of the governing unit such as a QC or catchment, an understanding of the scale-dependency is crucial for resource allocation and drought management. The spatio-temporal characteristic of droughts illustrated by Figures 4.21, 4.28 and 4.29 display that the

average area, maximum percentage of the area and total duration are found to be decreasing with an increase in the drought intensity for the different spatial scales. However, with respect to smaller spatial scales, drought occurrences persist for a shorter period compared to a larger spatial scale. Quantitatively this study was able to demonstrate that there is a visible variation within the drought characteristics (duration, intensity and spatial coverage) at different spatial scales. These findings emphasize and acknowledge that the management of droughts and the allocation of resources should be developed for different spatial scales, more so at smaller administrative units such as at a QC level.

To enable the improved management of drought impacts within any administrative area in any geographic location, the dependency of drought characteristics on the spatial scale should be studied at that location to derive the appropriate drought characteristics for that specific scale. Studies seeking to better quantify drought characteristics and their variations can prove to be valuable for society. In that context, studies focusing on the dependency of spatial scale of drought characteristics such as this will be helpful in drought management, resource allocation and improved water resources management.

The verification of the presence of the spatial scale's effect on drought characteristics for investigating the effect of the scale on the spatio-temporal characteristics of droughts was shown in this section of the study. Such scale investigations are necessary in order to account for the scale dependence of drought characteristics for effective management of droughts and allocation of water resources.

4.4.2 Standardized Precipitation Index (SPI) and Standardized Precipitation Evaporative Index (SPEI)

Despite all droughts originate from a lack of precipitation, hydrologists want to know how the precipitation shortage influences the hydrological system. Thus, the time scale over which water deficits accumulate becomes extremely important when assessing droughts. For these reasons, it is beneficial for drought indices to be associated with timescales to assist in managing and monitoring water resources. The popular SPI and SPEI indices can be computed at different time scales; however, the choice of a time scale is dependent on the choice of the drought analysis. SPI and SPEI are able to monitor wet and dry climates hence; an added

benefit of these indices includes the monitoring of wet periods. The SPEI holds the advantage of combining the effect of temperature and rainfall variability for drought assessment as well being more sensitive to global warming. As a result, the SPEI presents a more complete approach to explore the effects of climate change on drought conditions.

In this study the SPI and SPEI was calculated for QC's within the Umgeni and Upper Thukela Catchment based on the 22 meteorological stations together with satellite data, which covered the periods between 1986-2016. This study analysed the presence of trends in drought-affected areas across South Africa. In this section in order to define drought conditions, the SPI and SPEI was calculated on a 12-month (yearly) time scale. These indices were calculated to allow for comparison between the ETDI in detecting the occurrence of droughts or not. Calculations were carried out for four QC's within the Umgeni Catchment and four QC's within the Upper Thukela. The chosen QC's refer to those in which the calibration of the Hargreaves-LST was performed (Section 4.3.1). Table 4.4 provides details on the selected QC's, which were selected, based on the availability of meteorological data.

Sufficient meteorological data for a 30-year period was available for the Umgeni Catchment however, several years of historic data within the 30-year period was unavailable for the Upper Thukela Catchment. Hence, in order for the SPI and SPEI to be calculated for the Upper Thukela Catchment, the FEWS rainfall product was utilised to provide a 30-year record of rainfall and the temperature database for Southern Africa was able to provide the temperature data. The temperature database provides records only for 50 years from 1950-2000. However, the 30-year period considered in this study was from 1985-2016. Hence, to accommodate for the missing temperature for the period 2000-2016, temperature from nearby weather stations within the catchments were used to form a complete dataset.

Results of the SPI and SPEI produced by the R software are displayed with inputs of rainfall and temperature obtained from gauged data as well as from satellite data. The encouraging results produced from the use of the satellite data within the Umgeni catchment allowed for use of the satellite data to calculate the SPI and SPEI in the Upper Thukela Catchment.

Umgeni Catchment: using observed and satellite data to produce SPI and SPEI values.

Figure 4.30 to 4.33 represent the SPI and SPEI outputs and results from the SPEI-R software for the selected QC's. Cross comparisons between drought indicators was performed in order to investigate the ETDI in detecting the occurrences of droughts. Figure 4.30, Figure 4.31, Figure 4.32 and Figure 4.33 illustrate comparison of drought indices using observed data and using FEWS satellite rainfall data combined with the temperature database for the Umgeni catchment as inputs. Within these Figures, A-D represents results using observed data while E-H represent results using satellite rainfall estimates. In this study, SPEI results are displayed using two methods. The first method is through the Thornthwaite equation whereby evapotranspiration is computed as *PET* while the second uses the Hargreaves equation where evapotranspiration is computed using ET_o. The differences between the two methods and the results produced are not discussed in detail as it is found to be beyond the scope of the study. The SPEI results are only used to assess the ETDI in detecting the occurrence of a drought.

To interpret the SPI and SPEI, negative values represent a deficit in rainfall as well as dry conditions while, positive values represent rainfall and wet conditions occurring. Furthermore, negative SPI and SPEI trends account for an observed general increase in droughts. Technically, when SPI values drop below 0, droughts conditions prevail and the drought ends when the SPI becomes positive again. The duration of a drought is said to equal to the number of months the SPI was negative. However, the theoretical limits are $(-\infty,\infty)$. Figure 4.30, Figure 4.31, Figure 4.32 and Figure 4.33 display very slight discrepancies between the results obtained using observed data and satellite data. Overall, both instances correlate well and agree in detecting severe wetness and severe dryness. The 2015/2016 El Niño drought was detected by all SPI's and SPEI's within the study period. No significant difference in noted in the SPEI calculated using the Thornthwaite and Hargreaves equations. SPI and SPEI display similar results relating to drought variability and trends across the different QC's. Positive and negative trends exist across all QC's. Overall, it can be concluded that both SPI and SPEI trend analysis, yield similar results. From these results, incorporating satellite data for use in calculating SPI and SPEI within the R package is advocated. Utilizing satellite data is recommended especially in poor developing countries and regions where limited data is available to assist in water resources management and for decision-making purposes.

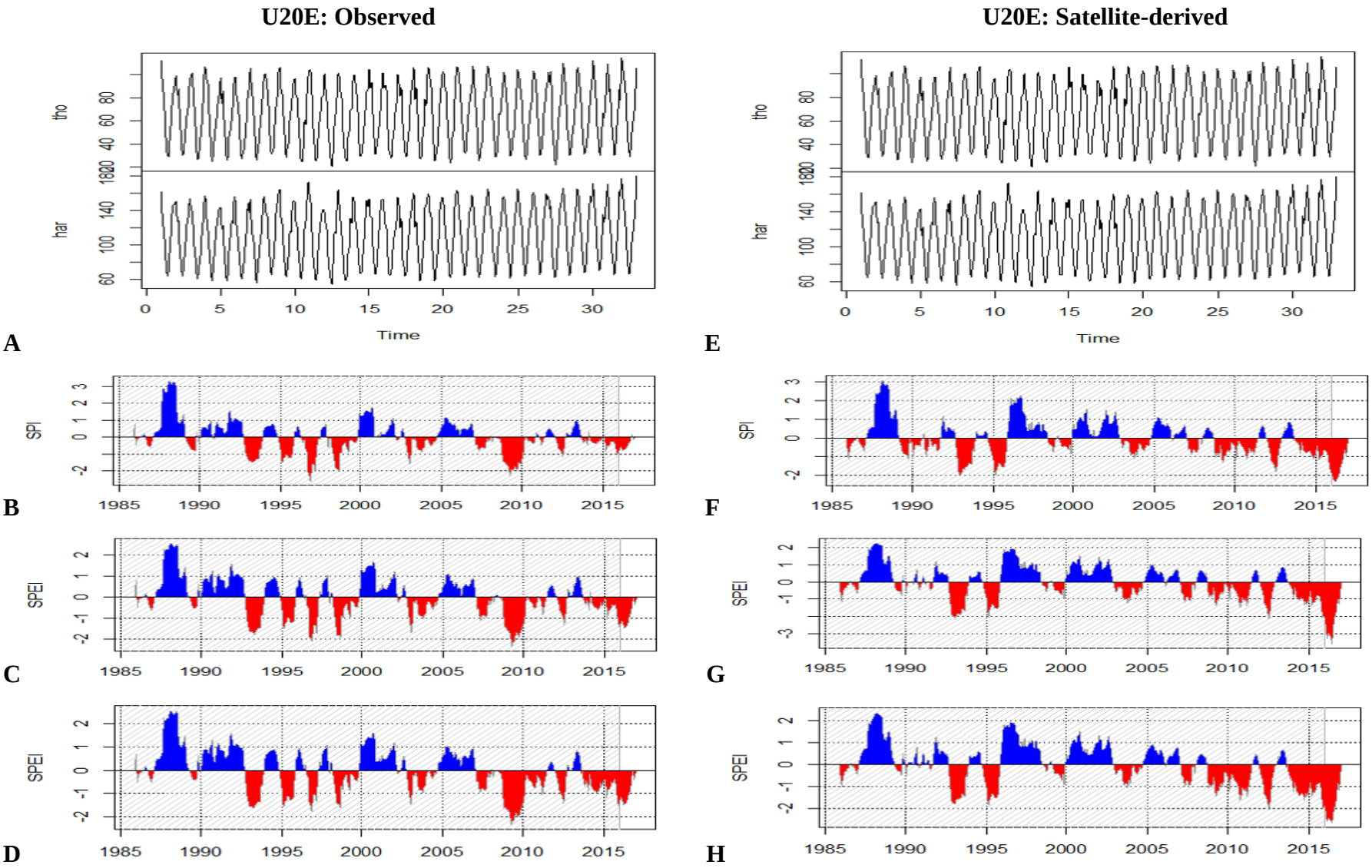

Figure 4.30 SPI and SPEI results for U20E.C and G represent SPEI calculated using the Thornthwaite method while Figure D and H the Hargreaves

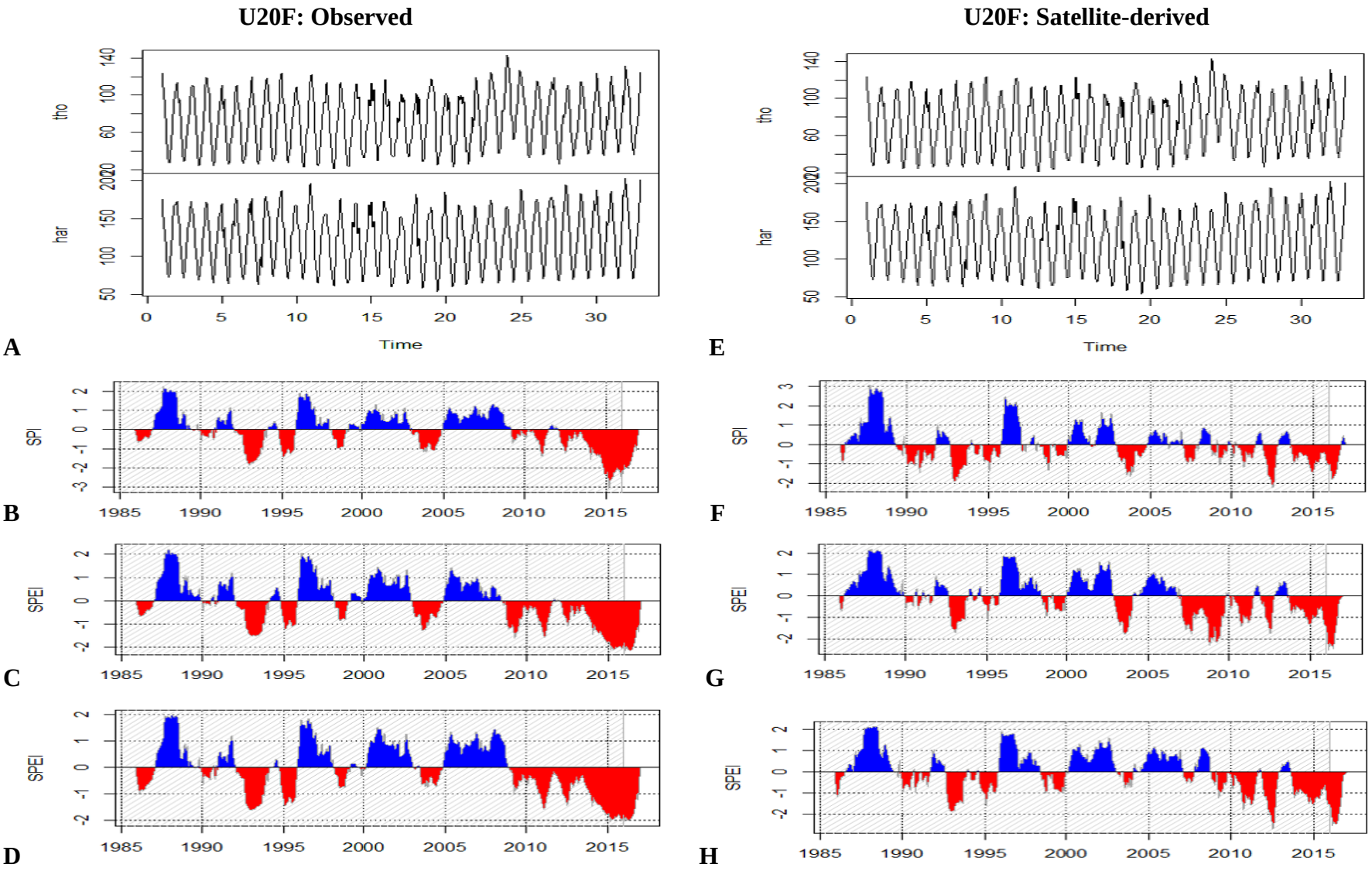

Figure 4.31 SPI and SPEI results for U20F.C and G represent SPEI calculated using the Thornthwaite method while Figure D and H the Hargreaves

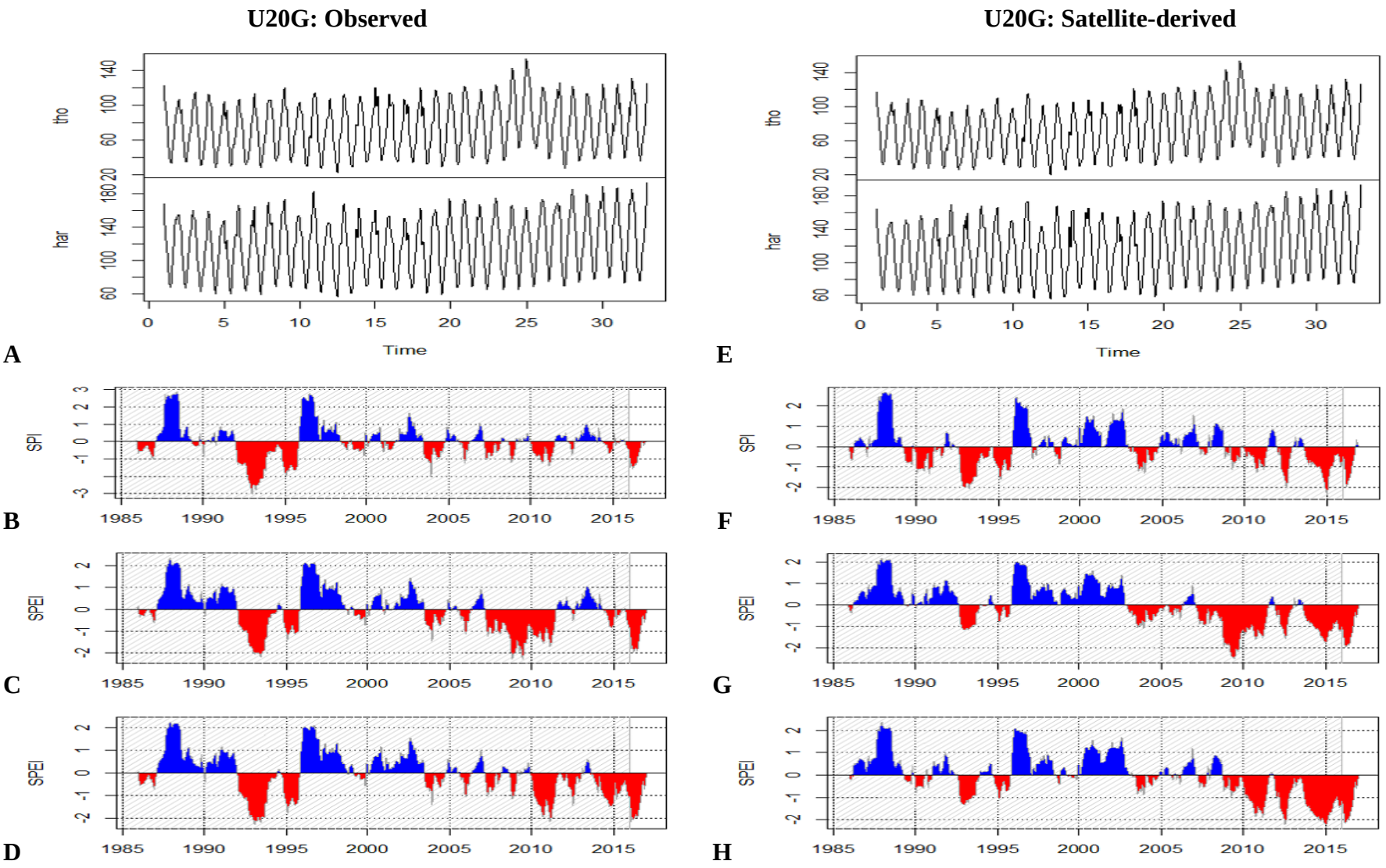

Figure 4.32 SPI and SPEI results for U20G.C and G represent SPEI calculated using the Thornthwaite method while Figure D and H the Hargreaves

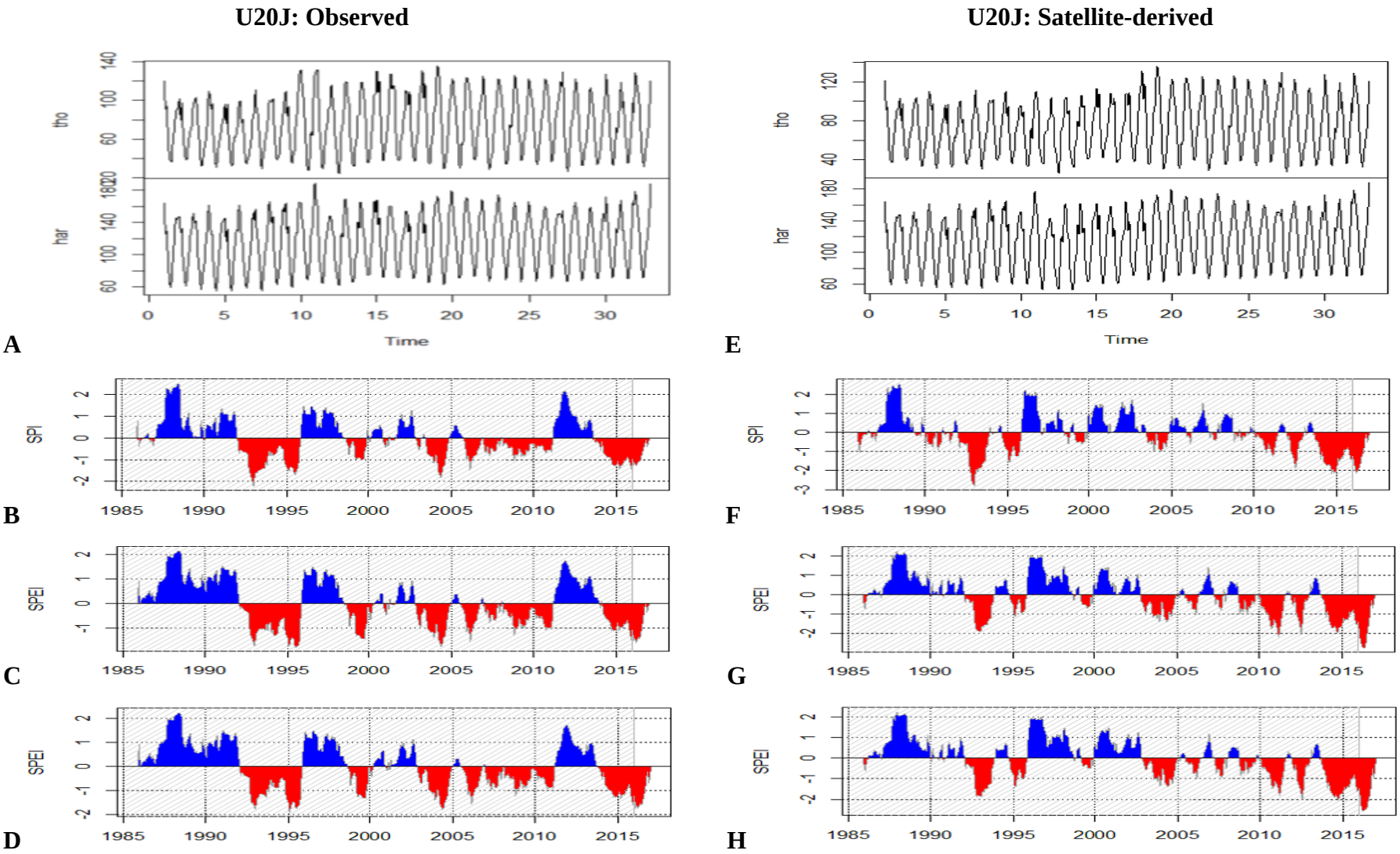

Figure 4.33 SPI and SPEI results for U20J.C and G represent SPEI calculated using the Thornthwaite method while Figure D and H the Hargreaves

4.4.3 Comparison of the SPI, SPEI (Thornthwaite, Hargreaves) with the ETDI: Umgeni Catchment

Cross comparisons between drought indicators was performed in order to investigate the ETDI in detecting the occurrences of droughts. Figure 4.34, Figure 4.36, Figure 4.38 and Figure 4.40 show comparison of drought indices using observed data as inputs. Figure 4.35, Figure 4.37, Figure 4.39 and Figure 4.41 illustrate the comparison of drought indices using FEWS satellite rainfall data, combined with the temperature database for southern Africa. In all Figures, the ETDI, when compared to the SPI and SPEI, displays a similar trend in peak and a drop in the amplitude of the indices. When closely observed, the ETDI shows subsequent peaks and drop in amplitude while the SPI and SPEI shows a gradual trend when compared. The SPI, SPEI-Thornthwaite and SPEI-Hargreaves are observed to be correlated.

Beguería *et al*. (2014), state that the Hargreaves equation does not have the limitations of the Thornthwaite equation as well as at a monthly and yearly timescale, ET_o estimates from both equations are found to be very similar, with differences being less than 2 mm per day. The study results are thus consistent with previous literature. The Hargreaves equation is the preferred option, when sufficient data is not available, or with the second option being the Thornthwaite.

Overall, all indices including the SPEI using observed and satellite data managed to display the similar trends in dryness and wetness that were experienced within the different quaternaries. The slight discrepancies in the peaks and drop in amplitude of the ETDI to the SPI and SPEI can be attributed to the fact that the indices are based on and account for different meteorological variables. Therefore, the environmental demand for the different meteorological variables vary. Additionally, in the case of the SPI and SPEI, it takes longer for precipitation shortage to become evident in soil moisture, which may explain the slight differences with the ETDI. The ETDI is derived from ET_o and ET_a while the SPI and SPEI is computed based on temperature and precipitation. Several studies have also reported on the SPEI correlating better with ecological and hydrological variables than other drought indices.

Despite the slight discrepancies, the SPI, SPEI and ETDI may all be used to detect drought occurrences.

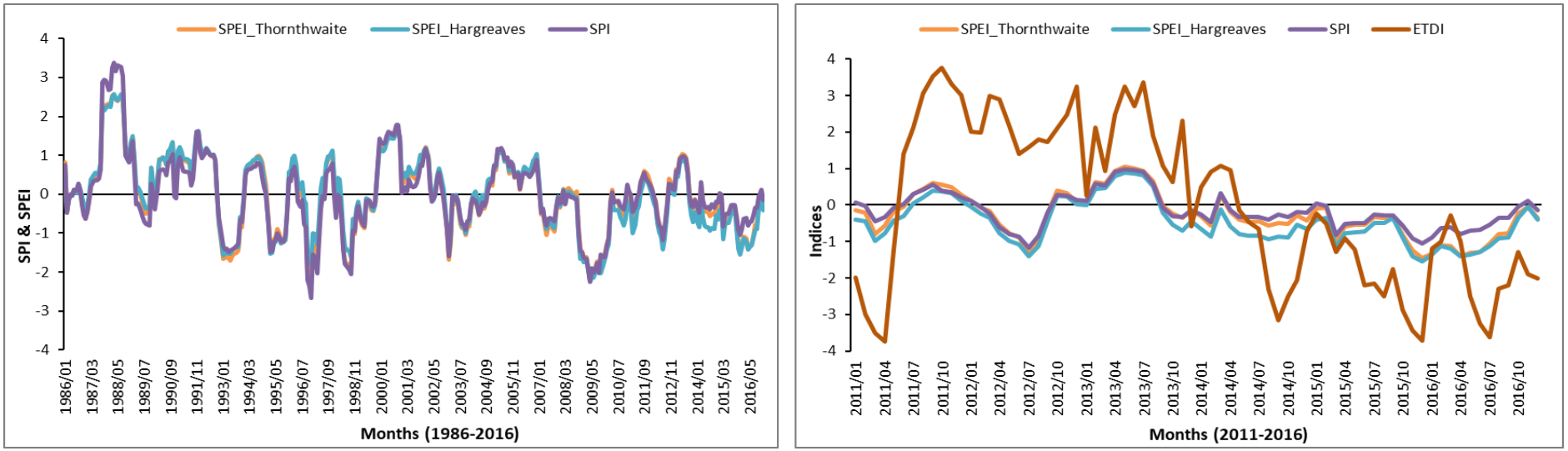

Figure 4.34 Comparison of drought indices for U20E using observed data

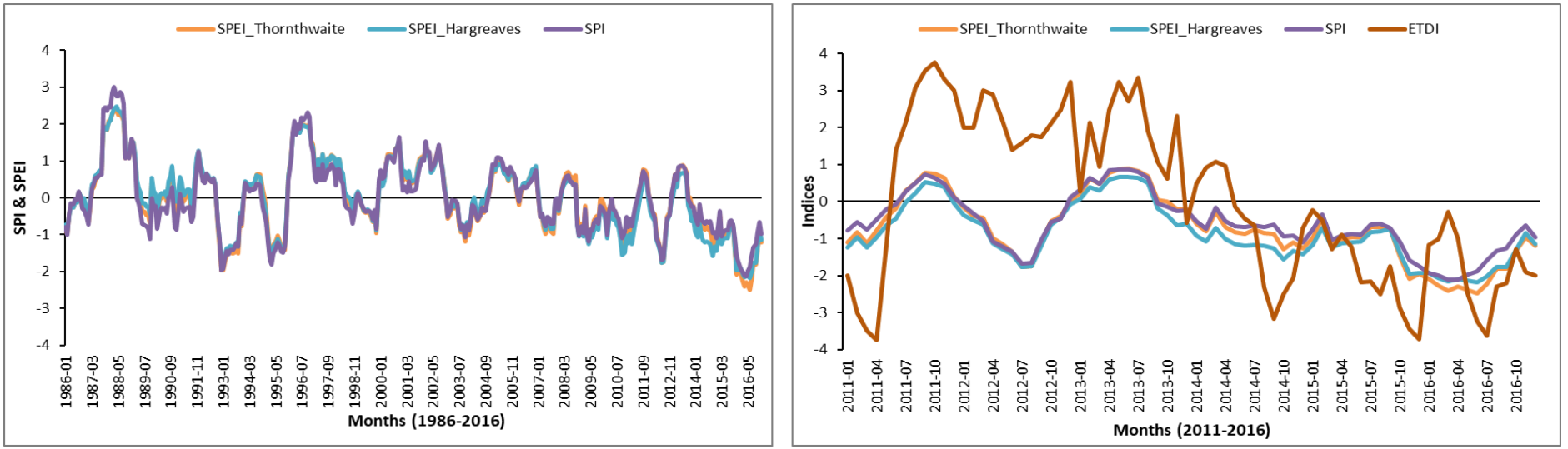

Figure 4.35 Comparison of drought indices for U20E using satellite-derived data

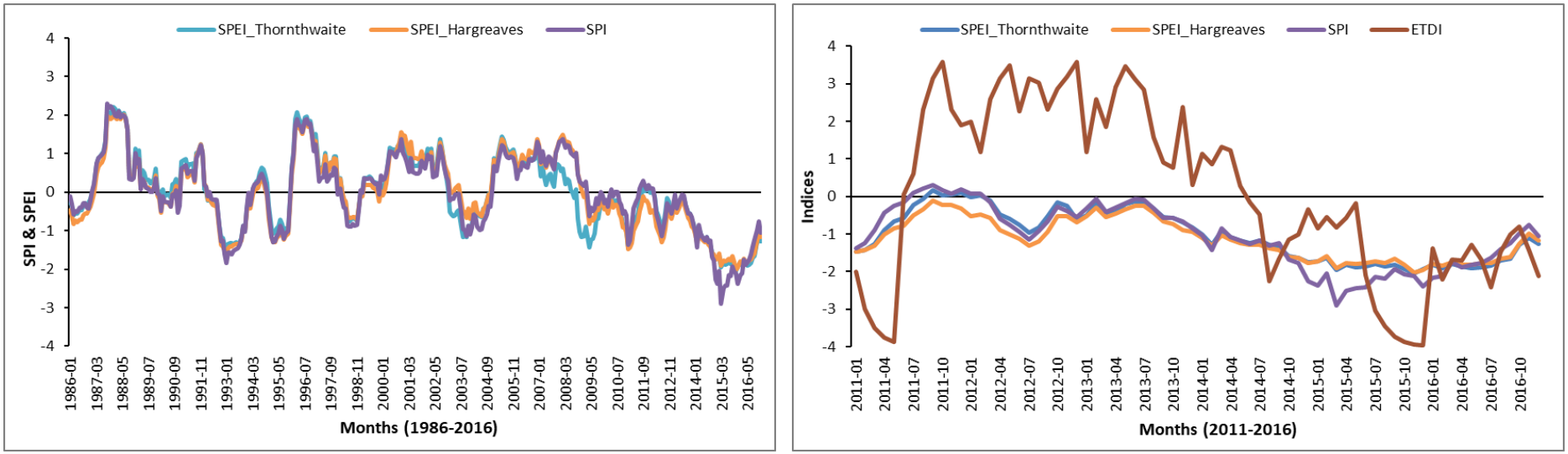

Figure 4.36 Comparison of drought indices for U20F using observed data

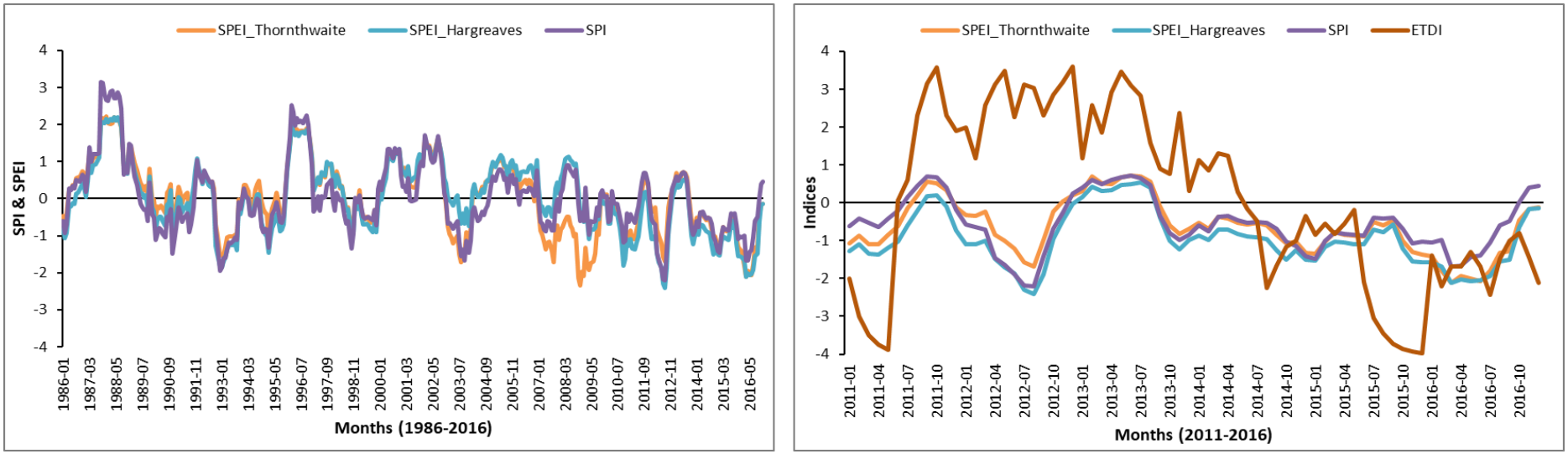

Figure 4.37 Comparison of drought indices for U20F using satellite-derived data

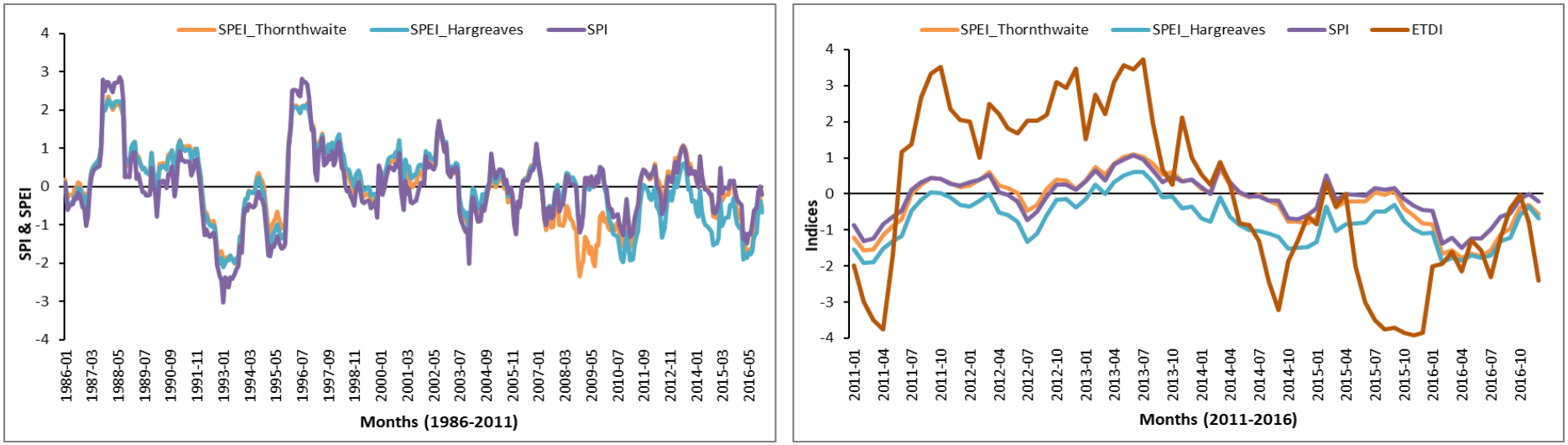

Figure 4.38 Comparison of drought indices for U20G using observed data

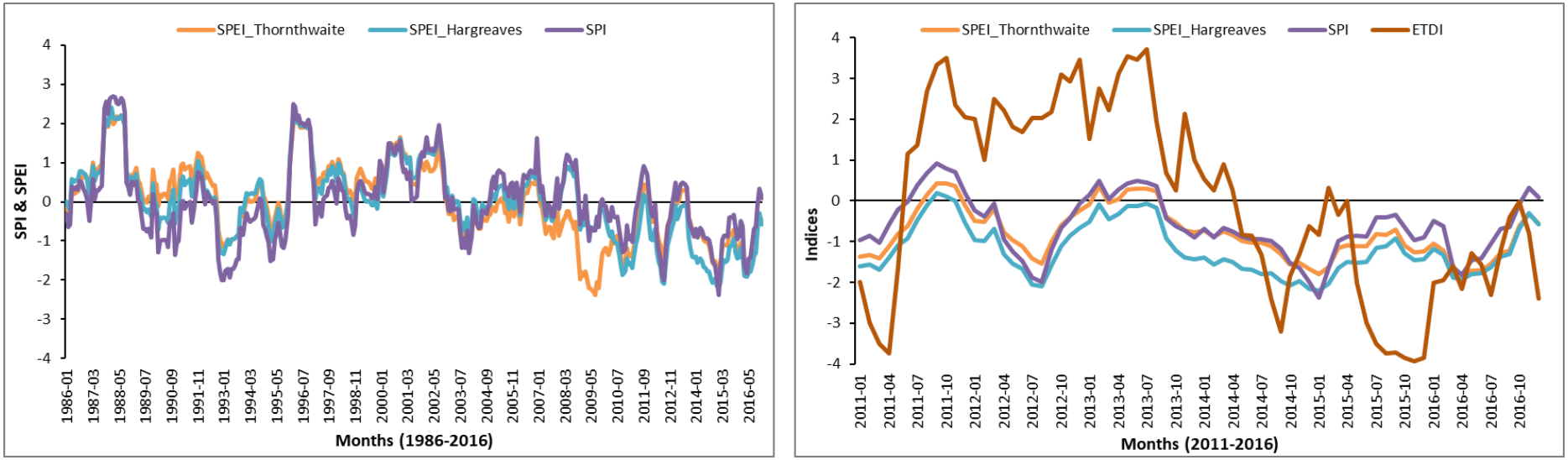

Figure 4.39 Comparison of drought indices for U20G using satellite-derived data

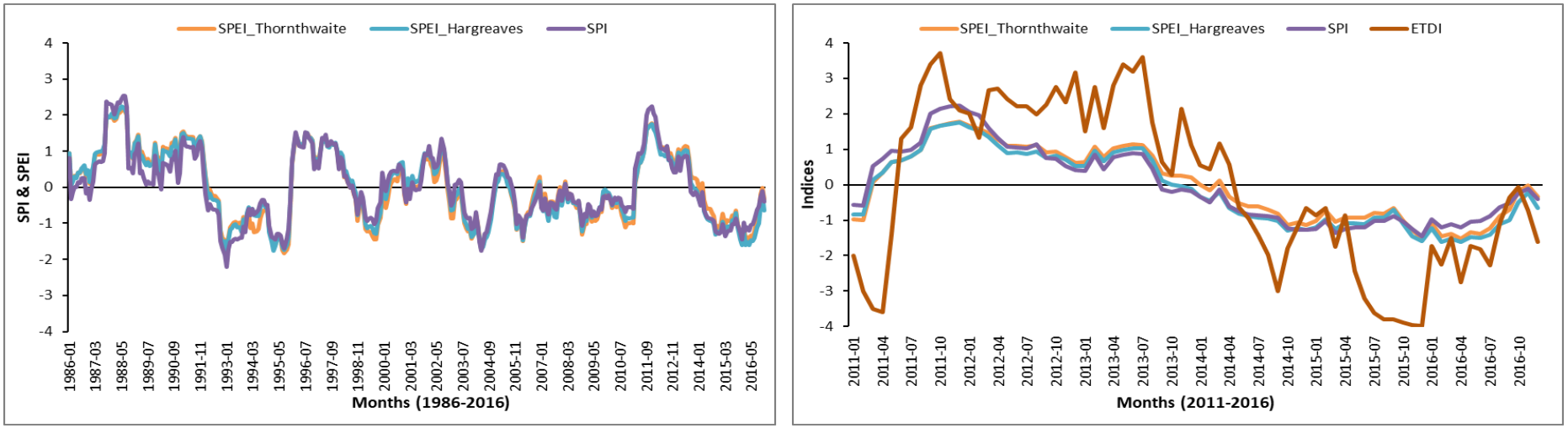

Figure 4.40 Comparison of drought indices for U20J using observed data

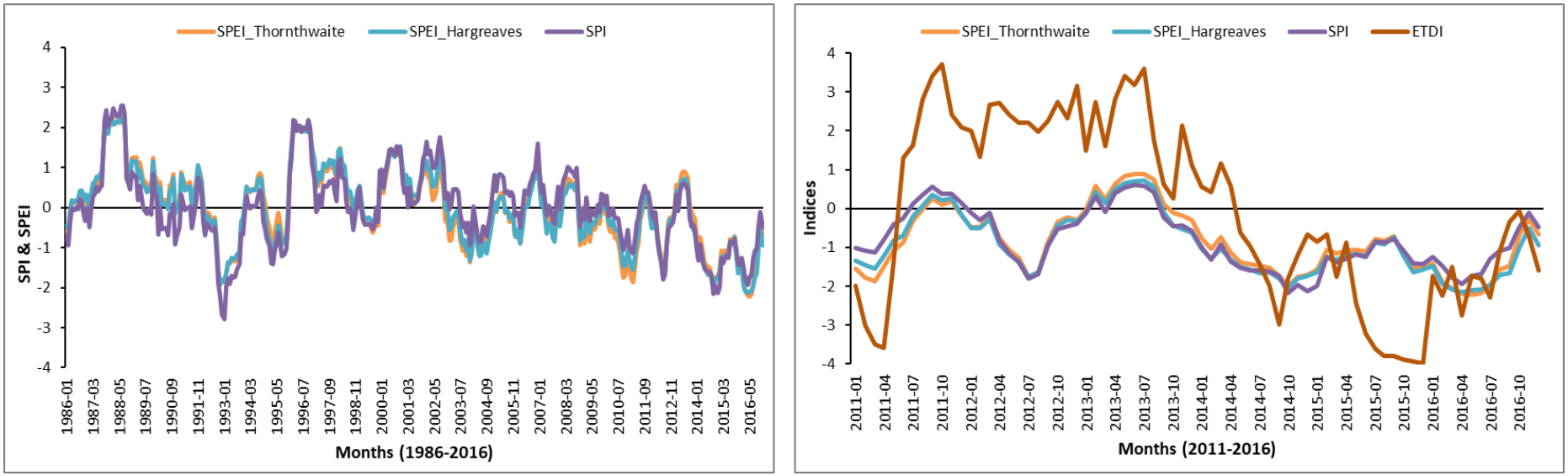

Figure 4.41 Comparison of drought indices for U20J using satellite-derived data

Cross correlation analyses were conducted between the ETDI, the SPI and the SPEI using observed data for the four selected QC's. Figure 4.42 displays the cross correlation results for QC U20J along with the R^2 values, while the R^2 values for the remaining three QC's are displayed in Table 4.6.

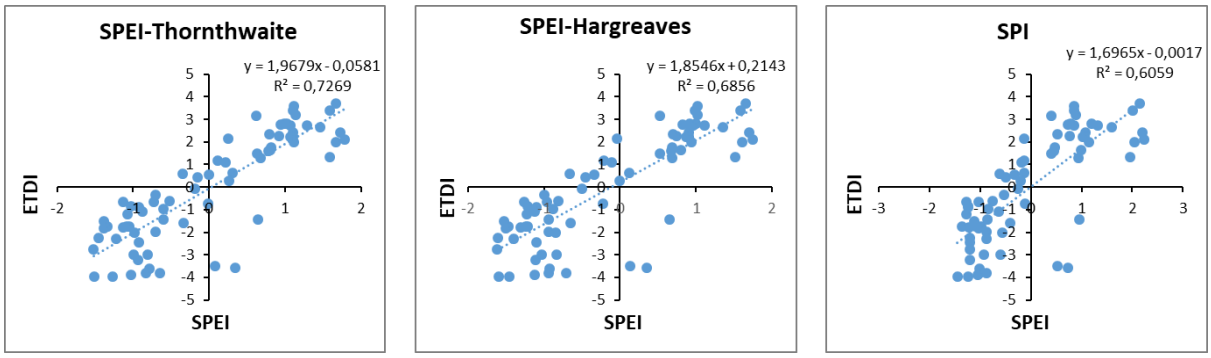

Figure 4.42 Correlation between the ETDI, SPI and SPEI for U20J (2011-2016)

Table 4.6 R^2 results obtained from performing ordinary least square regression analyses

	U20E	**U20F**	**U20G**	**U20J**
SPEI-Thornthwaite	0.43	0.62	0.48	0.73
SPEI-Hargreaves	0.42	0.57	0.48	0.69
SPI	0.31	0.44	0.40	0.61

The highest R^2 values for the QC's were obtained from the cross correlations between the ETDI and the SPEI-Thornthwaite, hence, displayed a better comparison to the ETDI. The SPEI-Thornthwaite requires mean daily temperature and the latitude of the study area. As with the Thornthwaite approach, the SPEI-Hargreaves also requires minimum and maximum daily temperatures. Beguería *et al*. (2010), reported on previous research that indicated that the Thornthwaite approach underestimates ET_o in arid and semi-arid environments and overestimates in tropical and humid equatorial regions. The negative y-intercept (-0.06) indicates an underestimation and is in line with the previous research results.

The greater difference between the ETDI and the SPEI-Hargreaves compared to the SPEI-Thornthwaite may be due to the discrepancies in the MOD11A2 maximum

temperature that was used within the Hargreaves-LST approach to obtain ET_o estimates as an input into the ETDI calculation.

Within this study, the Hargreaves and Thornthwaite equations were able to depict wet and dry events respectively and it was found to be valuable for use when limited meteorological data is available. The Hargreaves equation is preferred over the Thornthwaite, as it does not possess the limitations of the Thornthwaite equation (Begueria *et al.*, 2014); hence, use of the Hargreaves is recommended first and the second would be the Thornthwaite.

In comparison to the SPEI and the SPI with the ETDI, the SPEI results were better correlated to the ETDI. This is because the ETDI is an evaporative index and the SPEI techniques account for evaporation either through *PET* in the case of the SPEI-Thornthwaite approach or through ET_o with respect to the SPEI-Hargreaves approach. The SPI is calculated purely on rainfall and the index is unable to account for the evaporation component therefore, R^2 values were least correlated to the ETDI as opposed to the SPEI results.

4.4.4 Normalization performed on the indices using *in-situ* data: Umgeni Catchment

Normalization were performed on all three-drought indices for better comparison of the indices. The normalized indices were plotted for U20J as shown below in Figure 4.43 and the cross correlation of the normalized indices for U20J are shown in Figure 4.44. The Figures of the normalized indices for the remaining QC's are shown in Appendix A.

After normalization, a better comparison of the indices for U20J are displayed in Figure 4.43 than the previous without normalization, which is displayed in Figure 4.40. In terms of the correlation, R^2 values did not change after normalization, as values remained within the same range; however, the boxing co-ordinates of the plot changed, which resulted in a better display between the different indices (Figure 4.44). Computation of the ETDI based on the same time series as the SPI and SPEI is expected to result in a better correlation; however, the present results are suitable for assessing droughts within semi-arid to arid regions.

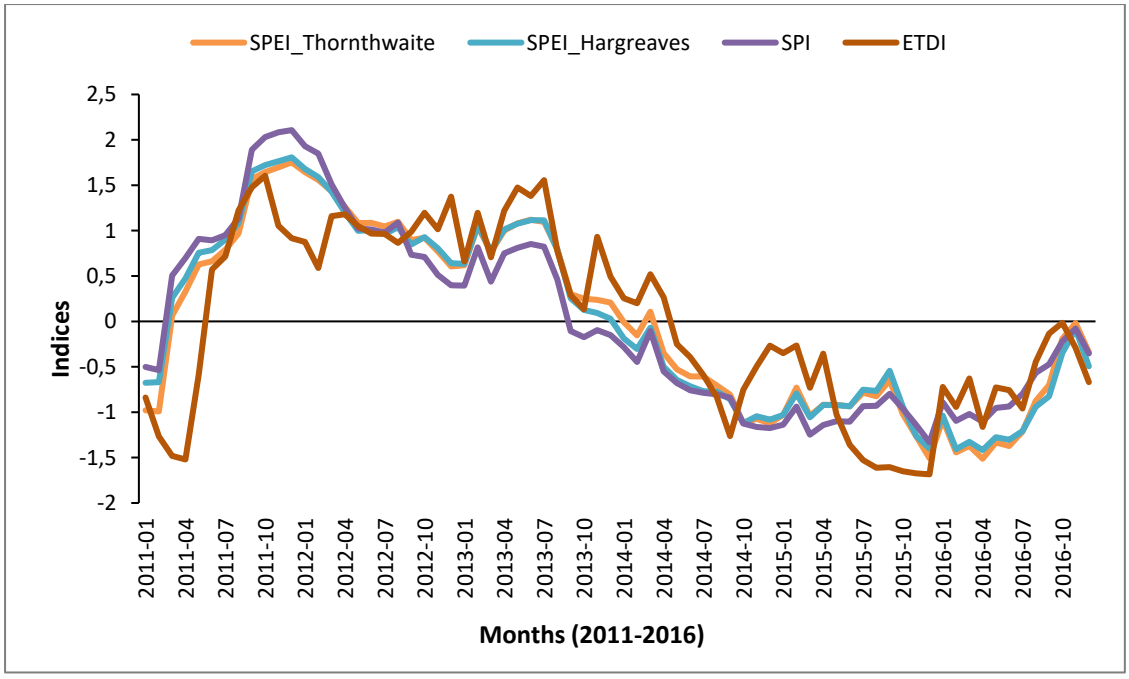

Figure 4.43 Comparison of normalized ETDI, SPI and SPEI for U20J (2011-2016)

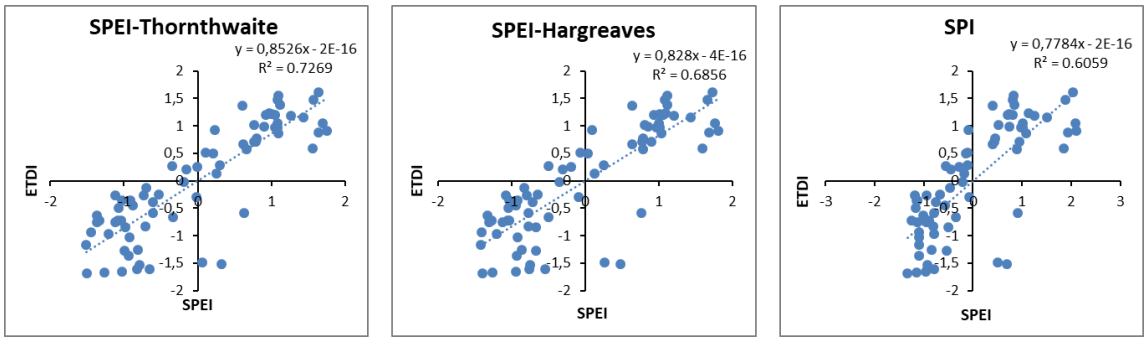

Figure 4.44 Correlation between normalized ETDI, SPI and SPEI for U20J (2011-2016)

The ETDI is suggested to be considered over the SPI and the SPEI where drought monitoring is concerned. The index accounts for the actual state of the land surface dryness through ET_a, which is known to be dependent on the current water availability that prevails. The ETDI is based on the evaporation deficit ($ET_a - ET_o$) and evaporation is considered to be a significant variable in semi-arid to arid regions like South Africa. At the land surface, evaporation provides the link between the energy and the water cycles, including between the water and the carbon cycle by means of vegetation transpiration. By accounting for evaporation and changes in the variable, a vital component of the water cycle can be accounted for. Evaporation is found to be a

significant contributor to droughts and drought severity, more so for semi-arid to arid regions. Bugan *et al*., 2012, states that ET_a can reach to 100% rainfall.

4.4.5 Comparison of SPI using *in-situ* rainfall data and satellite rainfall data within the Umgeni Catchment

SPI was calculated using 30 years precipitation data from *in-situ* data as well as from FEWS satellite rainfall data for the Umgeni Catchment. Comparisons between SPI calculated from observed data and SPI calculated from satellite data was performed. These comparisons were made to investigate how the two SPI's varied from each other and how they represented each other, because the SPI calculated from observed data was obtained from point measurements, and the SPI calculated from satellite data was from a spatially-averaged value of rainfall over a quaternary. Bar graphs were plotted to visually interpret and compare the two data sets for the four selected QC's within the Umgeni catchment (Figure 4.45). As shown in Figure 4.45 the satellite derived SPI for most months follow the same trend as the SPI values obtained from *in-situ* data. However, both datasets differed in a few cases, such as for the month of December and for the months within QC U20G. This difference could be attributed to the difference between the spatial scales at which rainfall estimates were obtained. It should also be noted that there were quite a few missing days of rainfall imagery seen within the FEWS rainfall product.

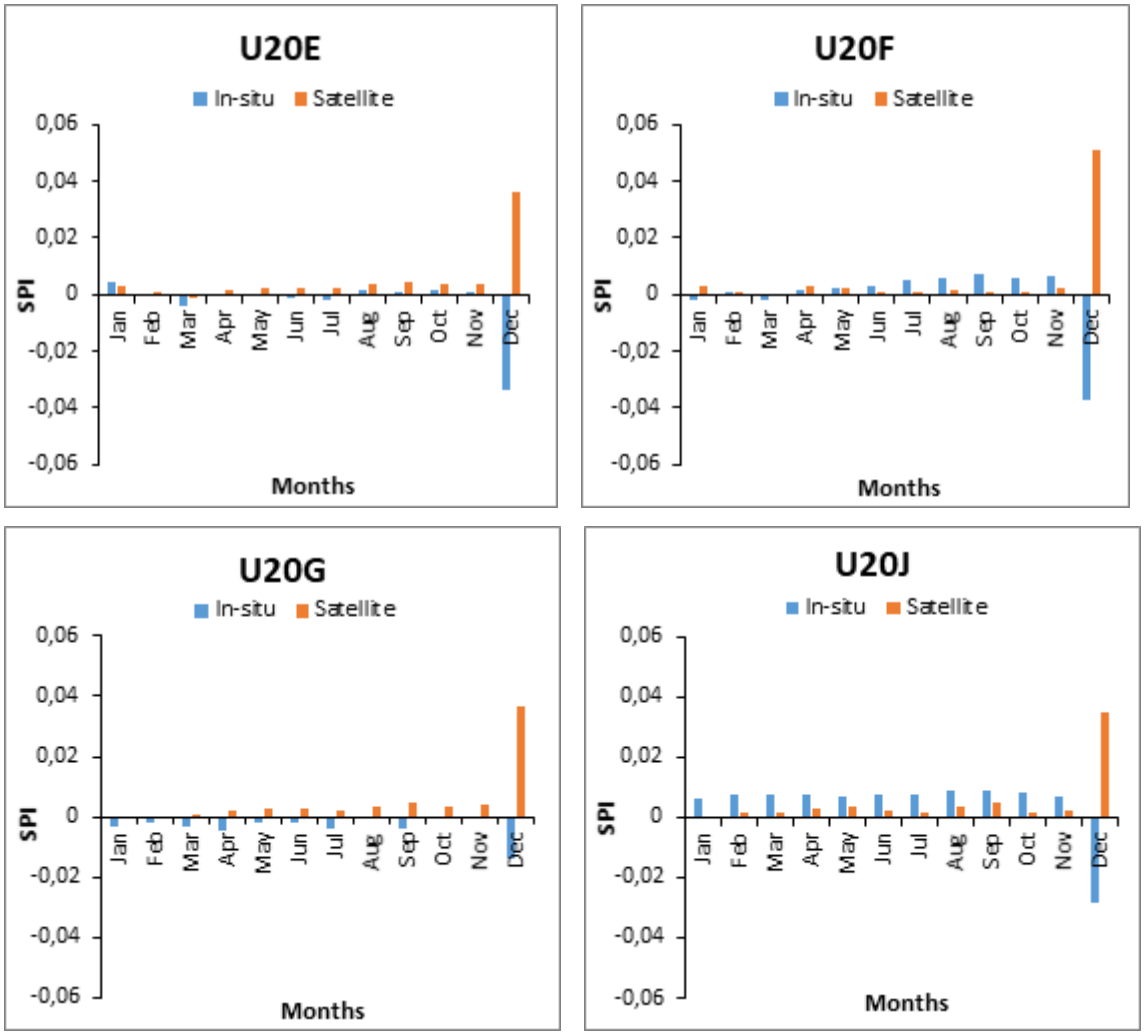

Figure 4.45 SPI calculated using *in-situ* and satellite rainfall data for the Umgeni Catchment (2011-2016)

A graph of correlation coefficients was plotted with SPI calculated from the representative *in-situ* dataset on the x-axis and the SPI calculated from satellite rainfall data on the y-axis. Figure 4.46 displays one common extreme outlier representing the difference in the SPI's for the month of December with majority of the points in close proximity to each other. The positive y-intercept for QC's U20E, U20F and U20J is indicative of an over-estimation by the satellite. Whereas, the negative y-intercept for QC U20G indicates an under-estimation by the satellite. The R^2 values for all four selected QC's range between 0.80 to 0.96, which is found to be close to 1 indicating that the datasets correlate well and are considered satisfactorily good. Overall, it can be seen that the FEWS rainfall product was suitable to provide spatial estimates of rainfall for use within the SPI and SPEI. This result encouraged the use of the FEWS rainfall product to enable calculations of the SPI and SPEI within the Upper Thukela Catchment as the catchment did not have sufficient meteorological data.

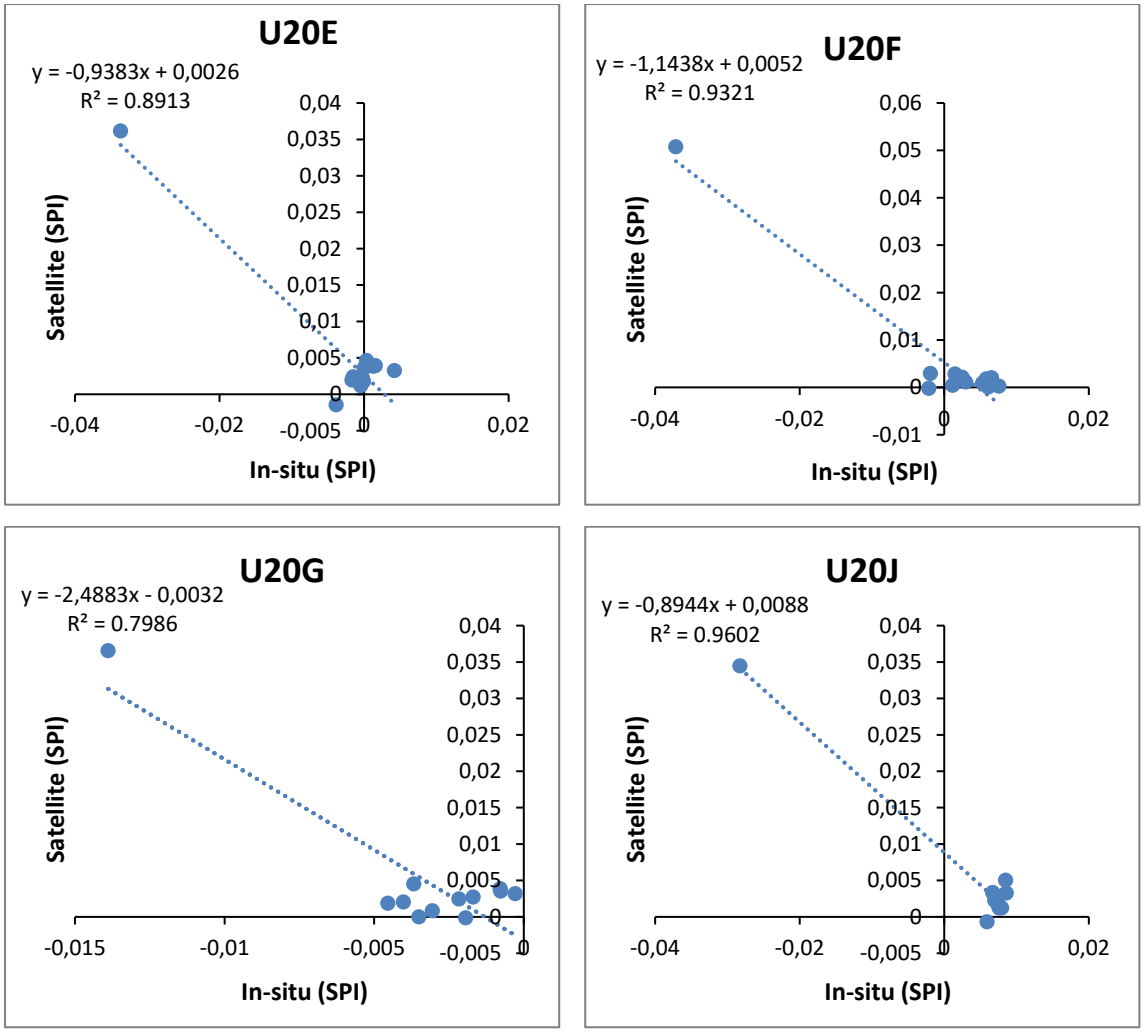

Figure 4.46 Scatterplot of *in-situ* calculated SPI values against FEWS rainfall calculated SPI values

4.4.6 Validation of the FEWS rainfall product within the Upper Thukela Catchment

Precipitation is notable the main factor that controls the persistence and development of droughts and since the quality of satellite rainfall products developed are subjective, it is beneficial for independent validation to be achieved.

The results from the previous section displayed the potential of using the FEWS satellite rainfall product to run the R package to obtain SPI and SPEI values for the Upper Thukela Catchment as a result of insufficient meteorological data to form 30 year precipitation and temperature datasets. Rainfall data from weather stations within the catchment consisted of data for a few years however not enough to form a 30 year record. A common period, 2011-2016 was identified whereby rainfall data was available for the selected QC's from weather

stations. This data was compared against rainfall data obtained from FEWS ARC 2.0 product for the same period to check the applicability of the product for use within the Upper Thukela Catchment.

Figure 4.47 illustrates a time-series analysis that was plotted to visually interpret and compare the FEWS dataset with the representative *in-situ* dataset. As shown in Figure 4.47 the FEWS estimates follow the same trend as the *in-situ* rainfall dataset and correlate with each other. Overall, the FEWS dataset followed the general trend of the *in-situ* rainfall estimates.

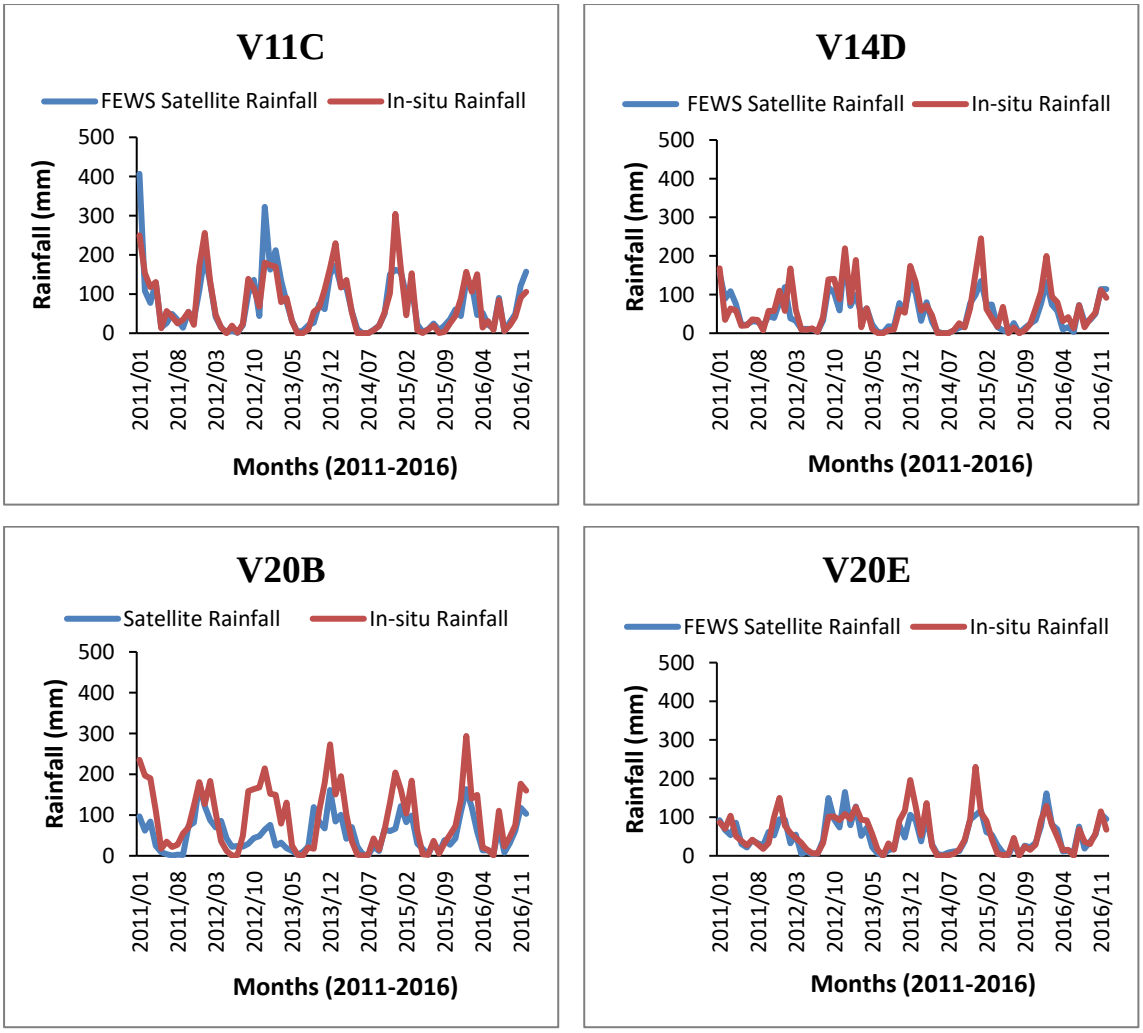

Figure 4.47 *In-situ* and FEWS annual rainfall estimates for the Upper Thukela (2011-2016)

Graphs of correlation coefficients were plotted with majority of the points in close proximity to the 1:1 line with no extreme outliers depicted (Figure 4.48). The positive y-intercepts for the four selected QC's within the Upper Thukela Catchment indicate an over-estimation of rainfall by the FEWS rainfall product. The slope is 0.88 for V11C, 0.64 for V14D, 0.42 for V20B and

0.68 for V20E, which represent the relationship between the two variables with regard to their increases and decreases. A value close to 1 is indicative of a good correlation between datasets. For this study, the values are considered acceptable. The R^2 for the quaternaries range from 0.55 to 0.72. This gives a further indication of the linear association that occurs between the datasets. Overall, it can be seen that the FEWS rainfall product was suitable to provide spatial estimates of rainfall. The FEWS rainfall product, together with the temperature database for Southern Africa, was therefore used to calculate the SPI and SPEI for the Upper Thukela Catchment.

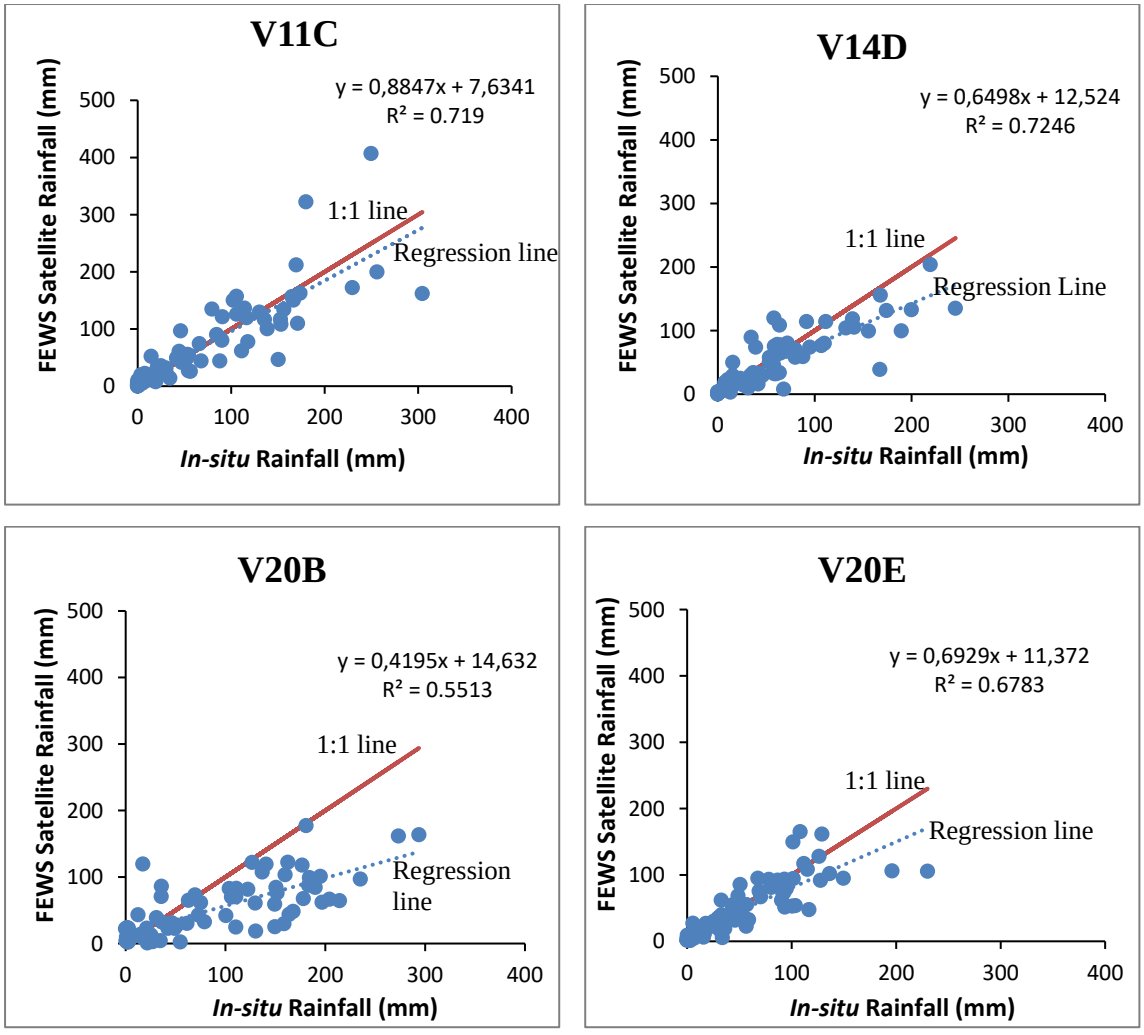

Figure 4.48 Scatterplots of *in-situ* rainfall estimates against FEWS estimates for the Upper Thukela Catchment

4.4.7 Calculation of the SPI and SPEI for the Upper Thukela Catchment incorporating satellite data

Given the situation of very few gauges being present with the catchment, the study opted to advocate the use of satellite data in such instances. However, various comparisons and analyses were performed prior to incorporating satellite data to generate SPI and SPEI results for the Upper Thukela catchment. The Umgeni Catchment, located directly below the Upper Thukela consisted of sufficient *in-situ* data to form 30-year records. Hence, comparison between the SPI's using different data inputs were performed and graph of correlation coefficients was plotted between the representative *in-situ* dataset and the satellite rainfall dataset for the Umgeni Catchment. R^2 values ranged from 0.80 to 0.96 and was considered satisfactorily good. Following these results for the Umgeni Catchment, time series analyses and graphs of correlation coefficients were then plotted between the representative *in-situ* rainfall dataset and the FEWS satellite rainfall estimates for the Upper Thukela Catchment. Majority of the points were in close proximity to the 1:1 line and it was observed that the FEWS rainfall product was suitable for providing spatial estimates of rainfall to calculate the SPI and SPEI for the Upper Thukela Catchment.

Following the promising results, the FEWS rainfall product together with the temperature database for Southern Africa formed 30-year records and the R software was able to produce SPI and SPEI results for the Upper Thukela Catchment. Figure 4.49 and Figure 4.50 present the results for the four selected QC's within the Upper Thukela catchment with SPEI results displayed using two methods. The first method used the Thornthwaite equation computed using *PET*, while the second used the Hargreaves equation computed using ET_o.

Figure 4.49 and Figure 4.50 results indicate that the 2015/2016 drought was detected within the catchment. Results display the potential of using SEO in an ungauged catchment or in a region with limited data availability. SEO can prove to be advantageous for water resources management and disaster risk monitoring in data-sparse areas. Satellite data provides a wealth of data on a large scale, which creates the potential for more intense drought research to be undertaken.

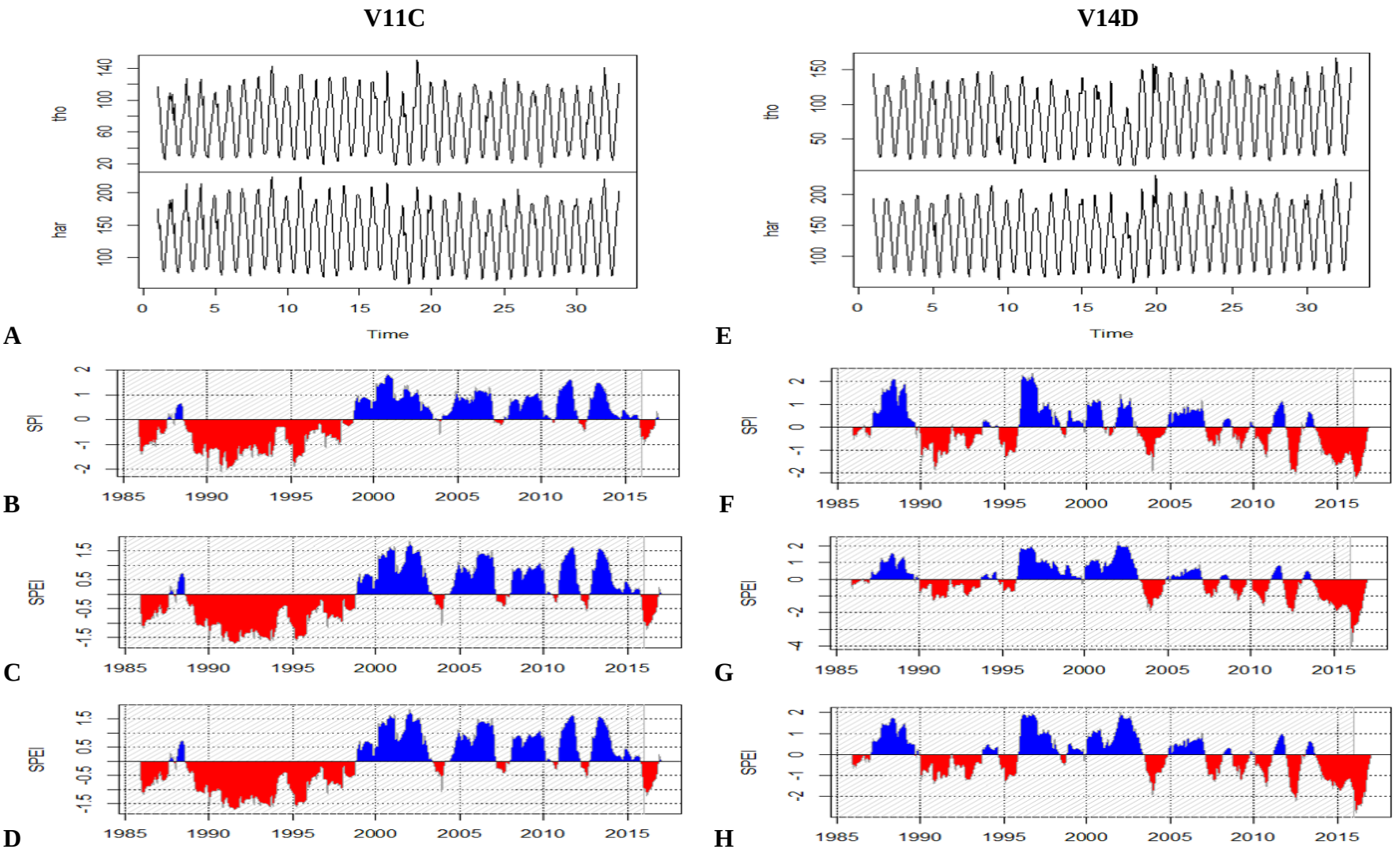

Figure 4.49 SPI and SPEI results for V11C and V14D.C and G represent SPEI using the Thornthwaite method while Figure D and H the Hargreaves

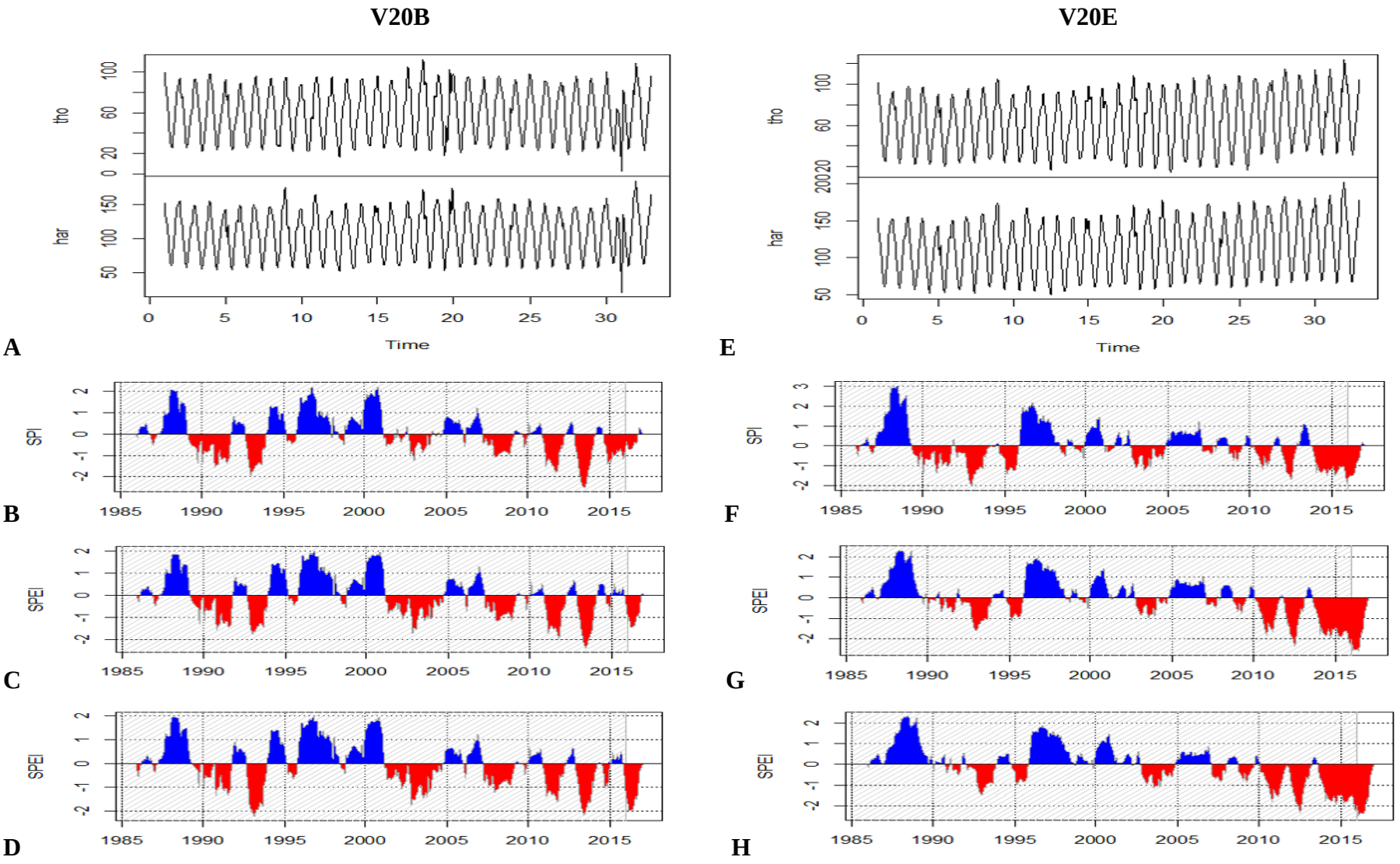

Figure 4.50 SPI and SPEI results for V20B and V20E.C and G represent SPEI using the Thornthwaite method while Figure D and H the Hargreaves

4.4.8 Comparison of SPI, SPEI (Thornthwaite, Hargreaves) and ETDI using satellite data in the Upper Thukela Catchment

Cross-comparisons between the different indices were undertaken to confirm the ETDI in detecting the occurrences of droughts. The comparison of drought indices using satellite data as inputs for QC's V11C, V14D, V20B and V20E are shown in Figure 4.51 to Figure 4.54. The figures display the SPI and SPEI to be well correlated as they follow the same trend and are in agreement with each other. Majority of instances display the ETDI following the general trend of the SPI and SPEI in most instances however, there are a few cases where an inverse in trend is observed.Additionally, the ETDI displays subsequent peaks, drops in amplitude while the SPI and SPEI show a gradual trend.

The differences may be attributed to the indices being based on different inputs and thereby accounting for different meteorological variables. The ETDI is computed from ET_o and ET_a variables, which may strongly depend on soil moisture, soil moisture holding capacity and the soil characteristics of the study area. Study by Vicente-Serrano *et al*. (2014), indicated that the SPI and SPEI display the largest sensitivity to ET_o variations. Furthermore, Beguería *et al*. (2010), stated that the climatic used in the SPEI does not represent the real moisture deficit that is experienced by a system. As a result, to overcome this, the different timescales offered by the index enables the user to find the appropriate time scale at which the response to droughts in said to be the highest. Hence, it may be beneficial for future studies to produce the drought indices at different time-scales. Several studies have also reported that the SPEI is known to correlate better with ecological and hydrological variables than with other drought indices within a number of natural and manages systems.

In respect to the SPI, it takes longer for precipitation shortage to become evident in soil moisture, streamflow, groundwater and dam levels. A 3-month SPI may be used to monitor soil moisture conditions at the start of the growing season or precipitation during the different stages of plant development or reproduction. Hence, it is recommended for the SPI to be calculated at different time scales to draw better comparisons between the ETDI and the SPI. Overall, all indices managed to display significant dry and wet periods well within the study period 2011-2016.

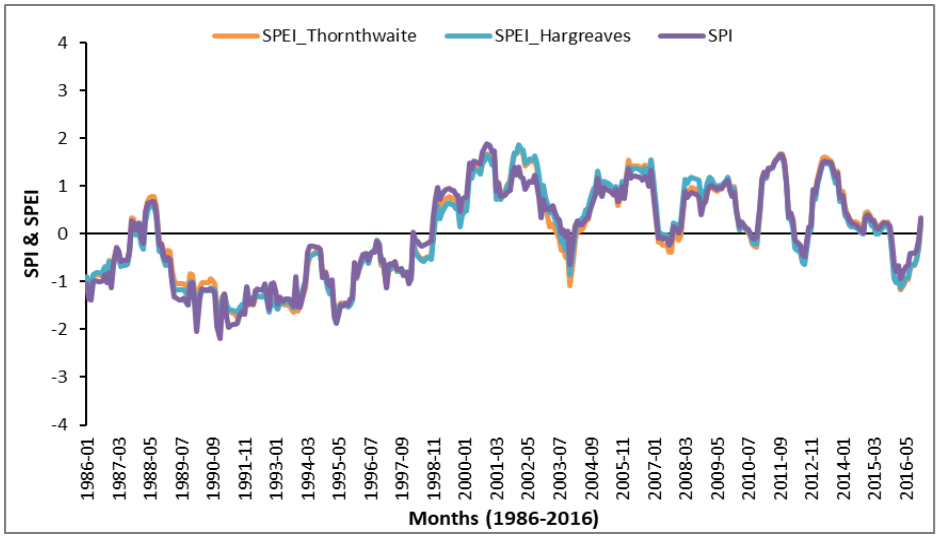

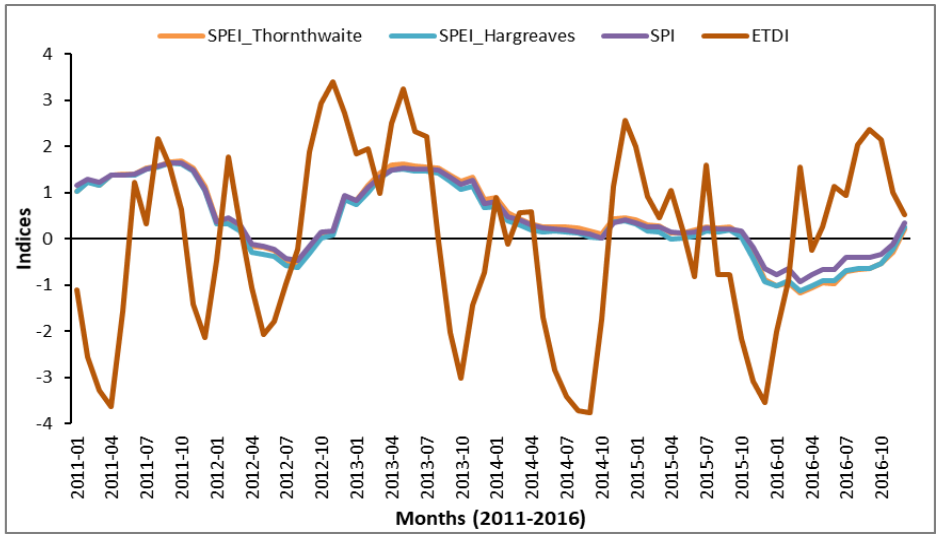

Figure 4.51 Comparison of drought indices for V11C

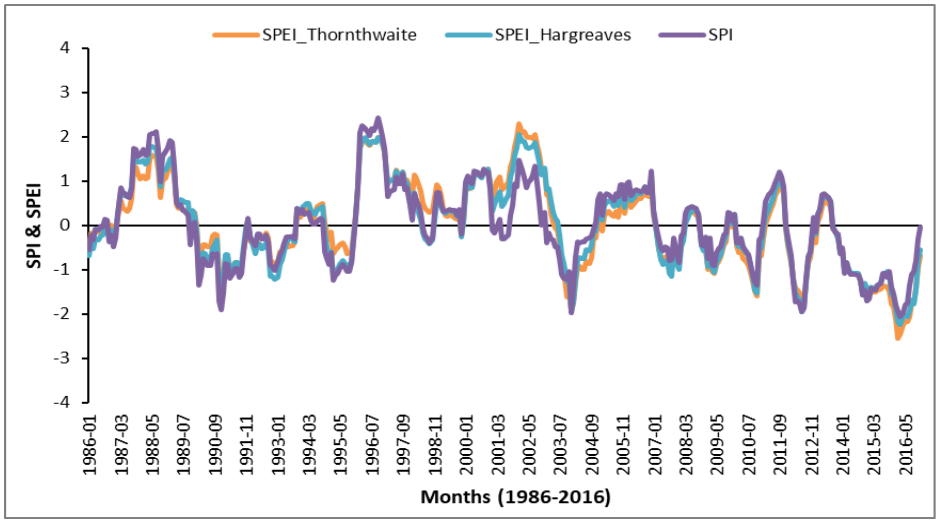

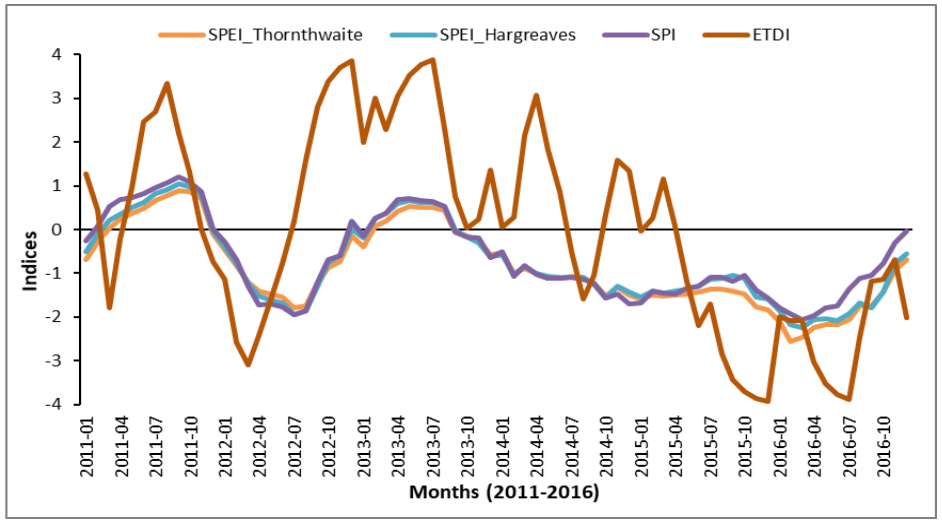

Figure 4.52 Comparison of drought indices for V14D

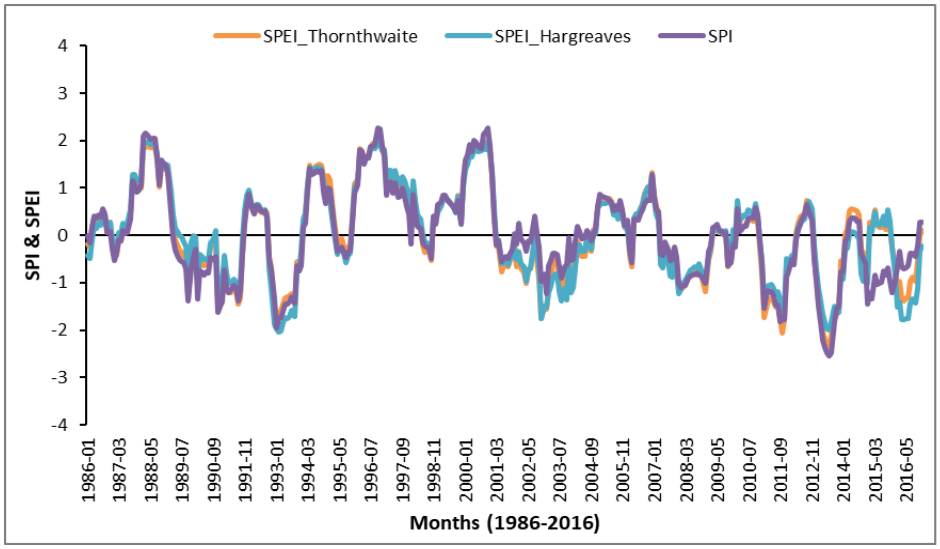

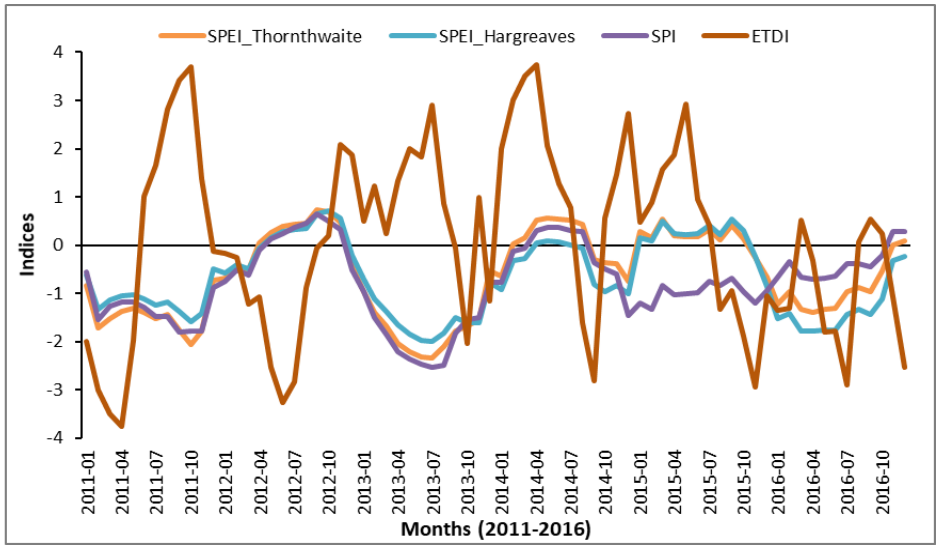

Figure 4.53 Comparison of drought indices for V20B

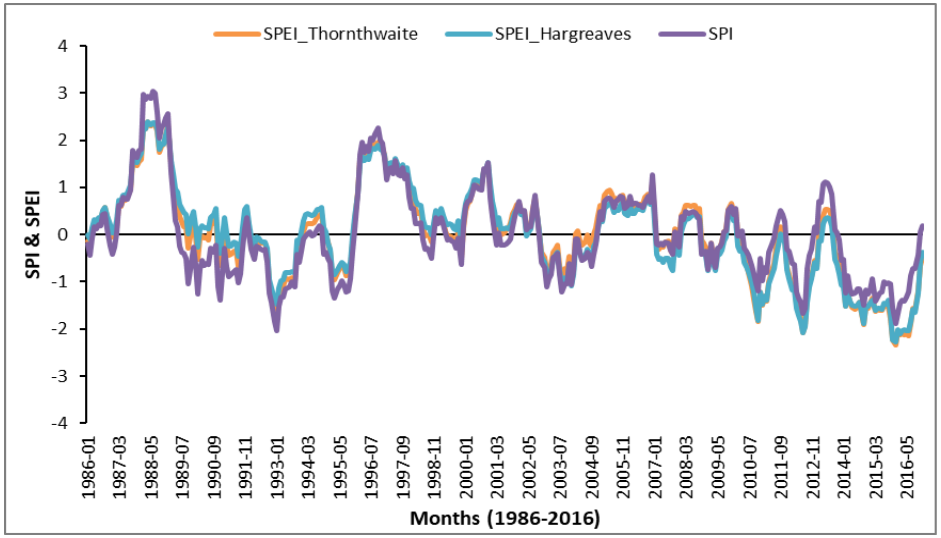

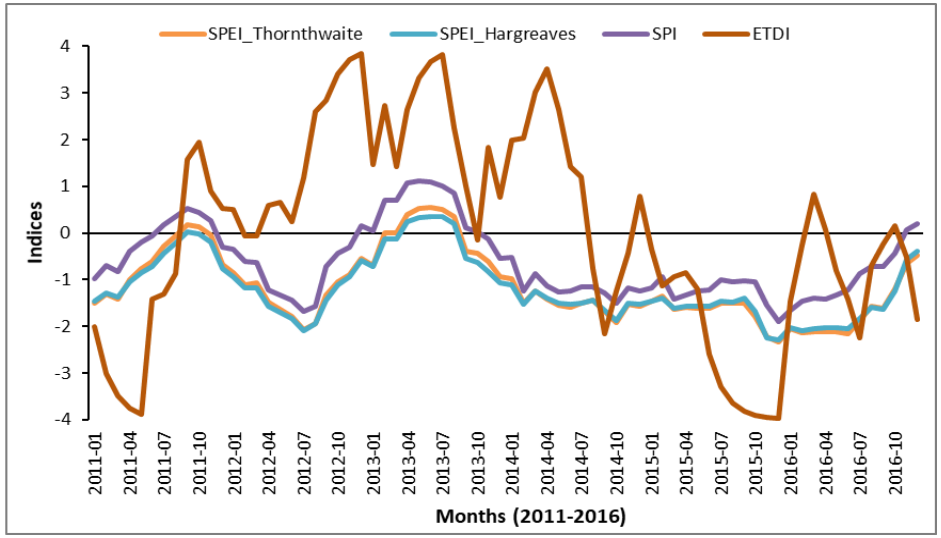

Figure 4.54 Comparison of drought indices for V20E

Several literatures discuss the various factors that contribute to triggering drought conditions, which include sea surface temperature (SSTs) and the ENSO (El Niño–Southern Oscillation) with SSTs being regarded as the major influencing factors. Nicholson (2000) conducted a study that showed SST, ENSO and land–atmospheric feedback, governs rainfall variability in South Africa. Results from the study further indicated that during the warm phase of the ENSO, droughts in Southern Africa are known to occur. A study by Rouault and Richard (2005) utilised the SPI to assess the spatial and temporal extent of droughts in South Africa and confirmed the strong relationship that exist between the ENSO and the drought conditions in southern Africa. According to the National Agro-meteorological Committee (NAC) Advisory on the 2015/2016 summer season, provinces including Kwa-Zulu-Natal displayed drought/very-dry conditions, which remained within the summer season. The drought indices including the ETDI was able to successfully detect those dry conditions that prevailed between 2015-2016. The report furthered stated that observations indicated that the ENSO was in a strong El Niño situation and the atmosphere was responding the strong SST warming.

SPI and SPEI produced for the Umgeni Catchment and for the Upper Thukela Catchment, based on ground measurements as well as those produced using satellite data were consistent to reports made by the media. According to the 1988 Global Register of Extreme Floods Events, Kwa-Zulu Natal was amongst some of the many areas within South Africa that experienced extreme flooding. The flooding resulted from heavy rains, which began on the 10/02/1988 and ended on the 02/03/1988. The SPI and SPEI values obtained within this study for the two study sites within the KwaZulu-Natal province was able to display this wetness through positive SPI's and were represented by blue shading indicating wet periods.

Additionally, numerous SAWS reports and media articles reported on what is known to be one of the greatest natural disasters in South Africa in September 1987, which resulted in several deaths and severe damage to the infrastructure. Areas within the province of KwaZulu-Natal interior were affected by the cut-off low, a significant synoptic-scale weather system that is responsible for most large-scale severe precipitation events to occur in South Africa. This resulted in large-scale extreme precipitation events. The SPI and SPEI values produced by the study was able to produce positive results indicating wetness. These correlating results prove the accuracy of the SPI and SPEI as they are in accordance to what we have experienced. In addition, the use of satellite data for drought indices is promoted as the results from this study, if given an ungauged catchment scenario, the drought indices were able to display previous wet

and dry events that occurred by displaying low, negative values for dry conditions and high, positive values for wet conditions.

All drought indices were able to successfully detect the 2015/2016 El Niño event that was experienced in KwaZulu-Natal. SPI and SPEI results for the 30-year period (1985-2016) clearly illustrate that from the year 2010 onwards sustained prolonged moderate to severe dryness has been occurring.

4.4.9 Discussion on drought propagation

The occurrences of droughts are termed complex due to them being dependent not only on the atmosphere, but as well as the hydrological processes that are responsible for feeding moisture to the atmosphere and causing water storage and runoff to streams (van Loon, 2014). Atmospheric processes take control of the development of a drought primarily due to climatic variability. Generally, prolonged durations of rainfall generates less input into the hydrological cycle triggering drought conditions (van Loon, 2014). Alternatively, anomalies in temperature also trigger drought condition. The abovementioned have been illustrated by the SPI, SPEI and ETDI results produced in this study.

Temperature and rainfall can both be associated with large-scale atmospheric or ocean patterns like ENSO, NAO (Northern Atlantic Oscillation), and SST's. Additionally, the depletion of soil moisture occurs resulting from antecedent conditions, evaporation from the soil, *ET* through the vegetation, drainage to groundwater as well as runoff contributing to stream flow. During dry conditions and lower than normal rainfall periods, runoff and drainage may be low; however, ET_a may increase as a result of increased wind speeds, radiation or vapour pressure. This paves the way for increases in ET_a, leading to extra water loss from open water bodies and the soil. Whilst during an extreme drought event, insufficient soil moisture and the wilting of plants can limit ET_a, further depleting soil moisture and restricting locally generated precipitation, thus contributing to drought conditions. This may explain why results produced by the ETDI were further enhanced compared to results produced by the SPI and SPEI (Figures 4.34-4.41, Figures 4.51-4.54).

Hence, the development of droughts are dependent on climate as during the warm seasonal climates, majority of the recharge occurs during the wet season. Whilst during the dry season,

ET_a is found to be higher than precipitation, thus ET_a plays a larger role during drought development. ET_a can aggravate a drought and during a typical dry season prevent the recovery of a drought. This aforementioned is further elaborate in the subsequent section (Section 4.4.10) and illustrated by Figure 4.55. The characteristic of a catchment may also play a role within drought development, the most significant characteristic being the storage capacity of the catchment.

It is noteworthy to mention that a study by Pozzi *et al*., (2013) explicitly mentions the diversity of variables that need to be monitored to capture the development of a hydrological drought and its impact on different water-related sectors. Furthermore, since declining groundwater levels are brought upon by a decreased recharge to the Ground Water (GW) system caused by a depletion of soil moisture, it may be valuable for further drought indices studies such as this study to account for GW levels.

4.4.10 Comparing the ETDI with hydrological parameters

When discussing droughts, the commonly employed variables within the definitions are often precipitation combined with other variables such as soil moisture and temperature, just to name a few. These hydrological variables are the driving forces to droughts (Eden, 2012). Previous research studies as well as results from this study have indicated that ETDI takes into account soil moisture with temperature, precipitation and elevation being interrelated. In order to further understanding these relationships, maps displaying the spatial distribution of these variables have been produced as shown in Figure 4.55. This analysis was carried out for a month (May 2015).

Elevation (Lynch, 2004) and precipitation (Weepener *et al*., 2011) are representative of the annual average expected ranges that are expected for the catchments as displayed in Figure 4.55. The Soil Saturation Index (SSI) is displayed for May 2015, which was retrieved from the SAHG-UKZN website and the average minimum and maximum temperatures had been obtained from the MOD11A2 LST product. The ET_o, ET_a, WS and ETDI are representative for May 2015.

Amongst the drought study years for this study (2011 to 2016), the year 2015 was considered to be the driest followed by 2016. Within the year 2015, the month of May was considered to

be amongst the dry season/winter season as well as produced ETDI values that were amongst the lowest. Hence, in order to display comparisons between the drought index and other hydrological variables, a dry season was considered appropriate.

The relationship that exists between the different variables of the hydrological system such as soil moisture, precipitation, discharge, GW, runoff and discharge may be an old concept in hydrology; however, the application of this knowledge to drought is relatively recent (van Loon, 2015). The precipitation regime in South Africa is characterized by high temporal and spatial variability, with the former being connected with seasonal cycles and inter-annual variability as well as the latter bring driven by marked topography (Figure 4.55).

Several studies that are linked to drought characteristics suggest that it is possible to quantify the hydrological variability that exists over an area, by combining monthly temperature and precipitation variability. The above-mentioned is illustrated by Figure 4.55 where those regions within the study areas that display high maximum temperatures along with poor precipitation are amongst those areas that received a more negative ETDI, indicating droughts conditions. The WS, which is computed from ET_o and ET_a displays low ET_a values for areas of low precipitation, low elevation, higher temperatures and low soil moisture, thus creating a favourable situation for droughts to develop, as indicated by the ETDI spatial maps.

The SSI and ETDI further display a distinct relationship, in that areas experiencing low soil moisture conditions, display lower ETDI values, which indicates more dryness for those areas with a low soil moisture. In concluding the discussion, when assessing, evaluating or monitoring drought conditions with the ETDI it is beneficial to account for the soil moisture within the region/area. It is also worth mentioning that the ETDI could be a useful indicator for monitoring soil moisture stress and that it can be used to assess the soil moisture of plants during their critical growth stages, thereby beneficial to agricultural sector. In addition, it is also clearly seen that the drivers of the hydrological cycle are all interrelated and each play a vital role when detecting droughts.

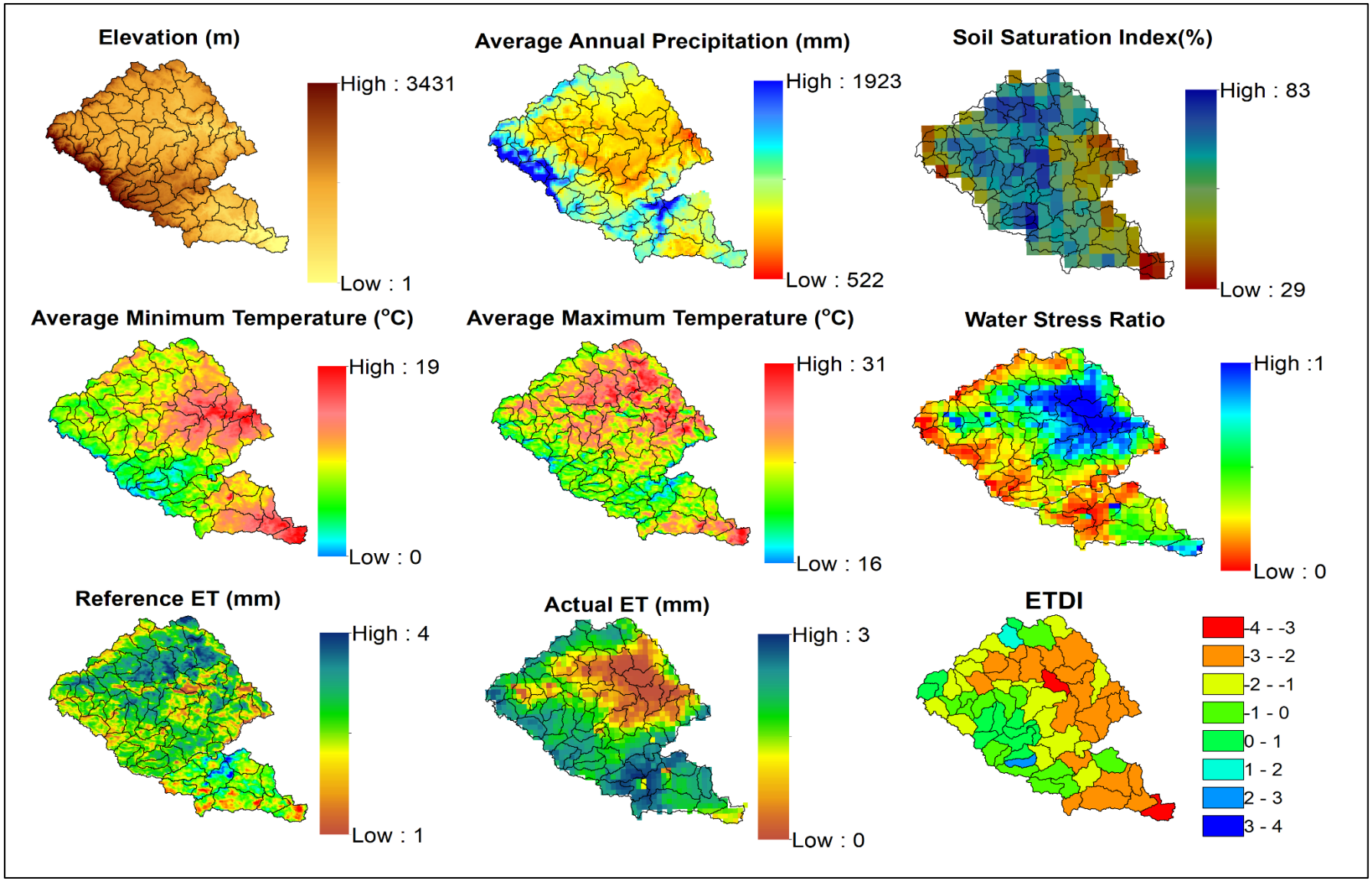

Figure 4.55 ETDI with the driving forces of droughts for the Upper Thukela and Umgeni Catchments for May 2015

5. CONCLUSION AND RECOMMENDATIONS

The conclusions and recommendations drawn from this research study are detailed in this chapter.

5.1 Conclusions

Droughts are a natural disaster and are driven by extremes in the natural variations in climate, which are forced by interactions found between the land surface, atmosphere and the oceans. With climate change, changes in rainfall patterns and projected increases in temperatures may result in an increase in the severity and intensity of droughts worldwide. Furthermore, the increasing demand from water supplies by growing populations and for socio-economic development affects the availability of water resources, creating unfavourable situations that places food, water and society at risk. There is a need to monitor droughts, and drought indices form a competent way of doing so.

In arid and semi-arid areas, ET_a forms a critical component of the hydrological cycle, which are crucial for assessing naturally varying climate and human-induced effects on hydrological systems as well as for better water resources management and disaster reduction plans. In recent years, the estimation of this variable has received substantial attention in an attempt to better quantify the loss of water from land surfaces and to assist in detecting the occurrences of droughts. Conventional field-based techniques, which are used to retrieve ET_a estimates have been utilised for several years to assist water resources management; however, the spatial resolution of the estimates along with the associated costs and time constraints have limited the practicality of this approach to the management of water resources over a larger-scale.

From the review of literature, it can be concluded that earth observation is seen to be an important tool in ET_a estimation over various spatial and temporal scales and it can be done in a cost-effective and timeous manner. The focus of this research study was to investigate and apply a satellite-derived evaporative drought index to assist in detecting the occurrence of drought conditions in South Africa. Recently, South Africa suffered one of the worst droughts of the century, linked to climate change and the El Niño phenomenon, which has resulted in warmer surface waters in the eastern tropical Pacific Ocean. The fact that South Africa is a

semi-arid country inundated by such conditions and, more so, that it faces a decrease in ground-based meteorological monitoring networks, has encouraged the use of satellite-derived data in the present drought monitoring study. To determine the potential risk of droughts in the future, it is critical to analyse the historical trends of drought events, and this has been aided by the use of drought indices.

In order to achieve the aim of this research study, specific objectives were outlined to inform the methodology and analyses that were performed. Three different drought indices (ETDI, SPI and SPEI) were used for the monitoring of droughts in this study. The drought indices were derived by using satellite earth observation data as inputs into the indices calculations.

The LSA-SAF DMET product was utilised to provide estimates of daily ET_a for input into the ETDI calculation. The product was validated for a period within the study period, with *in-situ* ET_a data being obtained from surface renewal (SR) and eddy covariance (EC) systems. Results showed that the DMET daily ET_a product is suitable in providing continuous spatial ET_a estimates as the product's temporal behaviour followed the general trend of the *in-situ* measured ET_a, although, the DMET estimates displayed a slight underestimation throughout the data period in comparison to *in-situ data*. Overall DMET was suitable for providing spatial estimates of ET_a for the ETDI calculation. However, the quality of the SVAT model should be further investigated due to its limited validation in the driest regions of the world (mainly in African countries) and be validated over other land covers to further improve results globally. The study was able to illustrate that the temporal distribution of ET_a for all the years followed a seasonal trend with maximum ET_a values occurring during summer months.

The Hargreaves method, developed by Hargreaves and Samani (1985), was used to obtain ET_o estimates for use within the ETDI calculations of this study. The Hargreaves equation was chosen as it is has been proven to be a feasible approach for use in semi-arid to arid environments, such as South Africa. This technique has received great attention within the research community due to its limited data requirements. To overcome the poor availability of meteorological data, LST data acquired by the MODIS sensor was used as input into the equation. The MOD11A2 product provided a spatial distribution of temperature for the study area, which depicted a clear spatial pattern with higher LST values during the spring-summer months and the lower LST values during the winter months and in high altitude areas. The spatial maps displayed the potential of the MOD11A2 product in providing information for

ungauged and for large geographical areas. Comparisons between air temperature data from ground-based meteorological stations indicated that the night and mean MODIS LST's were well correlated. However, discrepancies between the MODIS day LST and the maximum temperature from ground-based meteorological stations were observed as a result of variations occurring in accordance to the solar radiation, cloud cover ecosystems and vegetation phenology. These results indicate that further research is warranted for robust methods to retrieve maximum air temperature data. Overall, the estimates from the MOD11A2 product were found to be satisfactory and was used as an input in the Hargreaves equation to enable the retrievable of satellite-derived ET_o estimates.

The Hargreaves-LST method was calibrated by using FAO-PM ET_o estimates based on measured meteorological data. The calibrated Hargreaves-LST model estimates were found to closely follow the trends of the FAO-PM ET_o estimates and the results were in accordance with results observed in previous studies. It is recommended that the calibrated Hargreaves-LST estimates be used if sufficient data is available to allow for the calibration procedure to be performed. The Hargreaves-LST method of incorporating satellite LST data was therefore considered to be appropriate for the methodology of the study. Based on the statistics and regression analyses, the Hargreaves-LST approach was found to be applicable for use within South Africa. The methodology presented in this study provides a feasible alternative for estimating ET_o in South Africa as well as under limiting data conditions, without there being any additional data costs involved. The MODIS LST product is freely available and the method can be improved by using low cost direct methods to calibrate the empirical model. It is advised that calibration is necessary to signify the changes in the climatic variables. The Hargreaves-LST ET_o estimates were used as an input into the ETDI calculation for the assessment of droughts within the study.

The incorporation of satellite data into the Hargreaves equation is an advantage for water resources planning, agricultural water management and other hydrological related studies that can assist in the more viable and efficient management of water resources. In addition, ET_o is spatially variable due to the complex interaction that exists between the climate and the topography as well as solar radiation, which is influenced by cloud cover. Point estimates of these variables lack the spatial information required; however, to overcome this, satellite data can be incorporated. Hence, satellite data is advocated as an attractive tool for obtaining data and detecting change in an anomaly across vast areas as well as on a local scale. These findings

have critical implications for the water resources and agricultural sector of South Africa, which is already a water-stressed country.

The WS, WSA and the ETDI were calculated at different spatial scales for the Umgeni and Upper Thukela Catchments and were successful in detecting wet and dry periods, with results being in accordance with various recorded information. To confirm the occurrence of drought conditions that were detected by the ETDI, the SPI and SPEI were applied. All the indicators considered (SPI, SPEI, ETDI) were able to represent the most severe droughts within the study area including the 2015/2016 El Niño drought event as well the spatial variability of droughts. Results showed that persistent drought conditions affected the Upper Thukela and Umgeni Catchments. It was clear that from 2010 onwards there has been sustained prolonged moderate to severe dryness, with the longest and most intense drought recorded between 2010-2016, with 2015-2016 characterized by the occurrence of several widespread droughts in all three-drought indices. The ETDI was able to assist in the identification of the spatial and temporal evolution of droughts. There is added value in calculating indices based on variables such as rainfall in the case of the SPI and SPEI as they enable the identification of not only droughts but also floods and their severity. With droughts and floods receiving much attention and with the concern over how the threat of climate change may increase their severity and frequency over time, this study displays great relevance for further climate change studies. It is also suggested that the SPEI would be preferred to the SPI when exploring the evolution of climate change and the variation in drought events, since temperature is accounted for.

Overall, the SPI and SPEI confirmed the results that were produced by the ETDI. However, a comparative analysis of the different drought indices indicated that wet and dry conditions were more enhanced by the ETDI in comparison to the SPI and SPEI since the different indices account for different meteorological variables. The satellite-derived SPI and SPEI produced satisfactory results and were able to detect major dry and wet events including the 2015/2016 El Niño drought event for the Upper Thukela Catchment. The ETDI was further spatially compared to land surface variables namely precipitation, elevation, ET_a and soil moisture, which are recognisable driving forces to droughts. The results indicated that a distinct relationship exists between the land surface variables. The drivers of the hydrological cycle are all interrelated, each playing a vital role in detecting droughts.

The spatial distribution of droughts, using the ETDI was conducted in this study at different spatial scales displaying the creeping phenomenon of droughts. The results of this study were able to quantitatively demonstrate that there is a visible variation within the drought characteristics (the duration, intensity and spatial coverage) at different spatial scales. Spatially, the maps displayed how affected and severely affected areas gradually evolve and how the quaternary catchments (QC's) of maximum intensity expand. The spatial scale dependence of drought characteristics was evident in this particular study and such scale investigations are necessary for the effective management of droughts and the allocation of water resources. It was verified that droughts are a phenomenon of limited extension, in which several local factors act to determinate their extreme values. These findings emphasize and acknowledge that the management for the droughts and allocation of resources should be developed for different spatial scales, and more so at smaller administrative units such as at a QC level.

Aside from the general patterns, the analyses carried out in this study also indicated that the temporal evolution of droughts can be very diverse. Normal or humid conditions were observed in one QC, whilst another QC suffered drought over the same period. These patterns have been explained and attributed to the fact that the spatial differences are brought about by the influence of certain atmospheric patterns, such as the ENSO (Rodó *et al*., 1997). According to Rouault and Richard (2003), El Niño is usually linked to droughts in South Africa (van Heerden *et al*., 1988; Lindesay and Vogel, 1990). Overall, the combination of the spatial and temporal analyses of droughts can prove to be valuable in developing an improved understanding of droughts, assist in the establishment of effective and comprehensive tools for drought preparedness and they can be beneficial for the monitoring, which form the backbone of robust water resources planning to mitigate impacts at an adequate spatial division.

Overall, the ETDI was found to be a good indicator for the assessment and monitoring of drought conditions, due to its capability to timeously detect the onset of drought, and its realistic quantification of the severity of droughts within the study area. The spread of droughts over a large geographical area was successfully illustrated. One of the most important scientific developments is the growing view that droughts cannot simply be characterized by a lack of rainfall, and many recent papers including this study have shown the increased complexity of droughts including their hydrological processes. This study also displayed that the resulting differences in the indices can be attributed to the meteorological variables used to calculate them and that the choice of drought index is relevant.

This study has shown that the application of satellite products in water resource management is very promising. However, only their appropriate usage, an awareness of their limitations and the correct interpretation of remote-sensing data can facilitate water management and planning operations. SEO provides a great opportunity for identifying drought hot spots and geospatial differences (Rojas *et al*., 2011) as they enable the geospatial and temporal variability of droughts to be monitored. In this study, it was also demonstrated that the development of drought indices based on the merging of available climatic data with SEO and their implementation in GIS technologies, is a definite advance in assessing the spatial and temporal variability of droughts in South Africa. The study displayed that the low cost, good availability, accessibility, complete spatial coverage, and high temporal and spatial resolutions, are strong advantages for using SEO for the analysis of droughts in South Africa. This is because South Africa is a country where environmental and climatic data are often inaccessible, unavailable or expensive. Current earth observational satellites provide beneficial data to enable the assessment of vegetation, land cover and disasters, amongst several others, for example, the soil moisture product by (Sinclair and Pegram, 2010) by means of satellite imagery.

A major limitation of this study included the unavailability of good quality and undisturbed observational data as required by the SPI and SPEI as well as for the calibration of the Hargreaves-LST method for estimating ET_o. Another limitation included that this study conducted drought analyses within a 5-year period due to time constraints however; it is recommended that drought analyses be conducted preferably over a longer period such as 10 years and more. One of the main findings of this research is that the combined use of *in-situ* observations and satellite data is useful for ensuring that key variables of the water cycle are estimated adequately to meet the needs of national scale monitoring systems, planning tools and warning systems. In addition, for South Africa, education and training are critically needed to ensure that people in the country will be able to access and utilize such information, so that they can continue to research, in order to plan, prepare and avoid disasters.

5.2 Recommendations:

The following recommendations can be used to address some of the main limitations experienced within the study as well as provide assistance for future studies:

- The spatio-temporal drought analysis in this study can be improved using more observed ground-based meteorological data and different datasets, as there were slight discrepancies among the temperature, ET_a and ET_o data and datasets. The energy balance model, SEBS global monthly evapotranspiration product for the period between 1 April 2000 until 30 June 2017 has been made available recently, of which, the global daily evapotranspiration product is planned to be released end of 2017. It is recommended that for future research, the global monthly and daily evapotranspiration products be considered for drought monitoring. Interested users can access the monthly data through the FTP address: ftp://jmReGk8d:QR5X5cT2GLI@210.72.14.140 or visit the website of the TPE database http://en.tpedatabase.cn/portal/MetaDataInfo.jsp?MetaDataId=249454 .
- The METREF product, global SPI data set and SPEI Global Drought Monitor have not been attempt for use due to the scope of the current study however; they are recommended for future investigations into drought and within the ETDI.
- Comparison of the ETDI with the SPI and SPEI resulted in low correlation due to the differences in the calculation of the indices and the time-period. For further improvement on this, it is recommended that calculation of the indices for the same time-period to be conducted which may result in better assessments and correlations.
- For future studies, research on a study site's vegetation, soil moisture, runoff, discharge and ground water levels, is recommended for drought monitoring and prediction purposes. It is also recommended that when assessing, evaluating or monitoring drought conditions with the ETDI, it is beneficial to account for the soil moisture within the area.
- With declining gauging networks and poor correlation being detected between earth observation data and maximum air temperature data, research is needed on more robust methods to be able to retrieve accurate maximum air temperature data.
- For the comparison between drought indices using satellite data and *in-situ* data, spatial scale differences between the data must be accounted for in future studies.
- Studies focusing on ways of obtaining reliable short-term forecasts of ET may be beneficial for future drought studies. The investigation into the influence of ENSO on South Africa's droughts may also be beneficial to be included when analysing droughts using drought indices.

6. REFERENCES

Abouali, M, Timmermans, J, Castillo, JE and Su, BZ. 2013. A high performance GPU implementation of Surface Energy Balance System (SEBS) based on CUDA-C. *Environmental Modelling and Software* 41:134-138.

Aguilar, C and Polo, MJ. 2011. Generating reference evapotranspiration surfaces from the Hargreaves equation at watershed scale. *Hydrology and Earth System Sciences* 15: 2495-2508.

Ahmadi, SH and Fooladmand, HR. 2008. Spatially distributed monthly reference evapotranspiration derived from the calibration of Thornthwaite equation: a case study, South of Iran. *Irrigation Science* 26(4):303-312.

Allen, RG, Smith, M, Pereira, A and Pereira, LS. 1994. An update for the definition of reference evapotranspiration. *ICID Bulletin* 43(2):1-34.

Allen, RG, Pereira, LS, Raes, D and Smith, M. 1998, Crop evapotranspiration. Guidelines for computing crop water requirements, Irrigation and Drainage Paper 56, Food and Agric. Organization of the United Nations, Rome, Italy.

Andersson, JCM, Zehnder, AJB, Rockström, and Yanga, H. 2011. Potential impacts of water harvesting and ecological sanitation on crop yield, evaporation and river flow regimes in the Thukela River Basin, South Africa. *Agricultural Water Management* 98:1113-1124.

Anderson, MC, Allen, RG, Morse, A and Kustas, WP. 2012. Use of Landsat thermal imagery in monitoring evapotranspiration and managing water resources. *Remote Sensing of Environment* 122:50-65.

Arboleda, A, Ghilian, N and Gellens-Meulenberghs, F. 2011 EUMETSAT's LSA-SAF evapotranspiration: comparisons of operational product to observations and models at hydrological basin scale, *Proceedings of the EUMETSAT conference*. Oslo, Norway.

ARC-ISCW (Agricultural Research Council- Institute for Soil, Climate and Water). 2015. Umlindi:The Watchman. Issue No. 2015-12. ARC-ISCW, Pretoria, South Africa.

Bachour, R. 2013. Evapotranspiration modelling and forecasting for efficient management of irrigation command areas. Published Doctoral Irrigation Engineering Dissertation, Department of Civil and Environmental Engineering, Utah State University, Utah.

Balsamo, G, Viterbo, P, Beijaars, A, van den Hurk, B, Hirschi, M, Betts, AK and Scipal, K. 2009. A revised hydrology for the ECMWF model: verification from field site to

terrestrial water storage and impact in the integrated forecast system. *Journal of Hydrometeorology* 10(3):623-643.

Bastiaanssen, WGM, Molden, DJ and Makin, IW. 2000. Remote sensing for irrigated agriculture: examples from research and possible applications. *Agricultural Water Management* 146:137-155.

Bastiaanssen, W and Harshadeep, R. 2003. Managing scarce water resources in Asia: Nature of the Problem and can Remote Sensing help? ICID International Workshop on Remote Sensing of ET for Large Regions, WaterWatch and World Bank, Montpellier, France, 17 September 2003.

Bastiaanssen, WGM, Cheema, MJM, Immerzeel, WW, Miltenburg, IJ and Pelgrum, H. 2012. Surface energy balance and actual evapotranspiration of the transboundary Indus Basin estimated from satellite measurements and the ETLook model. *Water Resources Research* 48:1-16.

Bangira, T. 2013. Mapping of flash flood potential areas in the Western Cape (South Africa) using remote sensing and *in situ* data. Unpublished Master of Science in Geo-Information Science and Earth Observation thesis, Faculty of Geo-Information Science and Earth Observation, University of Twente, Enschede, Netherlands.

Bayissa, Y, Tadesse, T, Demisse, G and Shiferaw, A. 2017. Evaluation of satellite-based rainfall estimates and application to monitor meteorological drought for the Upper Blue Nile Basin, Ethiopia. *Remote Sensing* 9(669):1-17.

Beguería, S, Vicente-Serrano and Angulo, M. 2010. A multi-scalar global drought data set: the SPEIbase:A new gridded product for the analysis of drought variability and impacts. *Bulletin of the American Meteorological Society* 91:1351-1354.

Beguería, S, Vicente-Serrano, SM, Reig, F and Latorre, B. 2014. Standardized precipitation evapotranspiration index (SPEI) revisited: parameter fitting, evapotranspiration models, tools, datasets and drought monitoring. *International Journal of Climatology* 34:3001-3023.

Beljaars, ACM and Viterbo P. 1994.The sensitivity of winter evaporation to the formulation of aerodynamic resistance in the ECMWF model. *Boundary-Layer Meteorology* 71: 135-149.

Berhan, G, Hill, S, Tadesse, T and Atnafu, S. 2011. Using satellite images for drought monitoring: A knowledge discovery approach. *Journal of Strategic Innovation and Sustainability* 7(1):135-153.

Bhuiyan, C. 2004. Various drought indices for monitoring drought condition in Aravalli Terrain of India. In: *Proceeding 20th ISPRS Congress*, Istanbul, Turkey.

Botai, CM, Botai, JO, Dlamini, LC, Zwane, NS and Phaduli, E. 2016. Characteristics of droughts in South Africa: A case study of Free State and North West Provinces. *Water* 8(439):1-23.

Boyle, AS, Kennedy, CM, Torres, J, Colman, K, Perez-Estigarribia, PE and de la Sancha, NU. 2014. High-resolution satellite imagery is an important yet underutilized resource in conservation biology. *PLOS One Journal* 9:e86908.

Bulcock, HH and Jewitt, GPW. 2012. Field data collection and analysis of canopy and litter interception in commercial forest plantations in the KwaZulu-Natal Midlands, South Africa. *Hydrology and Earth System Sciences* 16:3717-3728.

Burke, EJ, Brown, SJ and Christidis, N. 2006. Modeling the recent evolution of global drought and projections for the twenty-first century with the Hadley centre climate model. *Journal Hydrometeorology* 7(5):1113-1125.

Byun, K, Liaqat, UW and Choi, M. 2014. Dual-model approaches for evapotranspiration analyses over homo- and heterogeneous land surface conditions. *Agricultural and Forest Meteorology* 197:169-187.

Cammalleri, C and Ciraolo, G. 2013. A simple method to directly retrieve reference evapotranspiration from geostationary satellite images. *International Journal of Applied Earth Observation and Geoinformation* 21:149-158.

Castro, M and Parra, JC. 2015. Estimation of the monthly reference evapotranspiration in the Araucania Region, Chile, from MODIS/TERRA satellite data. *Research Desk* 4(1):491-499.

Ceccato, P and Dinku, T. 2010. *Introduction to Remote Sensing for Monitoring Rainfall, Temperature, Vegetation and Water Bodies*. IRI Technical Report No 10-04. Earth Institute at Columbia University, International Research Institute for Climate and Society, New York.

Ceccherini, G, Russo, S, Ameztoy, I, Marchese, AF and Carmona-Moreno, C.2017. Heatwaves in Africa 1981-2015, observations and reanalysis. *Natural Hazards Earth System Sciences* 17:115-125.

Chehbouni, A, Lo Seen, D, Njoku, EG and Monteny, B. 1996. A Coupled Hydrological and Ecological modeling Approach to examine the Relationship between Radiative and Aerodynamic Surface Temperature over Sparsely Vegetated Surfaces. *Remote Sensing Environment* 58:177-186.

Chen, D, Gao, G, Xu, C, Guo, J and Ren, G. 2005. Comparison of the Thornthwaite method and pan data with the standard Penman-Monteith estimates of reference evapotranspiration in China. *Climate Research* 28:123-132.

Chen, Y, Xia, JZ, Liang, SL, Feng, JM, Fisher, JB, Li, X, Li, XL, Liu, SG, Ma, ZG, Miyata, A, Mu, QZ, Sun, L, Tang, JW, Wang, KC, Wen, J, Xue, YJ, Yu, GR, Zha, TG, Zhang, L, Zhang, Q, Zhoa, TB, Zhoa, L and Yuan, WP. 2014. Comparison of satellite-based evapotranspiration models over terrestrial ecosystems in China. *Remote Sensing Environment* 140:279-293.

Coll, C, Wan, Z and Galve, JM. 2009. Temperature-based and radiance-based validations of the V5 MODIS land surface temperature product. *Journal of Geophysical Research* 114.

CRED (Centre for Research on the Epidemiology of Disasters). 2015. EM-DAT: International Disaster database. [Internet]. CRED, Brussels, Belgium. Available from: [http://www.cred.be/]. [Accessed: [05 September 2017]].

Cristobal, J and Anderson, MC. 2013. Validation of a Meteosat Second Generation solar radiation dataset over the north-eastern Iberian Peninsula. *Hydrology and Earth System Sciences* 17:163-175.

Cruz-Blanco, M, Lorite, IJ and Santos, C. 2014. An innovative remote sensing based reference evapotranspiration method to support irrigation water management under semi-arid conditions. *Agricultural Water Management* 131:135-145.

Dai, A. 2011. Drought under global warming: a review. *Wiley Interdisciplinary Reviews: Climate Change* 2(1):45-65.

Dai, A. 2013. Increasing drought under global warming in observations and models. *Nature Climate Change* 3:52-58.

De Bruin, HAR, Trigo, IF, Gavilan, P, Martinez-Cob, A and Gonzalez-Dugo, M.P. 2010. Reference crop evapotranspiration estimated from geostationary satellite imagery. In: eds. *Remote Sensing and Hydrology,* Proceedings of a symposium held at Jackson Hole, 111- 114.Wyoming, USA. IAHS Press, Wallingford, Oxfordshire, UK.

De Bruin, HAR, Trigo, IR, Bosveld, FC and Meirink, JF. 2015. A thermodynamically based model for actual evapotranspiration of an extensive grass field close to FAO reference, suitable for remote sensing application. *Journal of Hydrometeorology* 17(5):1373-1382.

Dennis, I and Dennis, R. 2012. Climate change vulnerability for South African aquifers. Water SA 38(3):417-426.

De Winnaar, G and Jewitt, G. 2010. Ecohydrological implications of runoff harvesting in the headwaters of the Thukela River Basin, South Africa. *Physics and Chemistry of the Earth* 35:634-642.

Dorigo, WA, Scipal, K, Parinussa, RM, Liu, YY, Wagner, W, De Jeu, RAM and Naeimi, V. 2010. Error characterisation of global active and passive microwave soil moisture datasets. *Hydrology and Earth System Sciences* 15:2605-2616.

Douglas, EM, Jacobs, JM, Sumner, DM and Ray, RL. 2009. A comparison of models for estimating potential evapotranspiration for Florida land cover types. *Journal of Hydrology* 373(3-4):366-376.

Dube, T and Mutanga, O. 2015. Evaluating the utility of the medium-spatial resolution Landsat 8 multispectral sensor in quantifying aboveground biomass in uMgeni catchment, South Africa. *ISPRS Journal of Photogrammetry and Remote Sensing* 101:36-46.

Dube, T and Mutanga, O. 2016. The impact of integrating WorldView-2 sensor and environmental variables in estimating plantation forest species above ground biomass and carbon stocks in uMgeni Catchment, South Africa. *ISPRS Journal of Photogrammetry and Remote Sensing* 119:415-425.

Eden, U. 2012. Drought assessment by evapotranspiration mapping in Twente, the Netherlands. Unpublished MSc Dissertation, Faculty of Geo-Information Science and Earth Observation, University of Twente, Enschede, Netherlands.

Elhaddad, A, Garcia, LA and Chávez, JL. 2011. Using a surface energy balance model to calculate spatially distributed actual evapotranspiration. *Journal of Irrigation and Drainage Engineering* 137(1):17-26.

Everson, CS, Clulow, AD, Becker M, Watson, A Ngubo, C, Bulcock, H, Mengistu, M, Lorentz S and Demlie, M. 2014. *The long term impact of Acacia mearnsii trees on evaporation, streamflow, low flows and ground water resources. Phase II: Understanding the controlling environmental variables and soil water processes over a full crop rotation*. Report No 2022/1/13. Centre for Water Resources Research (CWRR), Pietermaritzburg, South Africa.

FEWS NET (Famine Early Warning Systems Network). 2016. FEWS NET El Niño and La El Niña monitoring resources. FEWS NET. USA. Available from: [http://www.fews.net/fews-net-el-ni%C3%B1o-monitoring-resources]. [Accessed: [08 November 2016]].

Feyen, L and Dankers, R. 2009. Impact of global warming on streamflow drought in Europe. *J. Geophysical Research Space* 114(D17):D17116.

Gavilán, P, Lorite, IJ, Tornero, S and Berengena, J. 2006. Regional calibration of Hargreaves equation for estimating reference ET in a semi-arid environment. *Agriculture Water Management* 81:257-281.

Gellens-Meulenberghs, F, Arboleda, A and Ghilain, N. 2007. Towards a continuous monitoring of evapotranspiration based on MSG data. In: eds. M, Owe and Ch, Neale, *Remote Sensing for Environmental Monitoring and Change Detection*, IAHS Publication 316, 228-234.

Gellens-Meulenberghs, F, Arboleda, A and Ghilain, N. 2008. Evapotranspiration assessment by LSA-SAF: methodology, status of validation and plans for the near future. In: *Proceedings of the 2008 EUMETSAT Meteorological Satellite Data User's Conference*,7, Darmstadt, Germany.

Gellens-Meulenberghs, F, Arboleda, A, Ghilain, N, de Crane, F and Sepulcre-Canto, G. 2009. Large scale evapotranspiration modeling using MSG SEVIRI derived data. *Proceedings of the Conference on Earth Observation and Water Cycle Science (ESA SP-674)*, Frascati, Italy.

GEOTERRAIMAGE. 2015. 2013-2014 South African National Land Data User Report and Metadata. [Internet]. South Africa National Biodiversity Institute, Claremont, South Africa. Available from: [http://bgis.sanbi.org.].[Accessed: [01 December 2016]].

Ghilain, N, Arboleda, A and Gellens-Meulenberghs, F. 2011. Evapotranspiration modelling at a large scale using near-real time MSG SEVIRI derived data. *Hydrology and Earth System Sciences* 15:771-786.

Ghilain, N, Arboleda, A and Gellens-Meulenberghs, F. 2013. Evapotranspiration monitoring in semi-arid areas using MSG-SEVIRI derived data: improvements from the use of leaf area index and land surface temperature. In: *Proceedings of the EUMETSAT'S User Conference*. Vienna, Austria.

Gibson, LA, Münch, Z, Engelbrecht, J, Petersen, N and Conrad, JE. 2009. *Remote sensing as a tool towards resource assessment and determination of the legal compliance of surface and groundwater use*. WRC Project K5/1690. Water Research Commission, Pretoria.

Gibson, LA. 2013. The application of the surface energy balance system model to estimate evapotranspiration in South Africa. Unpublished thesis, University of Cape Town, Cape Town, South Africa.

Gillette, HP. 1950. A creeping drought under way. In: *Water and Sewage Works*. March, 104-105.

Gokool S, Chetty KT, Jewitt, GPW and Heeralal, A. 2016. Estimating total evaporation at the field scale using the SEBS model and data infilling procedures. *Water SA* 42(4):1-11.

Gokmen, M, Verkerdy, Z, Verhoef, A, Verhoef, W, Batelaan, O and van der Tol, C. 2012. Integration of soil moisture in SEBS for improving evapotranspiration estimation under water stress conditions. *Remote Sensing of Environment* 121:261-274.

Graham, LP, Andersson, L, Horan, M, Kunz, R, Lumsden, T, Schulze, R, Warburton, M, Wilk, J and Yang, W. 2011. Using multiple climate projections for assessing hydrological response to climate change in the Thukela River Basin, South Africa. *Physics and Chemistry of the Earth* 36:727-735.

Hargreaves, GH and Samani, ZA. 1985. Reference crop evapotranspiration from temperature. *Applied Engineering in Agriculture* 1(2):96-99.

Hart, QJ, Brugnach, M, Temesgen, B, Rueda, C, Ustin, SL and Frame, K. 2009. Daily reference evapotranspiration for California using satellite imagery and weather station measurement interpolation. *Civil Engineering and Environmental Systems* 26(1):19-33.

Hayes, Dr MJ, Alvord, C and Lowrey, J. 2007. Drought Indices. In:eds. Western Water Assessment, *Intermountain West Climate Summary*, 1-6, Western Water Assessment, Colorado, USA.

Heim, RR. 2002. A review of twentieth-century drought indices used in the United States. *Bulletin of the American Meteorological Society* 83(8):1149-1165.

Hirpa, F, Gebremichael, M and Hopson, T. 2010. Evaluation of High-Resolution Satellite Precipitation Products over Very Complex Terrain in Ethiopia. *Journal of Applied Meteorology and Climatology* 49:1044-1051.

Holloway, A, Fortune, G, Zweig, P, Barrett, L, Benjamin, A, Chasi, V and de Waal, J. 2012. *Eden and Central Karoo Drought Disaster 2009 -2011: "The Scramble for Water".* Report No [LG 10/2011/2012]. Stellenbosch University, Western Cape, South Africa.

Houborg, R, Rodell, M, Li, B, Reichle, R and Zaitchik, BF. 2012. Drought indicators based on model-assimilated Gravity Recovery and Climate Experiment (GRACE) terrestrial water storage observations. *Water Resources Research* 48:1-17.

Huang, C, Li, Y, Gu, J, Lu, L and Li, X. 2015. Improving estimation of evapotranspiration under water-limited conditions based on SEBS and MODIS data in Arid Regions. *Remote Sensing* 7:16795-16814.

Hu, G, Jia, L and Menenti, M. 2015. Comparison of MOD16 and LSA-SAF MSG evapotranspiration products over Europe for 2011. *Remote Sensing of Environment* 156:510-526.

Jain, VK, Pandey, RP, Jain, MK and Byun, HR. 2015. Comparison of drought indices for appraisal of drought characteristics in the Ken River Basin. *Weather and Climate Extremes* 8:1-11.

Jarmain, C, Bastiaansen, W, Mengistu, MG and Kongo, V. 2009. *A methodology for near-real time spatial estimation of evaporation*, Water Resource Commission Report No. 1751/1/09, ISBN 978-1-77005-725-8.

Jarmaine, C, Singels, A, Obando, EB, Paraskevopoulos, A, Olivier, F, van der Laan, M, Turisan, DT, Dlamini, M, Munch, Z, Bastiaanssen, W, Annadale, J, Everson, C, Savage, M and Walker, S. 2014. *Water use efficiency of selected irrigated crops determined with satellite imagery*. Report No. [TT 602/14]. Water Research Commission and the Department of Agriculture, Forestry and Fisheries, Gezina, Republic of South Africa.

Jiang, L, Islam, S, Guo, W, Jutla, AS, Senarath, SUS, Ramsay, BH and Eltahir, E. 2009. A satellite-based Daily Actual Evapotranspiration estimation algorithm over South Florida. *Global and Planetary Change* 67:62-77.

Jovanovic, N, Garcia, CL, Bugan, RDH, Teich, I and Rodriguez, CMG. 2014. Validation of remotely-sensed evapotranspiration and NDWI using ground measurements at Riverlands, South Africa. *Water SA* 40:211-220.

Kershavarz, MR, Vazifedoust, M and Alizadeh, A. 2014. Drought monitoring using a Soil Wetness Deficit Index (SWDI) derived from MODIS satellite data. *Agricultural Water Management* 132:37-45.

Kiptala, JK, Mohamed, Y, Mul, ML and van der Zaag, P. 2013. Mapping evapotranspiration trends using MODIS and SEBAL model in a data scarce and heterogeneous landscape in Eastern Africa. *Water Resources Research* 49:8495-8510.

Kongo, MV, Jewitt, GWP and Lorentz, SA. 2011. Evaporative water use of different land uses in the upper-Thukela river basin assessed from satellite imagery. *Agricultural Water Management* 98:1727-1739.

Kovalskyy, V and Henebry, GM. 2012. Alternative methods to predict actual evapotranspiration illustrate the importance of accounting for phenology – Part 2: The event driven phenology model. *Biogeosciences* 9:161-177.

Kumar, R, Musuuza, JL, van Loon, AF, Teuling, AJ, Barthel, R, ten Broek, J, Mai, J, Samaniego, L and Attinger, S. 2016. Multiscale evaluation of the Standardized Precipitation Index as a groundwater drought indicator. *Hydrology and Earth System Sciences* 20:1117-1131.

Kustas, WP and Norman, JM. 1996. Use of remote sensing for evapotranspiration monitoring over land surfaces. *Hydrological Sciences Journal* 41(4):495-516.

Leelaruban, N and Padmanabhan, G. 2017. Drought occurrences and their characteristics across selected spatial scales in the contiguous United States. *Geosciences* 7(59):1-15.

Lehner, B, Dll, P, Alcamo, J, Henrichs, T and Kaspar, F. 2006. Estimating the impact of global change on flood and drought risks in Europe: a continental, integrated analysis. *Climate Change* 75(3):273-299.

Li, W, Hou, M, Chen, H and Chen, X. (2012). Study on drought trend in south China based on standardized precipitation evapotranspiration index. *Journal of Natural Disasters* 21:84-90.

Lindesay, JA and Vogel, CH. 1990. Historical evidence for Southern Oscillation-southern African rainfall relationships. *International Journal of Climatology* 10:679-689.

Lorentz, S, Thornthon-Dibb, S, Pretorius, C and Goba, P. 2004. *Hydrological systems modelling research programme: hydrological processes.* Report No. 1061 and 1086/1/04. School of Bioresources Engineering and Environmental Hydrology, University of Natal, Pietermaritzburg, South Africa.

LSA-SAF (Land Surface Analysis Satellite Applications Facility). 2015. Reference Evapotranspiration. [Internet]. EUMETSAT LSA SAF Land Surface Analysis, Darmstadt, Germany. Available from:[https://landsaf.ipma.pt/algorithms.jsp?seltab=6&starttab=]. [Accessed: 18 September 2015].

Lynch, SD. 2004. *Development of a Raster Database of Annual, Monthly and Daily Rainfall for Southern Africa*. WRC Report 1156/1/04. Water Research Commission, Pretoria, South Africa.

Maeda, EE, Wiberg, DA and Pellikka, PKE. 2011. Estimating reference evapotranspiration using remote sensing and empirical models in a region with limited ground data availability in Kenya. *Applied Geography* 31:251-258.

Maherry, AM, Horan, MJC, Smith-Adao, LB, van Deventer, H, Nel, JL, Schulze, RE and Kunz, RP. 2013. *Delineating river network quinary catchments for South Africa and allocating associated daily hydrological information*. WRC Report 2020/1/12. Water Research Commission, Pretoria, South Africa.

Manatsa, D, Mushore, T and Lenouo, A. 2017. Improved predictability of droughts over southern Africa using the standardized precipitation evapotranspiration index and ENSO. *Theory of Applied Climatology* 127:259-274.

Masih, I, Maskey, S, Mussa, FEF and Trambauer, P. 2014. A review of droughts on the African continent: a geospatial and long-term perspective. *Hydrology and Earth System Sciences* 18:3635-3649.

Masson, V, Champeaux, JL, Chauvin, F, Meriguet, Ch. and Lacaze. 2003. Global database of land surface parameters at 1-km resolution in meteorological and climate models. *Journal of Climate* 1(9):1261-1282.

McKee, TB, Doesken, NJ and Kleist, J. 1993: The relationship of drought frequency and duration to time scale. In: *Proceedings of the Eighth Conference on Applied Climatology*, Anaheim, California, 17–22 January 1993. Boston, American Meteorological Society, 179-184.

McKee, TB, Doesken, NJ and Kleist, J. 1995. Drought monitoring with multiple time scales. In: *Proceedings of the Ninth Conference on Applied Climatology*, 233-236. Dallas, TX, USA.

McMahon, TA, Peel, MC, Lowe, L, Srikanthan, R and McVicar, TR. 2012. Estimating actual, potential, reference crop and pan evaporation using standard meteorological data: a pragmatic synthesis. *Hydrology and Earth System Sciences Discussions* 9:11829-11910.

Merz, SK. 2010. *Evapotranspiration measurement: informing water management in Australia.* Report No. 35. Waterlines Report, National Water Commission, Canberra.

Miralles, DG, Holmes, TRH, de Jeu1, RAM, Gash, JH, Meesters, AGCA and Dolman, AJ. 2011. Global land-surface evaporation estimated from satellite-based observations. *Hydrology and Earth System Sciences* 15:453-469.

Miralles, DG, Jiménez, C, Jung, M, Michel, D, Ershadi, A, McCabe, MF, Hirschi, M, Martens, B, Dolman, AJ, Fisher, JB, Mu, Q, Seneviratne, SI,Wood, EF and Fernaìndez-Prieto, D. 2015. The WACMOS-ET project – Part 2: Evaluation of global terrestrial evaporation data sets. *Hydrology and Earth System Sciences* 12:10651-10700.

Minacapilli, M, Consoli, S, Vanella, D, Ciraoloc, G and Motisi, A. 2016. A time domain triangle method approach to estimate actual evapotranspiration: Application in a Mediterranean region using MODIS and MSG-SEVIRI products. *Remote Sensing of Environment* 174:10-23.

Molobela, IP and Sinha, P. 2011. Management of water resources in South Africa: A review. *African Journal of Environmental Science and Technology* 5(12):993-1002.

Morid, S, Smakhtin, V and Moghaddasi, M. 2006. Comparison of seven meteorological indices for drought monitoring in Iran. *International Journal of Climatology* 26:971-985.

Mucina, L and Rutherford, MC. 2006. The Vegetation of South Africa, Lesotho and Swaziland. Strelitzia 19, South African National Biodiversity Institute, Pretoria, South Africa.

Mutiga, JK, Su, Z and Woldai, T. 2010. Using satellite remote sensing to assess evapotranspiration: Case study of the upper Ewaso Ng'iro North Basin, Kenya. *International Journal of Applied Earth Observation and Geoinformation* 12S:S100-S108.

Mu, Q, Heinsch, FA, Zhao, M and Running, SW. 2007. Development of a global evapotranspiration algorithm based on MODIS and global meteorology data. *Remote Sensing Environment* 111:519-536.

Mu, Q, Zhao, M, Kimball, John S, McDowell, Nathan, G and Running, SW. 2013. A Remotely Sensed Global Terrestrial Drought Severity Index. *Bulletin of the American Meteorological Society (Drought severity index-measuring conditions from satellites)* 94(1):83-98.

Narasimharan, B and Srinivasen, R. 2005. Development and evaluation of Soil Moisture Deficit Index (SMDI) and Evapotranspiration Deficit Index (ETDI) for agricultural drought monitoring. *Agricultural and Forest Meteorology* 133:69-88.

Narongrit, C and Yasuoka, Y. 2003. The use of terra-MODIS data for estimating evapotranspiration and its change caused by global warming. *Environmental Informatics Archives* 1:505-511.

NOAA (National Oceanic And Atmospheric Administratiion). 2016. Experimental forecast reference crop evapotranspiration. [Internet]. USA.gov, United States. Available from: http://www.wrh.noaa.gov/forecast/evap/FRET/FRET.php?wfo=sto. [Accessed 29 March 2016].

Novella, NS and Thiaw, WM. 2012. African Rainfall Climatology Version 2 for Famine Early Warning Systems. *Journal of Applied Meteorology and Climatology* 52(3):588-606.

Palchaudhuri, M and Biswas, S. 2013. Analysis of meteorological drought using Standardized Precipitation Index –A case study of the Puruliya District, West Bengal, India. *International Journal of Environmental, Chemical, Ecological, Geological and Geophysical Engineering* 7(3):119-126.

Pandey, PK, Dabral, PP and Pandey, V. 2016. Evaluation of reference evapotranspiration methods for the north-eastern region of India. *International Soil and Water Conservation Research* http://dx.doi.org/10.1016/j.iswcr.2016.02.003. [Accessed: 12 February 2017].

Parry, ML, Carter, TR and Konijn, NT. 2012. *The Impact of Climatic Variations on Agriculture: Volume 2: Assessments in Semi-Arid Regions.* Springer Science and Business Media, Berlin, Germany.

Park, SJ, Park, JH, Ou, ML, Ryoo, SB and Han, KS. 2012. A Satellite-based daily actual evapotranspiration estimation over East Asia. National Institute of Meteorological Research, KMA, Republic of Korea.

Paulo, AA, Rosa, RD and Pereira, LS. 2012. Climate trends and behaviour of drought indices based on precipitation and evapotranspiration in Portugal. *Natural Hazards and Earth System Sciences* 12:1481-1491.

Pedro-Monzonís, M, Solera, A, Ferrer, J, Estrela, T and Paredes-Arquiola, J. 2015. A review of water scarcity and drought indexes in water resources planning and management. *Journal of Hydrology* 527:482-493.

Petja, BM, Moeletsi, ME, Van Zyl, D, Mpandeli, N and Sibandze, P. 2008. *Drought mapping in South Africa using coarse resolution satellite imagery*. Report No. GW/A/2008/44. ARC-Institute for Soil, Climate and Water. Pretoria.

Pitman. 2011 Overview of water resource assessment in South Africa: current state and future challenges. *Water SA* 37(5):659-664.

Potop, V. 2011. Evolution of drought severity and its impact on corn in the Republic of Moldova. *Theoretical and Applied Climatology* 105:469-483.

Pozzi, W, Sheffield, J, Stefanski, R, Cripe, D, Pulwarty, R, Vogt, JV, Heim, RR, Brewer, MJ, Svoboda, M, Westerhoff, R, van Dijk, A, Lloyd-Hughes, B, Pappenberger, F, Werner, M, Dutra, E, Wetterhall, F, Wagner, W, Schubert, S, Mo, K, Nicholson, M, Bettio, L, Nunuz, L, van Breek, R, Bierkens, M, de Goncalves, LGG, de Mattos, JGZ and Lawford, R. 2013. Towards global drought early warning capability: expanding international cooperation for the development of a framework for monitoring and forecasting. *Bulletin of the American Meteorological Society* 94(6):776-785.

Prudhomme, C, Giuntoli, I, Robinson, EL, Clark, DB, Arnell, NW, Dankers, R, Fekete, BM, Franssen, W, Gerten, D, Gosling, SN, Hagemann, S, Hannah, DM, Kim, H, Masaki, Y, Satoh, Y, Stacke, T, Wada, Y and Wisser, D. 2014. Hydrological droughts in the 21st century, hotspots and uncertainties from a global multi-model ensemble experiment. *Proceedings of the National Academy of Sci*ences 111(9):3262-3267.

Rahimi, S, Sefidkouhi, MAG, Raeini-Sarjaz, M and Valipour, M. 2015. Estimation of actual evapotranspiration by using MODIS images (a case study: Tajan catchment). *Archives of Agronomy and Soil Science* 61(5):695-709.

Rahimikhoob, A and Hosseinzadeh, M. 2014. Assessment of Blaney-Criddle equation for calculating reference evapotranspiration with NOAA/AVHRR data. *Water Resources Management* 28:3365-3375.

Rivas, R and Caselles, V. 2004. A simplified equation to estimate spatial reference evaporation from remote sensing-based surface temperature and local meteorological data. *Remote Sensing of Environment* 93:68-76.

Rivera, JA and Penalba, OC. 2014. Trends and spatial patterns of drought affected area in southern South America. *Climate* 2(4):264-278.

Rodo, X, Baert, E and Comn, FA. 1997. Variations in seasonal rainfall in Southern Europe during the present century: relationships with the North Atlantic Oscillation and the El-Nino Southern Oscillation. *Climate Dynamics* 13:275-284.

Rojas, O, Vrieling, A and Rembold, F. 2011. Assessing drought probability for agricultural areas in Africa with coarse resolution remote sensing imagery. *Remote Sensing of Environment* 26:343-352

Romaguera, M, Salama, Mhd.S, Krol, MS, Hoekstra, AY and Su, Z. 2014. Towards the improvement of blue water evapotranspiration estimates by combining remote sensing and model simulation. *Remote Sensing* 6:7026-7049.

Rosema, A. 2006. The energy and water balance monitoring system (EWBMS): Water resource monitoring and flow forecasting using geostationary satellite data. [Internet]. EARS, the Nederlands. Available from: http://www.a-a-r-s.org/ws-eowm/download/Plenary4/EWBMS.PDF. [Accessed 23 December 2016].

Rosema, A, De Weirdt, M, Foppes, S, Venneker, R, Maskey, S, Gu, Y, Zhao, W, Wang, C, Liu, X, Rao, S, Dai, D, Zhang, Y, Wen, L, Chen, D, Di, Y, Qiu, S, Wang, Q, Zhang, L, Liu, J, Liu, L, Xie, L, Zhang, R, Yang, J, Zhang, Y, Luo, M, Hou, B, Zhao, L, Zhu, L, Chen, X, Yang, T, Shang, H, Ren, S, Sun, F, Sun, Y, Zheng, F, Xue, Y, Yuan, Z, Pang, H, Lu, C, Liu, G, Guo, X, Du, D, He, X, Tu, X, Sun, W, Bink, B and Wu, X. 2008. *Satellite Monitoring and Flow Forecasting System for the Yellow River Basin: Scientific final report of ORET project*. Report No. 02/09-CN00069. EARS, Delft, the Netherlands.

Rouault, M and Richard, Y. 2003. Intensity and spatial extension of drought in South Africa at different time scales. *Water SA* 29(4):489-500.

Russo, AC, Gouveia, CM, Trigo, RM, Liberato, MLR and DaCamara, CC. 2015. The influence of circulation weather patterns at different spatial scales on drought variability in the Iberian Peninsula. *Frontiers in Environmental Science* 3(1):1-15.

SADC (Southern African Development Community). 2016. *SADC Regional Situation Update on EL Niño-induced drought*. Issue 01. SADC, Gaborone, Botswana.

Salama, MA, Yousef, Kh.M and Mostafa, AZ. 2015. Simple equation for estimating actual evapotranspiration using heat units for wheat in arid regions. *Journal of Radiation Research and Applied Sciences* 8:418-427.

Savenije, HHG. 2004. The importance of interception and why we should delete the term evapotranspiration from our vocabulary. *Hydrological Processes* 18:1507-1511.

Schubert, SD, Wang, H, Koster, RD, Suarez, MJ and Groisman, PY. 2014. Northern Eurasian heat waves and droughts. *Journal of Climate* 27:3169-3207.

Schneider, C, Aggett, G and Hattendorf, M. 2008. Comparison, Calibration and refinement of traditional crop coefficient curves in the South Platte River Basin using mapping evapotranspiration at high resolution with internalized calibration. In: *Pecora 17-The Future of Land Imaging*. Going Operational, Denver, Colorado.

Schulze, RE and Maharaj, M. 2003. *Development of a Database of Gridded Daily Temperatures for Southern Africa*. ACRUcons Report, 41. University of Natal, Pietermaritzburg, RSA, School of Bioresources Engineering and Environmental Hydrology.

Schulze, R. 2004. Case study 3: Modeling the impacts of land use and climate change on hydrological response in the mixed, underdeveloped/developed Mgeni Catchment, Southern Africa. In: ed. Kabat, P, Claussen, M, Dirmeyer PA, Gash, JHC, Bravo de Guenni, L, Meybeck, M, Pielke, RA, Sr and Vörösmarty, CJ. *Vegetation, Water, Humans and the Climate: A New Perspective on an Interactive System*, 441-464. Springer, Heidelberg.

Sepulcre-Canto, G, Vogt, J, Arboleda, A and Antofie, T. 2014. Assessment of the EUMETSAT LSA-SAF evapotranspiration product for drought monitoring in Europe. *International Journal of Applied Earth Observation and Geoinformation* 30:190-202.

Sheffield, J and Wood, EF. 2011. *Drought: past problems and future scenarios*. Earthscan, New York, USA.

Sheffield, J, Wood, EF, Chaney, N, Guan, K, Sadri, S, Yuan, X, Olang, L, Amani, A, Ali, A, Demuth, S and Ogallo, L. 2014. A drought monitoring and forecasting system for sub-Saharan African water resources and food security. *Bulletin of the American Meteorological Society*.

Shoko, C. 2013. Use of remote sensing for estimating total evaporation at a catchment scale. Unpublished MSc Bioresources Systems Dissertation, Centre for Water Resources Research, University of KwaZulu-Natal, Pietermaritzburg, South Africa.

Shoko, C, Dube, T, Sibanda, M and Adelabu, S. 2015. Applying the Surface Energy Balance System (SEBS) remote sensing model to estimate spatial variations in evapotranspiration in Southern Zimbabwe. *Transactions of the Royal Society of South Africa* 70(1):47-55.

Sinclair, S and Pegram, GGS. 2010. A comparison of ASCAT and modelled soil moisture over South Africa, using TOPKAPI in land surface mode. *Hydrology and Earth System Sciences* 14:613-626.

Singleton, A. 2012. *Forecasting drought in Europe with the Standardized Precipitation Index*. JRC Scientific and Technical Report, Publication Office of the European Union.

Siska, B and Takac, J. 2009. Drought analysis of agricultural regions as influenced by climatic conditions in the Slovak Republic. *Quarterly Journal of the Hungarian Meteorological Service* 113(1-2): 135-143.

Smakhtin, W and Hughes, DA. 2007. Automated estimation and analyses of drought characteristics from monthly rainfall data. *Environmental Modelling and Software* 22(6):880-890.

Sohn, SJ, Joong-Bae, A and Chi-Yung, T. 2013. Six month–lead downscaling prediction of winter to spring drought in South Korea based on a multi-model ensemble. *Geophysical Research Letter* 40:579-583.

Sorooshian, S and AghaKouchak, A. 2010. Advanced concepts on remote sensing of precipitation at multiple scales. Center for Hydrometeorology and Remote Sensing, Department of Civil and Environmental Engineering, University of California Irvine, USA.

Spinoni, J, Antofie, T, Barbosa, P, Bihari, Z, Lakatos, M, Szalai, S, Szentimrey T and Vogt, J (2013). An overview of drought events in the Carpathian Region in 1961-2010. *Advanced Scientific Research Journal* 10:21-32.

Srivastava, PK, Dawei, H, Ramirez, MAR and Islam, T, 2013. Comparative assessment of evapotranspiration derived from NCEP and ECMWF global datasets through Weather Research and Forecasting model. *Atmospheric Science Letters* 14:118-125.

Sun, Z, Gebremichael, M, Ardö, J, Nickless, A, Caquet, B, Merboldh, L and Kutschi, W. 2012. Estimation of daily evapotranspiration over Africa using MODIS/Terra and SEVIRI/MSG data. *Atmospheric Research* 112:35-44.

Sur, C, Kang, S, Kim, JS and Choi, M. 2015. Remote sensing-based evapotranspiration algorithm: a case study of all sky conditions on a regional scale. *GIScience and Remote Sensing* 52(5):627-642.

Su, Z, Schmugge TJ, Kustas WP and Massman WJ. 2001. An evaluation of two models for estimation of the roughness height for heat transfer between the land surface and the atmosphere. *Journal of Applied Meteorology* 40:1933-1951.

Su, Z, Dorigo, W, Fern´andez-Prieto, D, van Helvoirt, M, Hungershoefer, K, de Jeu, R, Parinussa, R, Timmermans, J, Roebeling, R, Schroder, M, Schulz, J, van der Tol, C, Stammes, P, Wagner, W, Wang, L, Wang, P and Wolters, E. 2010. Earth observation Water Cycle Multi-Mission Observation Strategy (WACMOS). *Hydrology and Earth System Sciences* 7:7899-7956.

Tadesse, T, Senay, G, Berhan, G, Regassa, T and Beyene, S. 2015. Evaluating a satellite-based seasonal evapotranspiration product and identifying its relationship with other satellite-derived products and crop yield: a case study for Ethiopia. *Journal of Applied Meteorology and Climatology* 40:39-54.

Ten Broek, J, Teuling, AJ and van Loon, AF. 2014. *Comparison of drought indices for the province of Gelderland, the Netherlands. DROUGHT-R and SPI.* Technical Report No. 16.

Tian, D and Martinez, CJ. 2012. Forecasting Reference Evapotranspiration Using Retrospective Forecast Analogs in the South-eastern United States. *Journal of Hydrometeorology* 13:1874-1892.

Tian, X, van der Tol, C, Su, Zhongo, Li, Zengyuan, Chen, E, Li, X, Yan, M, Chen, X, Wang, X, Pan, X, Ling, F, Li, C, Fan, W and Li, L. 2015. Simulation of forest evapotranspiration using time-series parameterization of the Surface Energy Balance System (SEBS) over the Qilian Mountains. *Remote Sensing* 7:15822-15843.

Timmermans, J, van der Tol, C and Su, Z. 2010. Increasing accuracy of daily evapotranspiration through synergistic use of MSG and MERIS/AATSR. *Geophysical Research Abstracts* 12:1.

Trambauer, P, Maskey, S, Werner, M, Pappenberger, F, van Beek, LPH and Uhlenbrook, S. 2014. Identification and simulation of space–time variability of past hydrological drought events in the Limpopo River Basin, southern Africa. *Hydrology and Earth System Sciences* 18:2925-2942.

Trenberth, KE, Dai, A, van der Schrier, G, Jones, PD, Barichivich, J, Briffa, KR and Sheffield, J. 2014. Global warming and changes in drought. *Nature Climate Change* 4(1):17-22.

UNFCCC (United Nations Framework Convention on Climate Change). 2011. Water and climate change impacts and adaptation strategies. United Nations Technical Paper No.5. UNFCCC, New York, United States of America.

Van Dijk and Renzullo, LJ. 2011. Water resource monitoring systems and the role of satellite observations. *Hydrological Earth System Sciences* 15:39-55.

Vancutsem, C, Ceccato, P, Dinku, T and Connor, SJ. 2010. Evaluation of MODIS land surface temperature data to estimate air temperature in different ecosystems over Africa. *Remote Sensing of Environment* 114(2):449-465.

Van den Hurk, BJJM, Viterbo, P, Beljaars, ACM and Betts, AK. 2000. *Offline validation of the ERA40 surface scheme*, ECMWF Technical Memorandum No. 295, p41.

Van Heerden, J, Terblanche, DE and Schulze, GC. 1998. The Southern Oscillation and South African summer rainfall. *Journal of Climatology* 8:577-597

Van Loon, AF and Laaha, G. 2014. Hydrological drought severity explained by climate and catchment characteristics. *Journal of Hydrology* 526:3-14.

Van Loon, 2015. Hydrological drought explained. *Wiley Interdisciplinary Reviews: Water* 2(4):2015.

Vicente-Serrano, SM. 2006. Differences in spatial patterns of droughts on different time scales: an analysis of the Iberian Peninsula. *Water Resources Management 20*(1):37-60.

Vicente-Serrano, SM, Beguería, S, López-Moreno, JI, Angulo, M., and El Kenawy, A. 2010a. A New Global 0.5_ Gridded Dataset (1901–2006) of a Multiscalar Drought Index: comparison with current drought index datasets based on the Palmer Drought Severity Index. *Journal of Hydrometeorology* (11):1033-1043.

Vicente-Serrano, SM, Beguería, S and López-Moreno, JI. 2010b. A multiscalar drought index sensitive to global warming: The standardized precipitation evapotranspiration index-SPEI. *Journal of Climate* 23(7):1696-1718.

Vicente-Serrano, SM, Begueria, S, and López-Moreno, JI. 2011. Characteristics and trends in various forms of the Palmer Drought Severity Index (PDSI) during 1900-2008. *Journal of Geophysical Research* 116:1-26.

Vicente-Serrano, SM, Begueria, S, Lorenzo-Lacruz, J, Camarero, JJ, López-Moreno, JI, Azorin-Molina, C, Revuelto, J, Morán-Tejeda, E and Sanchez-Lorenzo, A. 2012a. Performance of drought indices for ecological, agricultural, and hydrological applications. *Earth Interactions* 16(10):1-27.

Vicente-Serrano, SM, Zouber, A, Lasanta, T and Pueyo, Y. 2012b. Dryness is accelerating degradation of vulnerable shrublands in semi-arid Mediterranean environments. *Ecological Monographs* 82:407-428.

Vicente-Serrano, SM, Lopez-Moreno, JI, Bengueria, S, Lorenzo-Lacruz, J, Sanchez-Lorenzo, A, Garcia-Ruiz, JM, Azorin-Molina, C, Moran-Tejeda, EM, Revuelto, J, Trigo, R, Coelha, F and Espejo, F. 2014. Evidence of increasing drought severity caused by temperature rise in southern Europe. *Environmental Research Letters* 9(4):1-9.

Vicente-Serrano, SM and National Center for Atmospheric Research Staff. 2015. The Climate Data Guide: Standardized Precipitation Evapotranspiration Index (SPEI). [Internet]. National Center for Atmospheric Research, Boulder, Colorado, United States Available from: https://climatedataguide.ucar.edu/climate-data/standardized-precipitation-evapotranspiration-index-spei. [Accessed 20 December 2016].

Vicente-Serrano, SM, Van der Schrier, G, Beguería, S, Azorin-Molina, C and Lopez-Moreno, JI. 2015. Contribution of precipitation and reference evapotranspiration to drought indices under different climates. *Journal of Hydrology* 526:42-54.

Vicente-Serrano, SM and Begueria, S. 2016. Comment on "Candidate distributions for climatological drought indices (SPI and SPEI)" by James H. Stagge *et al*. *International Journal of Climatology* 36:212-213.

Vinukollu, RK, Wood, EF, Ferguson, CR and Fisher, JB. 2011. Global estimates of evapotranspiration for climate studies using multi-sensor remote sensing data: Evaluation of three process-based approaches. *Remote Sensing of Environment* 115:801-823.

Viterbo, P and Beljaars, A. 1995. An improved surface parameterization scheme in the ECMWF model and its validation. *Journal of Climate* 8:2716-2748.

Wagner, S, Kunstmann, H, Bárdossy, A, Conrad, C and Colditz, RR. 2008. Water balance estimation of a poorly gauged catchment in West Africa using dynamically downscaled meteorological fields and remote sensing information. *Physics and Chemistry of the Earth* 34(4-5):225-235.

Wanders, N and Wada, Y. 2014. Human and climate impacts on the 21st century hydrological drought. *Journal of Hydrology* 526:1-302.

Wan, Z, Zhang, Y, Zhang, YQ and Li, ZL. 2002. Validation of the land-surface temperature products retrieved from Moderate Resolution Imaging Spectroradiometer data. *Remote Sensing of Environment* 83:163-180.

Wan, Z, Zhang, Y, Zhang, YQ and Li, ZL. 2004. Quality assessment and validation of the global land surface temperature. *International Journal of Remote Sensing* 25:261-274.

Wan, Z. 2008. New refinements and validation of the MODIS land-surface temperature/emissivity products. *Remote Sensing of Environment* 112:59-74.

Wang, Kaicun, Wang, P, Zhanqing, L, Cribb, M and Sparrow, M. 2007. *Journal of Geophysical Research* 112:1-14.

Wanga, H, Chen, Y, Pan, Y and Li, W. 2015. Spatial and temporal variability of drought in the arid region of China and its relationships to teleconnection indices. *Journal of Hydrology* 523:283-296.

Warburton, ML, Schulze, RE and Jewitt, GPW. 2010. Confirmation of ACRU model results for applications in land use and climate change studies. *Hydrology and Earth Systems Science* 14:2399-2414.

Water Resource Commission (WRC). 2015. WRC Drought Factsheet 1: Background to current drought situation in South Africa. [Internet]. Water Research Commission, Pretoria, South Africa. Available from: http://www.droughtsa.org.za/images/Background_to_current_drought_situation_in_South_Africa.pdf. [Accessed 18 February 2016].

Weepener, HL, van den Berg, HM, Metz, M and Hamandawana, H. 2011. *Gap-filled DEM based on SRTM 90m DEM. SRTM90m_Gapfilled.tif*. WRC Report 1908/1/11, Water Resource Commission, Pretoria, South Africa.

Wei-Guang L, Xue Y, Mei-Ting H, Hui-Lin Ch and Zhen-Li Ch. 2012. Standardized precipitation evapotranspiration index shows drought trends in China. *Chinese Journal of Eco-Agriculture* 20(5):643-649.

Whitmore, JS. 1971. South Africa's water budget. *South African Journal of Science* 67(3):166-176.

Wilhite, DA, Sivakumar, MVK and Pulwarty, R. 2014. Managing drought risk in a changing climate: The role of national drought policy. *Weather and Climate Extremes* 3:4-13.

Wilhite, DA and Glantz MH, 1985. Understanding: the drought phenomenon: the role of definitions. *Water International* 10(3):111-120.

Wilk, J, Andersson, L and Warburton, M. 2013. Adaptation to climate change and other stressors among commercial and small-scale South African farmers. *Regional Environmental Change* 13:273-286.

Winkler, K, Gessner, U and Hochschild, V. 2017. Identifying droughts affecting agriculture in Africa based on remote sensing time series between 2000-2016: rainfall anomalies and vegetation condition in the context of ENSO. *Remote Sensing* 9(831):1-27.

World Meteorological Organization (WMO). 2012. Standardized Precipitation Index User Guide. WMO Publications, Geneva 2, Switzerland.

WWAP (United Nations World Water Assessment Programme). 2015. *The United Nations World Water Development Report 2015: Water for a Sustainable World*. Paris, UNESCO.

Zargar, A, Sadiq, R, Naser, B and Khan, FI. 2011. A review of drought indices. *Environ. Reviews* 19:333-349.

Zhang, K, Kimball, JS, Nemani, RR and Running, SW. 2010. A continuous satellite-derived global record of land surface evapotranspiration from 1983 to 2006. *Water Resources Research* 46 (9):1-21.

Zheng, X and Zhu, J. 2015. Temperature-based approaches for estimating monthly reference evapotranspiration based on MODIS data over North China. *Theoretical and Applied Climatology* 121:695-711.

Ziese, M, Schneider, U, Meyer-Christoffer, A, Schamm, K, Vido, J, Finger, P, Bissoli, P, Pietzsch, S and Becker, A. 2014. The GPCC drought index-a new, combined and gridded global drought index. *Earth System Science Data* 6:285-2.

Zotarelli, L, Dukes, MD, Romero, CC, Migliaccio, KW and Morgan, KT. 2013. Step by step calculation of the Penman-Monteith evapotranspiration (FAO-56 method). Institute of Food and Agricultural Sciences, University of Florida, Gainesville, Florida, United States of America.

7. APPENDIX A

In this appendix, the normalized drought indices (SPEI-Thornthwaite, SPEI-Hargreaves, SPI and ETDI) for U20E, U20F and U20G are displayed (Figures 7.1 to 7.3).

Normalization was performed for a better comparison of the indices. R^2 values produced by the correlation analyses remained unchanged from those presented in Table 4.5. Section 4.4.4 provides further details on the normalization that was performed.

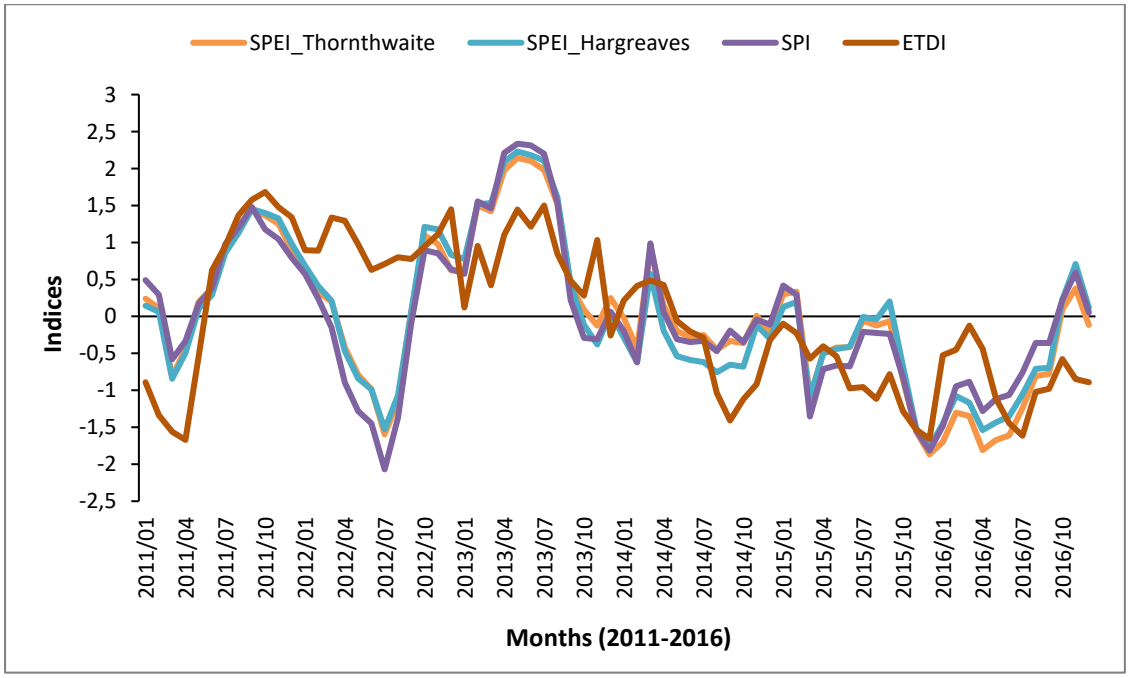

Figure 7.1 Comparison of normalized ETDI, SPI and SPEI for U20E (2011-2016)

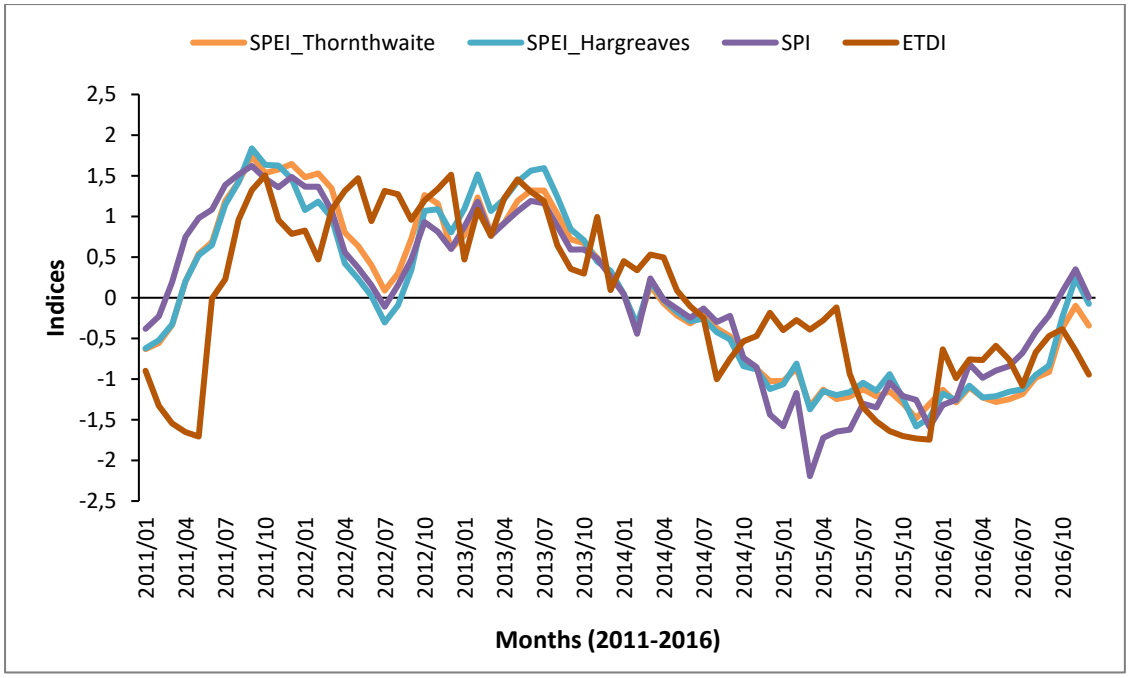

Figure 7.2 Comparison of normalized ETDI, SPI and SPEI for U20F (2011-2016)

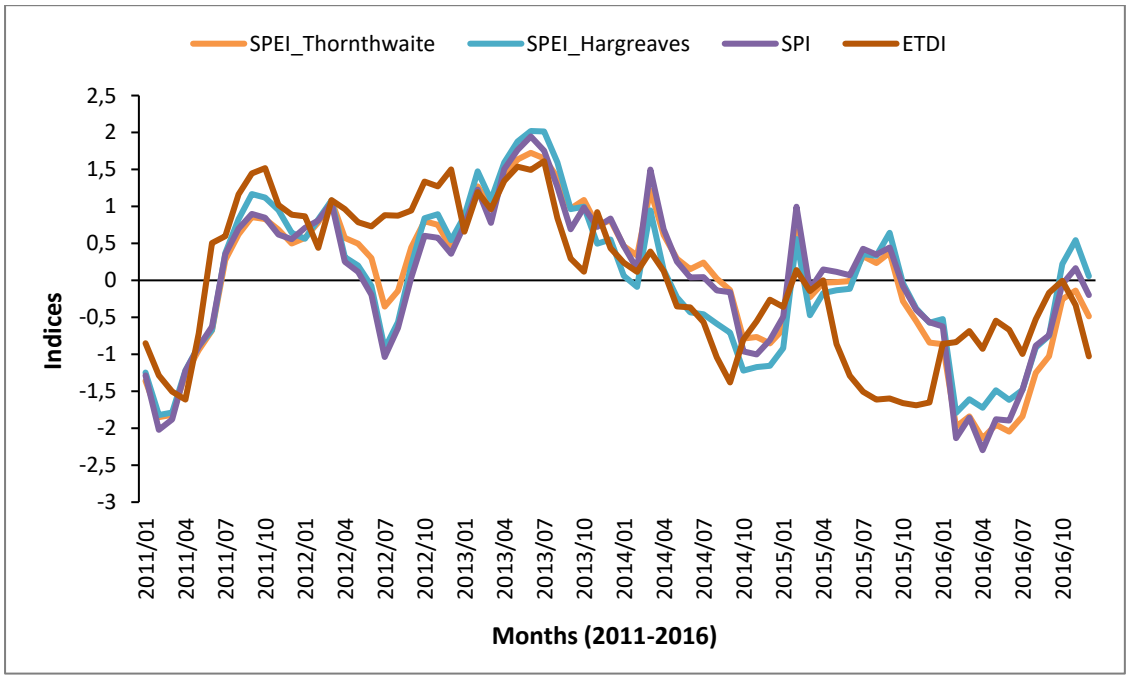

Figure 7.3 Comparison of normalized ETDI, SPI and SPEI for U20G (2011-2016)